Proceedings

MEA Meeting 2014

July 1 - July 4, 2014, Reutlingen, Germany

9th International Meeting on Substrate-Integrated Microelectrode Arrays

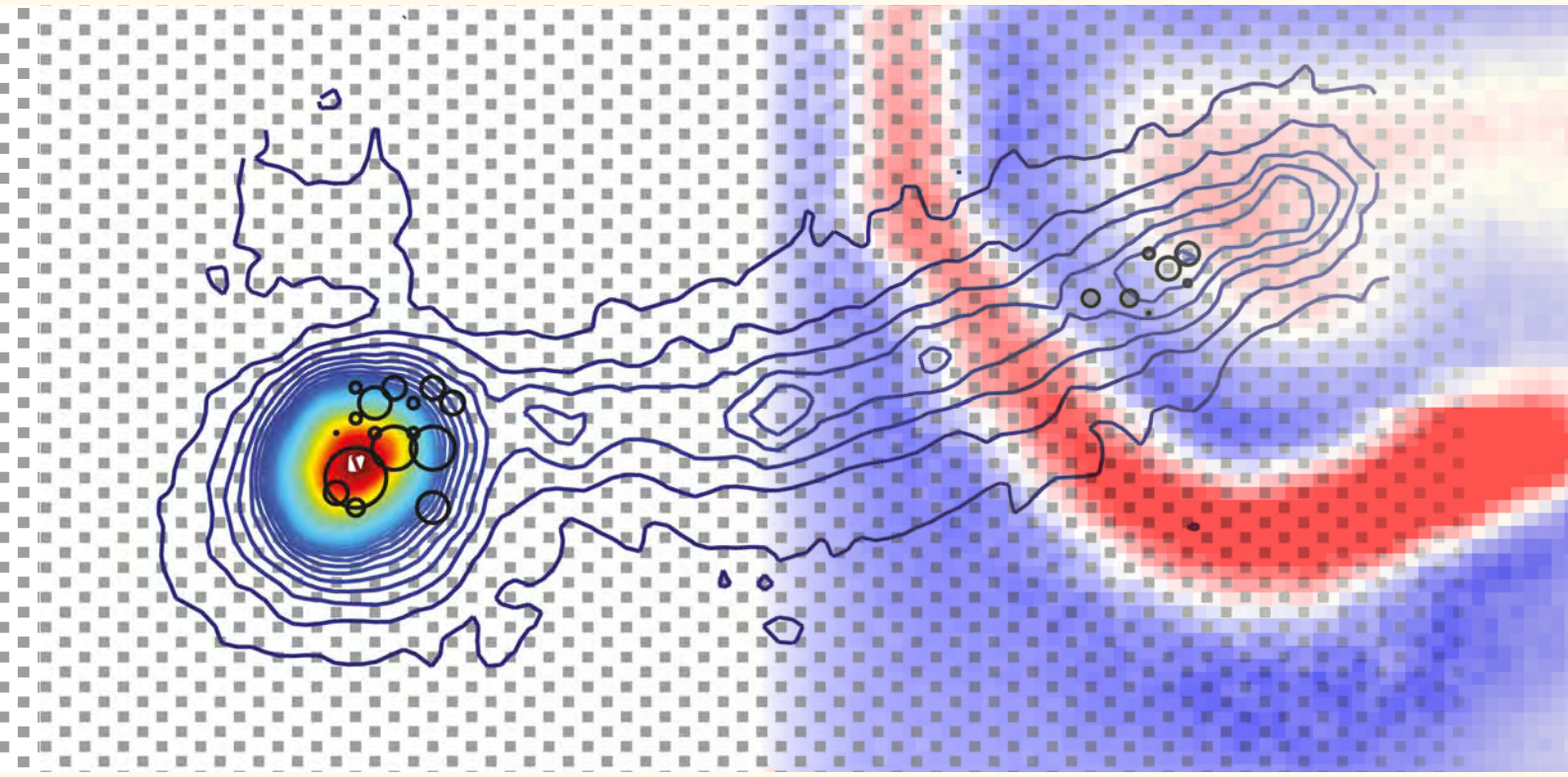

Tübingen Neurotech 2014

1st Tübingen Symposium on Current Topics in Neurotechnology

Bernstein Center Freiburg

NMI achieving results

Band 9

We are the MEA Powerhouse >>

NMI
achieving results

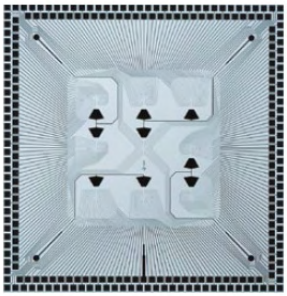

Custom-
designed MEAs

Flexible
MEAs

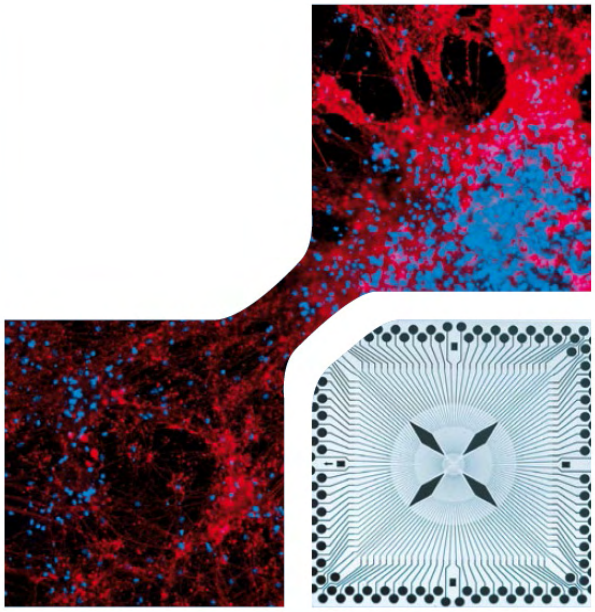

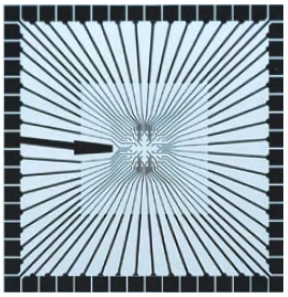

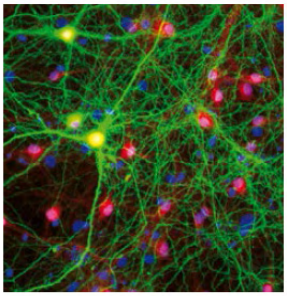

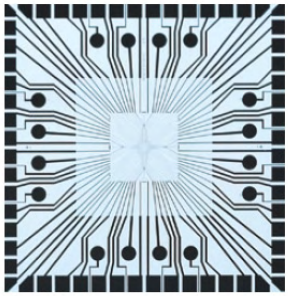

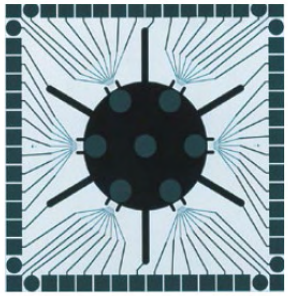

Innovating research
Improving health
Promoting safety

contact:
mea@nmi.de

NMI Natural and Medical Sciences Institute
Markwiesenstr,55
72770 Reutlingen, Germany
www.nmi.de

Best Pictures for Cover Image

Substrate-Integrated Microelectrode Arrays:
Electrophysiological Tools for Neuroscience, Biotechnology and Biomedical Engineering

9th International Meeting on Substrate-Integrated Microelectrode Arrays, July 1 - July 4, 2014, Reutlingen, Germany

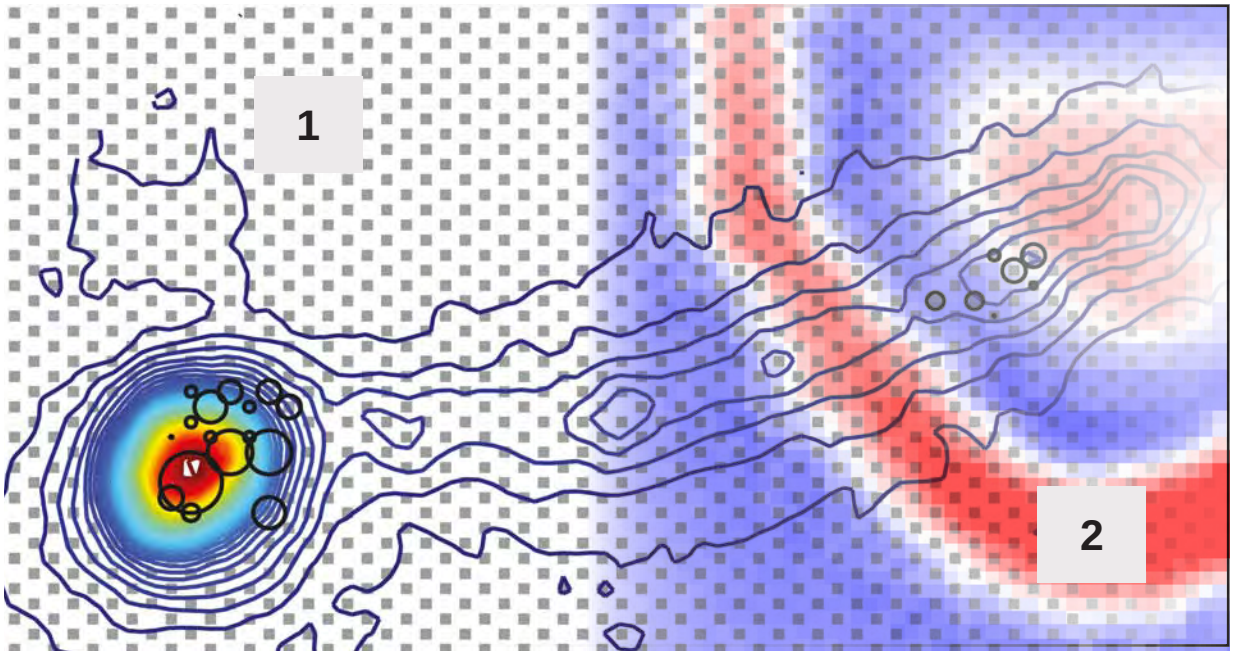

Cover images by courtesy of:
1 Jones Ian Lloyd et. al., Characterization of Mammalian Retinal Ganglion Cell Response to Voltage Stimulus, ETH Zürich, Basel, Switzerland
2 Lakshmi Channappa et. al., Electrical Imaging of Local Field Potentials in Organotypic and Acute Hippocampal Slices Using CMOS MEAs, NMI Reutlingen, Germany

Conference Proceedings of the
9th International Meeting on Substrate-Integrated Microelectrode Arrays
1st Tübingen Symposium on Current Topics in Neurotechnology
July 1 - July 4, 2014, Reutlingen, Germany

Meeting Organisation and Imprint

Organiser	NMI Natural and Medical Sciences Institute at the University of Tuebingen Markwiesenstrasse 55, 72770 Reutlingen, Germany Phone: +49 7121 - 51 530 -0; Fax: +49 7121 - 51 530 16; E-Mail: info@nmi.de Internet: www nmi.de
Publisher	NMI Natural and Medical Sciences Institute at the University of Tuebingen Markwiesenstrasse 55, 72770 Reutlingen, Germany Phone: +49 7121 - 51 530 -0; Fax: +49 7121 - 51 530 16; E-Mail: info@nmi.de Internet: www nmi.de
Editors	Dr. Alfred Stett and Dr. Günther Zeck
Co-organiser	Bernstein Center Freiburg Hansastraße 9, 79104 Freiburg, Germany Tel.: +49 (0)761 203 9549 ; Fax: +49 (0)761 203 9559 ; E-Mail: contact@bcf.uni-freiburg.de Internet: www.bcf.uni-freiburg.de
Organisation Team	Karla Bellack, Ira Digel, Nadja Gugeler, Priscilla Herrmann E-Mail: meameeting@nmi.de Internet: http://www.nmi.de/meameeting
Scientific Programme Committee	Dr. Michela Chiappalone, Italian Institute of Technology, Genova, Italy Prof. Ulrich Egert, University of Freiburg, Germany Prof. Gaute Einevoll, Norwegian University of Life Sciences (UMB), Norway Prof. Michele Giugliano, University of Antwerp, Belgium Prof. Yael Hanein, Tel-Aviv University, Israel Prof. Andreas Hierlemann, Swiss Federal Institute of Technology, Basel, Switzerland Prof. Jary Hyttinen, Tampere University of Technology, Finland Prof. Sven Ingebrandt, University of Applied Sciences, Kaiserslautern, Germany Dr. Udo Kraushaar, NMI Natural and Medical Sciences Institute, Reutlingen, Germany Prof. Sergio Martinoia, University of Genova, Italy Dr. Thomas Meyer, Multi Channel Systems MCS GmbH, Reutlingen, Germany Prof. Wim L.C. Rutten, University of Twente, The Netherlands Prof. Cornelius Schwarz, University of Tübingen, Germany Prof. Micha Spira, The Hebrew University of Jerusalem, Israel Prof. Bruce Wheeler, University of Florida, USA
Conference Chair	Dr. Alfred Stett and Dr. Günther Zeck, NMI Natural and Medical Sciences Institute, Reutlingen, Germany
Sponsor	Multi Channel Systems MCS GmbH, Reutlingen, Germany (www.multichannelsystems.com)
ISSN	2199-1596

NMI Natural and Medical Sciences Institute at the University of Tuebingen

NMI achieving results

Bernstein Center Freiburg

Bernstein Center Freiburg

Multi Channel Systems MCS GmbH

multichannel systems
Innovations in Electrophysiology

Foreword

Substrate-Integrated Microelectrode Arrays:
Electrophysiological Tools for Neuroscience, Biotechnology and Biomedical Engineering
9th International Meeting on Substrate-Integrated Microelectrodes, July 1 - 4, 2014

Current Topics in Neurotechnology – from Basic Research to Medical Application
1st Tübingen Neurotech Symposium, July 1, 2014

At present, the prime methodology for studying neuronal circuit-connectivity, physiology and pathol-ogy under in vitro or in vivo conditions is by using substrate-integrated microelectrode arrays.[1]

This quote from a recent review highlights the major research fields and topics in which microelectrode arrays (MEAs) are currently used. These areas, together with applications in electrical stimulation, stem cell research, and drug and toxicology tests will be addressed at this year's meeting on substrate-integrated microelectrode arrays (MEA 2014).

The broad range of bioelectric applications relies on customized hardware for efficient recording and stimulation. Today's microelectrode arrays comprise between 30 and 30,000 recording sites, which are embedded in glass, silicon or flexible polymers. The electrodes are either made of titanium nitride or carbon nanotubes, or they may be manufactured as field effect transistors or innovative organic materials. The entire range of technological developments in this area will be presented at the MEA Meeting 2014.

It is an honour and great pleasure for the Natural and Medicalw Sciences Institute (NMI) — which has been producing MEAs since the late 1980s — to organize and host the 9th MEA Meeting. We are pleased to welcome more than 250 students, senior researchers, developers, and new as well as experienced MEA us-ers to Reutlingen's new City Hall. Several hundred au-thors and co-authors from 26 countries submitted ab-stracts for MEA 2014, out of which we have chosen 25 for oral presentations and 115 for the poster exhibi-tion. All the accepted abstracts and papers will be pub-lished online as part of the meeting's proceedings.

These contributions, together with the eight key-note lectures which will be delivered by internation-ally-renowned scientists and leaders in the industrial sector, as well as the sizeable number of exhibitors showcasing their products and applications will cer-tainly make the MEA 2014 experience in Reutlingen a valuable and fruitful one for MEA developers and us-ers!

We are grateful to the Bernstein Center Freiburg for continuing to co-organize our MEA Meeting. We deeply appreciate the tremendous work done by the members of the Scientific Committee: they reviewed each submitted abstract and rated them carefully. We also thank the Scientific Committee for suggesting key-note speakers and appraising images for the best-picture award. This year's cover collage reflects the application of high-density CMOS-based arrays in single-cell analysis and systems neuroscience.

MEA 2014 will be preceded by the first *Tübingen Neurotech Symposium*, which has also been organized by the NMI. Speakers from local research institutes, hospitals and the industral sector will address current topics in neurotechnology – from basic research to medical application. The symposium features several state-of-the-art MEA applications which are likely to guide future MEA developments and applications. The highlight of this symposium is the evening session with keynote lectures and a panel discussion address-ing future directions and possibilities in brain research, as well as the international endeavours being made towards advancing neurotechnology, particularly in terms of large-scale brain mapping projects (BRAIN Initiative in the US, Human Brain Project in Europe).

We welcome you heartily to Reutlingen and are looking forward to an exciting meeting with lively and stimulating discussions – with old and new friends and colleagues.

Enjoy the meeting!

Dr. Alfred Stett, Dr. Günther Zeck
Conference chairs, NMI, Reutlingen

Prof. Dr. Ulrich Egert
Co-Organizer, Bernstein Center Freiburg

Follow us on facebook:
https://www.facebook.com/MEA.Meeting

Be part of the MEA user community on Yahoo:
https://groups.yahoo.com/neo/groups/mea-users/info

[1] M.E.Spira, A.Hai, Nature Nanotechnology, 8, 83-94, 2013

Program at a Glance

Tuesday, July 1	
13:30 - 18:00	Satellite Symposium: Tübingen Neurotech
19:00 - 20:30	Welcome Addresses and Opening Lectures by John Donoghue (Brown Institute for Brain Science, Brown University) and Katrin Amunts (Institute of Neuroscience and Medicine, Forschungszentrum Jülich)
20:30	Opening Reception

Wednesday, July 2	
8:30 - 10:10	Session: Stimulation strategies for neurons and fibers
10:10 - 10:40	Coffee break
10:40 - 12:40	Session: System Neuroscience (brain slices, retina, spinal cord)
12:40 - 14:00	Lunch break
14:00 - 15:40	Session: Pharmacology, toxicology, drug screening
15:40 - 16:10	Coffee break
16:10 - 17:50	Session: Neuron and network properties ("Analysis of (sub)-cellular neuron properties" and "signal analysis and statistics")
18:30	Social event: Punt ride on the river Neckar in Tübingen

Thursday, July 3	
9:00 - 14:15	Poster Sessions
12:00 - 13:00	Lunch break
15:00 - 16:00	Coffee break
16:00 - 17:30	Session: In vivo recordings and stimulation
18:30	Social event: Conference Dinner at Kelter, Metzingen

Friday, July 4	
8:30 - 9:30	Session: Primary and stem-cell derived cardiac myocyte cultures
9:30 - 10:00	Coffee break
10:00 - 12:00	Session: MEA technology (new materials, fabrication, culture techniques)
12:00 - 12:15	Closing remarks
12:15	Farewell lunch

Thank You to

Our Sponsors

multichannel systems
Innovations in Electrophysiology

Our Exhibitors

multichannel systems
Innovations in Electrophysiology

NMI TT
Technologie Transfer GmbH

National Bernstein Network Computational Neuroscience Germany

Qwane Biosciences
Innovative drug discovery tools

CorTec

Rapp OptoElectronic

CELLular Dynamics international

ALPHA MED SCIENTIFIC

nanion

The moment all the support you need
is just a phone call away.
This is the moment we work for.

ZEISS is the world's only one-stop manufacturer of light, X-ray and electron microscopes. Its extensive portfolio offers dedicated solutions for biosciences and materials microscopy in academia and industry.

www.zeiss.com/microscopy

ZEISS

We make it visible.

multichannel systems
Innovations in Electrophysiology

In vitro Electrophysiology

Recording and stimulating for all applications

- Standard MEAs from 32 to 256 electrodes
- Multiwell-MEA-System with 24 and 72 wells
- CMOS-System with over 5 000 electrodes

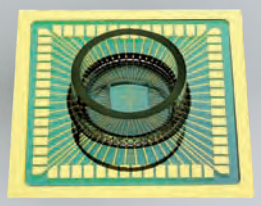

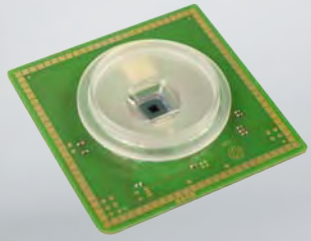

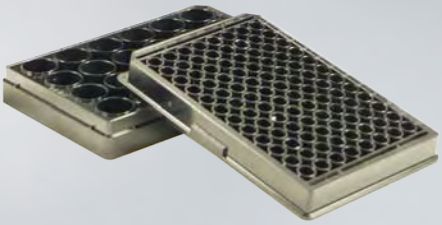

In vivo Electrophysiology

Powerful equipment for your experiment

- Wireless-System with 32 channels
- Tethered systems with up to 256 channels

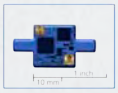

Visit us at our booth or at www.multichannelsystems.com

Contents

1st Tübingen Symposium on Current Topics in Neurotechnology - from Basic Research to Medical Application

Brain-Machine Interfaces and Algorithms

Brain-Machine-Interfaces (BMI) in Paralysis and Behavioral Disorders 29

N. Birbaumer[1,2,3], G. Gallegos-Ayala[1], R. Sitaram[4], U. Chaudhary[1], S. Soekadar[1], A. Ramos-Murguialday[1,5]

1 Institute of Medical Psychology and Behavioral Neurobiology, University of Tuebingen, Tuebingen, Germany
2 Ospedale San Camillo, IRCCS, Istituto di Ricovero e Cura a Carattere Scientifico, Venezia – Lido, Italy
3 Institute for Diabetes Research and Metabolic Diseases of the Helmholtz Center Munich at the University of Tübingen, Tübingen, Germany and German Center for Diabetes Research (DZDe.V.), Neuherberg, Germany
4 Department of Biomedical Engineering, University of Florida, Gainesville, FL, USA
5 Health Technologies Department, TECNALIA, San Sebastian, Spain

Combination of Brain-Machine Interfaces and Non-Invasive Brain Stimulation - from Basic Science to Clinical Applications 30

S. R. Soekadar[1,2], Matthias Witkowski[1,2], Niels Birbaumer[2,3,4]

1 University Hospital of Tübingen, Applied Neurotechnology Lab, Department of Psychiatry and Psychotherapy, Tübingen
2 Institute of Medical Psychology and Behavioral Neurobiology, University of Tübingen, Tübingen, Germany
3 Ospedale San Camillo, IRCCS, Istituto di Ricovero e Cura a Carattere Scientifico, Venezia – Lido, Italy
4 Institute for Diabetes Research and Metabolic Diseases of the Helmholtz Center Munich at the University of Tübingen, Tübingen, Germany and German Center for Diabetes Research (DZDe.V.), Neuherberg, Germany

Pharmaco-TMS-EEG: A Novel Approach for Probing GABAergic Activity in Human Cortex 32

Ulf Ziemann, Isabella Premoli, Florian Müller-Dahlhaus

Dept. Neurology & Stroke, and Hertie Institute for Clinical Brain Research, University of Tübingen, Germany

Near-Infrared Spectroscopy (NIRS) - A Promising Tool for Neurofeedback? 33

Andreas J. Fallgatter, Beatrix Barth, Ann-Christine Ehlis

Dept. of Psychiatry and Psychotherapy, University Hospital of Tübingen, Germany

Machine Learning Algorithms for Brain Signal Processing 34

Martin Spüler[1], Carina Walter[1], Armin Walter[1], Martin Bogdan[1,2], Wolfgang Rosenstiel[1]

1 Technische Informatik, Eberhard-Karls-Universität Tübingen, Germany
2 Technische Informatik, Universität Leipzig, Germany

Neurotechnology: Basic and Advanced Technologies

Implantable Bioelectronic Interfaces for Diagnosis, Therapy and Rehabilitation 38
Alfred Stett, Volker Bucher, Claus Burkhardt, Martina Cihova, Katja Gutöhrlein, Massimo Kubon, Gorden Link, Rene von Metzen, Wilfried Nisch, Sebastian Röhler, Ramona Samba, Michael Weinmann, Martin Stelzle
NMI Natural and Medical Sciences Institute at the University of Tübingen, Reutlingen, Germany

CMOS – Based Microelectrode Arrays ('Neurochips') for Simultaneous Stimulation and Detection Action Potentials at Sub-Cellular Resolution 41
Günther Zeck[1], Max Eickenscheidt, Lakshmi Channappa, Roland Thewes[2]
1 Natural and Medical Sciences Institute at the University of Tübingen
2 Chair of Sensor and Actuator Systems, Faculty of EECS, TU Berlin, Berlin, Germany

Electronic Systems for Electrophysiology and Implantable Devices 42
Clemens Boucsein, Karl-Heinz Boven, Andreas Möller
Multi Channel Systems MCS GmbH, Reutlingen, Germany

The Technology of Retinal Implants: Challenges and Solutions 43
Walter-G. Wrobel
Retina Implant AG, Reutlingen, Germany

Tapping Into Decision-Related Activity in Primary Somatosensory Cortex to Control the Subject's Percept 44
Cornelius Schwarz, Dominik Brugger and Stine Dehnke
Systems Neurophysiology, Werner Reichardt Centre for Integrative Neuroscience and Dept. for Cognitive Neurology, Hertie Institute for Clinical Brain Research

Neuroprosthesis and Neuromodulation: Applications and Prospects

To What Extent can Retinal Prostheses Restore Vision? 45
Zrenner, Eberhart[1]; Bartz-Schmidt, Karl-Ulrich[1]; Chee, Caroline[2]; Gekeler, Florian[1]; Jackson, Timothy L.[3]; MacLaren, Robert[4]; Nemeth, Janos[5]; Sachs, Helmut[6]; Stingl, Katarina[1]; Wong, David[7]
1 Werner Reichardt Center for Integrative Neurosciences and Institute for Ophthalmic Research, University of Tübingen, Germany
2 Dept.of Ophthalmology, National University Health System, Singapore, Singapore
3 Dept. of Ophthalmology, School of Medicine, King's College, London, United Kingdom
4 Dept. of Clinical Neurosciences, Nuffield Laboratory of Ophthalmology, University of Oxford, Oxford, United Kingdom
5 Semmelweis University, Budapest, Hungary
6 Städtisches Klinikum Dresden-Friedrichstadt, Dresden, Germany
7 Dept. of Ophthalmology, University of Hong Kong, Hong Kong

Brain-State Dependent Neuromodulation with Closed-Loop Neuroprosthetics for Neurorehabilitation 47
Alireza Gharabaghi
Functional and Restorative Neurosurgery, Neurosurgical University Hospital, University of Tübingen, Germany

9th International Meeting on Substrate-Integrated Microelectrode Arrays

Stimulation Strategies for Neurons and Fibers 49

Keynote Lecture: Bioelectronic Medicines: Can MEAs Help Bring About a New Class of Treatments? 50

Daniel Chew[1], Bryan McLaughlin[2], Arun Sridhar[1], Sonal Patel[1], Hannah Tipney[1], Roy Katso[1], Imran Eba[3] and Kristoffer Famm[1]

1 Bioelectronics R&D, GlaxoSmithKline, Stevenage, Hertfordshire SG1 2NY, UK
2 The Charles Stark Draper Laboratory, Cambridge, Massachusetts 02139, USA
3 Action Potential Venture Capital, Cambridge, Massachusetts 02142, USA

Oral Presentation: Response Profiles of Auditory Neurons on Multielectrode Arrays 51

Stefan Hahnewald[1], Anne Tscherter[3], Marta Roccio[1], Emanuele Marconi[1], Carolyn Garnham[2], Pavel Mistrik[2], Teresa Melchionna[2], Jürg Streit[3], Julien Brossard[4], Alexandra Homsy[4], Herbert Keppner[4], Hans-Rudolf Widmer[5], Pascal Senn[1]

1 Inner Ear Research Laboratory, Department of Clinical Research, University of Bern and University Department of Otorhinolaryngology, Head & Neck Surgery, Bern, Switzerland
2 MED-EL Elektromedizinische Geraete GmbH (MED-EL), Innsbruck, Austria
3 Department Physiology, University of Bern, Bern, Switzerland
4 Haute Ecole Arc Ingénierie, La Chaux-de-Fonds, Switzerland
5 Department of Neurosurgery, Bern University Hospital, Bern, Switzerland

Oral Presentation: PEDOT-CNT Coated Electrodes Stimulate Retinal Neurons with Low Voltage Amplitudes 54

Ramona Samba[1], Thoralf Herrmann[2], Günther Zeck[2]

1 BioMEMS and Sensors Group, NMI Natural and Medical Sciences Institute at the University of Tübingen, Reutlingen, Germany
2 Neurochip Research Group, NMI Natural and Medical Sciences Institute at the University of Tübingen, Reutlingen, Germany

Oral Presentation: Wide-Field Photostimulation of Cortical Networks: Selective Activation of Excitatory Neurons and Its Impact on Evoked Reverberating Responses In Vitro 56

Rocco Pulizzi[1], Gabriele Musumeci[1], Chris Van Den Haute[2], Veerle Baekelandt[2], and Michele Giugliano[1,3,4]

1 Department of Biomedical Sciences, University of Antwerp, Belgium
2 Department of Neurosciences, KU Leuven, B-3000 Belgium
3 Brain Mind Institute, EPFL, Switzerland
4 University of Sheffield, S1 4DP Sheffield, UK

Restoring Light Sensitivity in Blind Retinae Using Next-Generation Photopharmacology 58

Laura Laprell, Martin Sumser, Dirk Trauner

Ludwig-Maximilians-Universitaet, Munich, Germany

Finding the Most Effective Site for Extracellular Neuronal Stimulation 60

Milos Radivojevic, David Jäckel, Jan Müller, Vijay Viswam, Ian Lloyd Jones, Andreas Hierlemann, and Douglas Bakkum

ETH Zürich, Bio Engineering Laboratory, D-BSSE, Basel, Switzerland

Stimulation and Recording from the Same Microelectrode Using Low-Gain High-Resolution Data Acquisition System 62

Hyunjun Jung, Yoonkey Nam

Neural Engineering Laboratory, Department of Bio and Brain Engineering, Korea Advanced Institute of Science and Technology (KAIST), Daejeon, Republic of Korea

Combining an Optical Eye Model and MEA Recordings for Testing of Retinal Prostheses 64

John M Barrett[1], Lionel Chaudet[2], Mark Neil[2], Na Dong[3], Xiaohan Sun[3], Evelyne Sernagor[1], Patrick Degenaar[4]

1 Institute of Neuroscience, Newcastle University, United Kingdom
2 Imperial College, London, United Kingdom
3 South East University, Nanjing, China
4 School of Electrical and Electronic Engineering, Newcastle University, United Kingdom

Simultaneous Stimulation and Recording from Healthy and Blind Mouse Retinas Using Implantable Subretinal Microchips and Flexible Microelectrode Arrays 66

Henrike Stutzki, Florian Helmhold, Max Eickenscheidt, Günther Zeck

Neurochip Research Group,NMI Natural and Medical Sciences Institute at the University of Tübingen, Reutlingen, Germany

Localized Laser-Triggered Activity of Optogenetically Modified Neurons 68

Thoralf Herrmann[1], Christine Dürr[2], Martin Kriebel[2], Günther Zeck[1]

1 Neurochip Research Group, NMI Natural and Medical Sciences Institute at the University of Tübingen, Reutlingen, Germany
2 Molecular Biology, NMI Natural and Medical Sciences Institute at the University of Tübingen, Reutlingen, Germany

Effects of Long-term Electrical Stimulation on Retinal Ganglion Cell (RGC) Response in Retinal Degeneration Model (rd1) Mice 70

Joo Yeon Kim[1,2], Wang Woo Lee[1,2], Yong Sook Goo[1,2]

1 Department of Physiology, Chungbuk National University School of Medicine, Cheongju, S. Korea
2 Nano Artificial Vision Research Center, Seoul National University Hospital, Seoul, S. Korea

All Electrical or Optoelectrical Communication 72

Vanessa Maybeck, Wenfang Li1, Jan Schnitker, Andreas Offenhäusser

ICS/PGI-8 Bioelectronics, Forschungszentrum Jülich GmbH, Germany

Characterization of Mammalian Retinal Ganglion Cell Response to Voltage Stimulus 74

Jones Ian Lloyd, Russell Thomas, Fiscella Michele, Franke Felix, Müller Jan, Radivojevic Milos, Hierlemann Andreas

ETH Zürich, Bio Engineering Laboratory, D-BSSE, Basel, Switzerland

Autonomous Control of Network Activity 76

Sreedhar Saseendran Kumar[1,2], Jan Wülfing[2], Samora Okujeni[1], Joschka Boedecker[3], Ralf Wimmer[3], Martin Riedmiller[3], Bernd Becker[4], Ulrich Egert[1,2]

1 Biomicrotechnology, Institute of Microsystems Engineering, University of Freiburg, Freiburg, Germany
2 Bernstein Center Freiburg, Freiburg, Germany
3 Machine Learning Lab, University of Freiburg, Freiburg, Germany
4 Chair of Computer Architecture, University of Freiburg, Freiburg, Germany

Simultaneous Stimulation and Recording of Retinal Action Potentials Using Capacitively Coupled High- Density CMOS-based MEAs 78

Dmytro Velychko[1], Max Eickenscheidt[1], Roland Thewes[2], and Günther Zeck[1]

1 Neurochip Research Group, NMI Natural and Medical Sciences Institute at the University of Tübingen, Reutlingen, Germany
2 Chair of Sensor and Actuator Systems, Faculty of EECS, TU Berlin, Berlin, Germany

Systems Neuroscience (brain slices, retina, spinal cord) 80

Oral Presentation: On the Nature and Transmission of Information Among Cell-Assemblies: A Network and Information Analysis of Propagation Between Neural Populations in a Two-Chamber In Vitro System 81

DeMarse, Thomas[1], Alagapan, Sankarleengam[1], Pan, Liangbin[1], Franca, Eric[1], Leondopulos, Stathis[1], Brewer, Gregory[2], and Wheeler, Bruce[1]

1 Pruitt Dept. of Biomedical Engineering, University of Florida, Gainesville, Florida, USA
2 Dept. of Biomedical Engineering, University of California, Irvine, California, USA

Oral Presentation: Pairwise Reconstruction of the Hippocampal Tri-Synaptic Loop: EC-DG, DG-CA3, CA3-CA1 83

Gregory J. Brewer[1], Harsh Desai[1], Himanshi Agrawal[1], Stathis S. Leondopulos[2], Bruce C. Wheeler[2]

1 University of California Irvine, USA
2 University of Florida, Gainesville, FL USA

Oral Presentation: Electrical Imaging of Local Field Potentials in Organotypic and Acute Hippocampal Slices Using CMOS MEAs 85

Lakshmi Channappa, Florian Helmhold, Günther Zeck

Neurochip Research Group, NMI Natural and Medical Sciences Institute at the University of Tübingen, Reutlingen, Germany

Oral Presentation: Technique for Analysis of Purkinje Cell Sub-Cellular Functional Dynamics in Acute Cerebellar Slices Using a High-Density Microelectrode Array 88

Marie Engelene J. Obien[1], Andreas Hierlemann[2], Urs Frey[1,2]

1 RIKEN Quantitative Biology Center, Kobe Japan
2 Department of Biosystems Science and Engineering, ETH Zurich, Basel, Switzerland

Oral Presentation: Changes of Axonal Conduction in Bursting Activity 91

Kenta Shimba, Koji Sakai, Kiyoshi Kotani, Yasuhiko Jimbo

The University of Tokyo, Tokyo, Japan

Oral Presentation: Off-like Responses to the Blue-light in rd1/ChR2 Mouse Retina 95

Jae Hong Park, Hyuk-June Moon, Dong-Hoon Kang, Sujin Hyung, Hyun Jun Shin, Jun-Kyo Francis Suh

The Center for Bionics, Korea Institute of Science and Technology, Seoul, Republic of Korea

Decoding of Motion Directions by Direction-Selective Retina Cells 98

Michele Fiscella, Felix Franke, Jan Müller, Ian L. Jones, Andreas Hierlemann

Bio Engineering Laboratory, ETH Zurich, Basel, Switzerland

High Resolution Large-Scale Recordings of Light Responses from Mouse Retinal Ganglion Cells 100

Gerrit Hilgen[1], Alessandro Maccione[2], Stefano Di Marco[2], Luca Berdondini[2], Evelyne Sernagor[1]

1 Institute of Neuroscience, Medical Sciences, Newcastle University, Newcastle upon Tyne, UK
2 Neuroscience and Brain Technologies, Istituto Italiano di Tecnologia, Genova, Italy

Novel Insights into Visual Information Processing of Human Retina 102

Katja Reinhard[1], Marion Mutter[1], Michele Fiscella[2], Jan Müller[2], Felix Franke[2], Andreas Hierlemann[2], Thomas Münch[1]

1 Centre for Integrative Neuroscience, University of Tübingen, Tübingen, Germany
2 ETH Zürich, D-BSSE, Basel, Switzerland

Investigation of Functional Connectivity in Degenerative Retina Using MEA-STA System 103
Hyuk-June Moon, DongHoon Kang, JaeHong Park, SuJin Hyung, HyunJoon Shin, JunKyo Francis Suh
Center for Bionics, Biomedical Research Institute, KIST, Seoul, Korea

Pharmacology, Toxicology, and Drug Screening 105

Keynote Lecture: Neurotoxicity Screening Using Multi-Well Microelectrode Array Plates: Lessons Learned and a Path Forward 106
Timothy J Shafer
Integrated Systems Toxicology Division, NHEERL, ORD, United States Environmental Protection Agency, RTP, NC USA

Oral Presentation: Cytotoxicity of the Antimalarial Drug Mefloquine and Novel Protection by Quinolinic Acid 109
Katelyn E. Holmes, David Smith, Guenter W. Gross
Center for Network Neuroscience, Department of Biological Sciences, University of North Texas, Denton, USA

Oral Presentation: Norepinephrine Modulates Bursting Activity Differently During Development 112
Lui Yoshida, Kiyoshi Kotani, Yasuhiko Jimbo
The University of Tokyo, Tokyo, Japan

Oral Presentation: Microelectrode Array Recording and Ca^{2+} Imaging in Hippocampal Cultures Enzymatically Treated with Hyaluronidase 114
Mukhina Irina[1,2], Vedunova Maria[1,2], Mitrosina Elena[1,2], Sakharnova Tatiana[1,2], Zakharov Yury[1], Pimashkin Alexey[1], Dityatev Alexander[1,3]
1 N.I. Lobachevsky State University of Nizhny Novgorod, Nizhny Novgorod, Russia
2 Nizhny Novgorod State Medical Academy, Nizhny Novgorod, Russia
3 German Center for Neurodegenerative Diseases (DZNE), Magdeburg, Germany

Cortical Networks Respond with Major Activity Changes to Sildenafil Citrate (Viagra) 116
Nicole K Calderon[1,2], Daniel Ledee[1,2], Kamakshi Gopal[1,2], Guenter W. Gross[2,3]
1 Department of Speech and Hearing Sciences
2 Center for Network Neuroscience
3 Department of Biological Sciences University of North Texas, Denton, USA

Role of Tachykinin1 and αCGRP on Modulating Inflammatory Sensitization of TRPV1 118
Sakthikumar Mathivanan, Christoph Jakob Wolf, Isabel Devesa, Clotilde Ferrandiz Huertas, Antonio Ferrer-Montiel
Instituto de Biología Molecular y Celular, Universidad Miguel Hernandez de Elche, Alicante, Spain

Pharmacological Studies of Synaptic Communication in Maturing Human Pluripotent Stem Cell Derived Neural Networks 120
Meeri Mäkinen, Laura Ylä-Outinen, Dimitriy Fayuk, Susanna Narkilahti
NeuroGroup, BioMediTech, University of Tampere, Tampere, Finland

Automated Cytocentering™ Patch Clamp Recordings of Primary and iPSC-derived Cells Open New Paths in Basic and Applied Ion Channel Research 122
Dirck Lassen[1,2], Olaf Scheel[1], Stefanie Frech[1], Thomas Knott[1], Peter van Stiphout[2]
1 Cytocentrics Bioscience GmbH, Rostock, Germany
2 Cytocentrics BV, Eindhoven, The Netherlands

Ostreopsis cf. Ovata Toxicity Evaluation by Using Microelectrode Array Based Platform 124
Susanna Alloisio[1,2], Valentina Giussani[3], Marika Zanin[1], Valentina Asnaghi[3], Mariachiara Chiantore[3], Antonio Novellino[1,2]
1 ETT S.p.A., via Sestri 37, Genoa, Italy
2 Institute of Biophysics, National Research Council, Genoa, Italy
3 DiSTAV, University of Genoa, Genoa, Italy

Biphasic Reaction on Sodium Valproic Acid (NaVPA)- Treatment in Neuronal Networks 126
Matthias Nissen[1], Sebastian Bühler[2], Marco Stubbe[1] and Jan Gimsa[1]
1 University of Rostock, Biophysics, Rostock, Germany
2 Leibniz-Institut für Nutztierbiologie (FBN), Dummerstorf, Germany

Thymoquinone Protects Cultured Hippocampal and Human Induced Pluripotent Stem Cells-Derived Neurons Against α-Synuclein-Induced Synapse Damage 127
Alhebshi Amani, Odawara Aoi, Gotoh Masao,Suzuki Ikuro
Graduate School of Bionics, Tokyo University of Technology, Tokyo, Japan

Exciting New Easy-to-Use Hybrid Measurement System for Extracellular Potential And Impedance Recording in a 96-Well Format 129
David Guinot, Leo Doerr, Sonja Stoelzle-Feix, Ulrich Thomas, Matthias Beckler, Michael George, Niels Fertig
Nanion Technologies GmbH, Munich, Germany

Electrical Stimulation of Neuronal Cultures as a New Method for Neuropharmacological and Neurotoxicological Evaluation 131
Marika Zanin[2], Enrico Defranchi[1], Susanna Alloisio[2,3], Antonio Novellino[2,3], Sergio Martinoia[1]
1 DIBRIS, University of Genoa, Genoa, Italy
2 Alternative Toxicity Services, ETT s.p.a., Genoa, Italy
3 Institute of Biophysics, National Research Council, Genoa, Italy

Real-time Monitoring of Lesion Healing by Impedance Spectrometry on Chip 133
Heinz D. Wanzenboeck[1], Andreas Exler[1], Johann Mika[1], Emmerich Bertagnolli[1] Elisabeth Engleder[2], Michale Wirth[2], Franz Gabor[2]
1 Vienna University of Technology, Institute for Solid State Electronics, Vienna, AUSTRIA
2 University of Vienna, Department of Pharmaceutical Technology and Biopharmaceutics, Vienna, AUSTRIA

Functional Phenotypic Compound Screening with Primary Brain-Region Specific Cell Cultures 135
Alexandra Voss, Corina Ehnert, Konstantin Jügelt, Anna-Maria Pielka, Angela Podßun, Olaf H.-U. Schröder
NeuroProof GmbH, Rostock, Germany

MEA technology - a New Player in Diabetes Research 137
Sven Schönecker[1], Peter Krippeit-Drews[2], Gisela Drews[2], Karl-Heinz Boven[3], Elke Guenther[1], Udo Kraushaar[1]
1 NMI Natural and Medical Sciences Instute at the University of Tübingen, Dept. Electrophysiology, Reutlingen, Germany
2 University of Tübingen, Institute of Pharmacy, Dept. Pharmacology, Tübingen, Germany
3 Multi Channel Systems, Reutlingen, Germany

Neuron and Network Properties

Analysis of (Sub)-Cellular Neuron Properties ____ 138

Oral Presentation: Glutamate Mediated Astrocytic Filtering of Neuronal Activity 139

Gilad Wallach, Yael Hanein

School of Electrical Engineering, Faculty of Engineering, Tel Aviv University, Tel Aviv, Israel

Oral Presentation: Analysis of Related Molecules to Synchronized Burst Activity of Rat Cultured Cortical Networks 143

Daisuke Ito[1,2], Kazutoshi Gohara[3]

1 Division of Functional Life Science, Faculty of Advanced Life Science, Hokkaido University, Sapporo, Japan
2 Research Fellow of the Japan Society for the Promotion of Science, Tokyo, Japan
3 Division of Applied Physics, Faculty of Engineering, Hokkaido University, Sapporo, Japan

Oral Presentation: Functional Connectivity Estimate from Spontaneous and Stimulus Evoked Activities in Dissociated Cultured Neurons on a High-Density CMOS Microelectrode Array 147

Takeshi Mita[1], Douglas J. Bakkum[2], Urs Frey[3], Andreas Hierlemann[2], Ryohei Kanzaki[1], Hirokazu Takahashi[1]

1 The University of Tokyo, Tokyo, Japan
2 ETH Zurich, Basel, Switzerland
3 RIKEN Quantitative Biology Center, Kobe, Japan

Oral Presentation: Frequency Multiplications Accompanied by Sudden Synchrony Leaps and Ultrafast Neuronal Plasticity 149

Hagar Marmari[1], Roni Vardi[1], Amir Goldental[2] and Ido Kanter[1,2]

1 Gonda Interdisciplinary Brain Research Center and the Goodman Faculty of Life Sciences, Bar-Ilan University, Ramat-Gan, Israel
2 Department of Physics, Bar-Ilan University, Ramat-Gan, Israel

Oral Presentation: Simultaneous Intra- and Extracellular Recordings using a Combined High-Density Microelectrode Array and Patch-Clamp System 153

David Jäckel[1], Jan Müller[1], Thomas L. Russell[1], Milos Radivojevic[1], Felix Franke[1], Urs Frey[2], Douglas J. Bakkum[1] and Andreas Hierlemann[1]

1 ETH Zurich, Department of Biosystems Science and Engineering, Basel, Switzerland
2 RIKEN Quantitative Biology Center, Kobe, Japan.

An MEA-Based Model for Rapid Acceleration Injury to Neuronal Networks and Studies of Recovery 156

David C. Smith, Guenter W. Gross

Department of Biological Sciences, Center for Network Neuroscience University of North Texas, Denton, USA

Exploring the Role of Microtubule-Associated Protein Tau (Mapt) in Synaptic Plasticity 158

Torsten Bullmann[1,2], Tanja Treutlein[2], Jens T. Stieler[2], Max Holzer[2], Thomas Arendt[2], Urs Frey[1]

1 RIKEN Quantitative Biology Center, Kobe, Japan
2 Paul Flechsig Institute, Leipzig University, Leipzig, Germany

3D Finite Element Modeling of Single Neurons and the Microelectrode Array Microenvironment 160

Douglas J. Bakkum[1], Milos Radivojevic[1], David Jäckel[1], Felix Franke[1], Thomas L. Russell[1], Urs Frey[2], Hirokazu Takahashi[3], Andreas Hierlemann[1]

1 ETH Zurich, Basel, Switzerland
2 RIKEN Quantitative Biology Center, Kobe, Japan
3 The University of Tokyo, Tokyo, Japan

Multi-Parameter Analysis Platform for Neuronal Growth, Differentiation and Communication 162
L. Micholt, D. Braeken
Life Science Technologies, imec, Heverlee, Belgium

Characterizing the Human Embryonic Stem Cell – derived Neural Cultures: the Effect of Astrocytes on Network Properties 164
Marja Pajunen, Tanja Paavilainen, Dmitriy Fayuk, Laura Ylä-Outinen, Susanna Narkilahti
BioMediTech, University of Tampere, Finland

Neuronal Migration and Activity in Mature Primary Cultures on a High-Density CMOS Array 166
Hirokazu Takahashi[1], Takeshi Mita[1], Satoru Okawa[1], Ryohei Kanzaki[1], Urs Frey[2], Andreas Hierlemann[3], Douglas Bakkum[3]
1 The University of Tokyo, Tokyo, Japan
2 RIKEN Quantitative Biology Centre, Kobe, Japan
3 ETH Zurich, Basel, Switzerland

Simultaneous Microelectrode Array Recording and Intracellular $Ca^{2\pm}$ Imaging of Human Pluripotent Stem Cell–Derived Neural Cultures 168
Fayuk Dmitriy, Paavilainen Tanja, Meeri Mäkinen, Pajunen Marja, Heikkilä Juha, Narkilahti Susanna
BioMediTech, University of Tampere, Tampere, Finland

Spontaneous and Evoked Activity in Patterned Multi- Cluster Neuronal Networks 170
Margarita Anisimova[1], Keiko Yokoyama[1,2], Daisuke Ito[2,3], Masaaki Suzuki[4], Tsutomu Uchida[1], Kazutoshi Gohara[1]
1 Division of Applied Physics, Faculty of Engineering, Hokkaido University, Sapporo, Japan
2 Research Fellow of the Japan Society for the Promotion of Science, Tokyo, Japan
3 Division of Functional Life Science, Faculty of Advanced Life Science, Hokkaido University, Sapporo, Japan
4 National Institute of Advanced Industrial Science and Technology (AIST), Sapporo, Japan

Evaluation of Action Potential Conduction Velocity for Myelination Research 172
Koji Sakai, Kenta Shimba, Kiyoshi Kotani, Yasuhiko Jimbo
The University of Tokyo, Tokyo, Japan

Electrophysiological Characterization of Individual Neurons in Sparse Cortical Cultures 174
Weir Keiko, Blanquie Oriane, Kilb Werner, Luhmann Heiko J. and Sinning Anne
Institute of Physiology, University Medical Center Mainz, Mainz, Germany

Axon-Isolating Channels on a High Density Microelectrode Array 176
Marta K. Lewandowska, Douglas J. Bakkum, Andreas Hierlemann
Department of Biosystems Science and Engineering, ETH Zürich, Basel Switzerland

Pathomechanisms of Acquired Autoimmune Encephalitis Disorders Associated with Epilepsy and Anti- NMDA Receptors and Anti-LGI1 Autoantibodies 178
Elsen G. E.[1], Wolking S.[1], Maljevic S.[1], Wandinger K.P.[2], Lerche H.[1], Dihné M.[3]
1 Hertie Institute for Clinical Brain Research, Department of Neurology and Epileptology, University of Tübingen, Germany;
2 Institute for Clinical Chemistry and Department of Neurology, University Hospital Schleswig-Holstein, Lübeck, Germany
3 Department of Neurology, St. Lukas Klinik, Solingen, Germany

Effects of Epilepsy-Associated Ion Channel Mutations on Neuronal Network Activity 179
Snezana Maljevic, Yvonne Füll, Heidi Löffler, Filip Rosa, Yuanyuan Liu, Holger Lerche
Dept. of Neurology and Epileptology, Herti Institute for Clinical Brain Research, University of Tübingen, Tübingen, Germany

Neuron and Network Properties

Signal Analysis and Statistics ____ 180

Paired Spiking Is an Ubiquitous Response Property in Network Activity 181
Aurel Vasile Martiniuc[1], Rouhollah Habibey[2], Asiyeh Golabchi[2], Victor Bocos-Bintintan[3], Alois Knoll[1], Axel Blau[2]
1 Computer Science Department VI, Technical University Munich, Garching, Germany
2 Dept. of Neuroscience and Brain Technologies (NBT), Fondazione Istituto Italiano di Tecnologia (IIT), Genoa, Italy
3 Faculty of Environmental Science & Engineering, Babes- Bolyai University, Cluj-Napoca, Romania

Cultured Cortical Neurons Can Separate Source Signals from Mixture Inputs 183
Takuya Isomura[1,2], Kiyoshi Kotani[3], Yasuhiko Jimbo[3]
1 Department of Human and Engineered Environmental Studies, Graduate School of Frontier Sciences, The University of Tokyo, Tokyo, Japan
2 Japan Society for the Promotion of Science (JSPS), Tokyo, Japan
3 Department of Precision Engineering, School of Engineering, The University of Tokyo, Tokyo, Japan

High-Throughput, High-Performance, Low-Latency Spike-Sorting Hardware Platform..... 185
Dragas Jelena, Jäckel David, Franke Felix, Hierlemann Andreas
ETH Zurich, Department of Biosystems Science and Engineering, Basel, Switzerland

CARMEN, HDF5 and NDF: Reproducible Research on MEA Signals from Mouse and Ferret Retina. 187
L. S. Smith[1], S. J. Eglen[2], E. Sernagor[3]
1 Computing Science and Mathematics, University of Stirling, Stirling, Scotland UK
2 DAMTP, Centre for Mathematical Sciences, University of Cambridge, Cambridge, England, UK
3 Institute of Neuroscience, Faculty of Medical Sciences, University of Newcastle, Newcastle, England, UK

Post Stimulus Activity Patterns Reflect Stimulus Responses..... 188
Jelle Dijkstra[1] and Joost le Feber[1,2]
1 Biomedical Signals and Systems, University of Twente, Enschede, the Netherlands
2 Clinical Neurophysiology, University of Twente, Enschede, the Netherlands

Detecting Significant Changes in Oscillatory Power with Cluster-Based Permutation Testing..... 190
Ben van Lier[1,2], Andreas Hierlemann[2] and Frederic Knoflach[1]
1 F. Hoffmann - La Roche Ltd. Pharmaceutical Research and Early Development, Neuroscience, Basel, Switzerland
2 ETH Zürich, Department of Biosystems Science and Engineering, Basel, Switzerland.

Topological Effects on Bursting and Reverberation Dynamics..... 192
Chun-Chung Chen[1]
Institute of Physics, Academia Sinica, Taipei, Taiwan

A Multivariate Spike-Detection Algorithm to Asses Activity Patterns of Three-Dimensional In Vitro Models 194
Andreas W. Daus, Robert Bestel, Christiane Thielemann
Biomems lab, University of Applied Sciences Aschaffenburg, Germany

Partial Correlation Analysis for Functional Connectivity Studies in Cortical Networks..... 196
Daniele Poli, Vito Paolo Pastore, Simonluca Piazza, Paolo Massobrio and Sergio Martinoia
Department of Informatics, Bioengineering, Robotics and Systems Engineering (DIBRIS), University of Genova, Genova, Italy

Modulating Functional Connectivity in Hippocampal Cultures Using Hebbian Electrical Stimulation 198

Víctor Lorente[1], José Manuel Ferrández[1], Eduardo Fernández[2], Félix de la Paz[3]

1 Departamento de Electrónica, Tecnología de Computadores y Proyectos, Universidad Politécnica de Cartagena, Spain
2 Instituto de Bioingeniería, Universidad Miguel Hernández, Alicante, Spain
3 Departamento de Inteligencia Artificial, UNED, Madrid, Spain

Learning and Plasticity in Hippocampal Cultures Using Antiepilectic Drugs 200

José Manuel Ferrández[1], Victor Lorente[1], Arancha Alfaro[3], Eduardo Fernández[2]

1 Departamento de Electrónica, Tecnología de Computadores y Proyectos, Universidad Politécnica de Cartagena, Spain
2 Instituto de Bioingeniería, Universidad Miguel Hernández, Alicante, Spain
3 Departamento de Neurología, Hospital Vega Baja de Orihuela, Alicante, Spain

A Web-Based Framework for Semi-Online Parallel Processing of Extracellular Neuronal Signals Recorded by Microelectrode Arrays 202

Mufti Mahmud[1,2], Rocco Pulizzi[1], Eleni Vasilaki[3], Michele Giugliano[1,3,4]

1 Theoretical Neurobiology & Neuroengineering Lab, Dept. of Biomedical Sciences, University of Antwerp, Wilrijk, Belgium
2 Institute of Information Technology, Jahangirnagar University, Savar, Dhaka, Bangladesh
3 Department of Computer Science, University of Sheffield, Sheffield, UK
4 Brain Mind Institute, Swiss Federal Institute of Technology Lausanne, Lausanne, Switzerland

Comparison of Neuronal Dynamics in 2D and 3D In Silico Networks 204

Inkeri Vornanen, Jarno M. A. Tanskanen, Jari Hyttinen, Kerstin Lenk

Tampere University of Technology, Department of Electronics and Communications Engineering, and BioMediTech, Tampere

Estimating Stationary Functional Connection Underlying Switching-State Network Activity 206

Yuichiro Yada[1,2,3], Osamu Fukayama[1], Takayuki Hoshino[1], Kunihiko Mabuchi[1]

1 Graduate School of Information Science and Technology, The University of Tokyo, Tokyo, Japan
2 Research Center for Advanced Science and Technology, The University of Tokyo, Tokyo, Japan
3 Research Fellow of the Japan Society for the Promotion of Science, Tokyo, Japan

Network Dynamics in Connected Neuronal Sub-Populations During In Vitro Development 208

Marta Bisio, Alessandro Bosca, Valentina Pasquale, Luca Berdondini and Michela Chiappalone

Istituto Italiano di Tecnologia (IIT), Genova, Italy

Evoked Activity of Major Burst Leaders in Cultured Cortical Networks 210

Valentina Pasquale[1], Sergio Martinoia[2], Michela Chiappalone[1]

1 Department of Neuroscience and Brain Technologies, Istituto Italiano di Tecnologia, Genova, Italy
2 Department of Informatics, Bioengineering, Robotics and System Engineering, University of Genova, Genova, Italy

Use of Entropy to Discriminate Between Different Conditions in MEA Recordings 212

Capurro Alberto[1], Perrone Sandro[1], Heuschkel Marc[2], Makohliso Solomzi[2], Baez Candise[1] and Luthi-Carter Ruth[1]

1 Department of Cell Physiology and Pharmacology, University of Leicester, UK
2 Qwane Biosciences SA, EPFL Innovation Park, Lausanne, Switzerland

Initiation of Spontaneous Bursts in Dissociated Neuronal Cultures Is Poisson Process 214

Arthur Bikbaev[1], Abdelrahman Rayan[2], Martin Heine[1]

1 AG Molecular Physiology, Leibniz Institute for Neurobiology, Magdeburg, Germany
2 AG Molecular Neuroplasticity, Deutsches Zentrum für Neurodegenerative Erkrankungen, Magdeburg, Germany

Selective Laser Ablation of Interconnections Between Neuronal Sub-Populations: A Test-Bed for Novel Neuroprosthetic Applications 216

Alberto Averna[1], Marta Bisio[1], Valentina Pasquale[1], Paolo Bonifazi[2], Francesco Difato[1] and Michela Chiappalone[1]

1 Department of Neuroscience and Brain Technologies, Istituto Italiano di Tecnologia, Genova, Italy
2 School of Physics and Astronomy, Tel Aviv University (TAU), Israel

Simulation of hPSC Derived Neuronal Networks with Short and Long Reaching Axons 218

Kerstin Lenk[1], Laura Ylä-Outinen[2], Lukas H B Tietz[1], Susanna Narkilahti[2], Jari A K Hyttinen[1]

1 BioMediTech and Department of Electronics and Communications Engineering, Tampere University of Technology, Tampere, Finland
2 NeuroGroup, BioMediTech, University of Tampere, Tampere, Finland

Simplicial Complex and Betti Numbers to Characterize Co-Activation Patterns in Cortical Cultures 220

Virginia Pirino[1], Paolo Massobrio[1], Eva Riccomagno[2], Sergio Martinoia[1]

1 Neuroengineering and Bio-nano Technology Group (NBT), Department of Informatics Bioengineering Robotics and System Engineering, University o Genova, Genova, Italy
2 Department of Mathematics, University of Genova, Genoa, Italy

Investigation of Neuronal Activity Recorded with Multi-Electrode Arrays Using Principal Component Analysis 222

Patrick Schuller[1], Johann K. Mika[1], Heinz Wanzenböck[1], Petra Scholze[2], Emmerich Bertagnolli[1]

1 Institute of Solid State Electronics, Vienna University of Technology, Vienna, Austria
2 Center for Brain Research, Medical University of Vienna, Vienna, Austria

Modelling Seizure-Like Superburst Activity of Dissociated Neuronal Cultures 224

Simonov Alexander[1], Esir Pavel[1], Mukhina Irina[1,2], Kazantsev Victor[1,3]

1 Lobachevsky State University of Nizhny Novgorod, Russia
2 Nizhny Novgorod State Medical Academy, Nizhny Novgorod, Russia
3 Institute of Applied Physics RAS, Nizhny Novgorod, Russia

Cross-Correlation of Neural Culture Spiking Activity on Multielectrode Arrays is Strongly Dependent on Bursting Activity Pattern 226

Pimashkin Alexey[1,2], Gladkov Arseniy[1,3], Lepina Anastasia[1,3], Mukhina Irina[1,2,3], Kazantsev Victor[1,2]

1 Neuroscience Center, N.I. Lobachevsky State University of Nizhny Novgorod, Nizhny Novgorod, Russia
2 Department of Nonlinear Dynamics, Institute of Applied Physics RAS, Nizhny Novgorod, Russia
3 Normal Physiology Department, Nizhny Novgorod State Medical Academy, Nizhny Novgorod, Russia

Spontaneous and Stimulus Induced Connectivity Changes in Cultured Neural Network 228

Arseniy Gladkov[1,3], Alexey Pimashkin[1,2], Anastasia Lepina[1,3], Victor Kazantsev[1,2], Irina Mukhina[1,3]

1 Neuroscience Center, N.I. Lobachevsky State University of Nizhny Novgorod, Nizhny Novgorod, Russia
2 Department of Nonlinear Dynamics, Institute of Applied Physics RAS, Nizhny Novgorod, Russia
3 Normal Physiology Department, Nizhny Novgorod State Medical Academy, Nizhny Novgorod, Russia

Short ISI Stimulation Modifies Firing Property of a Cultured Neuronal Network 230

Hidekatsu Ito, Suguru N. Kudoh

School of Science and Technology, Kwansei Gakuin University, Sanda, Japan

In Vivo Recordings and Stimulation 232

Oral Presentation: Skin-like Neuroprosthesis Based on Elastomeric Composites for Chronic Epidural Electrical Stimulation of Paralyzed Rats 233

Alexandre Larmagnac[1], Niko Wenger[2], Pavel Musienko[2], Janos Vörös[1], Grégoire Courtine[2]

1 Laboratory of Biosensors and Bioelectronics, ETH Zurich, Switzerland
2 International Paraplegic Foundation Chair in Spinal Cord Repair, Center for Neuroprosthetics, EPFL, Switzerland

Electrical Stimulation of the Auditory Brainstem with a Flexible Polyimide Microelectrode Array 235

Amélie Guex[1], Rohit U. Verma[2], Ariel E. Hight[2], M. Christian Brown[2], Philippe Renaud[3], Daniel J. Lee[2], Stéphanie P. Lacour[1]

1 LSBI, Center for neuroprosthetics, EPFL, Lausanne, Switzerland
2 Eaton-Peabody Laboratories, Massachusetts Eye and Ear Infirmary, Boston, USA
3 LMIS4, STI, EPFL, Lausanne, Switzerland

PDMS Based µ-ECoG 237

Arthur Hirsch[1], Ivan Minev[1], Natalia Pavlova[2], Léonie Asboth[2], Grégoire Courtine[2], Stéphanie P. Lacour[1]

1 Laboratory for Soft Bioelectronic Interfaces, Centre for Neuroprosthetics, EPFL, Switzerland
2 UPCOURTINE, Brain Mind Institute, EPFL, Switzerland

MEA Technology

Oral Presentations 239

Keynote Lecture: Conducting Polymer Devices for In Vivo Electrophysiology....240

George G. Malliaras

Department of Bioelectronics, Ecole Nationale Supérieure des Mines, Gardanne, France

Oral Presentation: In-vitro Recordings of Electrogenic Cells Activity with Organic Field Effect Transistors....242

A. Spanu[1,2], S. Lai[1], P. Cosseddu[1], M. Tedesco[2], A.Bonfiglio[1,3], and S. Martinoia[2]

1 University of Cagliari – Dept. of Electrical and Electronic Engineering, Cagliari, Italy
2 University of Genova – Dept. of Informatics, Bioengineering, Robotics and System Engineering, Genova, Italy
3 CNR – Institute of Nanoscience, Modena, Italy

Oral Presentation: High-Density CMOS-based Microelectrode Array Platform for Large-Scale Neuronal Network Analysis....244

Jan Müller[1], Marco Ballini[1], Yihui Chen[1], Paolo Livi[1], Milos Radivojevic[1], Urs Frey[2], Douglas Bakkum[1] and Andreas Hierlemann[1]

1 ETH Zurich, Department of Biosystems Science and Engineering, Basel, Switzerland.
2 RIKEN Quantitative Biology Center, Kobe, Japan.

Oral Presentation: A Capacitively-Coupled CMOS-MEA with 4225 Recording Sites and 1024 Stimulation Sites....247

Gabriel Bertotti[1], Norman Dodel[1], Stefan Keil[1], Dirk Wolansky[2], Bernd Tillak[2], Matthias Schreiter[3], Max Eickenscheidt[4], Günther Zeck[4], Alfred Stett[4], Andreas Möller[5], Karl-Heinz Boven[5], and Roland Thewes[1]

1 TU Berlin, Faculty of EECS, Chair of Sensor and Actuator Systems, Berlin, Germany
2 IHP GmbH, Technology/Process Research, Frankfurt/Oder, Germany
3 Siemens AG, Corporate Technology, Research & Technology Center, Munich, Germany
4 NMI Natural and Medical Sciences Institute at the University of Tübingen, Neurochip Research Group, Reutlingen, Germany
5 Multi Channel Systems GmbH, Reutlingen, Germany

Oral Presentation: Electronic Motion Tracking of Single Migrating T Cells Using Field-Effect Transistor Arrays....251

Jessica Ka-Yan Law[1], Xuan-Thang Vu[1], Xiao Zhou[2], Saya Ri Heidingsfelder[1], Bin Qu[2], Markus Hoth[2], Sven Ingebrandt[1]

1 Department of Informatics & Microsystem Technology, University of Applied Sciences Kaiserslautern, Zweibrücken, Germany
2 Department of Biophysics, Saarland University, Homburg, Germany

Oral Presentation: Nano-Needle Gated Field Effect Transistor (NGFET) Array for Intracellular Recording and Stimulation of Neurons....255

Rao Rashmi B.[1], Singh Katyayani[1], Sikdar Sujit K.[2] and Bhat Navakanta[3]

1 Centre for Nano Science and Engineering
2 Molecular Biophysics Unit
3 Centre for Nano Science and Engineering & Electrical Communication Engineering, Indian Institute of Science, Bangalore, INDIA

Oral Presentation: Two-Chamber MEA to Unidirectionally Connect Neuronal Cultures....259

Joost le Feber[1,2], Wybren Postma[1], Wim Rutten[3], Eddy de Weerd[3], and Marcel Weusthof[1]

1 Biomedical Signals and Systems, University of Twente, Enschede, the Netherlands
2 Clinical Neurophysiology, University of Twente, Enschede, the Netherlands
3 Neural Engineering Dept./Biomedical Signals and Systems, University of Twente, Enschede , the Netherlands
4 BIOs-Lab on a Chip Group, University of Twente, Enschede, the Netherlands

MEA Technology

New Materials and Designs 263

Effect of Ion Sensitivity on Extracellular Recordings with Graphene Transistors 264
Lucas Hess, Martin Lottner, Michael Sejer Wismer, Jose A. Garrido
Walter Schottky Institut, Physik-Department, Technische Universität München, Germany

Boron Doped Diamond for Neural Stimulation or Recording 266
Fabien Sauter-Starace[1],Jean-LouisDivoux[2], Clément Herbert[3], Hugues Girard[3], Christine Mer[3], Philippe Bergonzo[3]
1 CEA LETI CLINATEC, Minatec Campus, Grenoble France
2 MXM Group,VALLAURIS, France
3 CEA-LIST, Diamond Sensors Laboratory, Gif-sur-Yvette, France

Impedance Considerations on MEA – the Effect of Electrode Materials and Coatings 268
Tomi Ryynänen[1], Manoj Sivasubramaniapandian[1], Marja Peltola[2], Susanna Narkilahti[2], Jukka Lekkala[1]
1 Department of Automation Science and Engineering and BioMediTech, Tampere University of Technology, Tampere, Finland
2 NeuroGroup, BioMediTech, University of Tampere, Tampere, Finland

Carbon Nanotube Multi-Electrode Array Chips for Noninvasive Real-Time Measurement of Dopamine, Action Potentials, and Postsynaptic Potentials 270
Mao Fukuda[1], Keiichi Shirakawa[1], Hideyasu Jiko[1], Ikuro Suzuki[2]
1 Alpha MED Scientific Inc., 209 Saito-incubator, 7-7-15 Saito-asagi, Ibaraki, Osaka, Japan
2 Graduate School of Bionics, Tokyo University of Technology, 1404-1 Katakura, Hachioji, Tokyo, Japan

Evaluation of Materials and Fabrication Techniques for Capacitive Electrodes 272
Sebastian Röhler[1], Claus J. Burkhardt[1], Dieter P. Kern[2], Alfred Stett[1]
1 NMI Natural and Medical Sciences Institute at the University of Tübingen, Reutlingen, Germany
2 Institute of Applied Physics, University of Tübingen, Tübingen, Germany

Chemical Vapor Deposition Grown Carbon Nanotubes on Recessed Contacts of Flexible Polyimide MEAs 274
Kerstin Schneider[1], Boris Stamm[2], Katja Gutöhrlein[2], Claus Burkhardt[2], Alfred Stett[2] and Dieter P. Kern[1]
1 Institute for Applied Physics, University of Tübingen, Tübingen, Germany
2 NMI Natural and Medical Sciences Institute at the University of Tübingen, Reutlingen, Germany

Diamond-Based Platforms for Long-Term Growth and Investigation of Neurons 276
Alexandra Voss[1], Hongying Wei[2], Maria Giese[2], Monika Stengl[2], Johann Peter Reithmaier[1], Cyril Popov[1]
1 Institute of Nanostructure Technologies and Analytics, CINSAT, University of Kassel, Germany
2 Department of Animal Physiology, CINSAT, University of Kassel, Germany

Cost-Effective Technique to Create CNTs Layers Enhancing Neuronal Network Development and Activity 278
Amélie Béduer[1], Arushi Varshney[1], Emmanuel Flahaut[2], Marc Heuschkel[3], Philippe Renaud[1]
1 Microsystems Laboratory, Ecole Polytechnique Fédérale de Lausanne (EPFL), Lausanne, Switzerland
2 University of Toulouse; UPS, INP; Institut Carnot Cirimat, Toulouse, France
3 Qwane Biosciences SA, EPFL Innovation Park, Lausanne, Switzerland

A Novel 3D Microelectrode Array for Extracellular Signal Recording of Acute Brain Slices 280
Carolin K. Kleber, Manuel Martina, Claus J. Burkhardt, Elke Guenther, Udo Kraushaar
NMI Natural and Medical Sciences Institute at the University of Tübingen, Reutlingen, Germany

Realisation of Co-Culture MEA Biochips Using a Novel SU-8 Fabrication Processfor Applications in Axonal and Synaptic Biology 282
Marc Heuschkel, Nader Jedidi, Solomzi Makohliso
Qwane Biosciences SA, EPFL Innovation Park, Building C, Lausanne, Switzerland

Advances in Diamond Microelectrode Arrays 284
T. Conte[1,2], Z. Gao[1], J.B. Destro-Filho[2], V. Carabelli[3], E. Carbone[3] and A. Pasquarelli[1]
1 Institute of Electron Devices and Circuit, Ulm University, Ulm, Germany
2 School of Electrical Engineering, Federal University of Uberlandia, Brazil
3 Department of Drug Science, NIS Centre, CNISM, University of Torino, Torino, Italy

Towards Stretchable High-Density Multielectrode Arrays 286
Flurin Stauffer[1], Vincent Martinez[1], Mohammed Adagunodo[2], Janos Vörös[1], Alexandre Larmagnac[1]
1 Laboratory of Biosensors and Bioelectronics, ETH Zurich, Switzerland
2 Faculty of Medicine, Biomedical Engineering, University of Bern, Switzerland

Towards Local Chemical Stimulation Through a Nanopore Array on a Microelectrode Array 287
Peter D. Jones, Paolo Cesare, and Martin Stelzle
NMI Natural and Medical Sciences Institute at the University of Tübingen, Reutlingen, Germany

Polymer-Based In Vivo Transducers with Conductive Polymer Mixture Polydimethylsiloxane Composite Electrodes 289
Asiyeh Golabchi, Rouhollah Habibey, Marina Nanni, Francesca Succol, Axel Blau
Fondazione Istituto Italiano di Tecnologia (IIT), Dept. of Neuroscience and Brain Technologies (NBT), Neurotechnologies (NTech), Genoa, Italy, www.iit.it

Nanostructured Diamond Microelectrode Arrays for Neural Recording and Stimulation 291
Gaëlle Piret[1,2], Clément Hébert[3], Lionel Rousseau[4], Emmanuel Scorsone[3], Raphaël Kiran[3], Myline Cottance[4], Gaëlle Lissorgues[4], Marc Heuschkel[5], Serge Picaud[6], Blaise Yvert[1,2], Philippe Bergonzo[3]
1 INSERM, Clinatec, U1167, Grenoble, France
2 CEA-Léti, Clinatec, U1167, Grenoble, France
3 CEA LIST, Diamond Sensors Laboratory, Gif-sur-Yvette, France
4 Université Paris-Est, ESYCOM, ESIEE Paris, Noisy le Grand, France
5 Qwane Biosciences SA, EPFL Innovation Park, Lausanne, Switzerland
6 Institut de la Vision, UMRS 968 Inserm/UPMC, UMR7210 CNRS, Paris, France

New Developments on the Fabrication of High Density and Low Density Diamond-Based MEA 293
A. Battiato[1,2,4], E. Bernardi[1,2,4], V. Carabelli[3,4], E. Carbone[3,4], S. Gosso[3,4], P. Olivero[1,2,4], A. Pasquarelli[5], F. Picollo[2,1,4]
1 Physics Department and NIS Inter-departmental Centre, University of Torino, Torino, Italy
2 INFN section of Torino, Torino, Italy
3 Department of Drug Science and Technology and NIS Inter-departmental Centre ,University of Torino, Torino, Italy
4 Consorzio Nazionale Inter-universitario per le Scienze fisiche della Materia (CNISM), Section of Torino
5 Institute of Electron Devices and Circuits, Ulm University, Ulm, Germany

Graphene and Silicon-Nanowire Field Effect Transistors for Neuronal Interfacing 295
Farida Veliev[1], Anne Briancon-Marjolet[2], Mireille Albrieux[3], Dipankar Kalita[1], Antoine Bourrier[1], Zheng Han[1], Vincent Bouchiat[1], Cécile Delacour[1]
1 Institut Néel, Grenoble France
2 Laboratoire HP2, UJF-INSERM U1042, Grenoble, France
3 Grenoble Institut des Neurosciences, Inserm, Univ. Joseph Fourier, Grenoble, France

MEA Technology

Advances in Fabrication and Instrumentation 297

A CMOS-based Microelectrode Array System for Stimulation and Recording in Neural Preparations In Vitro 298
Takashi Tateno
Graduate School of Information Science and Technology, Hokkaido University, Sapporo, Japan

A Novell LabVIEWTM based Multi-Channel Closed- Loop Stimulator 300
Christiane Thielemann, Maike Stern, Christoph Nick and Robert Bestel
University of Applied Sciences Aschaffenburg, BioMEMS lab, Germany

An Automated Method for Characterizing Electrode properties of High-Density Microelectrode Arrays 302
Vijay Viswam[1], David Jäckel[1], Marco Ballini[1], Jan Müller[1], Milos Radivojevic[1], Urs Frey[2], Felix Franke[1], Andreas Hierlemann[1]
1. ETH Zürich, Bio Engineering Laboratory, D-BSSE, Basel, Switzerland
2. RIKEN Quantitative Biology Center, Kobe, Japan

3D Electrodes for In-Cell Recording: Electrogenic Cell Membrane Deformation and Seal Resistance Estimation 304
Francesca Santoro, Jan Schnitker, Sabrina Ullmann, Andreas Offenhäusser
CS-8/PGI-8 Institute of Bioelectronics, Forschungszentrum Jülich, Germany

A Benchtop Device for Prolonged Experiments with Microelectrode Arrays 306
Regalia Giulia[1], Achilli Silvia[1], Biffi Emilia[2], Menegon Andrea[3], Ferrigno Giancarlo[1], Pedrocchi Alessandra[1]
1 Electronics, Information and Bioengineering Department, Politecnico di Milano, Milan, Italy
2 Bioengineering Laboratory, Scientific Institute IRCCS Eugenio Medea, Bosisio Parini, Italy
3 Advanced Light and Electron Microscopy Bio-Imaging Centre, San Raffaele Scientific Institute, Milan, Italy

Development of a Stand-alone Integrated MEA Biochip System for Chronic Recordings 308
Paolo De Pasquale[1,2], Antonin Sandoz[1], Igor Charvet[1], Philippe Passeraub[1], Michela Chiappalone[2], Luc Stoppini[1]
1 Hepia, HES-SO Geneva, Switzerland
2 Istituto Italiano di Tecnologia (IIT), Genova, Italy

3D Multi Electrode Arrays 310
Martin Baca[1], Heike Bartsch[2], Tom Porzig[2], Adam Williamson[1], Andreas Schober[1]
1 FG Nanobiosystemtechnik, Technische Universität Ilmenau (TUI), Germany
2 FG Elektroniktechnologie, Technische Universität Ilmenau (TUI), Germany

The Influence of Medium Conductivity on Cellular Impedance Measurements with Field-Effect Transistor Arrays 312
Felix Hempel, Nathalie Bernhard, Jessica Ka-Yan Law, Anna Susloparova, Dieter Koppenhöfer, Xuan-Thang Vu and Sven Ingebrandt
Department of Informatics & Microsystem Technology, University of Applied Sciences Kaiserslautern, Zweibruecken, Germany

Organic Field-Effect Transistor Arrays as a Possible Low-Cost Alternative for In-Vitro Monitoring of Different Cell Cultures 314

Lotta Emilia Delle[1], Anna Susloparova[1], Xuan Thang Vu[1,2], Olga Fominov[1], Felix Hempel[1], Jessica Ka-Yan Law[1], Sven Ingebrandt[1]

1 Department of Informatics & Microsystem Technology, University of Applied Sciences Kaiserslautern, Zweibruecken, Germany
2 Present address: Department of Physics IA, RWTH Aachen University, Aachen, Germany

Oriented Cortical Networks in Polydimethylsiloxane Microchannel Scaffolds for Recordings from Network Modules and Individual Connections 316

Rouhollah Habibey, Asiyeh Golabchi, Anilkrishna Konduri, Marina Nanni, Francesco Difato, Axel Blau

Fondazione Istituto Italiano di Tecnologia (IIT), Dept. of Neuroscience and Brain Technologies (NBT), Genoa, Italy, www.iit.it

A Microfluidic Device for Selective Positioning of Invertebrate Neurons 318

Katharina Krumpholz[1], Akram El Hasni[2], Andreas Neuhof[1], Rudolf Degen[1], Uwe Schnakenberg[2], Peter Bräunig[1], Katrin Bui-Göbbels[1]

1 RWTH Aachen University, Institute of Biology II, Aachen, Germany
2 RWTH Aachen University, Institute of Materials in Electrical Engineering (IWE 1), Aachen, Germany

Amplifier ASIC for Real 3D-Multichannel-MEA 320

Thomas Just, Peter Husar

Technische Universität Ilmenau, Germany

Simultaneous Electrical Investigation of Isolated Neurites Using a Neurite-Isolation Device as Neurite Regeneration Model 322

Johann K. Mika[1], Karin Schwarz[2], Heinz Wanzenböck[1], Petra Scholze[2], Emmerich Bertagnolli[1]

1 Institute of Solid State Electronics, Vienna University of Technology, Vienna, Austria
2 Center for Brain Research, Medical University of Vienna, Vienna, Austria

Ultra-Low Cost Arrays of Printed Carbon Electrodes for Extracellular Recordings 324

Jan Schnitker, Alexey Yakushenko, Francesca Santoro, Fabian Brings, Bernhard Wolfrum, Andreas Offenhäusser

ICS-8/PGI-8 Institute of Bioelectronics, Forschungszentrum Jülich, Germany

Stimulation Artifact Suppression Techniques for High-Density Microelectrode Arrays 326

A.Shadmani, J. Müller, P. Livi, M. Ballini, Y Chen, A. Hierlemann

ETH Zürich, Department of Biosystems Science and Engineering, Basel, Switzerland

Large-Area, High-Density Arrays of Micro-Needles for Acute Slice Electrophysiology 328

D.E. Gunning[1], P. Hottowy[2], W. Dabrowski[2], A. Sher[3], J.M. Beggs[4], C.J. Kenney[5], D.A. Young[1], A.M. Litke[3] and K. Mathieson[1]

1 Institute of Photonics, SUPA, University of Strathclyde, Glasgow, UK
2 AGH University of Science and Technology, Krakow, Poland
3 SCIPP, University of California Santa Cruz, Santa Cruz, California, USA
4 Biocomplexity Institute, Indiana University, Bloomington, Indiana, USA
5 SLAC National Accelerator Laboratory, Menlo Park, California, USA

A Hybrid Multi Optrode Electrode Array for Optogenetics 330

Luis Hoffman[1], Alexandru Andrei[1], Robert Puers[1,2], George Gielen[1,2], Dries Braeken[1]

1 Imec, Leuven, Belgium
2 ESAT, KULeuven, Leuven, Belgium

Image Processing Based Quantitative Analysis of MEA Cultured Neurons 332

João Fernando Mari[1,2], José Hiroki Saito[2,3], Amanda Ferreira Neves[5], Celina Monteiro da Cruz Lotufo[4], João-Batista Destro-Filho[4,] Alberto Pasquarelli[6]

1 Universidade Federal de Viçosa, Campus Rio Paranaíba, Brazil
2 Department of Computer Science, Federal University of São Carlos, Brazil
3 Faculty of Campo Limpo Paulista, Brazil
4 Federal University of Uberlândia, Campus Santa Mônica, Brazil
5 Department of Structural and Functional Biology, University of Campinas, Brazil
6 University of Ulm, Germany

MEA Technology

Culture Techniques 334

Long-Term Cultivation and Recording from Organotypic Brain Slices on High-density Micro-electrode Arrays 335

Wei Gong[1], David Jäckel[1], Jan Müller[1], Michele Fiscella[1], Milos Radivojevic[1], Douglas Bakkum[1], Felix Franke[1], Frederic Knoflach[2], Beat Gähwiler[3], Branka Roscic[1], Thomas Russell[1], Andreas Hierlemann[1]

1 Bio Engineering Laboratory, D-BSSE, ETH Zürich, Basel, Switzerland
2 F. Hoffmann-La Roche, Basel, Switzerland
3 University of Zürich, Brain Research Institute, Zürich, Switzerland

Four-Layer Closed-Loop Neuronal Networks 337

Gregory J. Brewer[1], Liangbin Pan[2], Sankaraleengam Alagapan[2], Eric Franca[2], Thomas De- Marse[2], Bruce C. Wheeler[2]

1 University of California Irvine, USA
2 University of Florida, Gainesville, FL USA

3D Neural Networks Coupled to Planar Microtransducer Arrays: An Innovative In-Vitro Experimental Model for Investigating Network Dynamics 339

Monica Frega[1], Mariateresa Tedesco[1], Paolo Massobrio[1], Mattia Pesce[2], Sergio Martinoia[1]

1 Neuroengineering and Bio-nano Technology Group (NBT), Department of Informatics Bioengineering Robotics and System Engineering, University of Genova, Genova, Italy
2 Department of Neuroscience and Brain Technologies, Italian Institute of Technology (IIT), Genova, Italy

Directed Neuronal Networks on Multi-Electrode Arrays 341

László Demkó, Csaba Forró, Harald Dermutz, János Vörös

Laboratory of Biosensors and Bioelectronics, Institute for Biomedical Engineering, ETH Zurich, Switzerland

Human Pluripotent Stem Cell Derived Neural Cells Obtained Either Using Adherent or Neurosphere Based Differentiation Have Ability to Form Spontaneously Active Neuronal Networks 342

Tiina Joki[1], Pauliina Salonen[2], Tarja Toimela[2], Riikka Äänismaa[1], Timo Ylikomi[2], Susanna Narkilahti[1]

1 NeuroGroup, BioMediTech, University of Tampere, Tampere, Finland
2 Finnish Centre for Alternative Methods (FICAM), University of Tampere, Tampere, Finland

Design and Fabrication of a Second-Generation Perfusion Cap for Enhanced Optical Access and Manipulation of Cell Cultures 344

Anil Krishna Konduri[1], Dirk Saalfrank[2], Rouhollah Habibey[1], Asiyeh Golabchi[1], Marina Nanni[1], Axel Blau[1]

1. Dept. of Neuroscience and Brain Technologies (NBT), the Italian Institute of Technology (IIT), Genoa, Italy, www.iit.it
2. Dept. of Informatics and Microsystem Technology, University of Applied Sciences Kaiserslautern, Zweibrücken, Germany, www.fh-kl.de

Primary and Stem-Cell Derived Cardiac Myocyte Cultures ____ 346

Keynote Lecture: Combined MEA Recording and Ca-Ratiometry in hiPSC-Derived Cardiomyocytes for Cardiac Safety Assessment 347

Georg Rast

Drug Discovery Support, Boehringer Ingelheim Pharma GmbH & Co. KG, Biberach an der Riss, Germany

Oral Presentation: Human Stem-Cell Derived Neuronal Cell Based In Vitro Platforms for Neurotoxicity and Disease Modelling 348

Susanna Narkilahti

NeuroGroup, BioMediTech, University of Tampere, Tampere, Finland

Comparative Assessment of Different Types of Human Stem Cell Derived Cardiomyocytes for Predictive Electrophysiological Safety Screening - Using Microelectrode Arrays (MEA) 351

Udo Kraushaar[1], Dietmar Hess[3], Hua Rong Lu[2], David Gallacher[2] and Elke Guenther[1]

1 NMI Natural and Medical Sciences Institute at the University of Tübingen, Reutlingen, Germany
2 Janssen Pharmaceutica NV, Beerse, Belgium
3 NMI-TT GmbH, Reutlingen, Germany

On-Chip Measuring of Drug-Induced Cardiac Action Potential Elongation of Single Cells with Patch Clamp Resolution 352

Danny Jans, Ben Huybrechts, Simon Schaerlaeken, Andim Stassen, Luis Hoffman, Jordi Cools, Geert Callewaert, Dries Braeken

imec, Leuven, Belgium

Pharmacological Response of a Human Induced Pluripotent Stem Cell-Derived Neuron and Astrocyte Co-Culture 354

Aoi Odawara[1,3], Masao Gotoh[1], Ikuro Suzuki[2]

1 School of Bioscience and Biotechnology, Tokyo University of Technology, Hachioji, Tokyo, Japan
2 Department of Electronics and Intelligent Systems, Tohoku Institute of Technology, Japan
3 Japan Society for the Promotion of Science, Tokyo, Japan

Human Embryonic and Induced Pluripotent Stem Cells Form Functional Neuronal Networks in MEA 356

Ylä-Outinen Laura, Hannuksela Eija, Narkilahti Susanna

NeuroGroup, BioMediTech, University of Tampere, Tampere, Finland

A Novel AFM-Based Technique for Measuring Coupled Phenomena in Cardiac Myocytes 358

Caluori Guido, Andrade_Caicedo Henry [1,2], Tedesco Mariateresa[1], Raiteri Roberto[1]

1 Department of Informatics Bioengineering and Systems Engineering, Università di Genova, Genova, Italy
2 Centro de Bioingeniería; Universidad Pontificia Bolivariana, Medellín, Colombia

Author Index ____ 361

1st Tübingen Symposium on Current Topics in Neurotechnology- from Basic Research to Medical Application

Brain-Machine-Interfaces (BMI) in Paralysis and Behavioral Disorders

N. Birbaumer[1,2,3], G. Gallegos-Ayala[1], R. Sitaram[4], U. Chaudhary[1], S. Soekadar[1], A. Ramos-Murguialday[1,5]

1 Institute of Medical Psychology and Behavioral Neurobiology, University of Tuebingen, Tuebingen, Germany
2 Ospedale San Camillo, IRCCS, Istituto di Ricovero e Cura a Carattere Scientifico, Venezia – Lido, Italy
3 Institute for Diabetes Research and Metabolic Diseases of the Helmholtz Center Munich at the University of Tübingen, Tübingen, Germany and German Center for Diabetes Research (DZDe.V.), Neuherberg, Germany
4 Department of Biomedical Engineering, University of Florida, Gainesville, FL, USA
5 Health Technologies Department, TECNALIA, Mikeletegi Pasalekua 1, 20009 San Sebastian, Spain

Abstract

Results from three applications of BMIs are described and their scientific, clinical and societal impact evaluated.
(1) BMIs for brain-communication in the locked-in patients
(2) BMIs as a rehabilitation modality for severe chronic stroke
(3) BMI-metabolic fMRI-neurofeedback in neuropsychiatric disorders

1 BMIs for brain-communication in the locked-in patients

BMIs using EEG, implanted Electrocorticogram (ECoG) were used extensively for brain communication in patients with severe paralysis, mainly amyotrophic lateral sclerosis (ALS). Up to the locked-in (LI) stage different types of EEG-ECoG-BMIs were used successfully to select letters or answers with brain oscillations (mainly sensorimotor rhythm, SMR) or cognitive event-related potentials from a computer menue. However, attempts to use BMI in the completely locked-in-syndrome (CLIS) were largely unsuccessful despite intensive research efforts. The first successful attempt in a CLIS patient using near-infrared-spectroscopy (NIRS) BMI-systems will be described (Gallegos-Ayala et al 2014).

2 BMIs as a rehabilitation modality for severe chronic stroke

A controlled outcome study of severe chronic stroke patients without residual hand mobility and without any available treatment modality left was recently published by this group (Ramos et al 2013) using a non-invasive extensive BMI-training with a neuroprosthetic device driven by sensorimotor brain oscillations (SMR) provides the first evidence of the clinical usefulness of BMI in this patient group. Reasons for this successful behavioral change and productive brain reorganization are presented and the necessity of future invasive BMI based on direct recordings from motor neurons comparable to those of Hochberg et al (2006, 2012) presented here by J. Donoghue in severe chronic stroke is emphasized.

3 BMI-metabolic fMRI-neurofeedback in neuropsychiatric disorders

Neurofeedback of EEG oscillations was used as a behavioral training-approach with considerable success in attentional disorders and epilepsy. Recently real-time-functional magnetic resonance (rt-fMRI) neurofeedback was developed by the Tuebingen group and tested in several neuropsychiatric disorders such as psychopathy, addiction, schizophrenia, obsessive-compulsive disorder and obesity (see Birbaumer et al 2013 for a review). Rt-fMRI-neurofeedback allows self-regulation of circumscribed well-defined cortical and subcortical brain systems and their connectivity. Some recent results in addiction are reported and the problem of brain-behavior associations related to BMI-training discussed.

Acknowledgement

Supported by Deutsche Forschungsgemeinschaft DFG (Koselleck BI 195/69-1), German Federal Ministry of Education and Research (BMBF) to the German Center for Diabetes Research (DZDe.V.,01GI0925), VW, Baden-Württemberg Stiftung, EU-FP7 and HORIZON 2020 (WAY, BRAINTRAIN, ERC to Rosenstiel & Birbaumer), CIN, FORTUNE (Faculty of Medicine, Univ. of Tuebingen).

Combination of brain-machine interfaces and non-invasive brain stimulation - from basic science to clinical applications

S. R. Soekadar[1,2*], Matthias Witkowski[1,2], Niels Birbaumer[2,3,4]

[1] University Hospital of Tübingen, Applied Neurotechnology Lab, Department of Psychiatry and Psychotherapy, Tübingen
[2] Institute of Medical Psychology and Behavioral Neurobiology, University of Tübingen, Tübingen, Germany
[3] Ospedale San Camillo, IRCCS, Istituto di Ricovero e Cura a Carattere Scientifico, Venezia – Lido, Italy
[4] Institute for Diabetes Research and Metabolic Diseases of the Helmholtz Center Munich at the University of Tübingen, Tübingen, Germany and German Center for Diabetes Research (DZDe.V.), Neuherberg, Germany
* Corresponding author. E-mail address: surjo.soekadar@uni-tuebingen.de

Abstract
Brain-machine interfaces (BMI) translate electric, magnetic or metabolic brain activity into control signals of external devices or machines, and allow restoration of communication or versatile control of prosthetic limbs or robots. By providing contingent feedback of brain activity, BMI systems can be used as training tools to augment these activities resulting in recovery of brain function. However, learning to control BMI systems can be cumbersome, particularly for individuals with brain lesions. Also, most BMI systems use sensory feedback for operant conditioning of BMI control-related brain activity, but do not provide a direct bidirectional link independent of afferent pathways. Based on previous work showing that non-invasive brain stimulation (NIBS) can improve learning while allowing for direct modulation of brain activity, the combination of NIBS and BMI seemed particularly desirable. Here we present the most recent technological advances developed in a collaborative research effort between the National Institutes of Health (USA) and the University of Tübingen that have successfully established combined NIBS and BMI. Different stimulation paradigms and recording methods, e.g. magnetoencephalography (MEG), electroencephalography (EEG) or functional near-infrared spectroscopy (NIRS), will be introduced and their clinical applications in neurological and psychiatric disorders described. Finally, current challenges and future developments will be discussed.

1 Introduction

While it was known for centuries that application of electric currents to the brain can regulate mood, cognition and behavior, the relevance of brain stimulation for both, basic and clinical science has substantially increased in the last two decades. Supported by the recent development of tools allowing systematic investigation of the physiological basis of such brain stimulation effects, its recent success may also relate to the potential specificity and immediacy of the intervention compared to other, e.g. pharmacological approaches. Besides invasive stimulation techniques, such as deep brain stimulation (DBS) or motor cortex stimulation (MCS), non-invasive brain stimulation (NIBS), including transcranial magnetic stimulation (TMS) and transcranial direct current stimulation (tDCS) are increasingly used. For instance, it was shown that tDCS, i.e. the application of weak transcranial direct currents at intensities of 1-2mA, can improve learning and skill consolidation throughout different domains. Moreover, when applied over the ipsilesional motor cortex of chronic stroke patients, reaction time and pinch force of the affected hand increased. However, simultaneous application of electric currents to the head during assessment of electric or magnetic brain oscillations was considered unfeasible due to stimulation artifacts. Recently, we overcame this limitation and established various paradigms allowing for combined application of transcranial electric currents during BMI control.

2. Combination of BMI and brain stimulation

In a first study conducted at the National Institute of Neurological Disorders and Stroke (NINDS, NIH, USA), it was investigated whether application of tDCS over the primary motor cortex (M1) can regulate the ability to control sensorimotor rhythms (SMR, 8-15Hz) used to control an orthotic device. 30 participants received either anodal, cathodal or sham stimulation prior to a daily BMI training performed over one week. At the end of the training, BMI control of participants who received anodal stimulation was superior to those who trained under cathodal stimulation. One month after the end of training, BMI control was still better in the group that received anodal stimulation compared to the other groups [1].

As several studies indicated that timing of stimulation relative to training can influence the stimulation effect, development of new strategies allowing simultaneous or brain state-dependent stimulation promises

to improve applicability and effectiveness of BMI training protocols.

Recently, feasibility of simultaneous tDCS during EEG-based BMI control was demonstrated and its limitations outlined [2]. While use of EEG limits the possibility to reconstruct brain activity of regions immediately underneath the stimulation electrode, another strategy recently introduced by the same group allows for *in vivo* assessment of neuromagnetic brain oscillations of brain regions directly below the stimulation electrode [3].

Using this paradigm, Soekadar et al. [4] showed for the first time that a chronic stroke patient without residual finger movements can utilize SMR of the M1 hand knob to control an orthotic device to perform grasping motions while this region, the ipsilesional M1, underwent anodal tDCS (Figure 1).

This new strategy may lead to the refinement of existing stimulation protocols and to a better understanding of the relationship between brain physiology, cognition and behavior, particularly in individuals with neurological and psychiatric disorders.

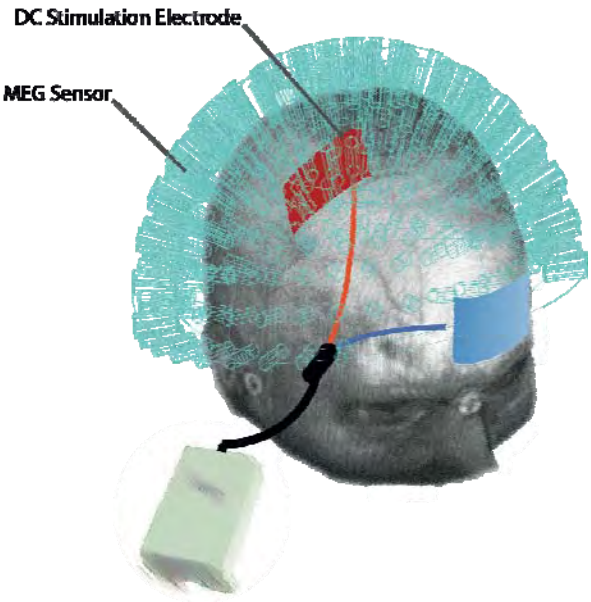

Fig. 1. Illustration of simultaneous electric brain stimulation during *in vivo* assessment of neuromagnetic brain oscillations using whole-head magnetoencephalography (MEG) [2]. As neuromagnetic brain activity passes through the stimulation electrodes, reconstruction of cortical activity of brain areas immediately below the stimulation electrode is possible.

3 Conclusion

Systems that combine BMI with direct, frequency tuned or brain-state dependent electric brain stimulation are novel and powerful tools to investigate the link between neurophysiology, brain function and behavior. Besides fostering neuroplasticity in the context of BMI training paradigms, this combination can provide direct bi-directional brain-machine interaction independent of afferent pathways, and thus become an effective novel treatment approach for various neurological and psychiatric disorders.

Acknowledgement

Supported by Deutsche Forschungsgemeinschaft DFG (Koselleck BI 195/69-1, NIH-DFG Research Career Transition Award to SRS, SO932-2), German Federal Ministry of Education and Research (BMBF, grant number 01GQ0831, 16SV5838K), the BMBF to the German Center for Diabetes Research (DZDe.V., grand number 01GI0925), VW, Baden-Württemberg Stiftung, EU-FP7 and HORIZON 2020 (WAY, grant number 288551, BRAINTRAIN, ERC to Rosenstiel & Birbaumer), CIN and FORTUNE (Faculty of Medicine, University of Tübingen).

References

[1] Soekadar SR, Witkowski M, Garcia-Cossio E, Birbaumer N, Cohen LG (2014b) Learned EEG-based brain self-regulation of motor-related oscillations during application of transcranial electric brain stimulation: feasibility and limitations. Front Behav Neurosci 8:93

[2] Soekadar SR, Witkowski M, Garcia-Cossio E, Birbaumer N, Robinson SE, Cohen LG (2013a) In vivo assessment of human brain oscillations during application of transcranial electric currents. Nature Communications 4:2032

[3] Soekadar SR, Witkowski M, Robinson SE, Birbaumer N (2013b) Combining electric brain stimulation and source-based brain-machine interface (BMI) training in neurorehabilitation of chronic stroke. Journal of the Neurological Sciences 333-e542

Pharmaco-TMS-EEG: A Novel Approach for Probing GABAergic Activity in Human Cortex

Ulf Ziemann, Isabella Premoli, Florian Müller-Dahlhaus

Dept. Neurology & Stroke, and Hertie Institute for Clinical Brain Research, University of Tübingen, Germany

Abstract

TMS-EEG, i.e. the combination of transcranial magnetic stimulation (TMS) with electroencephalography (EEG) has only recently become available because TMS-compatible EEG amplifiers had to be developed. TMS-EEG allows for recording responses directly from the brain to highly synchronized input by TMS. This is a major advance compared to conventional electromyographic (EMG) recording of muscle responses elicited by TMS of motor cortex (TMS-EMG). TMS-EEG reveals a number of TMS-evoked EEG responses (TEPs) that may represent brain excitability and connectivity, but much of the underlying physiology is still unknown. This talk will give an introduction into this novel technique and, in addition, will present some very recent data from our group where TMS-EEG was combined with pharmacology to characterize the pharmaco-physiology of TEPs.

1 Background / Aims

Combining transcranial magnetic stimulation (TMS) and electroencephalography (EEG) constitutes a powerful tool to directly assess human cortical excitability and connectivity (Ilmoniemi et al., 1997; Ilmoniemi and Kicic, 2010; Ziemann, 2011). TMS of the primary motor cortex elicits a sequence of TMS-evoked EEG potentials (TEPs) (Bonato et al., 2006). It is currently speculated that inhibitory neurotransmission through gamma-amino butyric acid type A receptors (GABAARs) modulates early TEPs (< 50ms after TMS), whereas gamma-amino butyric acid type B receptors (GABABRs) play a role for later TEPs (at around 100ms after TMS) (Rogasch and Fitzgerald, 2013). However, the physiological underpinnings of TEPs have not been directly tested yet.

2 Methods / Statistics

In a recent series of experiments (Premoli et al., 2014) we have studied the role of GABAAR/GABABR activation for TEPs in healthy subjects using a pharmaco-TMS-EEG approach. We tested the effects of a single oral dose of alprazolam or diazepam (classical benzodiazepines acting as allosteric positive modulators at α1-, α2-, α3- and α5-subunit-containing GABAARs), zolpidem (a hypnotic acting as positive modulator with high affinity at the α1-GABAAR), and baclofen (a GABABR agonist) on TEP amplitudes in double-blinded, placebo-controlled, crossover studies.

3 Results

Alprazolam and diazepam increased the amplitude of the negative potential at 45ms after stimulation (N45) and decreased the negative component at 100ms (N100), whereas zolpidem increased the N45 only. In contrast, baclofen specifically increased the N100 amplitude.

4 Conclusion/Summary

In conclusion, pharmaco-TMS-EEG allows study of the effects of CNS-active drugs directly on cortical activity. Findings demonstrate a differential effect of GABAAergic versus GABABergic neurotransmission on specific TEP components. Therefore, TMS-EEG may be used to study GABAAergic and GABABergic inhibition in neurological and psychiatric disorders, in which abnormal cortical inhibition has been implicated in the pathophysiology, such as epilepsy or schizophrenia. In addition, pharmaco-TMS-EEG offers the opportunity to study the actions of CNS-active drugs on human cortex in greater detail than it is hitherto possible with TMS or EEG alone. Future studies will have to address systematically the effects of other neurotransmitter systems (glutamate, dopamine, norepinephrine, serotonin, acetylcholine) on TEPs.

References

[1] Bonato C, Miniussi C, Rossini PM (2006) Transcranial magnetic stimulation and cortical evoked potentials: a TMS/EEG co-registration study. Clin Neurophysiol 117:1699-1707.

[2] Ilmoniemi RJ, Kicic D (2010) Methodology for combined TMS and EEG. Brain topography 22: 233-248.

[3] Ilmoniemi RJ, Virtanen J, Ruohonen J, Karhu J, Aronen HJ, Naatanen R, Katila T (1997) Neuronal responses to magnetic stimulation reveal cortical reactivity and connectivity. Neuroreport 8:3537-3540.

[4] Premoli I, Castellanos N, Rivolta D, Belardinelli P, Bajo R, Zipser C, Espenhahn S, Heidegger T, Müller-Dahlhaus F, Ziemann U (2014) TMS-EEG signatures of GABAergic neurotransmission in the human cortex. J Neurosci 34:5603–5612.

[5] Rogasch NC, Fitzgerald PB (2013) Assessing cortical network properties using TMS-EEG. Human brain mapping 34:1652-1669.

[6] Ziemann U (2011) Transcranial Magnetic Stimulation at the Interface with Other Techniques: A Powerful Tool for Studying the Human Cortex. The Neuroscientist: a review journal bringing neurobiology, neurology and psychiatry 17:368 - 381.

Near-Infrared Spectroscopy (NIRS) - a Promising Tool for Neurofeedback

Andreas J. Fallgatter, Beatrix Barth, Ann-Christine Ehlis

Dept. of Psychiatry, University of Tübingen, Germany

Abstract
Pharmacotherapy, mainly with stimulants and supplemented with psychotherapy are the standard therapies of ADHD in childhood and adulthood. As many patients don't accept pharmacotherapy for a sufficient time and in an adequate dose, alternative treatment starategies are urgently needed. In this respect, the development of neurofeedback training protocols in order to improve altered brain function in ADHD are proposed. In this talk the current status of NIRS-based neurofeedback protocols in our research group will be presented.

1 Backround / Aims

Hypofrontality, a decrease in frontal lobe activity that is associated with a number of clinical symptoms and psychiatric disorders, has been demonstrated in a wide range of fNIRS studies with psychiatric patients, and in particular in patients with ADHD. In more detail, dysfunctions of lateral prefrontal brain regions have been described in groups of ADHD patients during tasks probing working memory, response inhibition, word fluency and delay discounting. These findings from brain imaging may be used to directly identify hypofunctional brain regions underlying a disorder like ADHD and, in a second step, to specifically increase this brain function. This can be done by transforming this brain activity in a visible signal, e.g. an aeroplane flying on a computer screen, and allowing the subject to modulate the brain activity, e.g. by increasing the height of the aeroplane on the screen. This strategy is called neurofeedback.

2 Methods / Statistics

Based on such findings.Functional Near-Infrared Spectroscopy (fNIRS) can be used for an in-vivo assessment of activation changes in brain tissue. Due to its simple and quick applicability as well as the absence of side effects, fNIRS is particularly well tolerated by psychiatric patients and can hence markedly contribute to the understanding of the neurobiological basis of psychiatric disorders. Validity and reliability of fNIRS measurements to assess task-related cognitive activation have been repeatedly confirmed among healthy subjects.

3 Results

Beyond that, the application of fNIRS in order to detect altered cortical oxygenation in psychiatric patients during cognitive tasks has been highly intensified over the last two decades. Despite these encouraging findings in ADHD and the variety of beneficial properties of the method, the most apparent disadvantages of NIRS compared to other imaging techniques are its limited spatial as well as depth resolution and its restriction to cortical areas. Preliminary results for the application of NIRS as a neurofeedback method in children and adults with ADHD are shown. Advantages and disadvantages compared to other neurofeedback technologies like EEG or fMRI are discussed.

4 Conclusion/Summary

Further technical development and a broadened implementation are necessary in order to develop NIRS neurofeedback as an alternative or additional treatment option for ADHD,

References

[1] Ehlis, A.-C., Schneider, S., Dresler, T., Fallgatter, A.J. Application of functional near-infrared spectroscopy in psychiatry. In press: NeuroImage
[2] Haeussinger, F.B., Dresler, T., Heinzel, S., Schecklmann, M., Fallgatter, A.J., Ehlis, A.-C. Reconstructing functional near-infrared spectroscopy (fNIRS) signals impaired by extra-cranial confounds: An easy-to-use filter method. In press: Neuroimage
[3] Heinzel, S., Haeussinger, F.B., Hahn, T., Ehlis, A.-C., Plichta, M.M., Fallgatter, A.J. Variability of (functional) hemodynamics as measured with simultaneous fNIRS and fMRI. In press: Neuroimage
[3] Rea, M., Rana, M., Lugato, N., Terekhin, P., Gizzi, L., Brötz, D., Fallgatter, A., Birbaumer, N., Sitaram, R., Caria, A. Lower limb movement preparation in chronic stroke: towards anfNIRS-BCI for gait rehabilitation. In press: Neurorehabilitation and Neural Repair
[4] Schecklmann, M., Ehlis, A.-C., Plichta, M.M., Romanos, J., Heine, M., Boreatti-Hümmer, A., Jacob, C., Fallgatter, A.J. Diminished prefrontal oxygenation with normal and above-average verbal fluency performance in adult ADHD. Journal of Psychiatric Research 43:98-106, 2008.
[5] Schecklmann, M. Romanos, R., Bretscher F., Plichta M.M., Warnke A., Fallgatter, A.J. Prefrontal oxygenation during working memory in ADHD. Journal of Psychiatric Research 44:621-628, 2010.
[6] Schneider, S., Christensen, A, Hausinger, F.B., Fallgatter, A.J., Giese, M.A., Ehlis, A.-C. Show me how you walk and I tell you how you feel – A functional near-infrared spectroscopy study on emotion perception based on human gait. In press: NeuroImage

Machine Learning Algorithms for Brain Signal Processing

Martin Spüler[1], Carina Walter[1], Armin Walter[1], Martin Bogdan[1*,2], Wolfgang Rosenstiel [1]

1 Technische Informatik, Eberhard-Karls-Universität Tübingen, Germany
2 Technische Informatik, Universität Leipzig, Germany
* Corresponding author. E-mail address: martin.bogdan@informatik.uni-tuebingen.de

Abstract
The presented paper gives a brief overview of the activities of the research group “artificial neural networks and machine learning” related to current projects on brain signal processing and the application of machine learning techniques. The research group’s reputation regarding artificial neural networks and machine learning is based on the application, modification and further development of these algorithms in a manifold of different areas. Here we focus on machine learning methods for brain signal processing related to Brain-Computer Interfaces (BCIs), either for the detection of mental states, the use as communication device and for stroke rehabilitation. As a related aspect, we also demonstrate some works regarding the use of machine learning methods for brain stimulation.

1 Introduction

The research group „artificial neural networks and machine learning” has previously worked on the application, modification and development of machine learning and signal processing algorithms in different areas. For example, machine learning has been successfully applied to several projects with industrial cooperation such as quality control in chip fabrication, the prediction of workload in mainframes or the interpretation and processing of sensory data in chemical and biomedical applications. Despite these successful applications in the industrial area, most of the reputation has been achieved due to the working focus of the research group being in the field of biomedical applications. To name a few, the feasibility of controlling commercial limb prosthesis by means of recorded nerve signals has been proved. Also, the control of a pig’s limb due to functional neuroelectrical stimulation whereas stimulation patterns were provided by artificial neural nets have been demonstrated. On the way towards the interpretation of multi-electrode recordings in the central nervous system (CNS), remarkable advances have been achieved in the field of source separation as well as in the field of spike sorting. Together with the Hertie-Institute for Clinical Brain research (Systems Neurophysiology) outstanding results have been achieved in stimulating the CNS of the barrel cortex of rats in order to imprint neural activity. A further internationally renowned outcome of these close interdisciplinary cooperations are algorithms for feature extraction in EEG (electroencephalogram) and ECoG (electrocorticography) recordings as well as automatic electrode discrimination towards their impact of information content regarding communication possibilities in BCI. Currently, we are working on several funded projects to improve the processing of brain signals as well as functional electrical stimulation using machine learning methods.

2 Methods for Brain Signal Processing

In the following sections, we will present a selection of our recent work and give an overview how and where machine learning methods can be applied for brain signal processing. Our work has a strong focus on Brain-Computer Interface (BCI) [1] applications, where we develop methods to improve BCIs as a communication device. Further we investigate the use of machine learning to improve rehabilitation of stroke patients and for detection of mental states (i.e. workload = WL). Lastly, we will show how machine learning methods can be used in the context of functional brain stimulation.

2.1 Machine Learning to improve Brain-Computer Interfacing

One problem when using BCIs for communication is the non-stationarity of brain signals, meaning that the recorded brain signals change over time that leads to decreased performance over prolonged BCI usage.

To improve BCI performance, spatial filters generated by Canonical Correlation Analysis can be used [2] to enhance classification accuracy of evoked or event related potentials, which can be applied to a variety of different brain signals used for BCI control (i.e. P300, ErrP, c-VEP).

Further, we investigated the use of new BCI paradigms, like the use of code-modulated visual evoked potentials (c-VEPs) [3], to find new methods that can lead to faster BCI communication.

A screenshot of a spelling application being controlled by the c-VEP BCI is shown in figure 2, but the c-VEP system is not limited to this application and can be used to emulate mouse and keyboard on the

level of the operating system which theoretically allows the control of arbitrary applications.

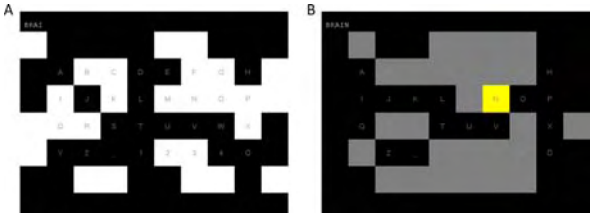

Fig. 1. Screenshot of the c-VEP BCI spelling application. A: screenshot during a trial. The letter Ö (lower right corner) serves as a backspace and allows the user to correct mistakes. B: screenshot of the letter N being selected and the other characters being grayed out to indicate a selection.

As a particularly promising approach to improve the robustness of a BCI system, several adaptive methods have been developed. We have shown that methods for adaptation can either be applied to the data before or in the classification process itself by implementing adaptive machine learning methods.

To reduce non-stationarity in the data we introduced a method that uses principal component analysis (PCA) to extract non-stationary components in the brain signals and use a covariate shift minimization technique to reduce their effect. We could show that the reduction of non-stationarity leads to significantly improved BCI performance [4].

By using an incremental training procedure for a Support Vector Machine (SVM) and combining it with a co-training approach, we realised an online adaptation of the SVM-classifier that is fast enough to work real-time even with high-dimensional MEG-data (275 channels). This approach was also shown to improve BCI performance significantly as well compared to non-adaptive methods [5].

While we have shown that error-related potentials can be detected in the brain signals and used to automatically correct erroneous responses of the BCI [6], we further used the detection of error-related potentials to improve adaptation of the c-VEP BCI. In combination with improved spatial filtering and the introduction of a one-class SVM for the classification of the c-VEP [7], a system which enables the user to write more than 20 error-free letters per minute have been developed which currently is the fastest non-invasive BCI system [8] and therefore an important step towards better BCI-driven communication.

Adaptive machine learning methods cannot only be used to improve BCI performance, but also to enable an unsupervised calibration. We have shown for the first time that an unsupervised online calibration of a BCI is possible [9] and argue that it potentially could be used for a new approach regarding the communication with complete locked-in patients

Since the use of adaptive methods opens many new questions about the interaction between the adaptive BCI system and the learning user, we addressed those questions by creating a simulation environment to easily explore the interaction between adaptive BCI and user to find out under which constraints the positive effect of BCI adaptation can reach its full potential [10].

2.2 BCI for mental state detection

The detection of mental states (i.e. effort of WL) using machine learning algorithms is the goal of our WissenschaftsCampus project, in cooperation with Prof. Gerjets (Knowledge Media Research Center, Tübingen). As the amount of WL during learning should be held within an optimal range of learner's memory capacity, our project is developing EEG based WL detection as well as prediction methods. These methods could be utilized in learning environments to adapt instructional material to the students individual WL online and thereby support the learning process successfully.

In contrast to BCI applications, it is not feasible for this application to use data from the same subject and same task for classifier training as well as testing since the subject may learn during training time. Therefore we developed two new classification methodologies based on EEG-signals, cross-task classification as well as cross-subject regression.

Prior to the application of machine learning methods characteristics in EEG-signals that reliably represent WL states has to be found. The power spectrum in θ- and α-frequencies composed of frontal as well as parietal electrodes (figure 2), can be used as features for WL classification.

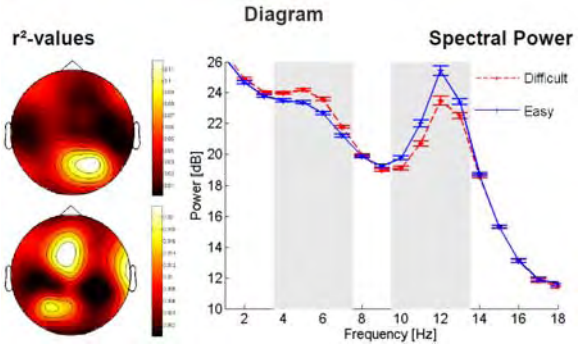

Fig. 2. Left: r²-values indicating the locations with highest differentiations while solving easy and difficult diagram tasks. Right: Spectral power plot for electrodes F3, Fz, F4, FC9, FC10, CP1, CP2, P3, Pz, P4) → significant increased θ-power as well as significant reduced α-power in diagram tasks.

Using cross-task classification, where a SVM was trained on EEG-data recorded while participants had to solve two working memory tasks (reading span, numerical n-back) and tested on EEG-data recorded during solving complex mathematical tasks, lead to accuracies around chance level [11]. To improve the relatively poor cross-task classification results, we used subjective cognitive-load ratings for defining classes, to reduce the varying difficulty across the tasks. A significant improvement of classifier performance ($p < 0.05$, permutation test) could be reached. The classifier was able to classify the subjectively eas-

ier versus harder set of math problems with a mean classification accuracy of 73 %.

While we have shown that modified cross-task classification can be used for WL detection, we further used a cross-subject regression method, for WL prediction. Therefore we applied a cross-subject linear regression method, using data from the same task but different subjects to calibrate the classifier. As most of the EEG-based WL classifications are subject-specific, this approach would enable training a classifier once that could handle multiple subjects. By applying linear regression cross-subjects a precise WL prediction could be reached (on average: Correlation Coefficient = 0.84).

In an upcoming study, these results will be used in an online learning environment to predict the user's WL and adapt the presented exercises accordingly, to support students successfully in their learning process.

2.3 BCI for stroke rehabilitation

One project in which we applied machine learning methods to improve BCI-based stroke rehabilitation is the “Bidirectional cortical communication interface” (BCCI) project led by Prof. Rosenstiel in cooperation with Prof. Birbaumer (Institute for Medical Psychology and Behavioral Neurobiology, University Hospital Tübingen) and Prof. Gharabaghi (Department of Neurosurgery, University Hospital Tübingen).

Over the course of this ERC-funded project, we have developed a BCI-based rehabilitation system, which detects the movement intention of the patient and couples this intention with haptic feedback given by an orthosis moving the paralyzed hand of the patient.

During this project, several stroke patients used this system for rehabilitation purposes. For the majority of the patients, the brain activity was measured non-invasively by EEG and the intention to move was detected by the BCI. Additionally, 3 patients were also implanted with epidural ECoG electrodes.

Based on those ECoG recordings, we could show that up to 7 different types of intended movements from the same limb could be classified successfully. These findings can further be used to improve BCI-guided rehabilitation, by not only coupling orthosis feedback to intended movement, but also giving different and more specific feedback for different movement intentions.

Further, we could show that ipsilesional ECoG activity yields enough information to not only discriminate different movement intentions, but also to reconstruct movement trajectories.

2.4 Machine Learning and Brain Stimulation

Since classical physiotherapy is often not very effective for stroke survivors with arm or hand paralysis and BCI-based rehabilitation might have its limits, new strategies are needed for rehabilitation. One idea to improve stroke rehabilitation is the use of brain stimulation techniques in combination with BCI technology as an addition to physiotherapy in order to facilitate neuroplasticity near the affected brain area. Within the BCCI project we took this next step by directly coupling brain stimulation and the hand orthosis with a BCI that detects the intention to move the paralyzed limb from the brain signal, forming the first bidirectional brain-computer interface applicable for the restoration of movement [12,14].

The main schematic setup for the new BCCI system is shown in figure 3.

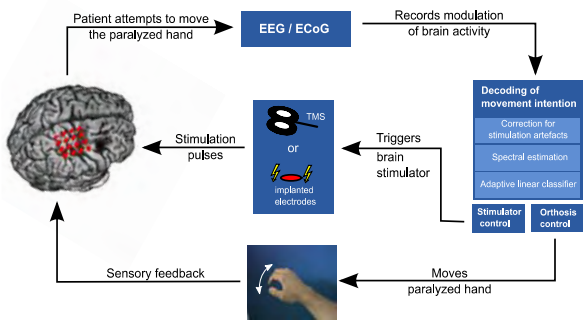

Fig. 3. Schematic setup of the BCCI system for hand movement restoration: A classifier detects the patient's intention to move the paralyzed hand using EEG or implanted ECoG electrodes. The output of the classifier controls an orthosis moving the hand and a brain stimulator, either transcranial magnetic stimulation (TMS) or electrical stimulation over the implanted electrodes.

As the signals are highly affected by stimulation artifacts this combination of BCI with brain stimulation introduces new challenges when recording and analysing the brain signals. Therefore new methods are needed [12] that are able to deal with these artifacts and allow a reliable estimation of the power spectrum despite the presence of stimulation artifacts.

Several chronic stroke patients were non-invasively treated with the combination of BCI and cortical stimulation, in addition to 3 stroke patients with a paralyzed hand that had been implanted with epidural electrocorticography (ECoG) electrodes. After 2-4 weeks of training with the BCCI system, 2 out of 3 implanted stroke patients regained control over some finger movements in the formerly paralyzed hand.

Furthermore, we conducted studies on the effects of cortical stimulation and the decoding of movement intention from these patients to optimize the system for future studies. We found that information about stimulation parameters and the intended movement at the moment of stimulation is encoded in the stimulation-evoked neural activity. Using appropriate machine learning methods, this information can be decoded even for single stimulation pulses and be used to identify optimal stimulation parameters and time points per patient [13].

Also, a change of the evoked potentials due to the stimulation of the cortex can be shown. Figure 4 shows the development of evoked potentials depending over different electrode sites over 4 weeks of stimulation. Please note, that only some of the recording sites of the

evoked potentials are changing during the 4 weeks whereas others don't. This effect is not correlated with the distance from the stimulation electrode. Thus the hypothesis can be formulated, that due to the stimulation some effects on the neural connections have been realized [14].

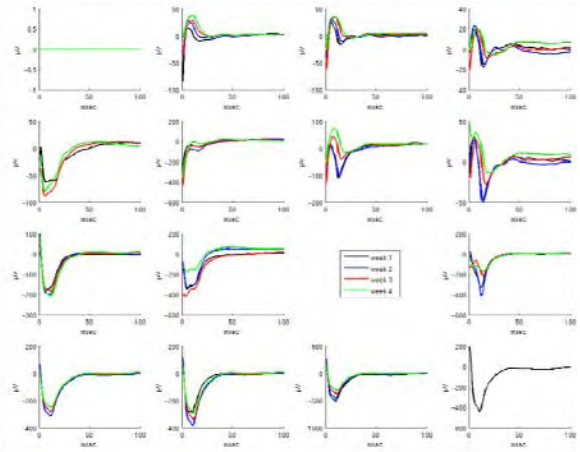

Fig. 4. Change of the evoked potentials over 4 weeks. Every diagram represents the corresponding electrode of the implanted 4x4 ECoG grid. The electrode without diagram represents the electrode used for the stimulation.

3 Summary

This paper summarizes the recent research effort of our group regarding the use of machine learning methods for brain signal processing. We have shown different applications where the use of machine learning algorithms is beneficial by advancing knowledge in the corresponding research applications and in the area of BCI in general as well. Future work will head the same research directions by further enhancing the performance of the applications in question. Also, the adaption of the presented algorithms to other applications mainly in the biomedical field will be investigated.

Acknowledgement

We are grateful to thank the supporters of the presented projects, namely WissenschaftsCampus, the Land Baden-Württemberg, BMBF (BFNT F*T, Grant UTü 01 GQ 0831), DFG (KOMEG) and the European Research Council ERC (Grant 227632).

References

[1] Wolpaw, J. R., Birbaumer, N., McFarland, D. J., Pfurtscheller, G., Vaughan, T. M. (2002). Brain–computer interfaces for communication and control. *Clinical neurophysiology*, *113*(6), 767-791.

[2] Spüler, M., Walter, A., Rosenstiel, W., Bogdan, M. (2014). Spatial Filtering Based on Canonical Correlation Analysis for Classification of Evoked or Event-Related Potentials in EEG Data," *IEEE Transactions on Neural Systems and Rehabilitation Engineering*.

[3] Bin, G., Gao, X., Wang, Y., Li, Y., Hong, B., & Gao, S. (2011). A high-speed BCI based on code modulation VEP. *Journal of neural engineering*, *8*(2), 025015.

[4] Spüler, M., Rosenstiel, W., Bogdan, M. (2012). Principal component based covariate shift adaption to reduce non-stationarity in a MEG-based brain-computer interface. *EURASIP Journal on Advances in Signal Processing, 2012:129.*

[5] Spüler, M., Rosenstiel, W., Bogdan, M. (2012). Adaptive SVM-based classification increases performance of a MEG-based Brain-Computer Interface (BCI). In *Artificial Neural Networks and Machine Learning–ICANN 2012*, pp.669-676.

[6] Spüler, M., Bensch, M., Kleih, S., Rosenstiel, W., Bogdan, M., Kübler, A. (2012). Online use of error-related potentials in healthy users and people with severe motor impairment increases performance of a P300-BCI. *Clinical Neurophysiology, 123*(7),pp. 1328-1337.

[7] Spüler, M., Rosenstiel, W., Bogdan, M. (2012). One class SVM and Canonical Correlation Analysis increase performance in a c-VEP based Brain-Computer Interface (BCI). In *Proceedings of 20th European Symposium on Artificial Neural Networks (ESANN 2012),pp.* 103-108.

[8] Spüler, M., Rosenstiel, W., Bogdan, M. (2012). Online adaptation of a c-VEP Brain-Computer Interface (BCI) based on Error-related potentials and unsupervised learning. *PloS one*, 7(12),e51077.

[9] Spüler, M., Rosenstiel, W., Bogdan, M. (2013). Unsupervised Online Calibration of a c-VEP Brain-Computer Interface (BCI). In *Artificial Neural Networks and Machine Learning–ICANN 2013*, pp. 224-231.

[10] Spüler, M., Rosenstiel, W., Bogdan, M. (2012). Co-adaptivity in Unsupervised Adaptive Brain-Computer Interfacing: a Simulation Approach. In *COGNITIVE 2012, The Fourth International Conference on Advanced Cognitive Technologies and Applications*, pp. 115-121.

[11] Walter, C., Schmidt, S., Rosenstiel, W., Gerjets, P., Bogdan, M. (2013). Using Cross-Task Classification for Classifying Workload Levels in Complex Learning Tasks. *In Proceedings of the 5th IEEE ACII 2013*, pp.876-881.

[12] Walter, A., Murguialday, A., Spüler, M., Naros, G., Leão, M. T., Gharabaghi, A., Birbaumer, N., Rosenstiel, W., Bogdan, M. (2012). Coupling BCI and cortical stimulation for brain-state-dependent stimulation: methods for spectral estimation in the presence of stimulation after-effects. *Frontiers in neural circuits*, *6*.

[13] Walter, A., Naros, G., Spüler, M., Gharabaghi, A., Rosenstiel, W., Bogdan, M. (2014). Decoding stimulation intensity from evoked ECoG activity. *Neurocomputing, http://dx.doi.org/10.1016/j.neucom.2014.01.048* .

[14] Walter, A., Naros, G., Spüler, M., Rosenstiel, W., Gharabaghi, A., Bogdan, M. (2013). Dynamics of a Stimulation-evoked ECoG Potential During Stroke Rehabilitation - A Case Study. *NEUROTECHNIX 2013 - International Congress on Neurotechnology, Electronics and Informatics*, pp.241-243.

Implantable bioelectronic interfaces for diagnosis, therapy and rehabilitation

Alfred Stett*, Volker Bucher, Claus Burkhardt, Martina Cihova, Katja Gutöhrlein, Massimo Kubon, Gorden Link, Rene von Metzen, Wilfried Nisch, Sebastian Röhler, Ramona Samba, Michael Weinmann, Martin Stelzle

NMI Natural and Medical Sciences Institute at the University of Tübingen, Reutlingen, Germany
* Corresponding author. E-mail address: stett@nmi.de

Abstract
Electrical implants like cardiac pacemakers and neuronal stimulators basically consist of a solid housing protecting the electronics and the energy storage. For applications, where only a small volume is available for inclusion of the implant like in the eye, ear and brain, and where cabling is not applicable, miniaturized, cable-free implants with wireless power supply and data transmission are required. The NMI together with its partners develops highly-integrated implantable systems for biosensor and electrical stimulation applications. For measurement and stimulation of biological signals the implants are equipped with multifunctional microelectrode arrays. The implant development aims at applications in diagnosis and therapy of neurological and metabolic disorders.

1 Background

Electrically active implantable medical devices (AIMD) are utilized for the management of numerous disorders, like cardiac pacing, eyesight, epilepsy, headaches, hearing, movement disorders, chronic pain, psychiatric and neurobehavioral disorders, gastric motility urinary frequency and urgency, and more [1]. Recently, the need for devices that targets single cells of neural circuits in the peripheral nervous system for the treatment of diseased organ functions has been described [2]. With regard to personalized medicine, implantable electrochemical biosensors raise the possibility for continuous monitoring of clinical biomarkers by direct tissue measurements [3] and for new therapies of metabolic disorders like diabetes [4].

State-of-the-art AIMDs for long-term use like cardiac pacemakers and deep brain stimulators basically consist of a solid metal housing protecting the electronics and the energy storage, and the stimulation electrode which is connected to the electronic circuitry via a lead and a interconnect header (Fig. 1) [5]. For applications, where only a small volume is available for inclusion of the implant like in the eye [6], brain and subcutaneous metabolic monitoring, and where large batteries and cabling are not applicable, miniaturized and compact system architectures are required, containing means for on-board data management and wireless communication with external devices for energy and data transmission. A special challenge is posed by the demand for biocompatibility and safe long-term function.

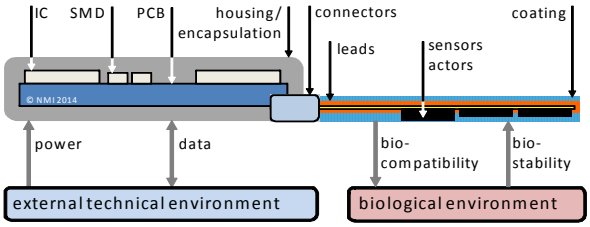

Fig. 1. Schematic drawing of an active electronic implant, its components and interactions with the external technical and biological environment. The implant has to be biocompatible and biostable under the condition of use. IC integrated circuit, SMD surface mounted passive device, PCB printed circuit board.

Ongoing research activities at the NMI pursue the idea of highly-integrated and miniaturized electronic implants with cable-free system architectures and multifunctional interfaces for stimulation and recording of neuronal activity and electrochemical detection of ions and biochemical molecules.

2. Cable-free electronic implants

2.1 Flexible active board for intracranial recording

For subchronic electrocorticography (ECoG) a polymer based system, which comprises a flexible printed circuit board (PCB) as well as the electronics and sensors without a hard shell, has been designed, manufactured and tested.

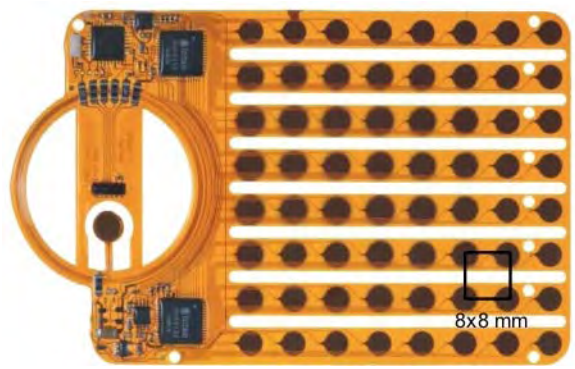

Fig. 2. Active ECoG grid with 64 channels for cortical recordings with implemented analog-to-digital conversion, multiplexing, optical data communication and a telemetric link for power supply.

The substrate is a flexible polyimide with embedded conductors. After assembly of the electronic components, the implant was coated with approx. 11 µm Parylene C. The active part of the grid was additionally coated with a PECVD SiO_X-layer and finally in silicone rubber to protect the thin encapsulation layers mechanically especially from the tools applied in the implantation surgery.

The approach of an active, cable-free, flexible and very thin implant for ECoG recordings is a substantial progress compared to the standard passive grids that are well-established but possess the drawback of the percutaneous cable. Moreover, the MEMS based manufacturing technologies offer more design freedom than conventional, hand crafted electrode grids, especially towards much smaller electrode sites, enabling an improved spatial resolution, while the number of recording sites is easily expandable.

2.2 PEEK capsule for in vivo biosensor applications

For subcutaneous electrochemical measurements a sensor capsule (Fig. 3) is being developed, where the electronic part of the system is housed in a sealed PEEK shell.

The capsule contains amperometric, potentiometric and impedance sensors allowing the electrochemical measurement of the oxygen concentration, pH-value and impedance in the vicinity of the implant. The implant system consists of application specific integrated circuits (ASICs) and microcontrollers for sensor readout, inductive power transmission and bidirectional data transfer, and a rechargeable battery.

Miniaturization of the implant comprising high functionality and a wireless link to the external device has been obtained by defining economical operation modes, designing energy efficient electronic circuits and the compact integration of the board and battery in a small capsule intended for subcutaneous implantation.

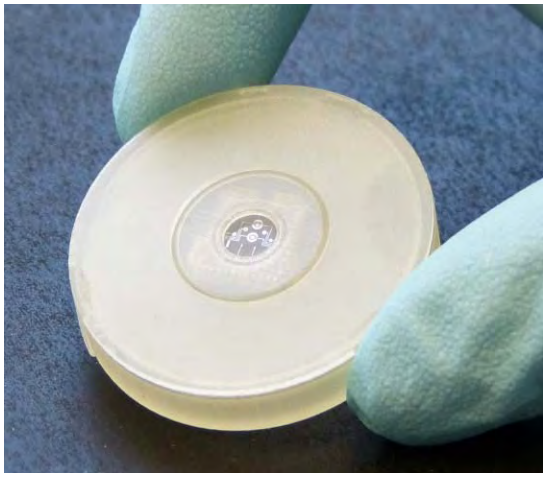

Fig. 3. Implantable electrochemical biosensor capsule (diameter 30 mm, height 7 mm).

3 Multifunctional sensor arrays

3.1 Microelectrodes for neuromonitoring and stimulation

Besides the encapsulated electronics, implants contain a number of contacts to record and stimulate cellular and molecular activity in the adjacent tissue. For this purpose we developed microelectrodes that are able to provide highly localized stimulation and to record cellular signals and local field potentials. Using MEMS technology, a wide variety of materials and insulators can be used to produce planar and 3D electrodes of small dimensions, high functionality and long-term stability (Fig. 4). For recording with a high signal-to-noise ratio, nano-columnar TiN electrodes are used, whereas for stimulation the high charge-injection capability of nanoporous Ir/IrOx is employed.

There is a strong demand for new materials to fabricate multifunctional microelectrodes that allow for recording, stimulation, and for electrochemical sensing of neuroactive chemical species [7]. As PEDOT–CNT composites are one of the most promising materials, we established a robust procedure for the production of PEDOT–CNT electrode arrays [8].

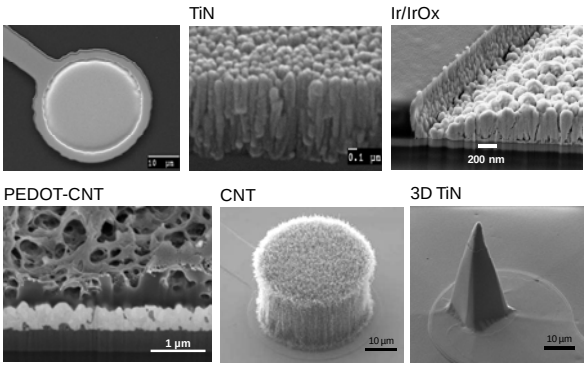

Fig. 4. Microelectrodes for recording and stimulation.

3.2 Electrochemical sensors

For electrochemical monitoring a sensor array comprising microelectrodes for O_2-, pH-value- and impedance measurement is available for integration into the implants (Fig. 5).

An amperometric sensor, realized in a three electrode configuration with working (Pt), counter (Pt) and reference (Ag/AgCl) electrode, is employed to measure oxygen concentration.

A potentiometric sensor in a two electrode configuration comprising a IrOx working and Ag/AgCl reference electrode is employed to measure the pH.

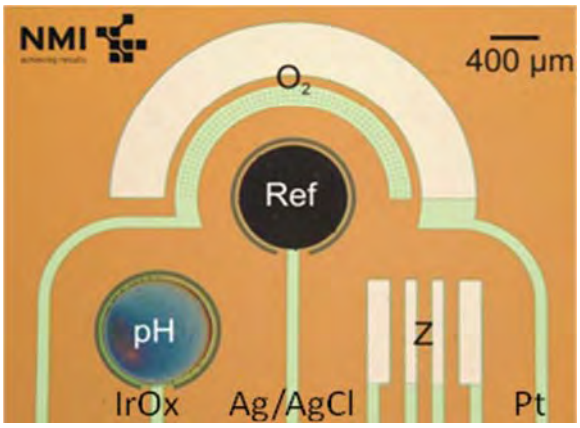

Fig. 5. Sensorarray with amperometric, potentiometric and impedance sensors allowing the electrochemical measurement of the oxygen concentration, the pH and the impedance in the vicinity of the implant.

4 Conclusion/Summary

Miniaturization of active, cable-free implants comprising high functionality and wireless links to external devices can be obtained by designing energy efficient electronic circuits and by using MEMS technology for fabrication of multifunctional sensor arrays and for their integration in compact substrates and housings to protect the electronics from body liquids.

Those miniaturized implants will open up a whole new spectrum of health care applications, facilitating more specific diagnosis, more effective therapies and aids used on a daily basis by patients suffering e.g. from neurological, movement or metabolic disorders.

Acknowledgement

This work was supported by the Federal Ministry of Education and Research (BMBF) through grants no. 01GQ0834 (Bernsteinfocus Neurotechnology: Hybrid brain), no. 16SV3782 (incrimp project, Rahmenprogramm Mikrosysteme, Förderinitiative Intelligente Implantate), no. 16SV5009 (Begleitforschung Intelligente Implantate), no. 16SV5979K (SMART Implant, a project of the SSI platform in the Cluster microTEC Südwest).

Contributions by and collaboration with Multi Channel Systems MCS GmbH and the SMART Implant consortium are kindly acknowledged.

References

[1] Krames, E.S., et al. What Is Neuromodulation? Chap. 1, p. 3-8. In: Krames E.S., Peckham P.H., Rezai A.R. (eds): Neuromodulation. Academic Press, 2009

[2] Famm, K.: A jump-start for electroceuticals. Nature (2013) 469:159-161

[3] Rogers M.L., Boutelle M.G.: Real-Time Clinical Monitoring of Biomolecules. Annual Review of An-alytical Chemistry (2013) 6:427-453

[4] Klonoff D.C.: The Benefits of Implanted Glucose Sensors. J Diabetes Sci Technol. (2007) 1(6): 797–800.

[5] Peckham P.H., Ackermann D.M.: Implantable Neural Stimulators. Chap. 18, p. 215-228. In: In: Krames E.S., Peckham P.H., Rezai A.R. (eds): Neuromodulation. Academic Press, 2009

[6] Zrenner E. et al.: Subretinal electronic chips allow blind patients to read letters and combine them to words. Proc. R. Soc. B (2011) 278:1489–1497

[7] Samba R et al. Application of PEDOT-CNT microelectrodes for neurotransmitter sensing. Electroanalysis (2014) 26:548-555

[8] Gerwig R et al.: PEDOT–CNT composite microelectrodes for recording and electrostimulation applications: fabrication, morphology, and electrical properties. Front. Neuroeng. (2012) 5:8.

CMOS – Based Microelectrode Arrays ('Neurochips') for Simultaneous Stimulation and Detection Action Potentials at Sub-Cellular Resolution

Günther Zeck[1], Max Eickenscheidt, Lakshmi Channappa, Roland Thewes [2]

1 Natural and Medical Sciences Institute at the University of Tübingen
2 Chair of Sensor and Actuator Systems, Faculty of EECS, TU Berlin, Berlin, Germany

Abstract
The action of arbitrary electrical stimuli upon neurons embedded in the complex tissue environment can be revealed by simultaneous recording of the evoked activity. Towards such goal integration of stimulation and recording sites at high-spatial resolution is required. Here we present first results obtained with a newly developed CMOS-based microelectrode array ("Neurochips") interfaced to either retina or hippocampal slices.

1 Backround / Aims

Microelectrode arrays (MEAs) based on integrated complementary metal oxide semiconductor (CMOS) technology have been introduced recently by our groups [1 – 3] towards efficient electrical stimulation and recording of neuronal activity at high spatial (~10 µm) and temporal resolution (~ 10 kHz). Although either stimulation or recording has been demonstrated a loss-free, bidirectional interfacing remained a challenge. Detection of the induced activity at a sub-millisecond timescale is desired to address the stimulation effect on single neurons or axons.

2 Methods / Statistics

A CMOS-based MEA comprising 4225 recording sites and 1024 stimulation sites has been developed [5] and tested with respect to detection and stimulation performance in neural tissue [6]. The recording site pitch is 16 µm or 32 µm, thus allowing for high-resolution electrical imaging of the interfaced neurons or neural tissue. *Ex vivo* light-responsive mammalian retina as well as hippocampal slices were interfaced to the planar sensor surface of the MEA. Single cell activity and local field potentials are induced by means of capacitive stimulation. The induced activity (action potentials and local field potentials respectively) and the propagation thereof are recorded and evaluated.

3 Results

Cathodal stimulus pulses applied at a remote position from retinal ganglion cell somata evoke back-propagating action potentials. This propagation is electrically imaged at subcellular resolution for a ganglion cell population. Cathodal stimulus pulses applied at different positions in a hippocampal slice evoke local field potentials. The propagation patterns of these local field potentials are discussed.

4 Conclusion/Summary

Capacitively coupled CMOS-based MEAs are an attractive tool to characterize the response of neurons in planar preparations to arbitrary electrical stimulus patterns. Such experiments may advance our understanding of the dynamic response properties of neuronal populations and lead to improved neuroprosthetic stimulation strategies.

References

[1] Eversmann, B., et al. (2004): *A 128 × 128 CMOS biosensor array for extracellular record-ing of neural activity.* IEEE Journal of Solid-State Circuits, 38 (12), 2306-2317.
[2] Zeck et al. (2011) *Axonal transmission in the retina introduces a small dispersion of relative timing in the ganglion cell population response* Plos One 6(6):e20810. doi:10.1371/journal.pone.0020810
[3] Eickenscheidt, M. et al (2012) *Electrical stimulation of retinal neurons in epiretinal and subretinal configuration using a multicapacitor array* J. Neurophysiol. 107(10):2742-55.
[4] Eickenscheidt, M. and Zeck, G. (2014) *Action potentials in retinal ganglion cells are initiated at the site of maximal curvature of the extracellular potential.* J.Neural.Eng. 11(3):036006
[5] Bertotti et al . (2014) *A Capacitively-Coupled CMOS-MEA with 4225 Recording Sites and 1024 Stimulation Sites.* Proc. of 9th Int. Meeting on Substrate-Integrated Microelectrodes
[6] Velychko et al. (2014) *Simultaneous Stimulation and Recording of Retinal Action Potentials Using Capacitively Coupled High-Density CMOS-based MEAs.* Proc. of 9th Int. Meeting on Substrate-Integrated Microelectrodes

Electronic systems for electrophysiology and implantable devices

Clemens Boucsein*, Karl-Heinz Boven, Andreas Möller

Multi Channel Systems MCS GmbH, Reutlingen
* Corresponding author. E-mail address: boucsein@multichannelsystems.com

1 Backround / Aims

Providing electronics for brain-machine interfaces and neuroprosthesis imposes several challenges from an engineering point of view. While the signals from neuronal tissue that have to be recorded are in the microvolt range, successful stimulation requires voltages four orders of magnitude larger [1]. At the same time, electronic components that should be attached to or implanted into the body need to be extremely compact and light-weight, and have to be optimized for low energy consumption. Finally, it is highly favorable to avoid cable connections to implanted devices, making radio technologies for energy and data transmission highly attractive for neurotechnology.

2 Results

Starting from cable-based miniature amplifiers for the recording of retinal signals, Multi Channel Systems has developed neurotechnology devices for several different applications, featuring the most important aspects for the successful interfacing of neuronal tissue for BMI and neuroprosthesis. Low-noise recording circuits (rms < 8µV) allow the acquisition

Fig. 1. Implant for EcOG-recordings with surface electrodes (provided by CorTec, Freiburg), which was tested in sheep and sucessfully passed the first long-term stability tests.

of local field potentials from 16 channels simultaneously, providing signal qualities sufficient for the application of epilepsy detection algorithms and prosthesis control. Miniaturization and implementation of trans-cutaneous energy transfer and data transmission led to fully implantable devices, which were successfully tested in sheep. Circuits can be assembled on flexible printed circuit boards, allowing for a versatile implantation procedure with high flexibility concerning the placement of the implant.

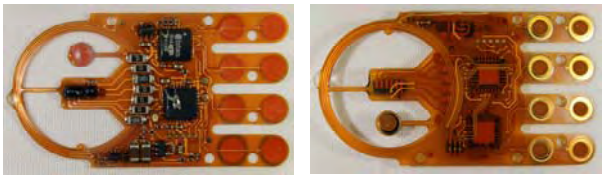

Fig. 2. Implant electronics and electrodes assembled on flexible substrate (provided by NMI, Reutlingen). Coil is used for energy transmission, while data exchange is achieved using infrared light.

Recent attempts to combine recording and stimulation on the same electrodes have led to the generation of a custom application-specific integrated circuit (ASIC), featuring high-voltage switches that protect the sensible amplifier circuits needed for low-noise recordings from the high voltages necessary for successful neurostimulation. With the help of these custom ASICs, a fully implantable device for EcOG recording and neurostimulation has been realized [2], and is currently tested in a suitable animal model (Fig.1).

3 Outlook

Following the successful introduction of retinal implants containing microelectronic devices, the next step will be the approval of implants for combined recordings from and stimulation of neuronal tissue, utilizing the very same electrodes. Animal testing of the respective prototypes is currently performed, and further developments in chip technology are likely to improve energy efficiency and noise levels of devices for BMI and neuroprosthesis control.

References

[1] Logothetis NK, Augath M, Murayama Y, Rauch A, Sultan F, Goense J, Oeltermann A, Merkle H (2010) The effects of electrical microstimulation on cortical signal propagation. Nat Neurosci. 13:1283-91.

[2] Gierthmuehlen M, Wang X, Gkogkidis A, Henle C, Fischer J, Fehrenbacher T, Kohler F, Raab M, Mader I, Kuehn C, Foerster K, Haberstroh J, Freiman TM, Stieglitz T, Rickert J, Schuettler M, Ball T (2014) Mapping of sheep sensory cortex with a novel micro-electrocorticography grid. J Comp Neurol. doi: 10.1002/cne.23631.

The Technology of Retinal Implants: Challenges and Solutions

Walter-G. Wrobel

Retina Implant AG, Reutlingen, Germany

Abstract

After more than a decade of development, the first retinal implants are being introduced to the market. The technical design deviates remarkably from other active implants and poses new challenges. Among them are: corrosion of electrical conductors and chips, lifetime of electrodes, eye movements and cable breakage. We present newly developed testing procedures and design solutions.

1 Introduction

Since the 1990's numerous groups around the world are working on retinal implants. To date two products have achieved market approval. We have been developing the subretinal implant Alpha IMS (see Fig.1), which in July 2013 received CE marking. Subretinal implants have the advantage that they use an anatomically natural separation between retina and choroid for implantion, which minimizes adverse tissue reaction and scarring. The subretinal space is humid and salty, and the electrode size has to be quite small (50x50µm²), the number of electrodes quite high (1500 electrodes), to achieve an acceptable optical resolution, and the device requires external electrical power.

2 Methods

Corrosion of metallic materials due to electrolyte migration can be tested by measuring electrical leakage currents. Current levels of > 1µA are an indicator of early failure. Manufacturing processes can be improved by evaluation of leakage current levels in the pA-range. For electrodes, iridium-oxide electrodes are preferred, as they survive > 500 mio. pulses. As the eye is one of the most mobile human organs, and Botox injections are unacceptable, power supply cables have to designed in such a way that they survive > 10 years of life. We have designed a testing apparatus and have compared results with clinical experiences.

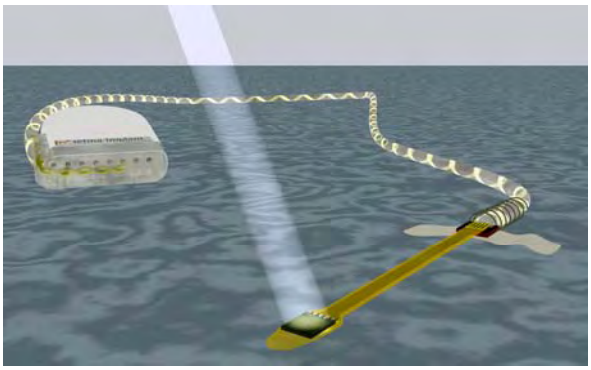

Fig. 1. Retina implant Alpha IMS

3 Results

By careful selection of components and optimization of manufacturing processes, polymer cables can achieve lifetimes acceptable for clinical application. Electrodes are not a challenge. Power supply cables can be designed in such a way that they survive an appropriate number of large eye movements.

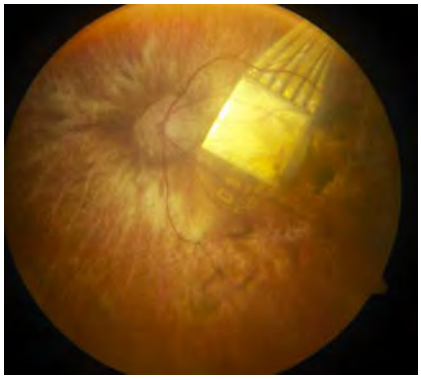

Fig.2. Alpha IMS implant in the human eye

4 Conclusion

There are no unsurmountable barriers to achieving with subretinal implants a lifetime of > 10 years. Required materials are available, and material properties are satisfactory. Careful and reproducible material processing is now the main challenge.

Acknowledgement

Many thanks to our collaborators, especially NMI Reutlingen, with special gratitude to more than 40 trial patients worldwide.

References

[1] K.Stingl et.al., Artificial vision with wirelessly powered subretinal electronic implant alpha-IMS, Proc.R.Soc. B280 : 20130077

Tapping into decision-related activity in primary somatosensory cortex to control the subject's percept

Brugger, Dominik, Dehnke, Stine and Schwarz, Cornelius

1Werner Reichardt Center for Integrative Neuroscience, Systems Neuroscience
2Hertie Institute for Clinical Brain Research, Dept. Cognitive Neurology
Eberhard Karls University, Tübingen, Germany*
Corresponding author. E-mail address: cornelius.schwarz@uni-tuebingen.de

Abstract
The input-output transformation of cortical neurons is highly activity-dependent ('context dependent') leading to a high variance of evoked neuronal responses on a trial by trial basis. We tested the hypothesis if part of this variability can be explained by local ongoing activity that is related to the upcoming decision of the animal. We used 'dynamic brain stimulation', a novel closed loop approach that applies cortical microstimulation dependent on immediately preceding cortical activity. Measuring the state of primary somatosensory via one electrode and dynamically adapting microstimulation pulses injected via another allowed us to stabilize evoked cortical activity and improve psychometric sensitivity of a rat trained to detect intracorticalmicrostimulation.

Support: DFG SCHW 577/9-1

To What Extent Can Retinal Prostheses Restore Vision?

Zrenner, Eberhart[1*]; Bartz-Schmidt, Karl-Ulrich[1]; Chee, Caroline[2]; Gekeler, Florian[1]; Jackson, Timothy L.[3]; MacLaren, Robert[4]; Nemeth, Janos[5]; Sachs, Helmut[6]; Stingl, Katarina[1]; Wong, David[7]

1 Werner Reichardt Center for Integrative Neurosciences and Institute for Ophthalmic Research, University of Tübingen Germany.
2 Dept.of Ophthalmology, National University Health System, Singapore, Singapore.
3 Dept. of Ophthalmology, School of Medicine,, King's College, London, United Kingdom.
4 Dept. of Clinical Neurosciences, Nuffield Laboratory of Ophthalmology, University of Oxford, Oxford, United Kingdom.
5 Semmelweis University, Budapest, Hungary.
6 Städtisches Klinikum Dresden-Friedrichstadt, Dresden, Germany.
7 Dept. of Ophthalmology, University of Hong Kong, Hong Kong.
*ezrenner@uni-tuebingen.de

Abstract
An interim report on a clinical trial is given that describes the results obtained in 26 patients blind from retinitis pigmentosa who have received the subretinal electronic implant Alpha IMS (Retina Implant AG, Reutlingen, Germany). It has turned out that the surgical procedure is safe and that the majority of patients have benefit for performing successfully visual tasks in daily life with this device that meanwhile has received approval for commercial use in Europe.

1 Backround

There exists no cure yet for blindness caused by hereditary retinal degeneration of the photoreceptors (e.g. retinitis pigmentosa (RP) but restoration of vision by various electronic retinal implants [1,2] has made rapid progress in recent years with remarkable results concerning visual localization of objects, mobility, even reading and face recognition in some cases [3,4]. There are, in principle, three different approaches (fig. 1, from Zrenner [5]): a) *Epiretinal* implants that are positioned on top of the neuroretina, placing electrodes, controlled by a camera outside the body, at the functional *output* of the retina, i.e. near to retinal ganglion cell fibers; b) *subretinal* implants that utilize light sensitive photodiodes, each connected to an electrode, both placed beneath the retina, contacting the functional *input* of the retina on the photoreceptor side, and c) the *suprachoroidal* approach that inserts electrode arrays from the back of the eye, positioning them on top of the choroid.

2 Methods / Statistics

Alpha-IMS subretinal implants (Retina Implant AG, Reutlingen, Germany) were positioned beneath the foveal region of 14 male and 12 female RP-patients (mean age 53.2 ± 8.2). Each of the 1500 subfoveal photodiodes within a 15° field (diagonal) controls an amplifier that, depending on the strength of the light, emits currents via planar electrodes to stimulate over-lying bipolar cells. Power and control signals are supplied inductively via a subdermal, retroauricular coil from which a subdermal cable leads to the eyeball.

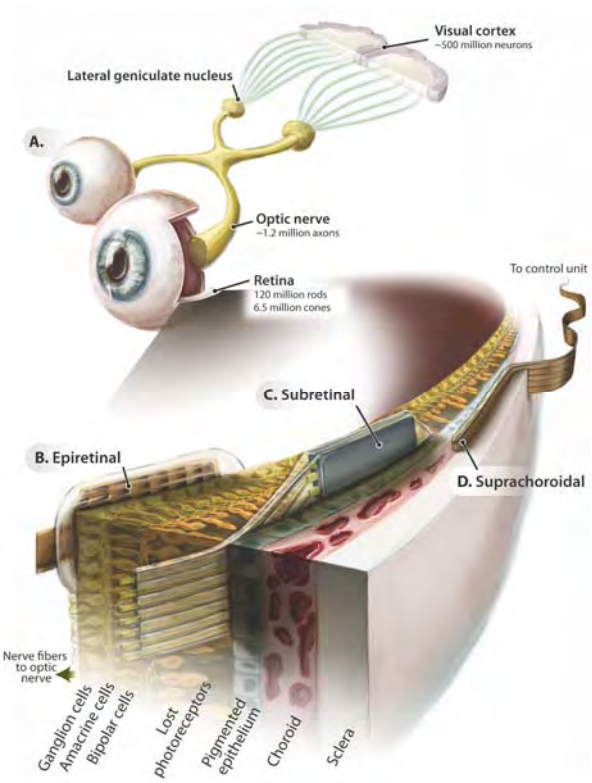

Fig. 1. The human ascending visual pathway (**A**) and sites in the retina where epiretinal (**B**), subretinal (**C**), and suprachoroidal (**D**) implants are inserted [5].

Function was tested by 4 procedures - 1: Monitor-based standardized tests for light perception, light localization, movement detection, grating acuity and visual acuity with Landolt C-rings (2- or 4 alternative-force-choice-tests); 2: Detection, localization and identification of objects placed on a table; 3: Reading letters; 4: Visual experiences during outdoor and daily-life activities.

3 Results

1: Implant-mediated light perception was possible for 22 (85%) patients; light localization for 15 (58%); movement detection (up to 35 cycles/degree) for 6 (23%); measurable grating acuity (up to 3.3 cycles/degree) for 14 (54%); and measurable visual acuity (up to 20/546) for 4 (18%).

2: On a visual ability scale from 0 (worst) to 4 (best) for 4 white geometric figures presented on a black table, patients averaged 3.12 ± 0.31 for detection, 2.94 ± 0.3 for localization and 1.06 ± 0.28 for identification at month 2 which was significantly better ($p < 0.012$) than with chip power switched off. Similar results were obtained with activities of daily living. Losses of approximately 1-1.5 units occured over 9-12 months.

3: Four patients (18%) could read letters 4-8 cm in size.

4: Twelve pa-tients (46%) reported useful visual experiences includ-ing recognition of details and 7 patients (27%) could localize objects in daily life without details.

5: Besides two treatable serious adverse events there were no safety concerns.

4 Summary

The Alpha-MS implant has meanwhile received a CE mark for commercial use in Europe. Psychophysical testing and self-reported outcomes show restoration of useful vision in a majority of patients. Subretinal implantation surgery is safe and a multicenter study is continuing with a slightly modified implant built for long term durability.

Acknowledgement

The authors thank the staff of the Retina Implant AG, Reutlingen, Germany, especially W. Wrobel, R. Rubow, A. Hekmat, A. Harscher, S. Kibbel, R. Rudorf, C. Eipper, C. Jansen, M. Kokelmann, G. Blaess, H. Wagner and E. Nestler for organizational background support in the trial. This work was supported by Retina Implant AG, Reutlingen, Germany and by the German Federal Ministry of Education and Research (BMBF; FKZ: 01GQ1002).

References

[1] Zrenner E. Will Retinal Implants Restore Vision? Science 295, 1022-1025 (2002)

[2] Zrenner E. Artificial vision: Solar cells for the blind. Nature photonics 6: 344-345 (2012)

[3] Zrenner E. Bartz-Schmidt KU, Benav H, Besch D, Bruckmann A, Gabel V-P, Gekeler F, Greppmaier U, Harscher A, Kibbel S, Koch J, Kusnyerik A, Peters T, Stingl K, Sachs H, Stett A, Szurman P, Wilhelm B, Wilke R. Subretinal electronic chips allow blind patients to read letters and combine them to words. Proc. R. Soc B - Biol.Sci. 278, 1489-1497 (2011)

[4] Stingl K, Bartz-Schmidt KU, Besch D, Braun A, Bruckmann A, Gekeler F, Greppmaier U, Hipp S, Hörtdörfer G, Kernstock C, Koitschev A, Kusnyerik A, Sachs H, Schatz A, Stingl KT, Peters T, Wilhelm B, Zrenner E. 2013 Artificial vision with wirelessly powered subretinal electronic implant alpha-IMS. Proc R Soc B - Biol Sci 280: 20130077. http://dx.doi.org/10.1098/rspb.2013.0077

[5] Zrenner E. Fighting Blindness with Microelectronics. Science Transl. Med. 5: 210ps16 (2013); DOI: 10.1126/scitranslmed.3007399

Brain-state dependent neuromodulation with closed-loop neuroprosthetics for neurorehabilitation

Alireza Gharabaghi[1*]

1 Division of Functional and Restorative Neurosurgery & Division of Translational Neurosurgery, University Hospital Tübingen; Neuroprosthetics Research, Centre for Integrative Neuroscience, University of Tübingen
* alireza.gharabaghi@uni-tuebingen.de

Abstract
We introduced a concept for movement-related and brain-state dependent stimulation of the human motor cortex for severely affected stroke survivors. Our findings suggest that closing the loop between intrinsic brain state, cortical stimulation and haptic feedback provides a novel neurorehabilitation strategy for stroke patients lacking residual hand function.

1 Backround / Aims

Motor deficits after stroke are an ongoing challenge. Brain stimulation and robotic rehabilitation have been explored as complementary therapeutic strategies for neurorehabilitation. Each of these approaches has methodological limitations, especially in the context of severely affected stroke patients: Up to now, brain stimulation protocols have been applied uncoupled to the ongoing brain activity of the patient. Similarly, current robotic training programs are not suitable for patients missing residual motor function.

2. Methods

A necessary prerequisite for the presented approach is a set-up that allows for closed-loop brain stimulation based on intrinsic neural properties at the time of stimulation. In parallel, this framework has to provide the patient with volitional motor control of a robotic device that moves the paralyzed hand contingent to movement intention.

3 Results

Here, we report on such brain state-dependent stimu-lation (BSDS) combined with haptic feedback provided by a robotic hand orthosis. Brain stimulation of the motor cortex and haptic feedback to the hand were controlled by sensorimotor desynchronization during motor-imagery and applied within a brain-machine interface environment in the chronic phase after stroke. BSDS significantly increased the excitability of the stimulated motor cortex, an effect not observed in non-BSDS protocols.

4 Conclusion/Summary

We present a novel intervention using self-generated brain-signals for the volitional control of concurrent brain stimulation and robotic control of a paralyzed hand. Thereby, this set-up provides a closed-loop framework to explore brain-activity dependent interventions in paralyzed patients for inducing targeted plasticity.

References

Becker HG, Haarmeier T, Tatagiba M, Gharabaghi A. Electrical stimulation of the human homolog of the medial superior temporal area induces visual motion blindness. J Neurosci. 2013 Nov 13;33(46):18288-97

Bensch M, Martens S, Halder S, Hill J, Nijboer F, Ramos A, Birbaumer N, Bogdan M, Kotchoubey B, Rosenstiel W, Schölkopf B, Gharabaghi A. Assessing attention and cognitive function in completely locked-in state with event-related brain potentials and epidural electrocorticography. J Neural Eng. 2014 Apr; 11(2):026006.

Gharabaghi A, Naros G, Walter A, Roth A, Bogdan M, Rosenstiel W, Mehring C, Birbaumer N. Epidural electrocor ticography of phantom hand movement following long-term upper limb amputation Front Hum Neurosci. 2014 May 6;8: 285.

Gharabaghi A, Kraus D, Leão MT, Spüler M, Walter A, Bogdan M, Rosenstiel W, Naros G, Ziemann U. Coupling brain- machine interfaces with cortical stimulation for brain-state dependent stimulation: enhancing motor cortex excitability for neurorehabilitation. Front Hum Neurosci. 2014 March 5;8:122.

Gharabaghi A, Naros G, Walter A, Grimm F, Schuermeyer M, Roth A, Bogdan M, Rosenstiel W, Birbaumer N. From assistance towards restoration with an implantaed brain-computer interface based on epidural electrocorticography. Restorative Neurology and Neuroscience 2014 (in press)

Walter, A., Ramos Murguialday, A., Spuler, M., Naros, G.,Leao, M.T., Gharabaghi, A., Rosenstiel, W., Birbaumer, N., and Bogdan, M. (2012). Coupling BCI and cortical stimulation for brain-state-dependent stimulation: methods for spectral estimation in the presence of stimulation after-effects. Frontiers in neural circuits 6, 87.

Vukelić M, Bauer R, Naros G, Naros I, Braun C, Gharabaghi A. Lateralized alpha-band cortical networks regulate volitional modulation of beta-band sensorimotor oscillations. Neuroimage. 2014 Feb 15;87: 147-53.

9th International Meeting on Substrate-Integrated Microelectrode Arrays

Stimulation Strategies for Neurons and Fibers

Bioelectronic Medicines: Can MEAs Help Bring About a New Class of Treatments?

Daniel Chew[1], Bryan McLaughlin[2], Arun Sridhar[1], Sonal Patel[1], Hannah Tipney[1], Roy Katso[1] Imran Eba[3] and Kristoffer Famm[1*]

1 Bioelectronics R&D, GlaxoSmithKline, Stevenage, Hertfordshire SG1 2NY, UK
2 The Charles Stark Draper Laboratory, Cambridge, Massachusetts 02139, USA
3 Action Potential Venture Capital, Cambridge, Massachusetts 02142, USA
* Corresponding author. E-mail address: kristoffer.h.famm@gsk.com

Abstract
Bioelectronic medicines have potential to be a new class of treatments for major chronic diseases, but require significant innovation in high-resolution, non-disruptive peripheral nerve interfacing to become a reality. GlaxoSmithKline (GSK) wants to work with the MEA community towards this goal.

1 Bioelectronic medicines – an intro

Virtually all visceral organs are under the influence of the nervous system - lungs, heart, liver, pancreas, kidney, bladder, gastrointestinal tract, and lymphoid and reproductive organs to mention a few. GSK believes modulation of neural signals in peripheral nerves to and from these organs could bring about a new class of treatments as neutrally-controlled organ functions are at the centre of major chronic diseases such as asthma, hypertension, diabetes, and arthritis. [1-3] In addition to offering a new approach to treat disease, bioelectronic medicines could offer higher specificity than current molecular treatments through the temporal and functional precision inherent in neural control. Our long-term ambition is to develop implantable micro-devices that directly interface with individual nerves, close to the end organ of interest. Such devices will read and write the full complexity of the signalling pattern within the nerve and operate in a closed loop fashion, regulating organ function with therapeutically optimised signatures. Electrical "treatment codes" could one day be used side by side with molecular medicines.

2 MEAs at a new challenging interface

To deliver bioelectronic medicines, a revolution in visceral peripheral nerve interfacing is necessary. [4] To address <100µm peripheral nerve branches a >10x increase in spatial recording and stimulation density above existing arrays could be required, plus a 10x increase in the number of parallel channels. Importantly, this must be achieved without a reduction in performance and with minimal axonal damage through displacement. Another challenge lies in providing intimate contact with irregular plexi, and ganglia embedded in adipose tissue. A third is related to minimising artefacts from pulsating vasculature and movement of cardiac, diaphragm, intestinal, and somatic muscles while maintaining contact with the same set of nerve fibres over time. Shape adaptability, flexibility, integrated active electronics, and new materials could be key for MEAs to overcoming these challenges.

3 Engaging with an emering community

Bioelectronic medicines will only reach its full potential if a broad range of disciplines together build a solid research foundation, backed by resourcing and a commitment to bring treatments all the way to patients. GSK is seeking to play such an integrating role through its exploratory research funding program that currently brings together near 30 academic groups around the world [5], its Innovation Challenge focused on rapidly developing visceral nerve research platforms to the community [6], and its $50m venture arm dedicated to the technology and early treatment manifestations of bioelectronic medicines [7]. Through this and potential other mechanisms, GSK wants to work with the MEA community and visionary research funding bodies to bring next-generation microelectrode arrays to bear on visceral nerves.

References

[1] Famm, K. *et al.* A jump start for electroceuticals. *Nature* **496**, 159–161 (2013).
[2] Gassler, J. P. & Bisognano, J. D. Baroreflex activation therapy in hypertension. *J. Hum. Hypertens.* http://dx.doi.org/ 10.1038/ jhh.2013.139 (2014).
[3] Olofsson PS. *et al.*Rethinking inflammation : neural circuits in the regulation of immunity. *Immunol Rev* 248(1):188-204 (2012)
[4] Birmingham, K. *et al.* Bioelectronic medicines: a research roadmap *Nature Reviews Drug Discovery* **In press**, June (2014)
[5] http://www.gsk.com/partnerships/bioelectronics.html?tab=tabexploratory-funding-programme
[6] http://www.gsk.com/partnerships/bioelectronics.html?tab=tabmillion-dollar-innovation-challenge
[7] http://www.actionpotentialvc.com/

Response Profiles of Auditory Neurons on Multi-electrode Arrays

Stefan Hahnewald[1*], Anne Tscherter[3], Marta Roccio[1], Emanuele Marconi[1], Carolyn Garnham[2], Pavel Mistrik[2], Teresa Melchionna[2], Jürg Streit[3], Julien Brossard[4], Alexandra Homsy[4], Herbert Keppner[4], Hans-Rudolf Widmer[5], Pascal Senn[1]

1 Inner Ear Research Laboratory, Department of Clinical Research, University of Bern and University Department of Otorhinolaryngology, Head & Neck Surgery, Bern, Switzerland.
2 MED-EL Elektromedizinische Geraete GmbH (MED-EL), Innsbruck, Austria.
3 Department Physiology, University of Bern, Bern, Switzerland.
4 Haute Ecole Arc Ingénierie, La Chaux-de-Fonds, Switzerland.
5 Department of Neurosurgery, Bern University Hospital, Bern, Switzerland.
* Corresponding author. E-mail address: stefan.hahnewald@dkf.unibe.ch

Abstract
Cochlear implants (CIs) have become the gold standard treatment for deafness. Despite all the success, some limitations remain. Our project: "NANOCI" (www.nanoci.org) aims at developing a new generation of CIs where the peripheral processes of the auditory neurons grow towards the electrode array to form a gapless interface in the cochlea. In theory, this strategy should result in *i*) a better auditory resolution and *ii*) lower energy consumption, two of the main limitations of current CI systems.
As a first step towards this ambitious goal, we are assessing auditory neuron activity on multi electrode arrays (MEAs) to investigate parameters that are relevant in the context of the project. If the distance of the stimulation electrodes to auditory neurons is changed, stimulation parameters will need to be adapted as well to fully exploit the theoretical advantages of a gapless interface. Optimum stimulation parameters and distance-related effects are experimentally addressed on a custom-made set up and first results confirmed the main hypothesis of the NANOCI project, namely that the smaller the distance between the stimulating electrode and the auditory neurons, the lower the Voltage needed to trigger neuronal activity and the larger the dynamic range of responses. Although preliminary, these results are the first of their kind in the auditory field and allow us to address more sophisticated stimulation protocols in the near future.

1 Background / Aims

Hearing is one of the most important senses to interact with the environment. Hearing loss therefore has a considerable negative impact on the communication ability of affected individuals and high socio-economic costs. For mild to moderate forms of hearing loss, hearing aids are widely used to alleviate the symptoms. In severe cases and deafness, a neuroprosthesis called cochlear implant (CI) can be surgically implanted to restore hearing. In the majority of CI-recipients, this treatment is effective, however, these devices still have limitations, which will be shown below, together with our attempts to address them. The potential impact in this field of research is considerable because over 360 Million people worldwide suffer from hearing loss (WHO, Feb. 2013; Fact Sheet N°300).

The inner ear is a complex biological structure composed of two major compartments containing the vestibular organs responsible for balance and the cochlea responsible for hearing, respectively. For hearing, hair cells (HCs) are critical because they transduce mechanical vibration into electrical stimulation of the auditory spiral ganglion neurons (SGNs). Many forms of sensorineural hearing loss originate from defects of HCs and CIs essentially bypass lost or not-functioning HCs by directly stimulating the SGNs electrically. One major limitation of CI systems is caused by the anatomical gap between the implant, consisting of linear array of 12 electrodes and the dendritic processes of the SGNs in the cochlea. As a consequence of this gap, stimulation from one electrode results in the simultaneous activation of a group of several hundreds of auditory neurons, thereby reducing the frequency resolution of the system and resulting in a high energy consumption of the device, a second drawback of the system. By creating a gapless interface between the electrode array and the auditory neurons, all these issues could be addressed simultaneously. The EU-FP7-funded project "NANOCI" (www.nanoci.org) (Grant agreement No.:281056) has been set up to achieve this ambitious goal combining biotechnology, nanotechnology and biomedical engineering in a balanced, multidisciplinary approach.

In order to simulate the NANOCI concept on a chip *in vitro*, we rely on Multi Electrode Array (MEA) as the basis of our *in vitro* experiments. MEAs are adequate to study the CI technology because stimulation and recording of neurons can be done simultaneously and distance related effects, resolution and response profiles can be assessed on multiple channels in parallel. The MEAs can also be seen as two dimensional cochlear implant where the electrodes are arranged on

a surface instead of a three dimensional helix. The MEA platform currently used in our laboratory (Qwane Biosciences, Lausanne) contains 64 platinum electrodes (40 x 40 µm with 200 µm space between two electrodes), which can all either be used for stimulation or for recording of extracellular single unit potentials. For our experiments, different culture types of mouse auditory neurons are tested on the MEA platform.

2 Methods

SGNs along with neighboring supporting cells and fibroblasts were isolated from 3-7 days old C57/Bl6 mice. Four different types of cell cultures were compared for best functional assessment on the MEA platform: single dissociated cells, partly dissociated micro explants, organotypic explants and stem/progenitor cell derived neurons. Single dissociated cells and partially dissociated explants were obtained by dissociating the SGN for 10 min with Accumax (Merck Millipore, Germany) at room temperature followed by mechanical trituration. Single dissociated cells were obtained by filtering the suspension through a 100µm strainer, whereas the micro explants were directly plated without filtering.

Organotypic explants correspond to linear sections from the SGN, keeping the original anatomy as intact as possible (Fig. 1). These three primary SGN cultures were grown in Neurobasal medium with 10% FBS (both Invitrogen, USA) for 2 weeks at 37°C. BDNF (25ng/ml; R&D Systems®, USA) was added to the medium for the first 4 days to initiate outgrowth of neurites. Stem/progenitor cells were isolated from the dissected SG tissue by an enzymatic digestion for 5 min with trypsin at 37°C and careful trituration. After filtering, single cells and small clumps were cultured in mitogen containing medium, following a published protocol to induce formation of floating spheres (Oshima *et al.,* 2009). Second generation spheres were plated and cultured for a two-week to induce differentiation into auditory neurons after withdrawal of mitogenic growth factors in serum free medium. For functional assessment, the four different cell cultures were differentiated directly on the MEA slides coated with either laminin/poly-L-lysine (laminin diluted 1:200 in 0.01% poly-l-lysine, both from Sigma) or matrigel (1:10, BD Biosciences) and grown for 2 weeks.

For immunohistochemistry, cultures were fixed and stained for βIII-tubulin (R&D, 1:200) to visualize the neurites, DAPI (Sigma, 10µg/ml) for cell nuclei and phalloidin (Sigma, 50µg/ml) for visualizing the actin cytoskeleton. The stained cultures were imaged using a fluorescent microscope (LSM700, Zeiss, Germany). Semiautomatic pixel counts were performed using the ImageJ™ software package.

For MEA recordings, cultures were perfused with an extra cellular solution (ECS) (145mM NaCl, 4mM KCl, 1mM MgCl2, 2mM CaCl2, 5mM Hepes, 2mM sodium pyruvate, and 5mM glucose [pH 7.4, room temperature]). To depolarize the cells and induce activity, cultures were perfused with ECS with 30mM potassium. To assess distance-related effects between the stimulating electrode and auditory neurons, cultures were stimulated via an external custom-designed MEDEL electrode (stimulus: 100ms, bi-phasic) that could be placed via a micromanipulator at distances ranging between 0 (gapless) and 70 µm (mimicking current CI systems) from the surface of the culture. The external electrode is a Teflon coated wire consisting of 90% platinum and 10% iridium and a diameter of 150µm. The stimuli were applied in 250 mV steps and ranged from 0 to 3 V.

Single unit potentials were recorded via LabView software and analyzed via IgorPro (Wavemetrics).

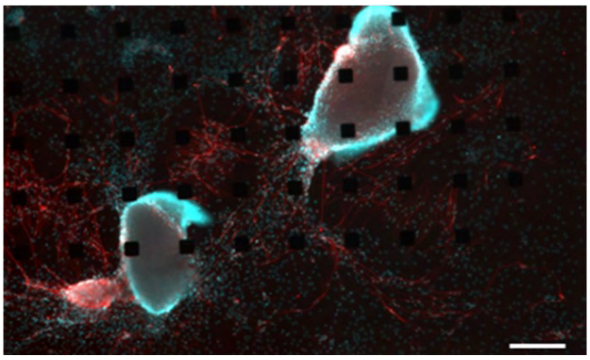

Fig. 1: Primary SGN culture (explants) cultured on MEA for 9 days, red (neurons, βIII-tubulin staining), blue (Nuclei, DAPI). Scale bar: 200µm.

3 Results

Comparative cell source assay: The morphological comparison of the four different culture types showed that SGN organotypic explants and micro explants had the highest densities of neurons quantified as number of βIII-tubulin positive pixels per DAPI positive pixels. In addition, the maximum length of neurites as assessed with ImageJ™ was highest in the same two preparations (data not shown). Density and length of neurites turned out to be important parameters for functional measurements, because a neurite has to cross at least two electrodes for stimulation/recording on the MEA setup. In case of single dissociated cells and stem/progenitor generated neuronal cells, the density on the MEA was not sufficient for stimulation and recording so far. For this reason, SGN organotypic explants were selected and further used for functional measurements on MEAs.

MEA experiments: Cultures were perfused with custom made physiological ECS. Some cultures showed spontaneous activity, whereas others were only active after depolarizing the auditory neurons with a perfusion of ECS containing 30mM potassium. In the latter case, neuron activity started 15s to 20s after onset of perfusion with action potentials occurring in a

variable range from 1 to 30 spikes per 100ms. We were also able to electrically stimulate the auditory neurons from MEA electrodes. Stimulation was reliably followed by one or more single unit events (action potentials) at one or more electrodes.

Distance related measurements: The stimulation with the external electrode mounted on the micromanipulator clearly showed distance-related effects. The experiment confirms that the higher the distance from the stimulating electrode to the auditory neuron culture, the higher was the voltage needed to trigger a first response (activation threshold) and thus to evoke neuronal activity (measured on MEA) (Fig. 2).

4 Conclusion/Summary

We were able to record single unit activity from organotypic cultures of spiral ganglion neurons on MEAs. Activity of these cultures was either spontaneous or could be triggered through a 30mM potassium perfusion or could be evoked by electrical stimulation from the MEA electrodes, which has not been reported previously. We were also able to do distance related stimulations in these cultures showing for the first time the efficacy of a cochlear implant might be increased dramatically by creating a gapless interface between the implant and the auditory neuron.

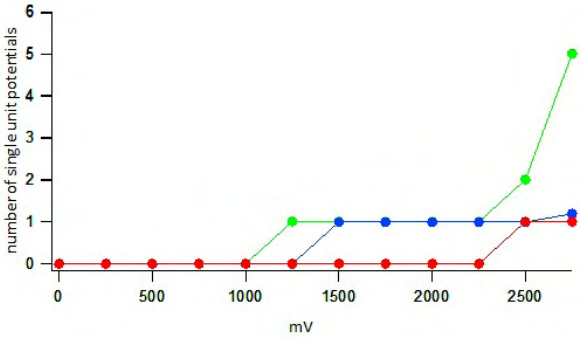

Fig. 2: Distance related effects on response profiles of auditory neurons when stimulated from an external electrode mounted on a micromanipulator positioned at a distance of 40µm (red), 20µm (green) and 0µm (gapless, blue). The average number of single unit potentials in response to 5 consecutive stimuli (y-axis) is plotted against the stimulation voltage (x-axis, mV).

Acknowledgement

This study was financially supported by the European Union`s Seventh Framework Programme (FP7/2007-2013 under grant agreement No. 281056). We thank Ruth Rubli, Department of Physiology, University of Bern, Bern, Switzerland for help with experimental cultures and Robin Davis, Department of Cell Biology and Neuroscience, Rutgers University, Piscataway, New Jersey for advice on neuronal culture.

References

[1] Oshima K., Senn P. And Heller S Isolation of sphere-forming stem cells from the mouse inner ear (2009) Auditory and Vestibular Research: Methods and Protocols. Humana Press. pp 141 – 162

PEDOT-CNT Coated Electrodes Stimulate Retinal Neurons with Low Voltage Amplitudes

Ramona Samba[1*], Thoralf Herrmann[2], Günther Zeck[2]

1 BioMEMS and Sensors Group, NMI at the University of Tübingen, Reutlingen, Germany
2 Neurochip Research Group, NMI at the University of Tübingen, Reutlingen, Germany
* Corresponding author. E-mail address: ramona.samba@nmi.de

Abstract
For electrical stimulation of neurons, methods that limit the polarization of the metal-based electrode to within safe electrochemical limits are desirable. Here we demonstrate that PEDOT-CNT coated electrodes are able to stimulate retinal circuitry presynaptic to the ganglion cells at stimulus thresholds between 200 – 600 mV for stimulus durations between 1000 – 100 ms respectively.

1 Background and aims

Electrical stimulation of the retina offers the possibility of partial restoration of visual function after degenerative diseases like retinitis pigmentosa[1, 2]. Challenges with current stimulation electrodes include side effects due to high stimulation thresholds and non-ideal electrode-tissue interface. PEDOT-CNT, a composite of the conducting polymer poly(3,4-ethylenedioxythiophene) and carbon nanotubes, has been recently presented as a highly biocompatible electrode material for neuronal applications, exceeding state-of-the-art electrodes in electrical performance[3]. In this work, PEDOT-CNT was investigated towards its performance in retinal stimulation, based on the hypothesis of lower stimulation thresholds due to higher charge transfer capacitance.

2 Methods

The details on the fabrication of PEDOT-CNT MEA can be found in Gerwig et al., 2012[3]. Briefly, a standard MEA with gold microelectrodes (30 µm diameter) was coated employing electropolymerization in a suspension of single-walled carbon nanotubes, poly(styrenesulfonate) and 3,4-ethylenedioxythiophene. Impedance at 1 kHz was measured in PBS after fabrication and in between different sets of stimulation experiments.

The retina of Sprague Dawley rats was prepared as described in Stutzki et al., 2014[4]. Briefly, isolated retinal portions were mounted ganglion cell side down on the MEA. During recordings, the retina was constantly perfused with warm oxygenated Ames' medium.

Extracellular stimulation was performed using constant cathodic voltage pulses applied to set of eight microelectrodes. Spikes from retinal ganglion cells (RGCs) were recorded by the electrode in the centre of the eight stimulation electrodes. Stimulus durations were 0.1, 0.2, 0.5 and 1 ms. Standard TiN microelectrodes served as control.

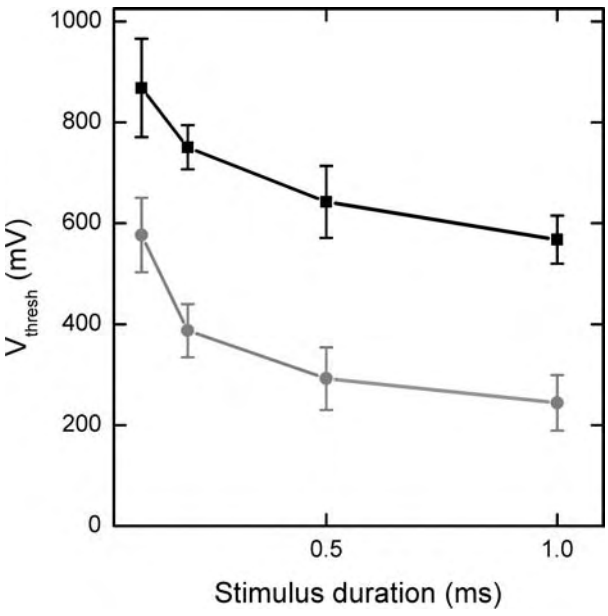

Fig. 1. Threshold stimulation voltages (V_{thresh}) are smaller for PEDOT-CNT electrodes as compared to TiN electrodes of the same size. Mean threshold voltage calculated for eight RGCs stimulated with TiN electrodes (black squares) and six RGCs stimulated with PEDOT-CNT coated gold electrodes (gray circles). Error bars represent standard error of the mean.

3 Results

For each stimulus duration the voltage amplitude was increased in incremental steps. Stimulated ganglion cell activity was detected in a time window of 10 – 20 ms after stimulus onset. Spikes in this time window are evoked by indirect stimulation, i.e. stimulation of the retinal circuitry presynaptic to the ganglion cell[5].

The voltage threshold activity was determined as that value which evoked a spike in 50 % of the stimu-

lus repetitions. Threshold voltages were estimated for each stimulus duration.

The mean threshold voltage for ganglion cells stimulated with TiN electrodes (n=8 RGCs) is about twice as high as the mean threshold voltage for stimulation with PEDOT-CNT coated gold electrodes (n=6 RGCs) (see figure 1).

Electrode impedance increased only slightly after several experiments and was still below 30 kΩ. No significant impedance difference was found between electrodes used for stimulation and unused ones.

4 Conclusion

PEDOT-CNT microelectrodes enable stimulation of retinal circuitry at lower voltages than state-of-the-art TiN microelectrodes. Lower voltages prevent damage by electrochemical side reactions. Therefore, PEDOT-CNT microelectrodes are attractive for neuroprosthetic applications.

Acknowledgement

Funding for this research was in part obtained from the German Federal Ministry of Education and Research through grant no. 01GQ0834 (RS) and grant no. 1312038 (TH and GZ). We thank NMI TT GmbH and Multi Channel Systems GmbH for support in MEA technology.

References

[1] A. Ahuja, et al., *British Journal of Ophthalmology* **2011**, *95*, 539-543.
[2] R. Wilke, et al., *Investigative ophthalmology & visual science* **2011**, *52*, 5995-6003.
[3] R. Gerwig, et al., *Frontiers in Neuroengineering* **2012**, *5*, 1-11.
[4] H. Stutzki, et al., *Frontiers in Cellular Neuroscience* **2014**, *8*, 38.
[5] M. Eickenscheidt, et al., *Journal of neurophysiology* **2012**, *107*, 2742-2755.

Wide-Field Photostimulation of Cortical Networks: Selective Activation of Excitatory Neurons and Its Impact on Evoked Reverberating Responses *In Vitro*

Rocco Pulizzi[1†], Gabriele Musumeci[1†], Chris Van Den Haute[2], Veerle Baekelandt[2], and Michele Giugliano[1,3,4*]

1 Department of Biomedical Sciences, University of Antwerp, Belgium;
2 Department of Neurosciences, KU Leuven, B-3000 Belgium;
3 Brain Mind Institute, EPFL, Switzerland;
4 University of Sheffield, S1 4DP Sheffield, UK.
† Equal contribution
* Corresponding author. E-mail address: michele.giugliano@uantwerpen.be

Abstract
Dissociated cortical networks developed on microelectrode arrays (MEAs) and expressing Channelrhodopsin-2 selectively in principal neurons, were our experimental model. We non-invasively monitored the spontaneous and light-evoked multi-unit responses to wide-field LED photoactivation. This approach allows us to manipulate the reverberating network response, thus proving to be a potential key tool for establishing closed-loop paradigms.

1 Background

Closed-loop control of cell assemblies via optogenetics has been suggested as a pivotal (causative) approach, required to advance our current (correlative) understanding of the neuronal substrates for memory and behaviour [1, 2]. However, due to present limitations, in vivo photostimulation in the cortex or hippocampus generally addresses a population of cells simultaneously, rather than one cell at the time [3, 4]. Thus, besides the downstream responses, arising from direct excitation or inhibition, photostimulation may also elicit reverberating local responses. These are a consequence of recurrent connectivity and may reflect a variety of time-scales and dynamical properties, whose precise control is complex. Here, we explored photostimulation in recurrent networks, by a reduced in vitro model.

2 Methods

We employed postnatal rat neocortical cell cultures, grown on substrate-integrated microelectrode arrays (MEAs) at 37°C, 5% CO2, 95% R.H. for several weeks. Five days after plating, neurons were transduced by adeno-associated viral particles (AAV) to express a double mutant version of ChannelRhodopsin-2 (C2-LCTC) conjugated with a reporter protein (mCherry). Exploiting the CaMKIIα promoter upstream the coding sequence, C2-LCTC could be restricted to excitatory neurons and enabling their activation by light [5]. We delivered wide-field LED photostimulation (2 mW*mm^{-2}, 470 nm, Rebel, Quadica Devel., Canada), employing a stimulus isolator (STG1002, Multichannel Systems, Germany) and an externally dimmable DC Driver (LuxDrive, Randolph, USA). We simultaneously recorded neuronal multiunit activity by the MEAs via an amplifier (MEA1060BC, Multichannel Systems) and studied spontaneous and light-evoked electrical activity, in mature cultures (i.e., 28-43 days in vitro). Recorded signals were analysed by using custom made software written in C and Matlab (The MathWorks, USA) [6]. The Pearson's coefficient and its significance were employed to assess correlations.

3 Results

ChannelRhodopsin-2 expression resulted in a large number of photosensitive (~80%) neurons, and led to normal ex vivo neuronal survival and development, with the typical irregular emergence of synchronized collective bursting, as in control cultures.

Brief light pulses evoked highly reproducible network-wide responses, consisting of i) an early phase (i.e., 0-20ms, immediately after the stimulus), and of ii) a late phase, lasting up to 400ms and fully abolished by bath-applied synaptic blockers. Interestingly, the duration of the pulses (i.e., 0.1-20ms) appeared linearly correlated with time course and profile of the evoked firing response, during its late but not its early phase.

In particular, a longer pulse reliably delayed the peak of the response (i.e., from 50 to 150ms). Furthermore, light stimulation elicited global coherent oscillatory firing, in the gamma range. Unexpectedly, the dominant oscillation frequency and its power were also linearly correlated with the duration of the light pulse.

4 Conclusion

Besides clarifying further the impact of optogenetic manipulations in recurrent microcircuits, our results provide a first indication that light duration can be employed to differentially manipulate network responses, altering feed forward or feedback components, which is extremely relevant for the design of closed-loop experimental paradigms aimed at steering network responses.

Acknowledgement

We are grateful to Mr. D. Van Dyck and Mr. M. Wijnants for excellent technical assistance. We thank Mr. J. Couto, Dr. M. Chiappalone and Dr. M. Mahmud for scientific discussions. Financial support from EC-FP7 (Marie Curie Network “NAMASEN”, grant n. 264872, ICT-FET project “ENLIGHTENMENT”, grant n. 284801), Research Foundation Flanders, grant n. G.0888.12N, and the Interuniversity Attraction Poles Program (IUAP), initiated by the Belgian Science Policy Office, is kindly acknowledged.

References

[1] Olsen, S. R., Bortone, D. S., Adesnik, H., & Scanziani, M. (2012). Gain control by layer six in cortical circuits of vision. Nature, 483(7387), 47–52.

[2] Lee, S.-H., Kwan, A. C., Zhang, S., Phoumthipphavong, V., Flannery, J. G., Masmanidis, S. C., Dan, Y. (2012). Activation of specific interneurons improves V1 feature selectivity and visual perception. Nature, 488(7411), 379–83.

[3] Belzung, C., Turiault, M., & Griebel, G. (2014). Optogenetics to study the circuits of fear- and depression-like behaviors: A critical analysis, Pharmacology, Biochemistry and Behavior, 122, 144–157.

[4] Roux, L., Stark, E., Sjulson, L., & Buzsáki, G. (2014). In vivo optogenetic identification and manipulation of GABAergic interneuron subtypes. Current Opinion in Neurobiology, 26C, 88–95.

[5] Prigge, M., Schneider, F., Tsunoda, S. P., Shilyansky, C., Wietek, J., Deisseroth, K., & Hegemann, P. (2012). Color-tuned channelrhodopsins for multiwavelength optogenetics. The Journal of Biological Chemistry, 287(38), 31804–12.

[6] Mahmud, M., Pulizzi, R., Vasilaki, E., & Giugliano, M. (2014). QSpike tools: a generic framework for parallel batch preprocessing of extracellular neuronal signals recorded by substrate microelectrode arrays. Frontiers in Neuroinformatics, 8 (March), 1–14.

Restoring Light Sensitivity in Blind Retinae Using Next-Generation Photopharmacology

Laura Laprell*, Martin Sumser, Dirk Trauner

Ludwig-Maximilians-Universitaet, Munich, Germany
* Corresponding author. E-mail address: laura.laprell@cup.lmu.de

Abstract
It has been estimated that more than 300 million people worldwide are suffering from blindness or impaired vision. Although the photoreceptor cells in some cases undergo complete degeneration, the remains of the retinal circuitry and especially the ganglion cells, which generate the output of the retina to the brain are often not affected and are still functionally intact. In order to restore light sensitivity to blind retinae, optochemical tools targeting receptors natively expressed in retinal cells provide a new photopharmacological strategy without the need of any genetic manipulation. We introduced the concept of photochromic ligands (PCL), which takes advantage of photoswitchable azobenzene molecules. These molecules are chemically modified in such a way that they enable optical control of neuronal activity by acting as selective photoswitchable receptor ligands or blockers of voltage-gated ion channels (VGIC). The molecule presented here is a photochromic potassium channel blocker and represents a very promising next-generation molecule for restoring light sensitivity in blind retinae.

1 Introduction

Recently, we introduced optochemical genetics as a new tool for the light-dependent control of intrinsic receptor function [3]. This photopharmacological approach is based on the application of photochromic ligands (PCLs) that bind non-covalently to their target receptors [1][7], consequentially activating/inactivating them in a reversible fashion (Fig. 1). Generally, PCLs are comprised of a ligand binding domain, a linker region and an azobenzene moiety. The azobenzene, responsible for the light-sensitivity, can exist either in the thermodynamically stable *trans*- or in the less stable *cis*-state. Upon irradiation with certain wavelengths one can switch between these two states. Only in one configuration the PCL can bind to the receptor, in the other it is sterically hindered (Fig. 1A). This strategy is not limited to control receptor activation, but can also be applied for blocking and unblocking ion channels [4] (Fig. 1B).

Since PCLs usually bind in a similar fashion as ligands to their respective receptors, the photopharmacological approach can easily be applied *in-vitro* or *in-vivo* to any tissue expressing the target receptor [4][6]. Polosukhina et al. (2012) could demonstrate that light-switchable open channel blockers applied to the eye (intravitreal injection) of blind mice are capable to restore light sensitivity [5]. One major drawback of this study was the use of the first generation open-channel blocker Acrylamide-Azo-Quaternary ammonium (AAQ) that has to be actively switched with 380 nm and 500 nm. Here, the requirement of UV-light illumination limits its applicability as a drug for vision restoration.

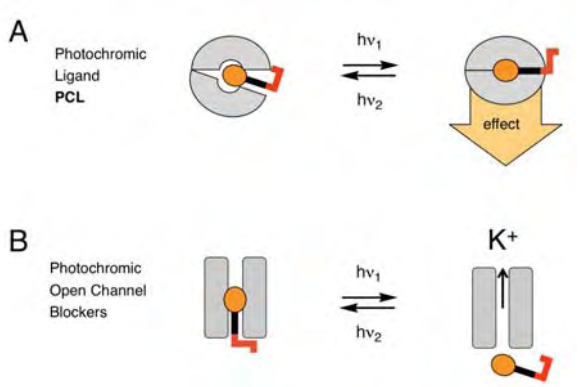

Fig. 1. (A) Schematic drawing of the photochromic ligand approach (PCL). The ligand carries a light-sensitive moiety, an azobenzene, which changes its conformation between the active and inactive state upon irradiation with specific wavelengths
(B) Photochromic open channel blockers represent a special case of PCLs. Only in one conformation the photoswitch blocks the pore of the channel, in this case a potassium channel.

Currently, we are working with a next-generation open-channel blocker 'red-DAD'. This molecule harbors several features, making it superior to AAQ for an application in vision restoration. First, the compound is not permanently charged and thereby crosses biological barriers more easily. Second, it is red-shifted, i.e. one can switch 'red-DAD' with blue or white light (440-480 nm, Fig.2). Third, lower light intensities in the range of bright ambient illumination are needed (data not shown). Finally, it relaxes back to the thermodynamically stable *trans*-configuration within 200 ms after turning of the light (data not shown).

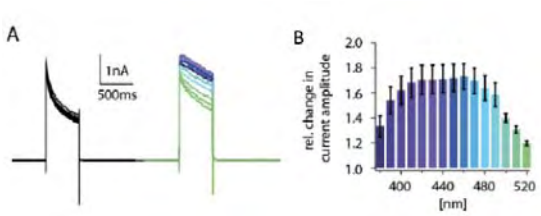

Fig. 2. (A) Potassium channel recordings in cortical neurons after application of red-DAD. In darkness channel pore is blocked by red-DAD.This block is optimally released with illumination between 420 and 460 nm light (B).

2 Methods

For *in-vitro* studies with completely light-insensitive murine retinae (cngA3$^{-/-}$, rho$^{-/-}$, opn4$^{-/-}$, similar to the mice used in [2]) retinal explants were shortly incubated with 'red-DAD' and mounted on a multi-electrode array (MEA). The detected spiking frequencies of RGCs integrate signals from all retinal cells, which are recorded by the MEA.

3 Results

By alternating 480 nm light and darkness it can be demonstrated that the pre-incubated retinae induce higher spiking frequency during illumination whereas the control retinae do not respond to light (Fig. 3).

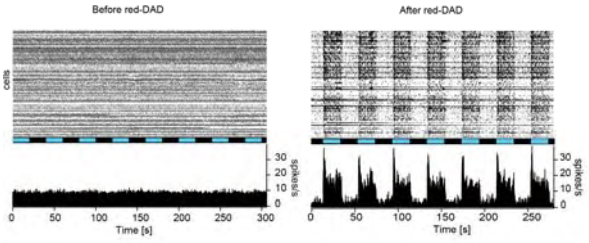

Fig. 3. (A) Top: Rasterplot of an MEA recording of an untreated cngA3$^{-/-}$, rho$^{-/-}$, opn4$^{-/-}$ mouse stimulated with 480nm light (blue bars). Bottom: Average histogram. Firing rate in Hz (spikes/s).
(B) Rasterplot and histogram of 'red-DAD' treated retina stimulated with 480nm light.

By blocking specific synaptic transmission pathways, one can identify, on which cell types 'red-DAD' acts in retinae. Carrying out similar pharmacological experiments as in [5] we identified bipolar cells as the primary target of red-DAD (data not shown).

4 Discussion

Taken together, 'red-DAD' is a promising next-generation molecule for restoring light-sensitivity in blind retinae. It penetrates easily into retinal cells, can be switch with moderately bright intensities of visible light and has the advantage of acting on bipolar cells. Activating bipolar cells will lead to highly complex RGC signal outputs to the brain due to lateral connections via amacrine cells. The more complex a signal is the more information it contains.

References

[1] Bartels E, Wassermann NH, Erlanger BF. Photochromic activators of the acetylcholine receptor. Proc Natl Acad Sci U S A. 1971, 68, 1820-3.
[2] Claes, E., Seeliger, M., Michalakis, S., Biel, M., Humphries, P. and Haverkamp, S. Morphological characterization of the retina of the cnga3(-/-)rho(-/-) mutant mouse lacking functional cones and rods. Inves Ophthalmol Vis Sci 2004, 45, 2039–48.
[3] Fehrentz T, Schönberger M, and Trauner D. Optochemical genetics. Angew Chem Int Ed Engl. 2011, 50, 12156-82.
[4] Mourot A, Kienzler MA, Banghart MR, Fehrentz T, Huber FM, Stein M, Kramer RH, Trauner D. Tuning photochromic ion channel blockers. ACS Chem Neurosci. 2011, 2, 536-43.
[5] Polosukhina A, Litt J, Tochitsky I, Nemargut J, Sychev Y, De Kouchkovsky I, Huang T, Borges K, Trauner D, Van Gelder RN, Kramer RH. Photochemical restoration of visual responses in blind mice. Neuron. 2012, 75, 271-82.
[6] Stawski P, Sumser M, Trauner D. A Photochromic Agonist of AMPA Receptors. Angew Chem Int Ed Engl. 2012, 51, 5748-5751.
[7] Volgraf M, Gorostiza P, Szobota S, Helix MR, Isacoff EY, Trauner D. Reversibly caged glutamate: a photochromic agonist of ionotropic glutamate receptors. J Am Chem Soc. 2007, 129, 260-1.

Finding the Most Effective Site for Extracellular Neuronal Stimulation

Milos Radivojevic, David Jäckel, Jan Müller, Vijay Viswam, Ian Lloyd Jones, Andreas Hierlemann, and Douglas Bakkum

ETH Zürich, Bio Engineering Laboratory, D-BSSE, Basel, Switzerland
* Corresponding author. E-mail address: milos.radivojevic@bsse.ethz.ch

Abstract
Here, we present a method to investigate the possibilities of selective, extracellular stimulation of rat cortical neurons grown over a high-density complementary metal–oxide–semiconductor microelectrode array.

1 Background / Aims

Knowledge of effective extracellular stimulation methods optimal stimulation locations and stimulation signal magnitudes to selectively stimulate single neurons is important for designing electrophysiological experiments. However, stimulation artifacts usually compromise the ability to record neuronal responses in close proximity to the stimulation site and to fully evaluate stimulus efficiency at single-cell resolution. To overcome this issue, we used a high-density complementary metal–oxide–semiconductor (CMOS) microelectrode array (HD-MEA), which allows for single-cell electrical activity to be recorded from a large number of electrodes and for stimulus efficacy to be judged by reading out the cell's somatic and axonal responses.

2 Methods / Statistics

We grew primary rat cortical neurons on CMOS-based HD-MEAs developed in our laboratory [1]. The array contains 11,011 densely packed electrodes, each of which can be used as recording or stimulation site. Thanks to an excellent signal-to-noise ratio, the array is sensitive enough to detect both somatic and propagating axonal action potentials [2]. To improve array performance, electrodes were covered with platinum-black. We measured the relative impedance of each electrode to confirm the homogeneity of platinum-black deposition and found negligible variations in impedance among electrodes. In our experiments, we used the CMOS MEA to simultaneously stimulate and sample electrical signals at spatially distant compartments of the same neuron (soma vs. axon) in order to reduce the influence of stimulation artifacts.

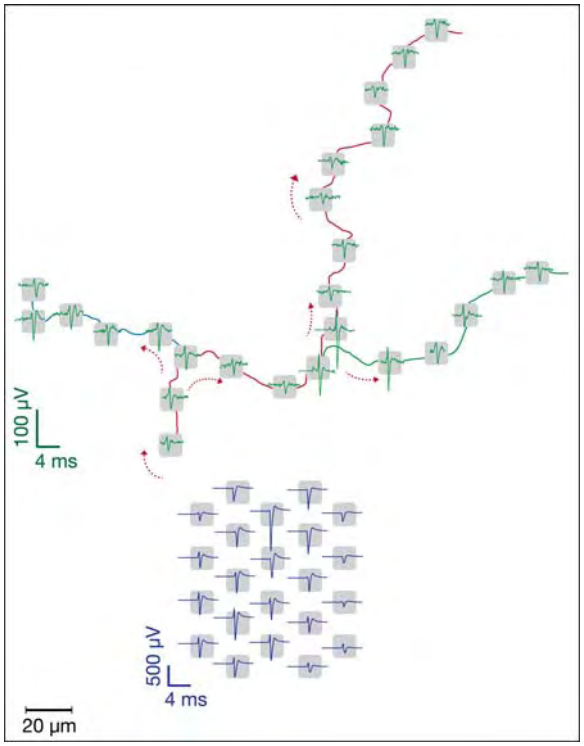

Fig. 1. Averaged electrical signals of a single neuron. Somatic (purple) and axonal (green) "footprints" are reconstructed based on antidromic and orthodromic stimulation-triggered neuronal responses,.

3 Results

Somatic and axonal locations of individual neurons were detected and identified according to their spontaneous and/or stimulation-triggered voltage traces (Figure 1) [2]. We used different electrode configurations to investigate somatic and axonal excitability. In a first configuration, "somatic electrodes" were used to apply stimulation and "axonal electrodes" were used for readout of triggered neuronal signals. In a second configuration, electrodes covering preselected areas of the axonal "footprint" were used to apply stimulation, while other available electrodes (axonal and somatic) were used as readout (Figure 2). Stimuli included biphasic voltage pulses

(between ±10 to 300 mV; 10 mV steps) and were applied 20 times per voltage value at a frequency of 5Hz. Each stimulation electrode was probed with increasing voltages until an evoked signal was detected on the readout electrodes. To get finer resolution excitability profiles, smaller 1 mV steps were used and applied in random order. We found that the most sensitive somatic site lies near the peak amplitude of the somatic voltage trace (8 out of 8 cases). Experiments, in which we probed all electrodes covering axonal locations, revealed higher excitability of the most sensitive somatic over axonal sites (3 out of 4 cases).

4 Conclusion/Summary

We established a method to reliably investigate somatic and axonal excitability of cortical neurons grown over CMOS HD-MEAs based on their spontaneous and/or stimulation-triggered electrical activity. Our preliminary data indicate that highly excitable neuronal sites co-localize with peaks of the reconstructed neuronal "footprint" (Figure 2) and suggest higher sensitivity of somatic over axonal sites to biphasic voltage stimulation.

Acknowledgement

Supported by the Swiss National Science Foundation Ambizione Grant PZ00P3_132245 and FP7 of the European Community through the ERC Advanced Grant 267351 'NeuroCMOS'.

References

[1] Frey, U. et al. (2010) Switch-matrix-based high-density microelectrode array in CMOS technology. *IEEE J. Solid-St. Circ. 45, 467–482*

[2] Bakkum, D. J. et al. (2013) Tracking axonal action potential propagation on a high-density microelectrode array across hundreds of sites. *Nature Commun. 4:2181.*

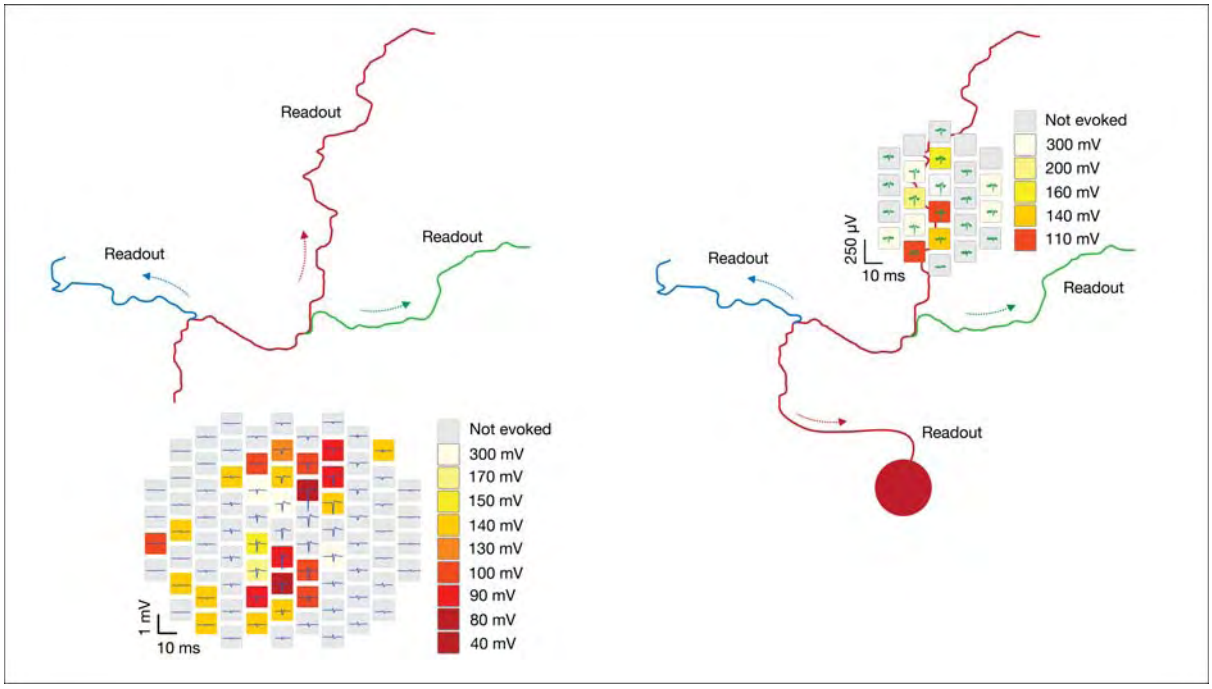

Fig. 2. Responsiveness of somatic (left) and axonal (right) sites to biphasic voltage stimulation.

Stimulation and Recording from the Same Microelectrode Using Low-Gain High-Resolution Data Acquisition System

Hyunjun Jung[1], Yoonkey Nam[1*]

1 Neural Engineering Laboratory, Department of Bio and Brain Engineering, Korea Advanced Institute of Science and Technology (KAIST), Daejeon, Republic of Korea
* Corresponding author. E-mail address: ynam@kaist.ac.kr

Abstract
Electrical stimulation is able to elicit neural activity by depolarizing the membrane potential. This technique is a powerful tool for clinical and physiological application. During the stimulation, a large artefact, which is thousands of times bigger than the spike, acts as an impulse input to High Pass Filter (HPF) that is essential to remove electrode dc potential. Fluctuating impulse response of HPF is clipped by the narrow input range of high gain amplifier. Because of this interaction between HPF and high gain amplifier, it is impossible to record the direct response on stimulating electrode for several milliseconds. Our goal is to record neural activity directly on a stimulating electrode. We used low gain single stage amplifier and 24-bit ADC to record neural signal without HPF. After stimulus potential from stimulating electrode was recorded totally and we applied revised SALPA algorithm to eliminate stimulus artefact (SA). Consequentially, our system can record neural signals in 2ms after stimulus and we recorded several non-synaptic responses which could not be recorded previously.

1 Introduction

Electrical stimulation is one of the essential techniques to modulate neural activity of neural circuits. Measuring neural responses after the electrical stimulation provides important information about the excitability or connectivity of targeted regions [1]. However, it is very difficult to record neural responses immediately after the stimulation due to stimulation artefacts implicated in neural recording system [2]. Despite various approaches (e.g., blanking and discharge circuitry, Wiener filtering, template subtraction method, subtraction of artefacts by local polynomial approximation algorithm)), it is still challenging to recover neural spikes directly from the stimulation electrodes within a few milliseconds [3].

Here we propose a novel neural recoding strategy to recover neural spikes from a microelectrode that was used for both electrical stimulation and recording. We were motivated by the fact that high resolution Analog-Digital Converters (ADC, 16 or 24 bit) are more commonly used in neural instrumentation, thus allowing us to use low-gain wide-bandwidth amplifiers for conditioning microelectrode signals containing large DC drift and small neural spikes. Here, we designed a fast responding data acquisition system and tested for the early recovery of neural spikes from a stimulating electrode.

2 Methods

Fig. 1 shows the experimental setup for the proposed neural signal processing system. A microelectrode was connected with both amplifier input and stimulator output. A non-inverting amplifier was designed with an FET-input OP-AMP (AD823, Anolog Devices, Norwood, USA). The amplifier was operated by 9-V battery to reduce power-line noise. The output of the amplifier stage was connected with 24-bit data acquisition system that was composed of 24-bit ADC and an anti-aliasing filter NI9239 (fs = 25 kHz, National instruments Corp, Austin, USA).

To elicit neural responses, biphasic current pulses (amplitude: 1 ~ 20 μA, pulse width: 200 μs) were generated by STG4002 (Multichannel Systems, Reutlingen, Germany). An analog switch was used to connect the stimulator with a microeletrode during the stimulation.

We used “SALPA” algorithm [4] that was developed to remove stimulation artefact in real-time neural signal processing. Two parameters (pre-window and post-window length) were tuned to achieve the minimum recovery time and spike conservation ratio. A dissociated hippocampal neuronal culture from E18 rat was used to verify the system performance and a planar-type microelectrode array with platinum black microelectrodes (diameter: 50 μm) was used for electrical stimulation and recording.

Continuous or triggered recording of electrode potential, on-line SA suppression were performed by customized LabVIEW program. (National instruments Corp, Austin, USA).

(a)

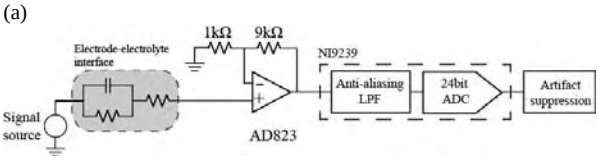

(b)

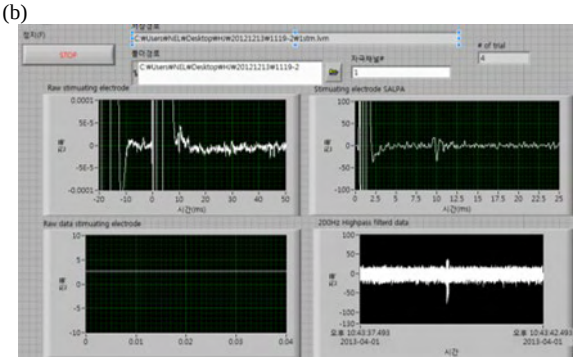

Fig. 1. System diagram of the LGHR system (a) and customized LabVIEW program (b)

3 Results

The 24-bit ADC provided two advantages in designing the neural recording system: low gain amplification(x10) and wide-bandwidth recording (0 – 12.5 kHz). System noise level was sufficiently small for low-noise neural recordings (input-referred noise: 20 μVpp (1 Hz- 8 kHz filtered)). The input dynamic range was ±875 mV. As there was no analog high-pass filter before the digitization, signal loss from amplifier saturation or clipping was minimized. After the digitization, we attempted to remove slowly recovering transient signals originated from metal-electrolyte double-layer capacitance. Fig 2(a) shows the removal of slowly decaying baseline using digital filters (200 Hz or 500 Hz high pass filter) or SALPA algorithm. We found that an asymmetric local curve fitting window was most effective in obtaining early baseline recovery time (2 ms) and low spike attenuation (64.9 %). Using this system, we were able to record neural spikes from an electrically stimulating microelectrodes reliably. Fig. 2(b) shows a representative recording from a cultured hippocampal neurons. Extracellular spikes as early as 2 ms were clearly recorded. Electrical stimulation can be as large as 30 μA or 500 mV and we can still recover neural spikes after 2 ms.

(a)

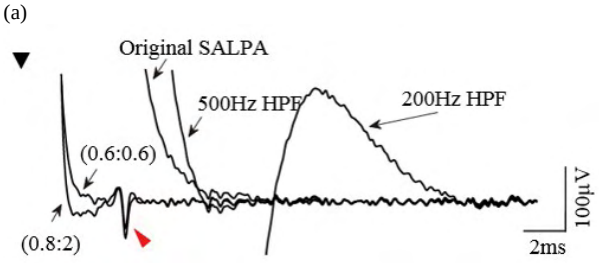

(b)

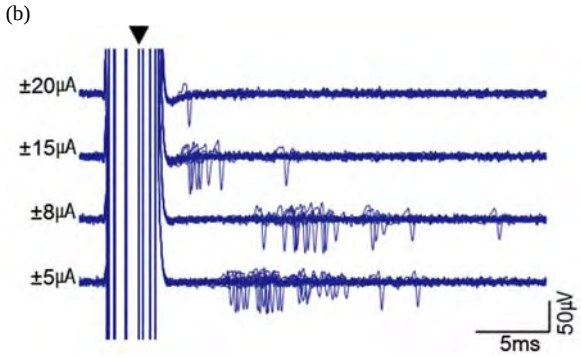

Fig. 2. Removal of SA and demonstration of direct response from stimulating electrode. Recovered signal through SALPA with 3 parameter sets and 2 HPF (a). Responses from 19 DIV cultured neural network was induced by 200 μs per phase negative first biphasic current pulse. 20 responses were overlaid. (b). Vertical lines near black arrow indicate SALPA artefact. (Black arrow: stimulus onset, Red arrow: spike)

4 Conclusion

We designed a simple system which can record neural responses from electrically stimulating electrode in 2 ms after stimulus robustly. Due to wide input dynamic range and omission of HPF, slowly changing after stimulus potential was totally recorded. Also, we revised SALPA for faster recovery and recorded signals in 2ms after stimulus which could not be recorded before. The proposed system can be piggy-backed to existing electrical neuro-modulation systems (e.g. deep brain stimulator) to investigate the effect of neural stimulations at the target spot.

Acknowledgement

This work was supported by National Leading Research Laboratory program (NRF-2012R1A2A1A01007327), from National Research Foundation of Korea.

References

[1] Y. Jimbo and A. Kawana, “Electrical stimulation and recording from cultured neurons using a planar electrode array,” Bioelectrochemistry Bioenerg., vol. 29, no. 2, pp. 193–204, Dec. 1992.

[2] E. a Brown, J. D. Ross, R. a Blum, Yoonkey Nam, B. C. Wheeler, and S. P. Deweerth, “Stimulus-artifact elimination in a multi-electrode system.,” IEEE Trans. Biomed. Circuits Syst., vol. 2, no. 1, pp. 10–21, Mar. 2008.

[3] K. Limnuson, H. Lu, H. J. Chiel, and P. Mohseni, “Real-Time Stimulus Artifact Rejection Via Template Subtraction.,” IEEE Trans. Biomed. Circuits Syst., pp. 1–10, Sep. 2013.

[4] D. a Wagenaar and S. M. Potter, “Real-time multi-channel stimulus artifact suppression by local curve fitting.,” J. Neurosci. Methods, vol. 120, no. 2, pp. 113–20, Oct. 2002.

Combining an Optical Eye Model and MEA Recordings for Testing of Retinal Prostheses

John M Barrett[1*], Lionel Chaudet[2], Mark Neil[2], Na Dong[3], Xiaohan Sun[3], Evelyne Sernagor[1], Patrick Degenaar[4]

1 Institute of Neuroscience, Newcastle University, United Kingdom
2 Imperial College, London, United Kingdom
3 South East University, Nanjing, China
4 School of Electrical and Electronic Engineering, Newcastle University, United Kingdom
* Corresponding author. E-mail address: j.m.barrett@ncl.ac.uk

Abstract
Typical light stimulation setups used in the investigation of optogenetic retinal prostheses do not take into account the modification of the incoming light by the optics of the eye itself. Thus, we developed an experimental setup that allows multielectrode array recordings from *ex-vivo* retinas while projecting light from an array of high-intensity Gallium Nitride microLEDs through an optical model of the human eye onto the retina. We were able to focus the LED array image onto the retina successfully and evoked channelrhodpsin-2 mediated light responses in healthy and in genetically blind retinas. We will use this system to explore improved strategies for optogenetic retinal prostheses.

1 Background

Retinal prostheses seek to restore vision to patients affected by retinal dystrophies (characterised by photoreceptor degeneration) by stimulating the surviving neurons. Current devices return only limited vision, still within the range of legal blindness [1]. One promising approach is optogenetics – photosensitizing the surviving neurons with light-sensitive ion channels or pumps.

In our lab, we investigate this approach *in-vitro* using retinas from transgenic mice with photoreceptor degeneration and retinal ganglion cells (RGCs) expressing the light-sensitive cation channel, channelrhodopsin-2 (ChR2). As ChR2 requires high radiance stimulation, we aimed to demonstrate scalability of microLED (µLED) optical stimulator arrays [2,3] to head-mounted prostheses.

In *in-vitro* studies of optogenetic RGC stimulation, light is typically delivered onto the retina using microscope objectives (e.g. [4]), but this does not take into account how the image is altered by the optics of the eye itself and the virtual reality optics required to deliver it. We therefore designed and built a system for projecting µLED array light through a realistic optical model of the human eye onto isolated mouse retinas, while recording RGC responses using microelectrode arrays (MEAs).

2 Methods

The OEMI-7 (Ocular Instruments, Cordova, USA) is an optical model of the human eye for ophthalmological training. We constructed an adapter to attach the OEMI-7 to an MEA1060-Inv amplifier (MultiChannel Systems (MCS), Reutlingen, Germany). We used 60-channel ITO MEAs (MCS) to record from isolated B6.Cg-Tg(Thy1-ChR2/EYFP)9Gfng/J (*ChR2*) mouse retinas with channelrhodopsin-expressing RGCs and retinas from a cross between *ChR2* mice and the C3H/HeNHsd mouse model of retinitis pigmentosa (*ChR2rd1* mice).

Fig.1. View of the artificial eye and virtual reality lens from below. Light is projected from the LEDs (not pictured), through microlenses and focussing optics onto a mirror (bottom right), then reflected and refracted through the virtual reality lens into the artificial eye (top), which focuses the light on the retina. The blue line shows the approximate path taken by the LED light. The metal plate at the top holds the eye and the MEA amplifier

We provided light stimulation using a 256-pixel microLED array, custom fabricated using 0.35µm CMOS and GaN LED technologies [2,3]. We project-

ed the LED light onto the MEA holding the retina through a microlens array and projection optics [5] (to improve efficiency and fill factor), an eMagin z800 virtual reality prism lens (eMagin, Bellevue, USA), and the OEMI-7 (Fig 1).

3 Results

We successfully focussed the LED array image through the OEMI-7 and the translucent MEA onto the RGC layer (Fig 2) and recorded ChR2-mediated spiking responses. The transmission efficiency was approximately 2.5%, a 3-fold improvement over the 0.86% efficiency of focussing similar LEDs through a 2X objective via the camera port of an inverted microscope (Olympus IX-71; Olympus, Tokyo, Japan).

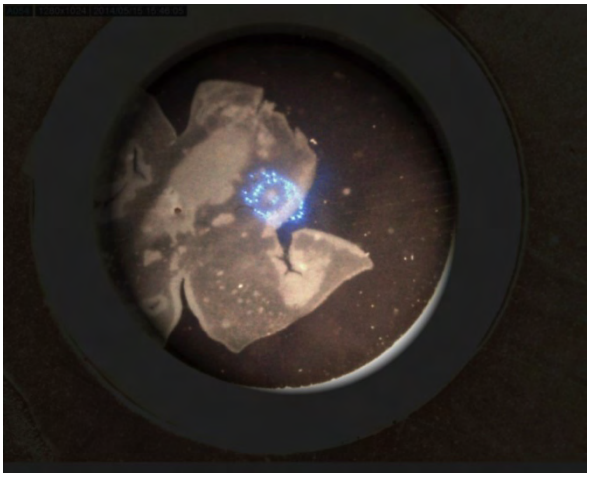

Fig.2. Photomicrograph of an isolated *ChR2rd1* retina mounted on a 60-channel ITO MEA. An image projected by the LEDs is focussed onto the retina by the optical system.

We were able to evoke light-driven spikes with a minimal irradiance on the retina of 14.3 μW/mm^2 (3.4×10^{13} photons/mm^2/s at 470nm) in *ChR2* retinas and 82.6μW/mm^2 (2.0×10^{14} photons/mm^2/s) in *ChR2rd1* retinas (Fig 3). The median threshold light flash duration (i.e. the duration required to evoke a response on 50% of trials) at the stated intensities was 23.3ms and 63.7ms, respectively. The energy supplied to the LEDs for successful full-field stimulation in the *ChR2rd1* retinas was approximately 1J, but future improvements in both optoelectronic and optical efficiencies, in addition to improved channelrhodopsin sensitivities, are likely to reduce this.

Furthermore, this 1J is equivalent to an all-white image, whereas real world image transfer only requires 10-15% of the scene to be illuminated after retinal processing [6]. As such, the total power requirement, including 0.5-1W for processing, can be kept below the <5W limit for passive cooling. This is similar to current mobile phone and tablet technologies.

4 Conclusion

We developed an optical system for stimulating retinas in a way that mimics how light would realistically stimulate optogenetically engineered RGCs in retinal dystrophy patients. Our results indicate that microLED arrays are scalable to wearable optogenetic prostheses. We will use this system to explore improved stimulator technology and signal processing strategies for optogenetic retinal prosthetics.

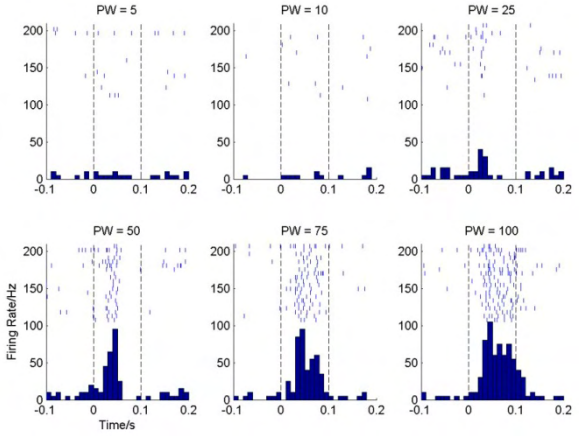

Fig.2. Raster plots and peristimulus time histograms showing responses of an example cell from a *ChR2rd1* retina to μLED stimulation at 82.6μW/mm^2. Each plot represents responses to a 5, 10, 25, 50, 75 or 100ms full-field light flash.

Acknowledgement

This work was supported by the Wellcome Trust [096975/Z/11/Z] (JB, ES, PD) and EU FP7 research project OPTONEURO [249867] (LC, PD).

References

[1] Stingl, K. K. et al. (2013): Artificial vision with wirelessly powered subretinal electronic implant alpha-IMS. *Proc R Soc B, 280, 20130077*

[2] Grossman, N. et al. (2010): Multi-site optical excitation using ChR2 and micro-LED array. *J Neural Eng, 7, 016004*

[3] McGovern, B. et al. (2010): A new individually addressable micro-LED array for photogenetic neural stimulation. *IEEE Trans Biomed Circuits Syst, 4(6, part 2), 469-476*

[4] Nirenberg, S. & Pandarinath, C. (2012): Retinal prosthetic strategy with the capacity to restore normal vision. *PNAS, 109, 15012-15017*

[5] Chaudet, L. et al. (2013): Development of optics with micro-LED arrays for improved opto-electronic neural stimulation. *Proc. SPIE, 8586, 85860R*

[6] Degenaar, P et al. (2009): Optobionic vision: a new genetically enhanced light on retinal prosthesis. *J Neural Eng, 6(3), 035007*

Simultaneous Stimulation and Recording from Healthy and Blind Mouse Retinas Using Implantable Subretinal Microchips and Flexible Microelectrode Arrays

Henrike Stutzki[1], Florian Helmhold[1], Max Eickenscheidt[1], Günther Zeck[1*]

1 Neurochip Research Group, Natural and Medical Sciences Institute at the University of Tübingen, Reutlingen, Germany
* Corresponding author. E-mail address: guenther.zeck@nmi.de

Abstract
Electrical stimulation using neuroprosthetic devices aims to evoke neural activity in a localized area. Here we show that subretinal stimulation of blind retinas is able to activate a spatial region of comparable size as the light-activated so-called receptive field in healthy retinas. Our experiments may guide the improvement of stimulation patterns of retinal implants used in patients suffering from retinitis pigmentosa.

1 Backround / Aims

The aim of this study is to compare the electrical response patterns evoked by subretinal stimulation of healthy and blind retinas. Stimulation was performed using a microchip which is part of a subretinal implant. The microchip aims to replace missing photoreceptors by electrically stimulating inner retinal neurons [1, 2]. Specifically, we asked to what extent the spatio-temporal response patterns of electrically stimulated blind retinas are comparable to the light-induced response patterns of wild type retinas.

2 Methods / Statistics

Whole-mount retinas from adult wild type (C57Bl6) and adult *rd10* mice were interfaced in subretinal configuration on the microchip. This chip contains an array of 1600 stimulation electrodes with an electrode spacing of 70 µm. Individual photodiodes on the microchip were illuminated by an oLED monitor. The change in photocurrent was transferred to constant stimulation pulses (voltage controlled stimulation +/- 1.6V, cathodic pre-pulse duration: 0.1 ms, anodic pulse: 2 ms).

The spiking response of retinal ganglion cells (RGCs) was recorded using a flexible, transparent and perforated microelectrode array (**Fig.1A**; FLEX-MEA, 16 electrodes, 10 or 30 µm electrode diameter respectively). Perforation allowed for appropriate oxygenation of the retina and therefore for recording times exceeding more than one hour. The ganglion cell spiking to repetitive electrical stimuli was revealed either in the raw trace (**Fig. 1B**) or after subtracting the average extracellular signal and a local polynomial interpolation. The amplitude of the recorded extracellular waveforms reached up to 1 mV (**Fig. 1C**) resulting in a signal-to-noise ratio of up to 30 (**Fig.1D**).

Electrically evoked receptive field sizes were mapped using narrow stripe-like stimuli (dimensions: 70 x 3000 μm^2 – 420 x 3000 μm^2). As a reference, light-stimuli with identical spatial characteristics were presented to wild type retinas. At each stimulus position the number of induced RGC spikes was calculated as an average over multiple stimulus presentations.

3 Results

The spatial activity distribution for RGCs in both, wild type and blind retinas was well approximated by a Gaussian distribution. In wild type retinas light-induced receptive field sizes were slightly smaller than electrically evoked ones. Comparison between wild type and blind retinas did not show any significant difference in electrically evoked receptive field sizes.
Moreover the spatio-temporal response patterns in retinas of both mouse strains shared similar features.

4 Conclusion / Summary

The main result is that similar spatio-temporal response patterns are detected upon light- or electrical stimulation in wild type and blind mouse retinas. This indicates that (i) the inner retinal circuitry remains intact to a large degree upon photoreceptor degeneration and (ii) that the implantable microchip is able to elicit near - physiological responses in these retinas.

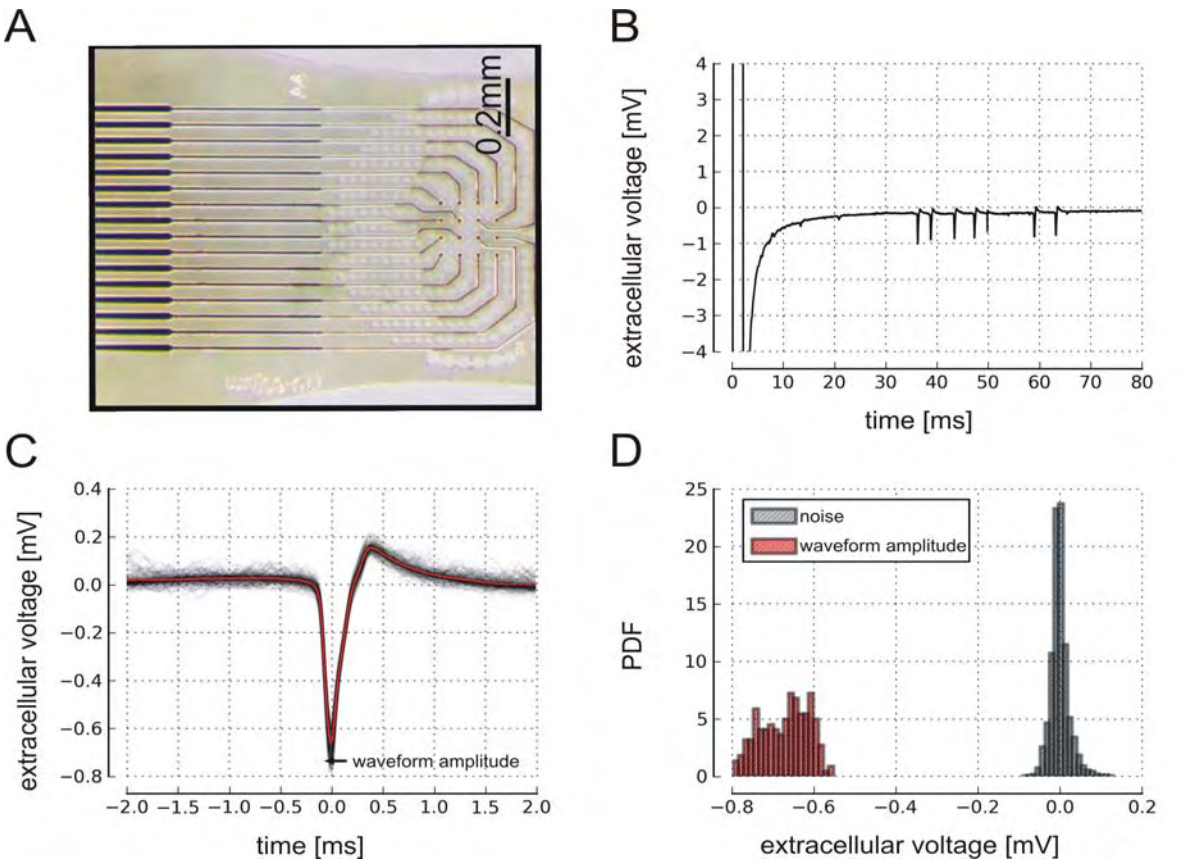

Fig.1: A Photograph of the flexible, transparent and perforated microelectrode array. **B** Raw trace of the recorded signal on one electrode with the stimulus artefact followed by spiking activity. **C** Superimposed, aligned spike waveforms from the electrode shown in (B). **D** Probability density function of the extracellular noise and of the waveform amplitude.

Acknowledgement

BMBF Grant (no. 1312038) to HS, FH, ME and GZ. We thank Retina Implant AG for providing us the subretinal microchip used here.

References

[1] Zrenner E. et al. (2011) Subretinal electronic chips allow blind patients to read letters and combine them to words.. Proc Biol Sci. 278(1711):1489-97.

[2] Eickenscheidt M. et al.,(2012) Electrical stimulation of retinal neurons in epiretinal and subretinal configuration using a multicapacitor array J.Neurophysiol. 107(10):2742-55.

Localized, Laser-Triggered Activity of Optogenetically Modified Neurons

Thoralf Herrmann[1], Christine Dürr[2], Martin Kriebel[2], Günther Zeck[1]

1 Neurochip Research Group, NMI at the University of Tübingen, Reutlingen, Germany
2 Molecular Biology, NMI at the University of Tübingen, Reutlingen, Germany

Abstract
Optogenetically modified neuronal cell cultures on microelectrode arrays are stimulated with brief localized laser flashes. Extracellular recordings show significantly altered activity after the application of the optical stimulation. Correlated responses occurred as fast single spikes and spike trains.

1 Background/Aims

Optical stimulation of genetically modified neuronal cultures promises to be more specific than electrical stimulation due to the local activation of individual neurons or of a small group thereof [1, 2]. In neuronal cultures with densely photosensitized neurons local activation has not been demonstrated. Here we report on first steps investigating the precision of stimulation in dense neuronal cultures.

2 Methods

Genetic modification of cell cultures.

Neuronal cell cultures (rat cortex, 5000 neurons/mm^2) are plated on micro electrode arrays (252 TiN electrodes, diameter = 30µm). After an incubation phase of 1-2 weeks the cultures are treated by lentiviral transduction (pLenti_CaMKIIa-hChR2(H134R)-EYFP-WPRE) to express exogeneous channelrhodopsin. The morphologic condition of the cultures is monitored by means of light and fluorescence microscopy.

Optical stimulation and signal detection.

A laser stimulation setup (Rapp OptoElectronic) composed of a laser unit for providing brief intense light flashes and a digital mirror device (DMD) to facilitate fast pattern transitions is coupled to a upright microscope (Olympus). The incident light pathway is used to project light patterns through the microscope objective onto a MEA with a neuronal cell culture.

Electrical signals are recorded using the MEA256-System (multi channel systems) and digitized. Areas which show spontaneous neuronal activity are repeatedly exposed to localized light stimuli. Offline signal analysis includes filtering, threshold detection of spikes and extraction of timestamps.

Control cultures without lentiviral treatment are exposed to the same laser stimuli to exclude thermal effects.

3 Results

Cell bodies and neurites of transduced cultures can be identified in fluorescence microscopy. (Fig.1)

Stimulation with brief laser pulses (duration 2ms, λ = 473nm, 24mW/mm^2) in most cases elicited a spike within the first 5ms after the stimulus onset. In some cases the first spike was followed by a spike burst (Fig. 2). Furthermore, it was possible to evoke single spikes by reducing the stimulus area to 0.002mm^2. No stimulus correlated activity was detected in the control cultures.

4 Conclusion

Single stimulus-locked spikes can be evoked using small optical stimuli (0.002mm^2). Larger stimuli (0.14 mm2) evoke spike burst indicating the activation of pre-synaptic circuitry.

Acknowledgement

The work is supported by the BMBF (FKZ: 1312038).

References

[1] Takahasi H. et al, 2012, *Biosystems*
[2] Dranias M.R. et al., 2013, *J.Neurosci.*

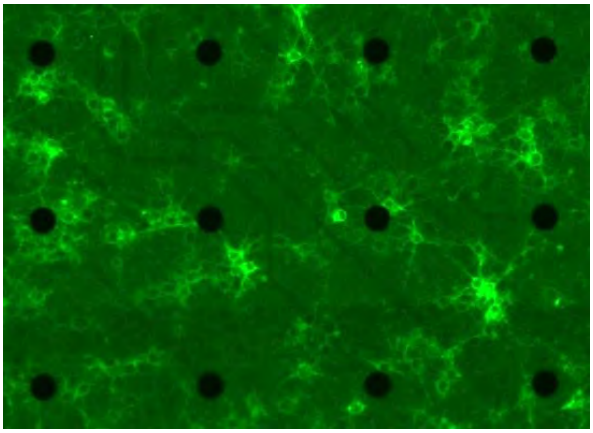

Fig. 1: Fluorescence image of a neuronal cell culture after lentiviral transduction. After the expression of channelrhodopsin cell bodies as well as neurites show a clear fluorescence signal and can therefore be easily identified.

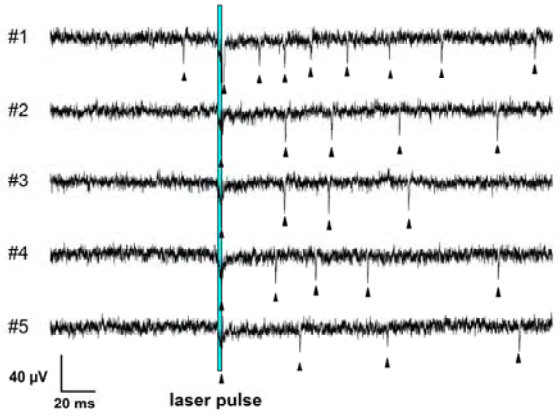

Fig. 2: Neuronal activity following optical stimulation with a laser pulse (duration 2ms, λ = 473nm, 24mW/mm^2, area: 0.14mm^2). Subsequently recorded raw MEA electrode signals at the center of the stimulated area. Increased activity is measured after each of the laser stimulus (action potentials are indicated by arrowheads).

Effects of Long-term Electrical Stimulation on Retinal Ganglion Cell (RGC) Response in Retinal Degeneration Model (*rd1)* Mice

Joo Yeon Kim[1,2], Wang Woo Lee[1,2], Yong Sook Goo[1,2,*]

1 Department of Physiology, Chungbuk National University School of Medicine, Cheongju, S. Korea
2 Nano Artificial Vision Research Center, Seoul National University Hospital, Seoul, S. Korea
* Corresponding author. E-mail address: ysgoo@chungbuk.ac.kr

Background/Aims

Retinal prosthesis is being developed for patients with retinitis pigmentosa (RP) and age-related macular degeneration (AMD), and this is regarded as the most feasible method to restore vision. Extracting optimal electrical stimulation parameters for the prosthesis is one of the most important elements. Previously, we investigated polarity effect of current pulse, and established that cathodic phase-1st pulse is more efficient than the anodic phase-1st pulse on evoking RGC spikes [1]. Here, we used charge-balanced, cathodic phase-1st biphasic current pulse and we compared the firing pattern of RGC spikes while applying electrical stimulation or without any stimulation.

1 Methods/Statistics

1.1 Recording of retinal ganglion cell activity

The well-known animal model for RP, *rd1 (Pde6b^{rd1})* mice at postnatal 8 weeks were used. From the e*x-vivo* retinal preparation, retinal patches were placed ganglion cell layer down onto 8 × 8 MEA. MEA60 system (Multi-Channel Systems GmbH, Reutlingen, Germany) was used as data acquisition system. Multi-electrode recordings of the retinal activity were obtained from 60 electrode channels with a bandwidth ranging from 10 to 3000 Hz at a gain of 1200. The data sampling rate was 25 kHz/channel. From the raw waveform of retinal recording, RGC spikes and local field potential were isolated by using 100 Hz high-pass filter and 50 Hz low-pass filter, respectively.

1.2 Electrical stimulation & data analysis

8 X 8 grid MEA with perforated layout (electrode diameter: 30 μm, electrode spacing: 200 μm, and impedance: 50 kΩ at 1 kHz) was used for stimulation and recording the ganglion cell activity. The 60 identical pulses consisted of symmetric biphasic current pulses were applied with 1 Hz frequency. From previous experiment, the maximal evoked RGC responses were almost always observed at 500 μs pulse duration and 30 μA pulse amplitude, therefore we fixed pulse duration and pulse amplitude at 500 μs and 30 μA, respectively. Multielectrode data were analyzed off-line using Offline sorter, Neuroexplorer. Images were processed in Origin. When we identified electrically-evoked retinal ganglion cell (RGC) spikes, we used same criteria with our previous paper [2]. By this definition, we included both short- and long-latency spikes, different from others [3]. We compared mean frequency of RGC spikes both in retinal patches (n = 4) with electrical stimulus for 5, 10, 20, 30, and 60 minutes and the time matched control patches (n = 4) without electrical stimulus. The mean frequency of RGC spikes was calculated for the last one minute time frame for each group. We fitted RGC response curve with sigmoidal fit using Boltzmann equation.

2 Results

In stimulus-applied group, out of 4 retinal patches, 114 ~125 RGCs (n = 4 patches) were included for analysis and 124 ~151 RGCs (n= 4 patches) for no stimulus-applied group. The 2nd peak in interspike interval histogram (ISIH) was observed significantly later at 156 ± 17 ms in stimulus group for 60 minutes than other stimulus groups for 5, 10, 20, and 30 minutes ($p<0.001$, ANOVA) (Fig. 2). The mean frequency of RGC spikes significantly increased in 10, 20, 30, and 60 minutes stimulus group relative to control group with no stimulus (Fig. 3).

3 Conclusion/Summary

The result showed that the RGC spikes were well evoked by our current stimulus protocol up to 60 minutes stimulus. Now we are applying longer stimulus than 60 minutes to find long-term safety limit for electrical stimulus. Since our relatively long 400 ms criteria for evoked RGC spikes includes both short- and long-latency spikes, we are dissecting short-latency RGC spikes evoked by direct stimulation of RGC and long-latency RGC spikes evoked through synaptic transmission for better analysis. SALPA based Matlab code was used for short-latency spikes [4]. Our ex-vivo result

might be beneficial for clinical study for retinal prosthesis.

Acknowledgement

This study was supported by grants from MEST (2009-0065444), and happy tech program of MEST (2010-0020852).

References

[1] Ahn K. N, Lee W. W, Goo Y.S. (2012). Effects of symmetric and asymmetric current stimuli on retinal ganglion cell (RGC) responses modulation in retinal degeneration model (*rd1*) mice. Proceedings of 8th Int. Meeting on Substrate-Integrated Microelectrode Arrays, 2012. pp130-131.

[2] Goo Y.S., Ye J.H., Lee S., Nam Y., Ryu S.B., Kim K.H. (2011). Retinal ganglion cell responses to voltage and current stimulation in wild-type and *rd1* mouse retinas. *J. Neural Eng.*, 8, 035003(12pp).

[3] Sekirnjak C, Hottowy P, Sher A, Dabrowski W, Litke A. M., Chichilnisky E. J. (2006) Electrical stimulation of Mammalian retinal ganglion cells with multielectrode arrays. *J. Neurophysiol.* 95, 3311-3327.

[4] Wagenaar D.A., Potter S. M. (2002) Real-time multi-channel stimulus artefact suppression by local curve fitting. *J. Neurosci. Meth.* 120, 113-120.

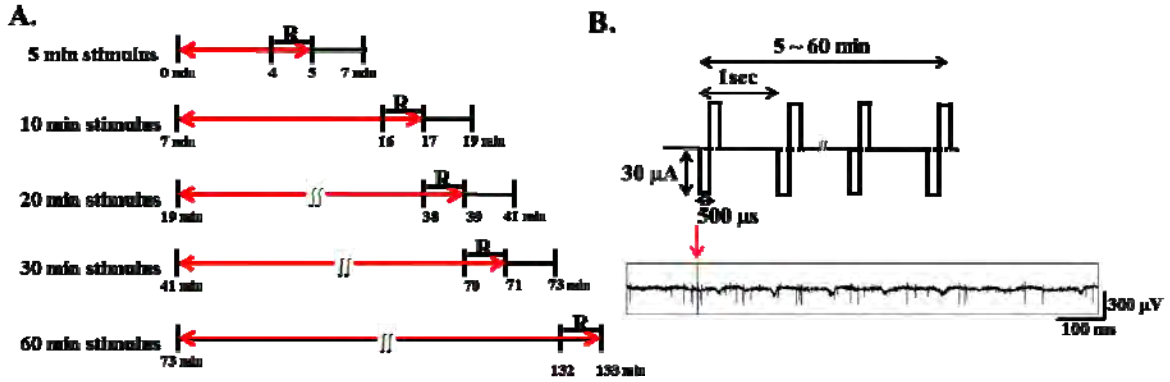

Fig. 1. Experimental protocol and retinal ganglion cell (RGC) spike response to electrical stimulus. A. Electrical stimulus was applied for 5, 10, 20, 30, and 60 minutes. For each stimulus group and time-matched control group, retinal activity was recorded for the last one minute time frame (R in figure) and mean frequency of RGC spikes for one minute was calculated. B. Standard biphasic current pulse used to stimulate RGCs and RGC response (bottom trace).

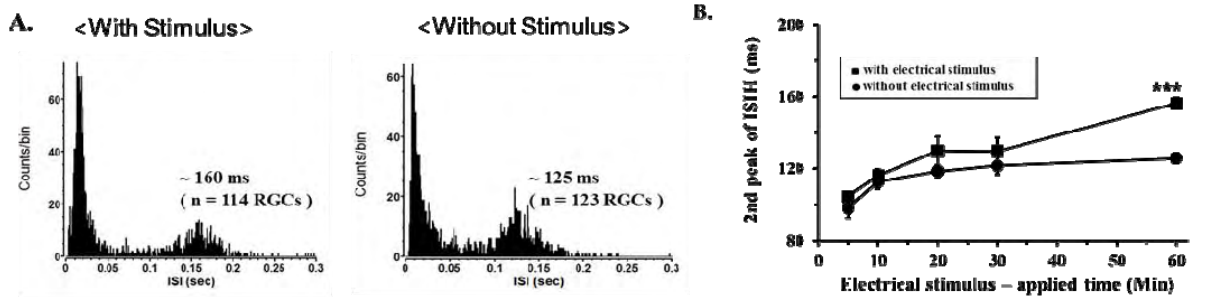

Fig. 2. Comparison of 2nd peak in interspike interval histogram (ISIH) of RGC. A. Typical example of ISIH both in 60 min stimulus applied group (Lt) and time-matched control group (Rt). B. Among electrical stimulus-applied group, 60 min stimulus significantly increases 2nd peak of ISIH ($p<0.001$), while among time-matched control group, there is no significant difference.

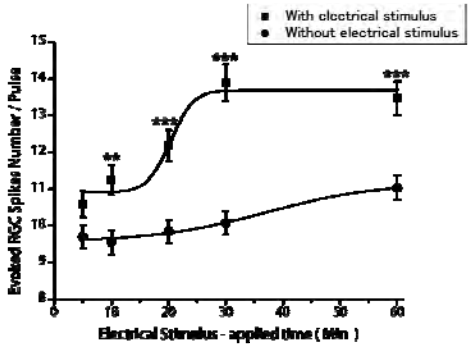

Fig. 3. Comparison of retinal ganglion cell (RGC) spike number in stimulus applied group (■) and time-matched control group without stimulus (●). Significant differences were observed in 10 min ($p<0.01$), and 20, 30, and 60 min stimulus group ($p<0.001$).

All Electrical or Optoelectrical Communication

Vanessa Maybeck[1*], Wenfang Li[1], Jan Schnitker[1], Andreas Offenhäusser[1]

1 ICS/PGI-8 Bioelectronics, Forschungszentrum Jülich GmbH, Germany
* Corresponding author. E-mail address: v.maybeck@fz-juelich.de

Abstract
MEAs hold great promise as therapeutic devices for their ability to modify neural network activity. Considering the importance of continual feedback from the network in determining stimulation protocols, we compare the advantages and challenges of all-electrical bi-directional MEA-neuron interfaces with combined optical and electrical methods combining optogenetics and MEAs. Among our criteria are the resolution of stimulation in space, resolution and reliability of stimulation in time, and cross-talk considerations.

1 Bi-directional Bioelectronic Communication

1.1 Pure Electrical

Background

Neurons may be stimulated to fire action potentials (APs) by single voltage or current controlled pulses applied over a microelectrode, or by summation of multiple pulses. The stimulation artefact may prevent AP recordings on the stimulation electrode, or neighbouring channels [1]. A key goal is to reduce the size of stimulation pixels, while maintaining high current injection, and temporal accuracy.

Results

We tested planar Au and Pt MEAs of varying electrode size for the range of stimulation in the SECW. Where stimulation was successful, we determined the ability of the other channels in the array to detect APs. This is dependent on not only the detection capabilities of the electrodes but also on the delay to the AP, which should be reproducible to maintain temporal accuracy, and the stimulation artefact. The blind time (taken as a return to within 1 µV of baseline in the pre amplification signal) observed on the stimulation electrode prevented chip based AP recordings from the stimulated cell. However, only the closest array points to the stimulation electrode had stimulation artefacts that would prevent recording. Planar metal electrodes with the highest spatial accuracy in our tests (36µm diameter) could stimulate up to 225% their radius away. We also encountered stimulation of very distant cells when applying pulses to very small electrodes. In these cases, the cells were on larger electrodes whose feed lines run near to the stimulation channel. We propose that the crosstalk-coupled signal was sufficient to stimulate the neuron on the second electrode.

The distribution of delay to AP during electrical stimulation was much narrower, and only showed a trend in delay time in some cases, resulting in a tail in the delay distribution (Fig. 1). Though MEA stimulation was temporally very accurate, stimulation is limited to the predetermined points on the chip. Reducing the pitch of electrodes may exasperate the cross-talk issue and require design elements to shield individual channels from one another.

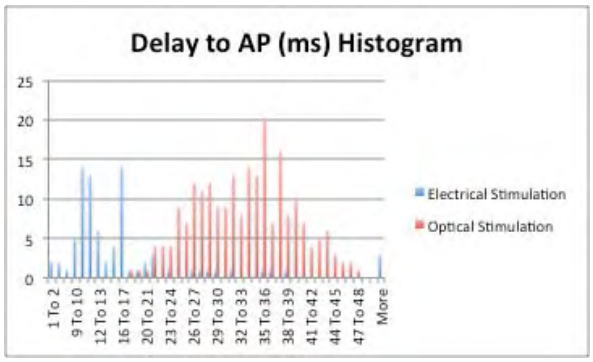

Fig. 1. Delay to AP with subsequent electrical or optical stimulation pulses. Optogenetic stimulation results in a broader Gaussian distribution, while electrical stimulation is generally specific but with a significant tail.

1.2 Optogenetic and Electrical

Background

Optogenetics introduces a light sensitive protein to control neurons by illumination. Channelrhodopsin 2 is a major tool in the class of optogenetic actuators, depolarizing cells by opening a non-specific cation channel when in blue light [2]. Optogenetics can be combined with MEAs in both on-chip and off-chip configurations. We evaluated external illumination of the modified Ch2opt, design considerations for light sources are beyond our current scope.

Results

We tested if light based stimulation combined with MEA recordings could improve the accuracy of feedback based stimulation by avoiding the stimulation artefact, increasing the available stimulation

points beyond the number of electrodes, and increasing stimulation resolution without reducing detection sensitivity. We tested a variety of wafer, electrode, and passivation material combinations to determine that the optimal MEA for optogenetics is Pt electrodes on glass, passivated with SU8. Typically favoured MEA materials, such as platinum black, showed large laser artefacts. We found that among the trade-offs between optical and electrical stimulation to consider are the variability of delay to AP in optical stimulation (Fig. 2) and device sensitivity to laser pulses. We describe the blind time in optogenetic stimulation from the start of the light pulse, noting that APs should be detectable even during illumination. This is in contrast to electrical stimulation where the channel is in saturation during the stimulation pulse. In MEA materials where light pulses induce an electrical response, similar considerations apply as in the case of electrical stimulation artefacts.

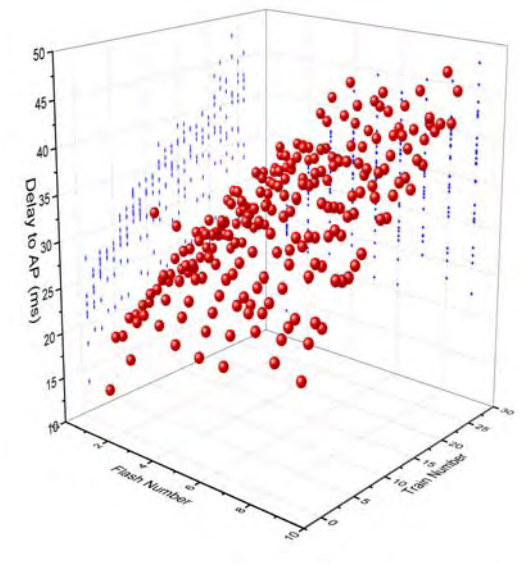

Fig. 2. Delay to AP with subsequent optical stimulation trains.

Overall, we found that the major gain for a combined opto-electrical approach is to avoid the stimulation artefact in the recording, and to access more points in the network via optics. Optogenetic stimulation exhibited an order of magnitude smaller artefact peak and six-fold shorter blind time. The trade-off being the wider time band in which the stimulated APs fall (Fig. 1). The standard deviation of electrically stimulated APs is larger, but this is skewed by rare, very late APs that skew an otherwise narrower peak in AP distribution. Surprisingly, the spatial accuracy relative to electrode size or illumination spot size is similar. However, since intensity and channel expression can be manipulated without changing the illumination spot diameter, there is greater flexibility to increase optogenetically delivered currents than in altering the electrode for higher charge injection at small electrode sizes. An overview of the relative performance across the various factors can be found in Table 1.

Acknowledgement

We thank QWANE and the HNF for MEAs as part of the FP7 program NeuroCare and Helmholtz POF BioSoft, respectively.

References

[1] Dura, B. (2012): High-frequency electrical stimulation of cardiac cells and application to artefact reduction. *IEEE transactions on biomedical engineering, 59(5), 1381-90.*

[2] Nagel, G. (2003): Channelrhodopsin-2, a directly light-gated cation-selective membrane channel. *PNAS, 100(24), 13940-5.*

	Electrical	*Optogenetic*
Peak Artifact	0.883 ± 0.172 mV pre amplification	-0.068 ± 0.050 mV (ø 12 µm) -0.121 ± 0.030 mV (ø 24 µm)
Artifact Tau	13.2 ± 6.5 ms	13.795 ± 0.807 ms (ø 12 µm) 16.355 ± 0.075 ms (ø 24 µm)
Total Blind Time	263 ± 34 ms post pulse (ø 64 or 36 µm) threshold raw .001	42.1 ± 8.5 ms from start of pulse (ø 24 µm) threshold raw .001
AP Accuracy	±10.3 ms	± 6.3 ms
Spatial Accuracy	225% - 460% electrode size	250% spot size
Error Rate	50 ± 35%	7 ± 14%

Table 1. Summary of parameters.

Characterization of Mammalian Retinal Ganglion Cell Response to Voltage Stimulus

Jones Ian Lloyd[1*], Russell Thomas[1], Fiscella Michele[1], Franke Felix[1], Müller Jan[1], Radivojevic Milos[1], Hierlemann Andreas[1]

1 ETH Zürich, Bio Engineering Laboratory, D-BSSE, Basel, Switzerland
* Corresponding author. E-mail address: ian.jones@bsse.ethz.ch

Abstract
A high-density CMOS-MEA device with 11,011 electrodes and 126 active recording channels at 18 µm pitch was used to record from and to stimulate ex-vivo rat retinal tissue. First, light stimuli projected onto the retina were used to stimulate the RGCs while recording with different groups of electrodes. Then, selective electrical stimulation of retinal ganglion cells was performed using the high-density microelectrode array.

1 Background/Aims

Microelectrode arrays (MEAs) have significant potential as a tool to interface with the neurons in the retina, and are used in visual prosthetic devices [1]. We used a high-resolution CMOS-based microelectrode array to select, electrically stimulate and record from retinal ganglion cells (RGCs). We investigated the question of how to selectively stimulate RGCs without stimulating nearby axons and neighboring neurons. Furthermore, we characterized how the cell responded to voltage stimulation at different anatomical regions (i.e., the soma and axon) to improve selectivity of stimulation.

2 Methods/Statistics

A high-density CMOS-MEA device with 11,011 electrodes and 126 active recording channels at 18 µm pitch [2] was used to record from and to stimulate ex-vivo rat retinal tissue. First, light stimuli projected onto the retina were used to stimulate the RGCs while recording with different groups of electrodes. Spike sorting was then applied to a fixed group of electrodes in order to distinguish the spikes produced by the RGC of interest. The responses on all groups of electrodes were then merged so as to create the electrical footprint of the RGC. A biphasic voltage stimulus was subsequently applied to one electrode at different locations of the RGC (near the soma and axon). The RGC responses were recorded at distal electrodes under the RGC in order to reduce the interference of the stimulation artifact.

3 Results

RGCs were located, and the electrical footprint was obtained for the RGCs of interest; the propagating action potential of one single RGC was detected on hundreds of electrodes (Fig. 1). The lowest threshold for stimulating the RGC near the soma was found to be near the highest-amplitude waveforms of the electrical footprint, which we assumed was most likely close to the soma or axonal initial segment. Peak-to-peak voltage pulses on the order of 200 - 400 mV were required to elicit responses from the RGCs.

4 Conclusion/Summary

The distinct advantage of being able to electrically “visualize” an RGC at subcellular resolution using the high resolution of the electrode array was demonstrated for this high-density MEA system; furthermore, since the electrodes are bidirectional, an RGC could be accessed at many different anatomical locations for electrical stimulation. Thus far, we have applied voltage pulses on single electrodes near the putative soma and at an axonal portion of the RGC; the next steps will involve the application of different voltage waveforms on multiple electrodes for the purpose of selectively producing pre-determined spike trains in single RGCs.

Acknowledgement
This work was supported by the ERC Advanced Grant “NeuroCMOS” under contract number AdG 267351.

References

[1] Chuang, A. T., Margo C. E., Greenberg, P. B. (2014). Retinal implants: a systematic review. *Br J Ophthalmol*, 10.1136/bjophthalmol-2013-303708.
[2] Frey, U., Sedivy J., Heer, F., Pedron, R., Ballini, M., Mueller, J., Bakkum, D., Hafizovic, S., Faraci, F. D., Greve, F., Kirstein, K. U., Hierlemann, A. (2010). Switch-Matrix-Based High-Density Microelectrode Array in CMOS Technology. *IEEE Journal of Solid-State Circuits*, 45(2): 467-482.

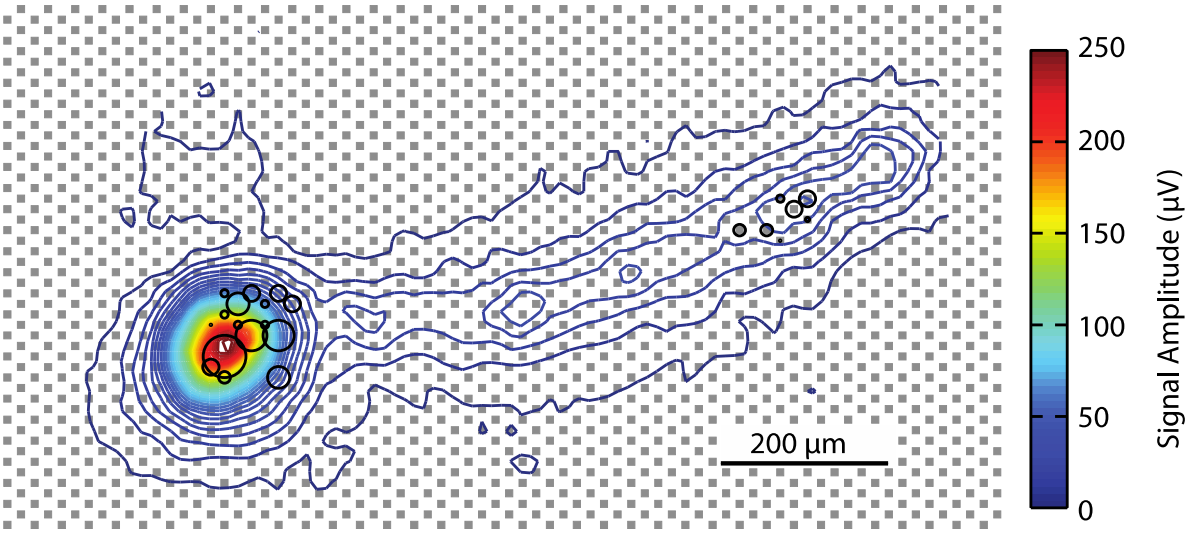

Fig. 1. The topographical map depicts the relative amplitudes of the electrical footprint of a rat RGC. The region to the left with highest amplitude is the putative soma of the cell, and to the right, the region with lower amplitude is the axon. The black circles represent the stimulability: the relative area of each circle indicates the inverse of the stimulus voltage threshold (the smaller the circle, the more difficult the stimulation) required for eliciting an RGC response with a voltage stimulus. The grey squares represent electrodes that can or have been used to stimulate and/or record cellular signals.

Autonomous Control of Network Activity

Sreedhar Saseendran Kumar[1,2], Jan Wülfing[2], Samora Okujeni[1], Joschka Boedecker[3], Ralf Wimmer[3], Martin Riedmiller[3], Bernd Becker[4], Ulrich Egert[1,2*]

1 Biomicrotechnology, Institute of Microsystems Engineering, University of Freiburg, Freiburg, Germany
2 Bernstein Center Freiburg, Freiburg, Germany
3 Machine Learning Lab, University of Freiburg, Freiburg, Germany
4 Chair of Computer Architecture, University of Freiburg, Freiburg, Germany
* Corresponding author. E-mail address: egert@imtek.uni-freiburg.de

Abstract
Electrical stimulation of the brain is used to treat neurological disorders. Yet it is unknown how to find stimulation patterns that produce desired results with the least interference. Towards this goal, we tested a generic closed-loop paradigm that autonomously optimizes stimulation settings. We used neuronal networks coupled to a reinforcement learning based controller to maximize response lengths.

1 Background

High-frequency electrical stimulation is effective in managing the symptoms of neurological disorders (Parkinson's disease, dystonia). Major problems are: 1) stimulation settings do not adapt to the needs, 2) undesired network responses result in serious side effects, and 3) non-optimal energy consumption necessitates frequent battery replacement.

Closed-loop paradigms that autonomously learn could be useful to optimize stimulation settings. We present a proof-of-concept in a simple control task. A controller had to find the optimal timing of electrical stimuli applied to a neuronal network *in-vitro* at one electrode to maximize the response length at another electrode of a microelectrode array (MEA).

2 Methods

The full parameter space for such a controller currently cannot be scanned *in vivo*. To develop concepts and techniques, we stimulated neuronal networks on MEAs. We trained a controller with reinforcement learning techniques (Q-learning, Watkin, C.J., *Learning from Delayed Rewards*, PhD thesis, Cambridge University, 1989) (fig.1). Following each spontaneous burst (SB), a training episode began. It ended with the controller either stimulating (rewarded) or being disrupted by another SB (punished). During training (n = 5, 1000 episodes) the controller learned an optimal stimulation time. The learned controller was then tested in a 500 episode session.

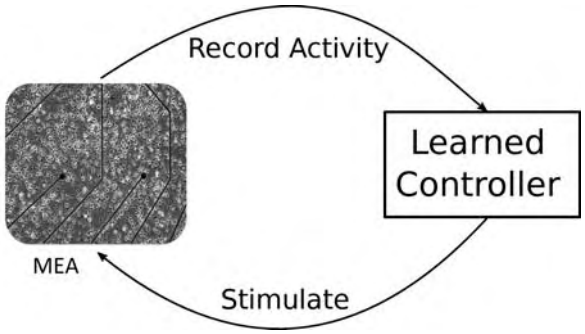

Fig. 1. Closed-loop experimental scheme

3 Results

Response length increases with the duration of pre-stimulus inactivity (fig. 2a, Weihberger et al. (2012), J.Neurophysiol 109:1764-1774). Our training data fits this exponential model indicating that the controller was able to identify this underlying relationship. Overall, the fit parameter *A* varied across cultures with the longest response, while the parameter λ stayed around $1.44 \pm 0.88\ s^{-1}$ (n = 5).

With increasing waiting periods SBs may occur before the stimulus. The controller learned the delay that minimized such disruptions. The ratio of the learned delay to the mode of the inter-burst interval (IBI) distribution of spontaneous activity was 0.98 ± 0.33 (n = 5), suggesting that the learned delay was always very close to the most frequent IBI (fig. 2 b-d).

4 Conclusion

Coupling closed-loop configurations with machine-learning techniques are promising strategies to adjust stimulation parameters autonomously. A simple controller was able to 1) identify stimulus-response relationships, and 2) balance stimulus timing between response lengths and the probability of disruptions by spontaneous bursts.

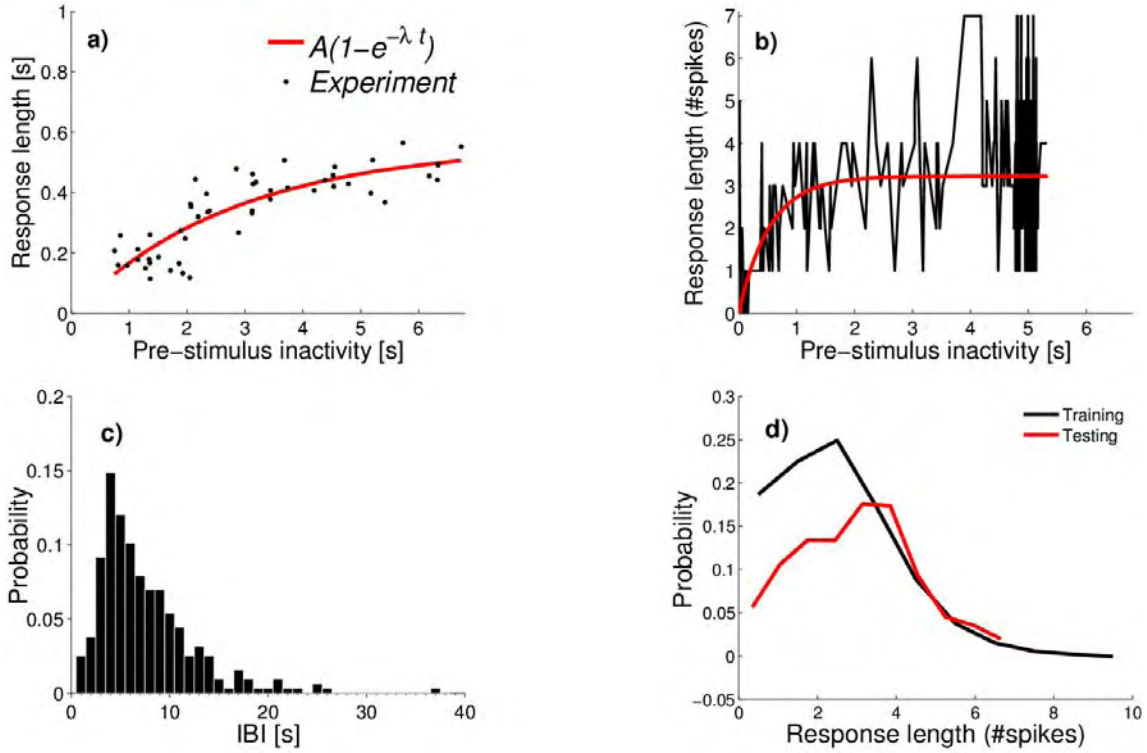

Fig. 2 a) Response length vs. pre-stimulus inactivity (Adapted from Weihberger et al. 2012). **b)** Stimulus-response relations learned by the controller for a culture. The controller 'chooses' to mostly stimulate at the peak of the spontaneous IBI distribution, ~5s **c)**. This improves the chances of evoking a consistent long response, without interruption by an intervening SB. At the same time, the shift in the peak of the response length distribution for the testing session towards a longer response suggests that the learned delay also improved the response lengths, **d)**.

Acknowledgements

Supported by BrainLinks-BrainTools Cluster of Excellence (DFG, EXC 1086), BMBF (FKZ 01GQ0830) and the EU (NAMASEN #264872).

Simultaneous Stimulation and Recording of Retinal Action Potentials Using Capacitively Coupled High-Density CMOS-based MEAs

Dmytro Velychko [1], Max Eickenscheidt [1], Roland Thewes [2], and Günther Zeck [1]

1 Neurochip Research Group, Natural and Medical Sciences Institute at the University Tübingen, Reutlingen, Germany
2 Chair of Sensor and Actuator Systems, Faculty of EECS, TU Berlin, Berlin, Germany

Abstract
Light responses of retinal ganglion cells (RGCs) were recorded by a capacitively coupled CMOS-based MEA. Simultaneous electrical stimulation and recording with capacitive electrodes is presented. The work demonstrates applicability of the new CMOS MEAs for electrophysiological experiments and neural tissue response analysis.

1 Background/goal

CMOS based capacitive microelectrode arrays (MEAs) are used to record and stimulate neuronal activity at high spatial resolution. Previous MEAs from our labs were used to investigate light-induced activity of retinal ganglion cells [1] or the specificity of electrically stimulated retinal neurons [2, 3]. Simultaneous, artefact-free electrical stimulation and recording of many neurons in the same tissue has not yet been possible. Here, we overcome this restriction by using a recently developed capacitively coupled MEA which comprises 4225 recording sites at 16 µm pitch interlaced with 1024 capacitive stimulation sites at 32 µm pitch.

2 Methods

Retinas from adult guinea pigs are isolated and interfaced to the planar dielectric surface of the CMOS MEA with the ganglion cell layer in close contact to the array. Light stimuli were projected onto the MEA using a customized setup employing LEDs of specified wavelength and intensity. During light-stimulation, action potentials of the retinal ganglion cells (RGCs) can be detected online thus allowing for a rough classification of the cell types. Offline analysis allows for a more precise classification. Sinusoidal electrical stimuli (voltage range: 0 -3.3V) are applied to the capacitive stimulation sites using arbitrary patterns of combined sites. Electrical stimulation using different frequencies (range 10 – 40 Hz) is analyzed here.

3 Results

ON and OFF light flashes applied to the entire active area at a rate of 1 Hz are used to characterize RGCs (Fig. 1). Different ganglion cell subtypes react either at onset or offset of the light stimuli with either a transient burst of spikes or a tonic response pattern. The light-induced response pattern can be measured over a large intensity range (up to 2.5 mW/mm2). Electrically stimulated RGC activity is detected during application of sinusoidal voltage pulses to large capacitive areas. The stimulus amplitude is adjusted to keep the stimulation amplitude constant. After subtraction of the passive tissue response phase-locked ganglion cell activity becomes clearly visible (Fig. 2). Different RGC types show different phase-shifted activity.

4 Conclusions

Capacitively coupled CMOS-based MEAs are an attractive tool to characterize the response of (retinal) neurons to arbitrary electrical stimuli patterns of variable frequency and electrode size. Such experiments may advance our understanding of the dynamic response properties of neuronal populations and lead to improved neuroprosthetic stimulation strategies.

Support
This work is supported by BMBF Grant 1312038 to DV, ME and GZ, and BMBF Grant 0315636A to RT.

References:

[1] Zeck G, Lambacher A., Fromherz P. Plos One 6(6):e20810, (2011)
[2] Eickenscheidt M., Jenkner M., Thewes R., Fromherz P., Zeck G. J. Neurophysiol. 107(10):2742-55, (2012)
[3] Eickenscheidt, M., Zeck, G. J. Neural.Eng., 11(3):036006 (2014)

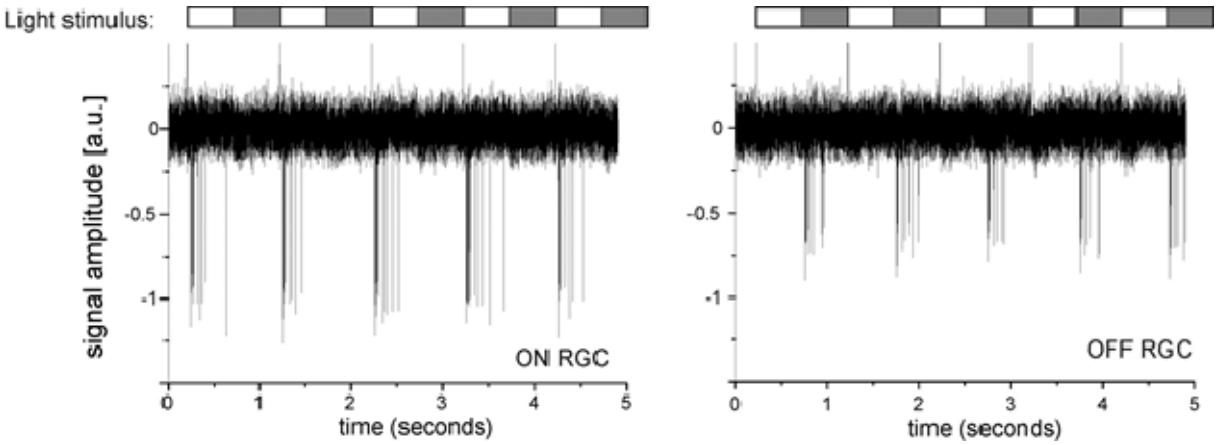

Figure 1: Light-stimulated activity of two RGCs recorded using a capacitive CMOS MEA. Extracellular voltages recorded below two different retinal ganglion cells in the same retina during stimulation with flickering stimuli (indicated above the recorded traces). (Left) Spiking of an ON transient RGC to the presentation of five stimulus repetitions. (Right) Spiking of an OFF transient RGC to the presentation of five stimulus repetitions. The signal amplitude is shown in arbitrary units.

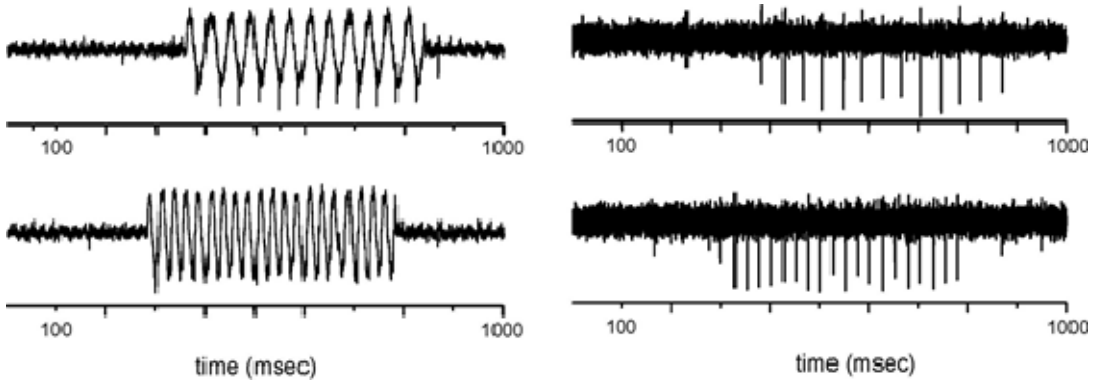

Figure 2: Simultaneous electrical stimulation and recording of evoked action potentials with the CMOS MEA. Sinusoidal stimuli are applied through a dielectric capacitively coupling electrodes leading to rhythmic changes of the extracellular voltage as well as neuronal activity of RGCs. (Left) Application of 25 Hz stimulus (upper row) and 40 Hz stimulus (lower row). (Right) Filtered signal traces reveal phase-locked RGC spiking. The signal amplitude is shown in arbitrary units.

Systems Neuroscience
(brain slices, retina, spinal cord)

On the Nature and Transmission of Information Among Cell-Assemblies: A Network and Information Analysis of Propagation Between Neural Populations in a Two-Chamber In Vitro System

DeMarse*, Thomas[1], Alagapan, Sankarleengam[1], Pan, Liangbin[1], Franca, Eric[1], Leondopulos, Stathis[1], Brewer, Gregory[2], and Wheeler, Bruce[1]

1 Pruitt Dept. of Biomedical Engineering, University of Florida, Gainesville, Florida, USA
2 Dept. of Biomedical Engineering, University of California, Irvine, California, USA
* Corresponding author. E-mail address: tdemarse@bme.ufl.edu

Abstract
Transient synchrony and propagation of neural activity between cortical areas is thought to underly many cognitive processes. In this study we create an in vitro feed-forward network composed of living cortical neurons. Each layer of the network was separated by and communicated through a series of micro-tunnels in which we varied the number of tunnels to manipulate the degree of communication between layers. We study the formation of small synchronous neuronal assemblies within each layer and measure the communication between layers in terms of the fidelity with which assemblies are able to reproduce spike trains across layers containing robust rate based and temporal information within those spike trains.

1 Backround / Aims

Cognition is associated with rapidly changing and widely distributed neural activation patterns involving numerous cortical and sub-cortical regions. While this fact is now widely appreciated, our understanding of the computational ability of these networks or the nature of information stored or transmitted between regions remains poorly understood. We created a simple two-chamber in vitro system (**Fig.1B,C**) representing two small cortical populations interconnected through tunnels in a feed-forward network topology (**Fig.1A**). These cortical networks spontaneously form network wide bursts of activity (oscillations) occurring with delta and theta frequencies. One of the most fundamental issues in neuroscience is the nature of the neural representation of information.

We then study the communication between small functional cell-assemblies that dynamically form during each burst event, transmit information in the form of spike trains within and between each network, before fading away at the end of each oscillation. We manipulate the number of communication pathways between each neural population and measure the effects this reduction has on the nature and fidelity of information as it is transmitted between assemblies embedded within each layer.

2 Methods / Statistics

Rat cortical cells were placed into one chamber of a PDMS device (**Fig.1B-E**) followed 10 days later with cells into the second chamber forming two layers

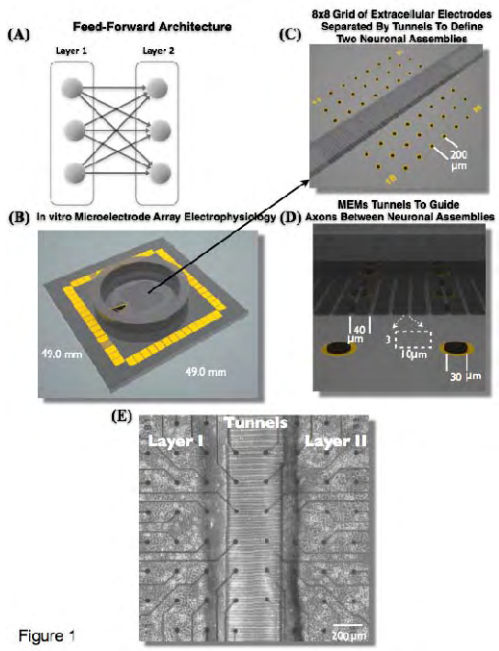

Fig. 1. In vitro Feed-forward network composed of two cortical networks that communicate through micro-tunnels separating each layer.

of a feed-forward network containing ~5000 cells each. Each layer was interconnected by 10 µm wide tunnels (**Fig.1C-D**) over an MEA (**Fig.1B,E**). Groups with 2 tunnels (2T), 5T, 15T, 51T MEA cultures were created (n=18). Functional connectivity was estimated using a Granger causal [1, 2] and scaled cross-correlation metric [3] across the entire recording and individually during burst events. These estimates were

compared to the fidelity of neural transmission during bursts, computed between each pair of neurons within each population and between layers using the Victor-Purpura [4] cost based metric of spike-train similarity. Cost, ***q***, was varied from (2<***q***<150 ms) representing similarity at time scales associated with temporal (2<***q***<20 ms) to rate based neural coding (80<*q*<150 ms). Similarity, $\boldsymbol{D_v}$, ranged from 0<$\boldsymbol{D_v}$<1.0 (dissimilar to identical).

3 Results

Fig.2 depicts spike train similarity, D_v, for each pair of neurons between layers I and II estimated during periods in which bursts propagated across layers and for each value of cost parameter: *q* in ms. Similarity of spike trains transmitted across layers was greater for rate relative to temporal neural coding for all groups. Increasing the number of tunnels from 2 to 51 resulted in increased similarity of spike trains propagated between layers (Fig.2 Inset), particularly at temporal scales.

4 Conclusion/Summary

Our results support the presence of both rate and temporal neuronal coding whose fidelity increased with increasing number of communication pathways, was maximal within bursting, and varied with network characteristics based on functional connectivity from our network analysis.

References

[1] Ding M., Chen Y. and Bressler S.L. (2006) Granger Causality: Basic Theory and Application to Neuroscience. **I**n Handbook of Time Series Analysis: Recent Theoretical Developments and Applications. Wiley-VCH Verlag GMBh & Co., Berlin

[2] Cadotte A. C., DeMarse T. D., He P. H. and Ding M. (2008). Causal Measures of Structure and Plasticity in Simulated and Living Neural Networks. *PLOS: One* 3(10):e3355.

[3] Nikolić D., Mureşan R. C., Feng W. and Singer W. (2012) Scaled correlation analysis: a better way to compute a cross-correlogram. *Eur J Neurosci* 35(5):742-62.

[4] Victor J. D. and Purpura K. P. (1996). Nature and precision of temporal coding in visual cortex: a metric-space analysis. *J Neurophysiol* 76(2):1310-26.

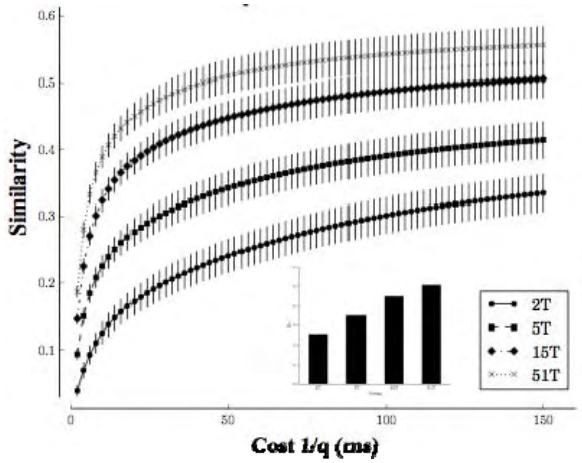

Fig. 2. Similarity of spike trains between neurons in Layer I and Layer II.

Pairwise Reconstruction of the Hippocampal Tri-Synaptic Loop: EC-DG, DG-CA3, CA3-CA1

Gregory J. Brewer[1*], Harsh Desai[1], Himanshi Agrawal[1], Stathis S. Leondopulos[2], Bruce C. Wheeler[2]

1 University of California Irvine, USA
2 University of Florida, Gainesville, FL USA
*Corresponding author. E-mail address: GJBrewer@uci.edu

Abstract
Sub-regions of the hippocampus are thought to contribute differently to stages of learning and memory, but we don't yet know the code for how this information is created. Here our goal was to determine if these regions could be distinguished as they self-wire into the anatomically accurate tri-synaptic network from the entorhinal cortex (EC) to the dentate gyrus (DG) to the CA3 or to the CA1, in pairs. Despite removal from the developing brain, hippocampal subregions maintain their developmental course as distinct elements of a learning and memory processing cascade. Several spike dynamics measures were enhanced by anatomically appropriate connections. This technology will enable determination of the network integration of stimulation-dependent plasticity and how subregion-specific information patterns are reliably transmitted but differentially processed within each hippocampal subregion.

1 Background/Aims

Sub-regions of the hippocampus are thought to contribute differently to stages of learning and memory, but we don't yet know the code for how this information is created. Here our goal was to determine if these regions could be distinguished as they self-wire into the anatomically accurate tri-synaptic network from the entorhinal cortex (EC) to the dentate gyrus (DG) to the CA3 or to the CA1, in pairs. Monitoring activity from each hippocampal region in behaving animals produces specific patterns of activity for each region, but we lack information about the inputs necessary to evoke these patterns and their relationships.

2 Methods

Here we reconstructed paired components of the tri-synaptic pathway: EC-DG, DG-CA3, CA3-CA1 in culture. We confined each subregion in a 20 mm^2 compartment. Compartments were connected by 51 microtunnels each 3 µm high x 10 µm wide x 400 µm long, fabricated in PDMS. This device was aligned with a 60 electrode array (MEA) and allowed to adhere. Neurons from subregions of the hippocampus were dissected and plated into separate subcompartments. Spiking activity was recorded after network development of 3 weeks in culture and analyzed for differences in activity dynamics.

3 Results

Previously we showed sub-region-restricted gene expression by quantitative PCR [1]. These results indicate that distinct subregions can be micro-dissected and that they maintain their phenotype in these cultured networks. By monitoring the timing of large action potentials over two electrodes in the tunnels [2], the DG-CA3 pair maintained anatomically accurate direction of communication from the DG to the CA3, despite being plated at the same times. Compared to controls of DG on each side, a DG subregion connected to EC showed lower spike rates and burst rates. With EC connected to DG, the EC subregion showed even lower spike and burst rates but now spikes per burst and extraburst spike rates were also lower. These differences occurred with equal percent active electrodes and burst durations. For the DG-CA3 pair, CA3 was generally less active than DG, except for a higher rate of intraburst spikes in the CA3 than the DG. Other combinations with CA3 and CA1 will be described in comparison to homologous pairs as controls.

4 Conclusion/Summary

Despite removal from the developing brain, hippocampal subregions maintain their developmental course as distinct elements of a learning and memory processing cascade. Several spike dynamics measures were enhanced by anatomically appropriate connections. This technology will enable determination of the network integration of stimulation-dependent plasticity and how subregion-specific information patterns are reliably transmitted but differentially processed within each hippocampal subregion.

Acknowledgement
We thank NIH for their support (R01 NS052233).

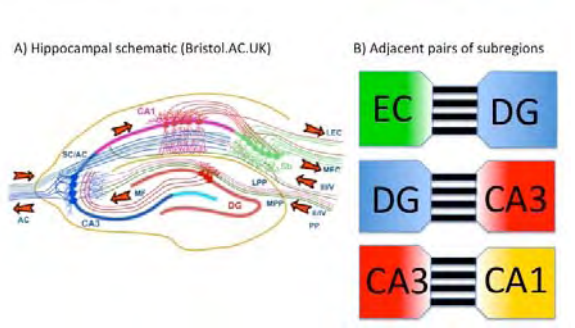

Fig. 1. A) Schematic of the tri-synaptic pathway in a slice of the hippocampus. MEC, medial entorhinal cortex (EC); LEC, lateral EC; DG, dentate gyrus. B) Experimental design to culture neurons from hippocampal regions into pairs of compartments connected with tunnels for axonal communication.

Reference

[1] Brewer G.J., Boehler M.D., Leondopulos S., Pan L., Alagapan S., DeMarse T.B., Wheeler B.C. (2013). Toward a self-wired active reconstruction of the hippocampal trisynaptic loop: DG-CA3. *Frontiers in Neural Circuits* 7,165 DOI=10.3389/fncir.2013.00165. PM:24155693

[2] Pan L, Alagapan S, Franca E, DeMarse, T, Brewer GJ, Wheeler BC. 2013. Large extracellular spikes recordable from axons in microtunnels. IEEE Trans. Neural Sys. Rehab. Eng. 22:453-459. doi: 10.1109/TNSRE.2013.2289911. Epub 2013 Nov 13.

Electrical Imaging of Local Field Potentials in Organotypic and Acute Hippocampal Slices Using CMOS MEAs

Lakshmi Channappa, Florian Helmhold, Günther Zeck

Neurochip Research Group, NMI at the University of Tübingen, Reutlingen, Germany

Abstract
In neural tissues network activity is driven by interconnected neuronal populations comprising inhibitory and excitatory neurons. These cell populations form local networks which can generate spontaneous oscillations or field potentials. However, when an imbalance between these cell populations occurs, it leads to an aberrant network activity which is one underlying cause of neurological disorders. Here we report on the recording of spontaneous and aberrant neural network activity in hippocampal slices using high density CMOS-based microelectrode arrays (MEAs).

1 Background

Hippocampal slices are well-suited to investigate epileptiform like activity *in vitro*, which mimics the process of epileptogenesis observed with *in vivo* animal models [1]. Electrical imaging of local field potentials (LFPs) in organotypic hippocampal slices (OHCs) using high-density multi-transistor array of 16,384 sensors (1mm^2) has been reported recently [2]. However, aberrant epileptiform like activity and putative mechanisms are still unclear [3]. Here we aim for characterization of LFPs under different pharmacological conditions in organotypic and in acute slice preparations using CMOS-based MEAs.

2 Methods

For extracellular recordings, transverse sections of cortico - hippocampal slices of 400µm thickness were prepared from new-born SD rats (P6-P8). for OHCs [4]. Acute hippocampal slices were prepared from older SD rats (P13 to P30) under otherwise unchanged conditions. Before each recording, the slices were tightly interfaced to the CMOS MEA. Epileptiform like activity was elicited by both omitting Mg^{2+} and elevating K^+ or by addition of $GABA_A$ receptor antagonist bicuculline methiodide to artificial cerebrospinal fluid (ACSF) LFPs in the OHCs were recorded from different subfields (CA1 or CA3 or DG) between 4 to 12 DIV in culture (**Fig.1**). Similarly, LFPs were recorded from acute slice preparations to compare the LFPs to OHC slices.

The recordings were performed on CMOS MEAs with a sensor pitch of either 7.4 µm [2] or of 16 µm [5] covering an area of either 1 or 2 mm^2. The sampling frequency ranged between 6 – 25 kHz. LFP identification and propagation velocities were calculated using custom-written software (Python).

3 Results

Spontaneous LFPs were identified in OHC but not in acute slice preparations .During induced epileptiform like activity we observed LFPs of high-amplitude and high-frequency in both hyper-excited slices and in disinhibited slices. Here, the LFP propagation velocity and the propagation path were evaluated for the p-spike component along the pyramidal cell layer. In many cases the propagation occurred along the classical direction, i.e. from DG along the mossy fibers to CA3 and further along the Schaffer collaterals to CA1 (**Fig.2A**). The propagation speed evaluated from more than 100 LFPS ranged between ~200 - 300mm/s (LFPs evaluated in 9 slices). However, “backward” LFP propagation (CA1 to CA3 to DG, n > 100) was observed with a similar propagation velocity (**Fig. 2B**) (n = 9 slices). The velocities of individual LFPs in each slice follow a Raleigh distribution. The LFP propagation was inhibited by addition of ionotrophic glutamate receptor blocker or by addition of a gap junction blocker, suggesting a potential contribution of excitatory receptors and of electrical coupling for the LFP propagation.

4 Conclusion

The occurrence of spontaneous LFPs in OHCs reflects an imbalance of the neural network, possibly due to cultivation. The values for the propagation velocities suggest axonal transmission. Although excitatory receptors and electrical coupling appears to be involved, the mechanism for aberrantly propagating LFPs cannot be clarified yet.

Acknowledgement
We thank the German Federal Ministry of Education and Research (BMBF grant 1312038) for funding of the project.

References
[1] Ziobro JM, Desphande LS, DeLorenzo RJ. (2010), *Brain Res*. 1372: 110-120
[2] Hutzler M, Lambacher A, Eversmann B, Jenkner M, Thewes R, Fromherz P. (2006), *J. Neurophysiol.* **96:** 1638-1645
[3] Zhang M, Ladas TP, Qiu C, Shivacharan RS, Gonzalez-Reyes LE. (2014), *J.Neurosci*. 34(4): 1409 - 1419
[4] Stoppini L, Buchs PA, Muller D. (1991), *J Neurosci Methods*. **37**(2): 173-82
[5] Bertotti G. et al., Proc. 9th International Meeting on Substrate-Integrated Microelectrodes, 2014

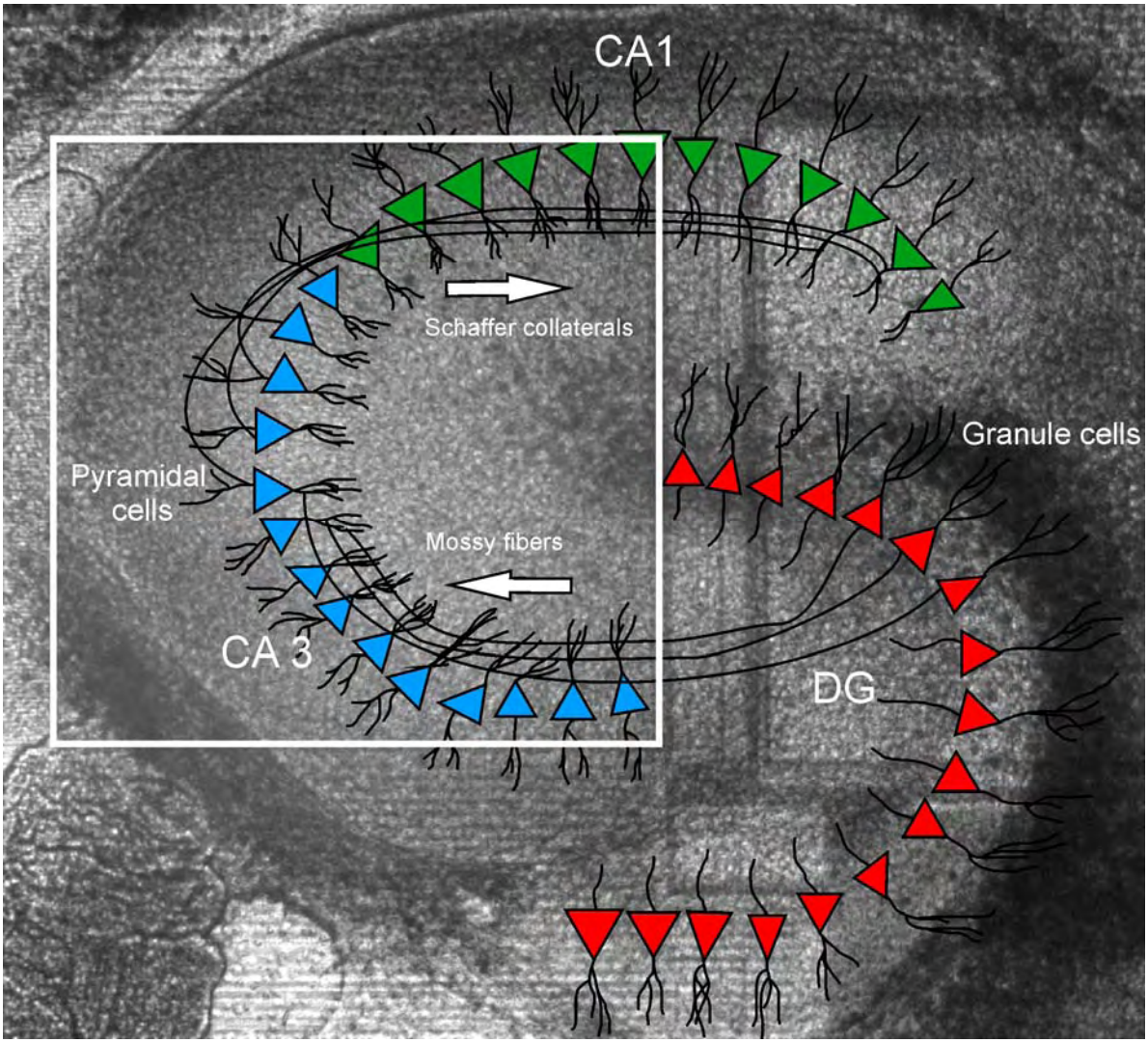

Figure 1: Bright field image of an organotypic hippocampal slice interfaced to the CMOS MEA recording array (white square). The image shows schematically the position of different cell types (pyramidal cells in CA3 (blue), pyramidal cells in CA1 (green) and granule cells of dentate gyrus (red)), subfields and fiber systems of the hippocampus.

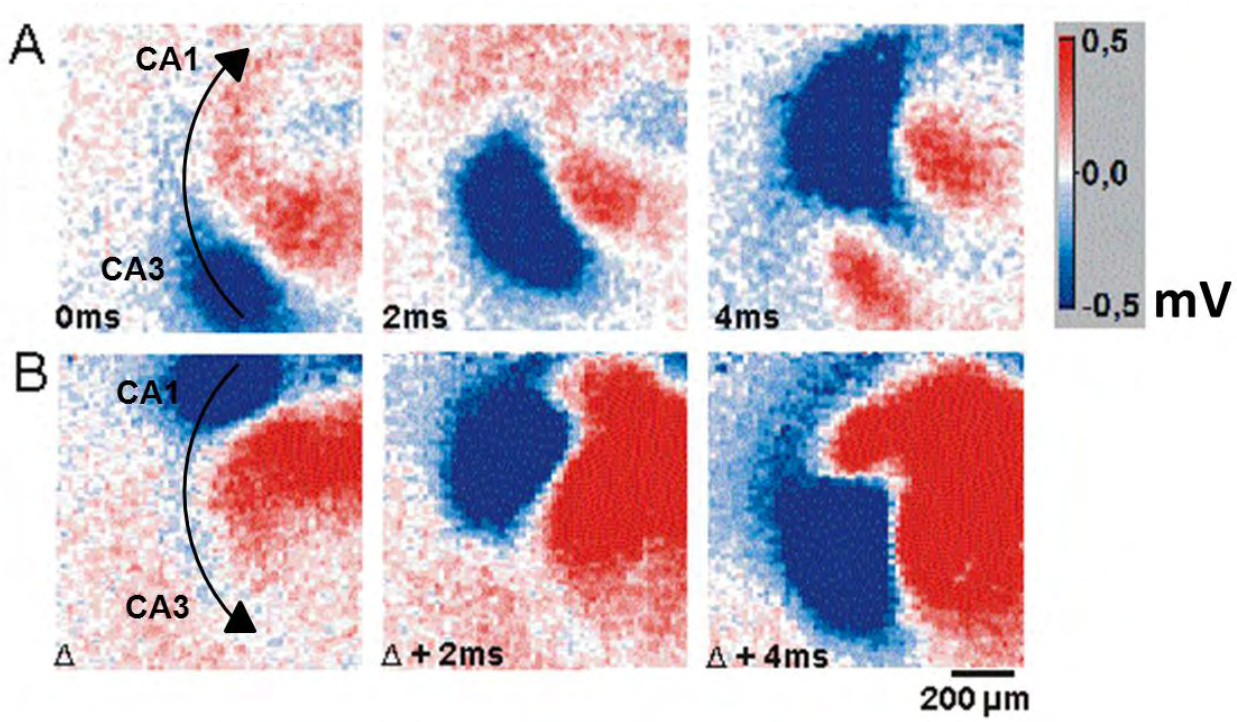

Figure 2: Propagating LFPs in the hippocampal slice shown in **Fig. 1** upon chemical induction of epileptiform like activity.
(A) Three electrical images at (equidistant time points) of one LFP which propagates from CA3 to CA1.
(B) Three electrical images of a second LFP which propagates in the opposite direction along nearly the same path in the same hippocampal slice.

Technique for Analysis of Purkinje Cell Sub-Cellular Functional Dynamics in Acute Cerebellar Slices Using a High-Density Microelectrode Array

Marie Engelene J. Obien[1*], Andreas Hierlemann[2], Urs Frey[1,2]

1 RIKEN Quantitative Biology Center, Kobe Japan
2 Department of Biosystems Science and Engineering, ETH Zurich, Basel, Switzerland
* Corresponding author. E-mail address: meobien@riken.jp

Abstract
High-density microelectrode arrays (HDMEAs) allow for recording neuronal extracellular action potentials (EAP) at sub-cellular resolution *in vitro*. In slice preparations, however, we face the following challenges: (a) neurons may have specific orientations in 3D, depending on the tissue structure, and (b) there is a need for powerful spike sorting techniques, especially to cope with bursts and to detect dendritic spikes. In this work, we present approaches to overcome these challenges. We analyzed Purkinje cell (PC) signals in acute brain slices using a combination of HDMEAs and patch clamp with the main goal to understand the PC spiking states [1] and to observe the effects of PC dendritic arborization on their function.

1 Background and Aims

1.1 HDMEA and acute brain slices

Microelectrode arrays have been used for single-unit recording in acute slices [2], which allowed for analysis of the fast dynamics of single neurons and of the slower local field potentials (LFP). High-resolution recordings with high-density microelectrode arrays (HDMEAs) enabled to obtain the shapes of extracellular action potentials (EAPs) across the soma and processes of single neurons [3]–[5]. Planar HDMEAs can be used to record from the entire Purkinje cell (PC) structure in acute cerebellar slices due to their almost planar fan-shaped anatomy. The sagittal cut only slightly damages the flat dendrites [2], and, although the inputs to the PC are lost, i.e., parallel and climbing fibers are severed, PCs remain spontaneously active—which is characteristic for GABA-ergic neurons. Hence, HDMEAs are a suitable tool to study the function of PCs. One caveat, however, includes assigning the recorded EAPs to their source. PCs in acute slices can have different z-distances (heights) and angles with respect to the HDMEA-electrode plane. Moreover, since the neuronal density in cerebellar slices is high, and since all PCs are in the same layer, there is a need for powerful spike sorting to obtain EAP footprints that can be unambiguously assigned to the respective PCs. Here, we present developments to overcome some of the challenges mentioned above.

1.2 Studying Purkinje cell spiking dynamics

PC spontaneous spiking is tonic. In order to study the different spiking dynamics of PCs, there is a need to stimulate either directly the neuron or in other layers, such as the granular layer, to simulate climbing fiber input, or such as the molecular layer, to mimic parallel fiber input (see Fig. 1). In this work, we directly stimulated the PC by whole-cell current clamp. Complex spiking activity can be observed upon stimulation of the PC soma with large currents [1]. It has been discovered that complex spiking of PCs includes calcium-mediated dendritic spikes [6]. Hence, it is our goal to detect the origin of the dendritic spikes by using the HDMEA during spiking events. We intend to study the contributions of the dendritic arbor t PC signaling by investigating PCs at different developmental stages.

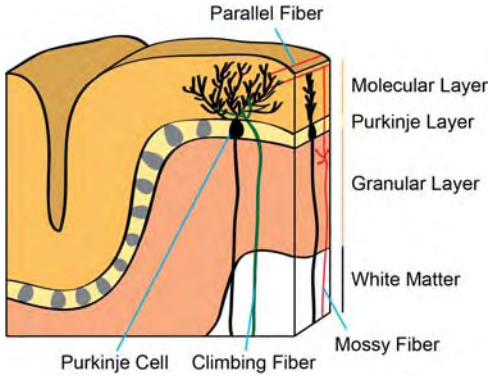

Fig. 1. Cerebellar layers.

2 Methodology

2.1 Acute slice preparation

Wild-type CD-1 mice (P18-P23) were obtained from the Laboratory for Animal Resources and Genetic Engineering in RIKEN Center for Developmental Biology Kobe, Japan. The mice were anaesthetized by isoflurane inhalation and then decapitated. The brain

was dissected and immediately immersed in ice-cold artificial cerebrospinal fluid (ACSF (calcium free); contents in mM: NaCl 125 , KCl 2.5, NaH_2PO_4 1.25, $MgSO_4$ 1.9, Glucose 20, $NaHCO_3$ 25). Then, the cerebellum was separated from the cortex by cutting with a blade and glued onto the vibratome tray along its sagittal plane. Parasagittal cerebellar slices (150-200µm) were obtained and kept under carbogen-bubbled ice cold ACSF (Leica VT-1200S). The slices were incubated at 35°C ACSF (with 2mM $CaCl_2$) for 30-45 minutes and then maintained at room temperature until measurement. All experimental procedures were approved and executed in accordance to RIKEN guidelines.

2.2 Electrophysiology

The acute slice was placed on the HDMEA and continuously perfused with carbogen-loaded ACSF (~30-33°C) throughout the experiment. We combined the HDMEA (11,011 planar electrodes, 3,150 electrodes/mm^2, 126 channels) [7] with conventional patch-clamp (Axon Multiclamp 700B and Digidata 1440A). The recordings were triggered through external signals to precisely synchronize patch and HDMEA data acquisition. The patch pipette was controlled via an automated micromanipulator (PatchStar, Scientifica). The glass pipettes were pulled to have tip resistances of 6-8MΩ (P-97, Sutter Instruments).

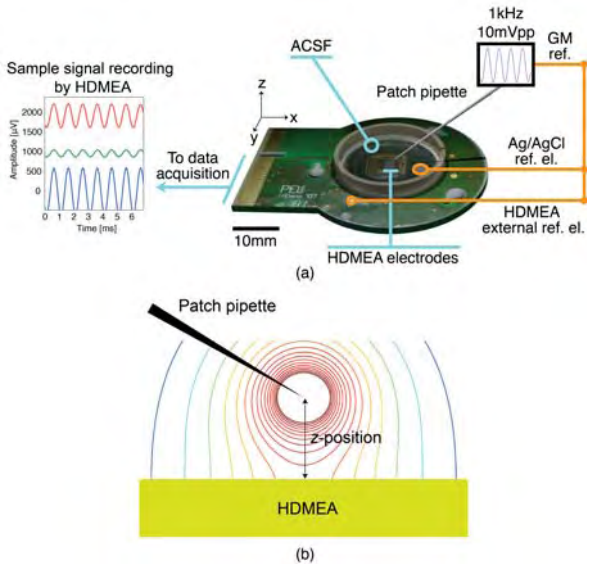

Fig. 2. (a) Setup for localization of the patch pipette on the HDMEA. (b) Simulated potential distribution of a point source corresponding to the patch pipette tip above the HDMEA.

2.3 Blind localization

We used blind localization [8] to navigate the patch pipette towards a PC soma in an acute slice without using a microscope: (1) a current sine-wave of 1kHz was applied to the patch pipette; (2) the signals were recorded with the HDMEA; (3) the patch pipette location was estimated by fitting the measured HDMEA signal amplitudes. The setup is presented in Fig. 2a. We assumed the HDMEA surface to be an insulator and the extracellular space to be homogeneous and isotropic. Hence, the potential of a point source, located anywhere above the HDMEA plane, is measured at the insulator surface with twice its value in the homogeneous space given as:

$$\Phi_e = 2(A) / \sqrt{(x^2+y^2+z^2)},$$

where $A = I/(4\pi\sigma)$, I is the stimulation current, σ is the medium conductivity, and $\sqrt{(x^2+y^2+z^2)}$ is the distance between the point source and the electrode. We show a visualization of the potential distribution from a point source above the HDMEA in Fig. 2b.

Through blind localization, we moved the patch pipette towards PC layer locations, where the HDMEA detected the highest EAPs. The PC somas were initially assumed to be located near the largest recorded negative signal peaks. The patch pipette was maneuvered to the presumable PC location until a Giga-ohm seal was achieved (cell-attached patch).

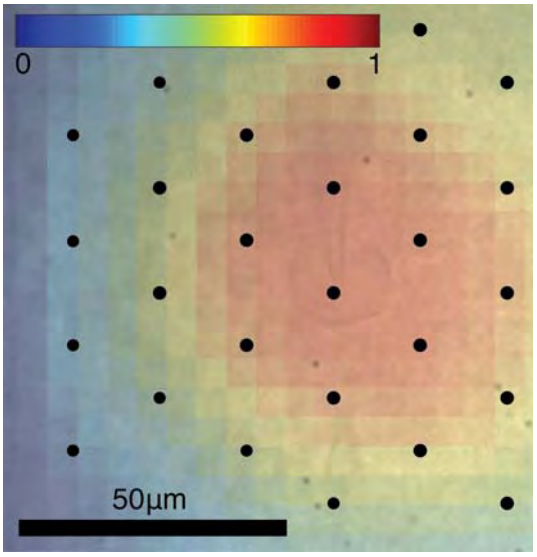

Fig. 3. Heat map showing the interpolation of relative signal amplitudes measured by the HDMEA to estimate the patch pipette location upon issuing a patch pipette stimulation signal. A value of 1 corresponds to the highest recorded amplitude.

3 Results

3.1 HDMEA and patch recordings

We have used blind source localization to move the patch pipette towards a PC soma in an acute slice without visualization. We confirmed that the patch pipette was indeed on a PC soma by using IR-DIC microscopy (BX-61, Olympus). An image of the measured PC soma and the heat map of the signal amplitudes for localizing the patch pipette are provided in Fig. 3. Simultaneous cell-attached patch clamp and HDMEA recordings are obtained from the spontaneously spiking PC.

3.2 Observing different PC spiking states

There are several ways to evoke complex spikes and dendritic spikes in PCs *in vitro*, e.g., through

climbing fiber stimulation or high somatic current injection [1]. Using whole-cell patch-clamp, it is possible to stimulate the PC and observe three different spiking activities (regular simple, fast simple, and complex spikes), shown in Fig. 4. When the corresponding extracellular signals are recorded by using the HDMEA, it is possible to determine the activity at the dendritic area during somatic complex spikes. This is an alternative to multiple patch-clamp recordings at different locations of the neuron, which is a tedious and complicated task.

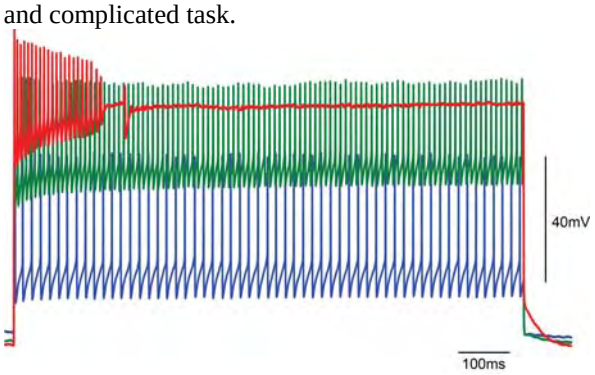

Fig. 4. Whole-cell current clamp measurements of a PC show three different spiking states upon stimulation at different intensities. Blue: Regular simple spiking (0.75nA). Green: Fast simple spiking (2nA). Red: Complex spiking (2.5nA).

4 Conclusion

We have described a methodology to study Purkinje cells using simultaneous HDMEA and patch clamp recordings. We also used blind localization to navigate the patch pipette towards a PC soma in an acute slice.

Acknowledgement

This work was supported by the Japan Society for Promotion of Science (JSPS) under Grants-in-Aid for Young Scientists (B) (No. 25730183).

References

[1] J. T. Davie, B. a Clark, and M. Häusser, “The origin of the complex spike in cerebellar Purkinje cells.,” *J. Neurosci.*, vol. 28, no. 30, pp. 7599–609, Jul. 2008.

[2] U. Egert, D. Heck, and A. Aertsen, “Two-dimensional monitoring of spiking networks in acute brain slices.,” *Exp. Brain Res.*, vol. 142, no. 2, pp. 268–74, Jan. 2002.

[3] U. Frey, U. Egert, F. Heer, S. Hafizovic, and A. Hierlemann, “Microelectronic system for high-resolution mapping of extracellular electric fields applied to brain slices.,” *Biosens. Bioelectron.*, vol. 24, no. 7, pp. 2191–2198, Mar. 2009.

[4] T. J. Blanche, M. a Spacek, J. F. Hetke, and N. V Swindale, “Polytrodes: high-density silicon electrode arrays for large-scale multiunit recording.,” *J. Neurophysiol.*, vol. 93, no. 5, pp. 2987–3000, May 2005.

[5] C. Gold, D. a Henze, C. Koch, G. Buzsáki, Carl Gold, Darrell A. Henze, Christof Koch, and György Buzsáki, “On the origin of the extracellular action potential waveform: A modeling study.,” *J. Neurophysiol.*, vol. 95, no. 5, pp. 3113–28, May 2006.

[6] R. Llinás, M. Sugimori, and R. Llinas, “Electrophysiological properties of in vitro Purkinje cell dendrites in mammalian cerebellar slices.,” *J. Physiol.*, vol. 305, no. 1, pp. 197–213, Aug. 1980.

[7] U. Frey, U. Egert, F. Heer, S. Hafizovic, and A. Hierlemann, “Microelectronic system for high-resolution mapping of extracellular electric fields applied to brain slices.,” *Biosens. Bioelectron.*, vol. 24, no. 7, pp. 2191–2198, Mar. 2009.

[8] M. E. J. Obien, A. Hierlemann, and U. Frey, “Factors Affecting Blind Localization of a Glass Micropipette Using a High-Density Microelectrode Array,” in *Proceedings of IEEE Sensors, 2013*, 2013, pp. 932–935.

Changes of Axonal Conduction in Bursting Activity

Kenta Shimba[1*], Koji Sakai[1], Kiyoshi Kotani[1], Yasuhiko Jimbo[1]

1 The University of Tokyo, Tokyo, Japan
* Corresponding author. E-mail address: shimba@neuron.t.u-tokyo.ac.jp

Abstract
Microelectrode array (MEA) techniques were broadly used to evaluate properties of neuronal networks at various levels from the sub-cellular to the multi-cellular levels. For example, we can record synchronized bursting of neuronal population from multi electrodes and propagating action potentials along axon by using microfabricated devices attached with MEAs. However, there is no method to evaluate neuronal properties of both sub-cellular and multi-cellular level at the same time. In this study, we analysed propagating action potentials along axon at the multi-cellular and sub-cellular level. Results show that shifts of major propagation direction occurred repeatedly in long bursts and bursting activity slows conduction velocity of axons in some neurons. These results suggest that our experimental system is capable of studying changes of axonal conduction in bursting activity at both sub-cellular and multi-cellular levels in the same time.

1 Introduction

Microelectrode arrays (MEA) have been broadly used to evaluate properties of neuronal networks at various levels from the sub-cellular to the multi-cellular levels. At the sub-cellular level, previous study developed a method for detection of propagating action potentials along axons with MEA [1]. Moreover, it was reported that the axon has potentials to control their conduction parameters, depending on neural firings [2]. Thus, network activity is modulated by not only synaptic transmission and plasticity, but changes in axonal conduction parameters. However, there is no method to evaluate neuronal properties of both sub-cellular and multi-cellular level at the same time.

In this study, we attempted to evaluate changes in conduction delay of axonal conduction and the direction of signal propagation between two neuronal networks from bursting activities.

2 Materials and Methods

2.1 Microfabrication

The design and the fabrication method of the culture device is previously described [3]. Briefly, the culture device is composed of a MEA substrate and a ring-shaped chamber made of polydimethylsiloxane (PDMS) as sown in Fig. 1. The inside and the outside of the chamber are connected with 36 microtunnels (750 um in length, 30 um in width and 5 um in height). A half of microtunnels are aligned on three electrodes which have a pitch of 300 um.

The PDMS chamber were developed with a master mold made of SU-8 photoresists. Then, the chamber was attached on a MEA substrate pre-coated with 0.1% poly-ethyleneimine and 20 ug/ml laminin.

2.2 Cell Culture

Cortices were taken from E16 ICR mice and dissociated with 0.25% trypsin and DNase. The cortical cells were seeded in the culture device with the cell density of 5.0×10^3 cells/mm^2. The culture medium was Neurobasal medium supplemented with 2 mM GlutaMAX, a set of B27 supplement and 1% penicillin-streptomycin. Cortical cells were cultured in a CO_2 incubator (5% CO_2, 37 ºC). Half the medium were replaced with fresh one every three days.

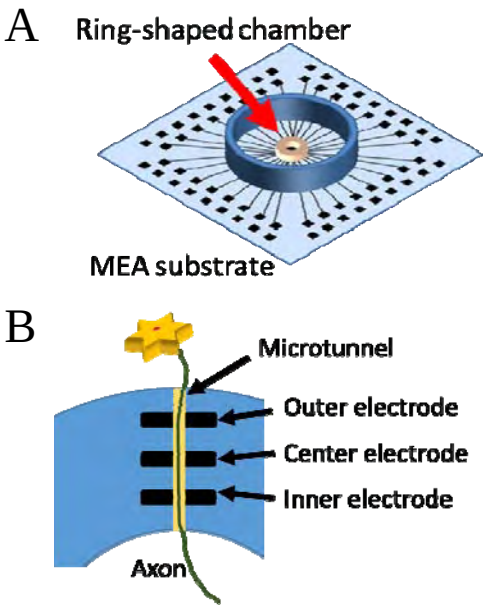

Fig. 1 Schematics of culture device. The culture device is composed of a MEA and a ring-shaped chamber (A). The inside and the outside of the chamber are connected with 36 microtunnels. A half of microtunnels are aligned on three electrodes (B). These structure enables recording of propagating action potentials along axon.

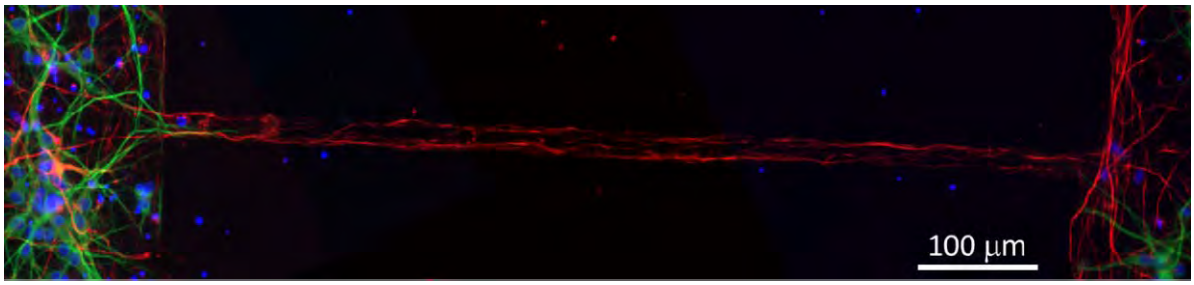

Fig. 2 Immunofluorescent image of cultured cortical neurons. Axons and dendrites were stained with antibodies against neurofilament middle (red) and MAP2 (green), respectively. Nuclei were counterstained with DAPI (blue). It was confirmed that axons entered the microtunnel at 7 days in vitro.

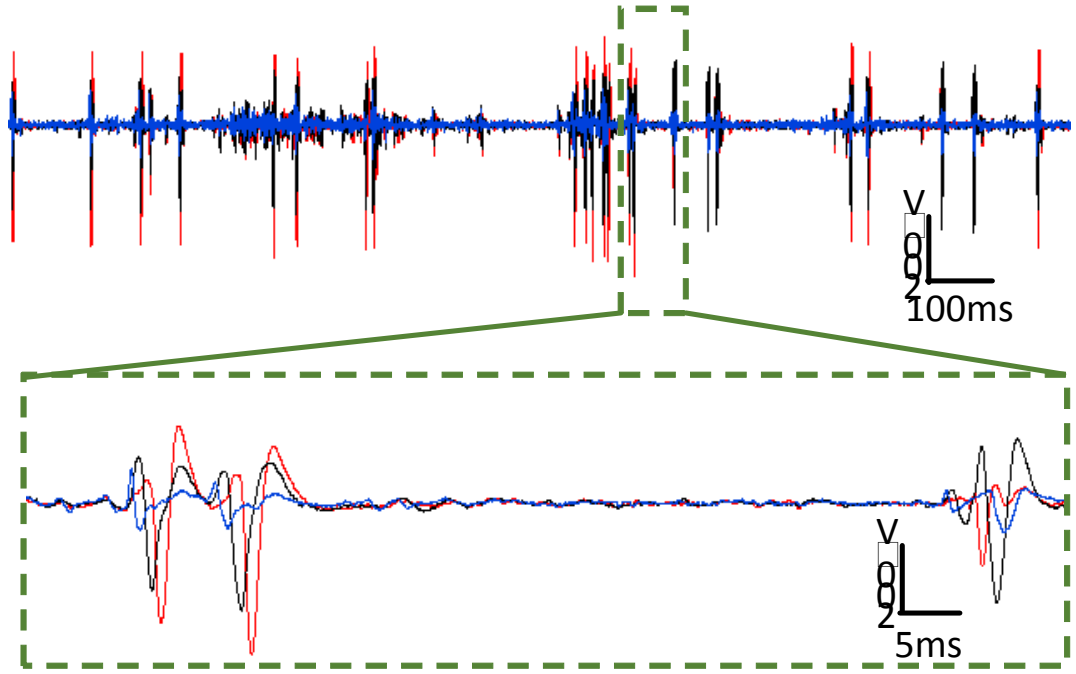

Fig. 3 Spontaneous activity recorded from axons. Neuronal activities were recorded almost simultaneously from three electrodes. Both directions of propagations were observed.

2.3 Data Recording and Analysis

Spontaneous activities were recorded with a recording system previously described [4]. The data from MEA electrodes were processed using amplifiers (× 5000) and a band-pass filter (100 - 2000 Hz). Then, the processed data were converted to digital signal with the sampling frequency of 50 kHz and the resolution of 12 bits and recorded.

Data analysis procedure is composed of spike detection, spike sorting and burst detection. First, neuronal activities were detected from signals of electrodes which had been aligned on the center of each microtunnel. Threshold were set at five times the background noise level of each electrode. Second, spike trains recorded from each electrode were classified into clusters representing individual neurons. We employed EToS software to perform spike sorting [5]. Finally, network bursts were detected from spikes with Wagenaar's method [6].

3 Results and Discussion

3.1 Axonal elongation in microtunnel

Fig. 2 shows an immunofluorescent image of microtunnel. In Fig. 2, multiple images of a microtunnel were pieced together in order to visualize axonal elongation in whole length of the microtunnel. Axons (red) and dendrites (green) were labeled with anti-neurofilament middle and anti-MAP2 antibody, respectively. Results suggest that only axons can pass through microtunnels and few nuclei enter microtunnels.

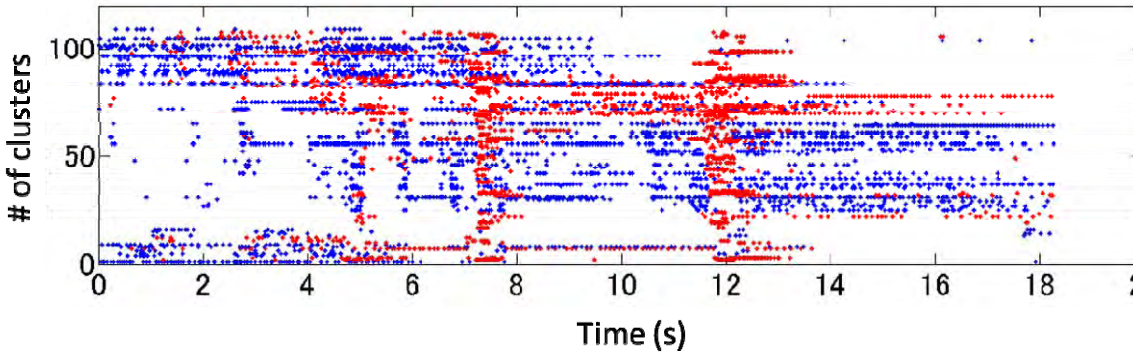

Fig. 4 Raster plot of conductions in a bursting activity. Inward and outward conductions were shown as blue and red dots, respectively. Major directions of conductions were shifted repeatedly. Data were recorded at 10 days in vitro.

3.2 Propagating action potentials

Neuronal activities were recorded almost simultaneously from three electrodes aligned on same microtunnel. Fig. 3 shows a representative waveforms of spontaneous activity. Blue, black and red lines indicate raw traces recorded from outer, center and inner electrode, respectively. We have considered delay time between outer and inner electrodes as conduction delay.

Patterns of network bursts changed with culture days. Long bursting activity (> 10 s) was observed from cortical networks at only 10 days in vitro as shown in Fig. 4. Major directions of propagation were shifted repeatedly in the long burst. However, in short bursts, shift of conduction direction occurred only once or twice.

3.3 Change in conduction delay

We evaluated relationships between the conduction delay and the network activity. As a result, there were some clusters whose conduction delays increased as activity- or time-dependent manner in bursting activities (Fig. 5A). It means that conduction velocity of axon gradually slows down in high frequency firing. In order to determine how many clusters have these kind of property, ratio of conduction delays of the first and last five spikes in each bursting activity were calculated as change index by each clusters. Fig. 5B shows the change index of each cluster in a sample at 10 DIV. The conduction velocity slowing was observed in approximately 15% of all clusters. These results is consistent with early reports which studied axonal conduction slowing with electrical stimulation [7].

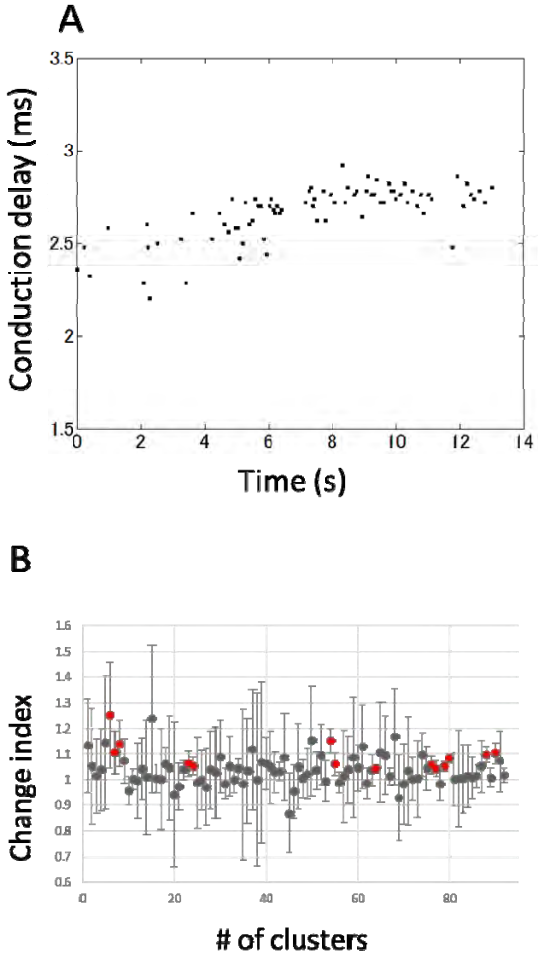

Fig. 5 Changes of conduction delays in bursting activity. (A) A time course of an increase in the conduction delay of a cluster. (B) Changes in conduction delays of all clusters. Change index is defined as ratio of conduction delays of the first and the last five spikes in each bursting activity. Change Index increased in approximately 15% of all clusters (red dots). (mean ± SD)

4 Conclusion

In this study, we analysed propagating action potentials along axon at the multi-cellular and sub-cellular levels. Results show that shifts of major propagation direction occurred repeatedly in long bursts and conduction velocity of some neurons slowed down in bursting activities. These results suggest that our experimental system is capable of studying changes of axonal conduction in bursting activity at both sub-cellular and multi-cellular levels at the same time.

Acknowledgement

We gratefully acknowledge the partial financial support provided by the Japan Society for the Promotion of Science (JSPS) via Grant-in-Aid for JSPS Fellows (25-4923) and a Grant-in-Aid for Scientific Research A (23240065).

References

[1] Dworak, B. J., & Wheeler, B. C. (2009). Novel MEA platform with PDMS microtunnels enables the detection of action potential propagation from isolated axons in culture. *Lab on a Chip*, 9(3), 404-410.

[2] Debanne, D. (2004). Information processing in the axon. *Nature Reviews Neuroscience*, 5(4), 304-316.

[3] Shimba, K., Sakai, K., Arimatsu, K., Kotani, K., Jimbo, Y. (2013). Long term observation of propagating action potentials along the axon in a microtunnel device. *6th International IEEE/EMBS Conference on Neural Engineering*, 945-948.

[4] Jimbo, Y., Kasai, N., Torimitsu, K., Tateno, T., Robinson, H. P. (2003). A system for MEA-based multisite stimulation. *IEEE Transactions on Biomedical Engineering*, 50(2), 241-248.

[5] Takekawa, T., Isomura, Y., Fukai, T. (2010). Accurate spike sorting for multi‐unit recordings. *European Journal of Neuroscience*, 31(2), 263-272.

[6] Wagenaar, D., DeMarse, T. B., Potter, S. M. (2005). MEABench: A toolset for multi-electrode data acquisition and online analysis. *2nd International IEEE/EMBS Conference on Neural Engineering*, 518-521.

[7] Soleng, A. F., Chiu, K., Raastad, M. (2003). Unmyelinated axons in the rat hippocampus hyperpolarize and activate an H current when spike frequency exceeds 1 Hz. *The Journal of physiology*, 552(2), 459-470.

Off-like Responses to the Blue-light in rd1/ChR2 Mouse Retina

Jae Hong Park[1], Hyuk-June Moon[1], Dong-Hoon Kang[1],Sujin Hyung[1] , Hyun Jun Shin[1], Jun-Kyo Francis Suh[1*]

[1]The Center for Bionics, Korea Institute of Science and Technology, Seoul, Republic of Korea
* Corresponding author. E-mail address: jkfsuh@kist.re.kr

Abstract
Optogenetics, a technique to utilize a variety of microbial opsin genes to control cellular behaviors with light, has been shown as a potential means to restore light-sensing functions in the retina of animal model of retinitis pigmentosa. One of the strategies for optogenetic vision restoration was to express channelrhodopsin (ChR2) genes to retina ganglion cells which are the only gateway for visual data transmission from retina to brain. Previous study reported that ganglion cells expressing ChR2 by Thy-1 promoter were depolarized by blue light, regardless of whether they were ON or OFF ganglion cells. In this study, however, we report that a few OFF-like ganglion cells were observed in the rd1/ChR2 mouse retina, showing decreased firing rates with blue light illumination. ChR2-eYFP was widely expressed in the rd1/ChR2 retina and the layer of outer nuclear was absent. Many ganglion cells showed increased firing rates with blue light illumination, a typical ON-like response by the direct ChR2-induced depolarization. However, a few ganglion cells with OFF-like responses were also observed with a decreased firing rate when blue light was illuminated onto the retina. The same retina sample did not respond to yellow light, indicating that OFF responses of ganglion cell was not photoreceptor-mediated but optogenetically-mediated. Treatment of GABA antagonist, picrotoxin can enhance response of ganglion cells to the optogenetic stimulation. We speculate that this OFF response may be resulted by a pathway involving amacrine cells which may suppress the ganglion cells activity by an inhibitory neurotransmitter, GABA. This speculation warrants a further study to confirm the mechanism of OFF response in rd1/ChR2 retina.

1 Introduction

Converting visual signals into electrical signals in photoreceptors is the first step for transmitting visual information to the brain (Baylor, D 1996). Therefore severe or complete loss of photoreceptor causes visual dysfunction or blindness even though other cells remained in the retina including bipolar or ganglion cells are intact. Diseases such as retinitis pigmentosa (RP) or age-related macular degeneration (AMD) destroy photoreceptor cells in the retina, often resulting in complete blindness.

Recently, many studies (Senthil et al., 2010, Bi et al., 2006, Lagali et al., 2008) have shown that regaining photo-sensitivity with channelrhodopsin (ChR2) which can give to cells an ability of responding to light is one of the solutions for restoring visual dysfunction or blindness due to photoreceptor loss. Most of these studies focused on bipolar cells or ganglion cells, which are known for direct visual signal transmitter.

Retinal ganglion cells which are the sole output of retina to the brain receive the signals not only from bipolar cells but also from amacrine cells, the most variable types in the retina. So manipulating an activity of amacrine cells by optogenetics would be also a candidate method for restoring vision.

2 Materials and Methods

A rd1/ChR2 mouse were obtained from cross-breeding with a ChR2-eYFP ((B6.Cg-Tg(Thy1-COP4/EYFP) 9Gfng/J from Jackson Laboratory) and C3H mouse line. To make mice homozygous to the Pde6brd1 mutant, rd1/ChR2 mouse and C3H mouse were continuously crossbred and the gene expression was identified with PCR genotyping. The mice used in this study were the 5th generation offspring. The electrical activity of ganglion cells in the enucleated retina in response to the blue laser (duration 2 seconds, 470nm, ~10mW/mm2) was recorded using a MEA with 256 channels (256MEA200/30iR-ITO-gr, Multi-Channel Systems MCS Gmbh). The electrical signals were sampled at 10 kHz, band-pass-filtered between 100 Hz and 3000 Hz, and segmented and clustered into groups using WaveClus, an open source spike sorting program. The neuronal spike data acquired from the system was analysed with peri-stimulus time histogram(PSTH).

3 Results

As previously reported (Senthil et al., 2010), we have crossbred Thy1::ChR2-eYFP mice with rd1 mutant mice to generate a mouse line that expresses ChR2 in the ganglion cells in the retina, which can not respond to the normal light stimuli otherwise due to photoreceptor loss. ChR2-eYFP was widely expressed in the rd1/ChR2 retina (Figure 1) and the layer of outer nuclear was absent (data not shown here).

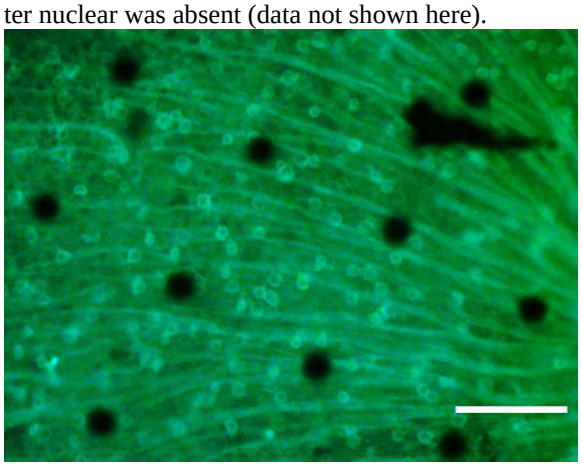

Figure 1. ChR2-eYFP is widely expressed in the rd1/ChR2 retina

Most of the recorded ganglion cells in the rd1/ChR2 mice showed increased firing rates with blue light illumination, a typical ON-like response by the direct ChR2-induced depolarization (Figure 2A). However, a few ganglion cells with OFF-like responses were also observed with a decreased firing rate when blue light was illuminated on the retina (Figure 2B).

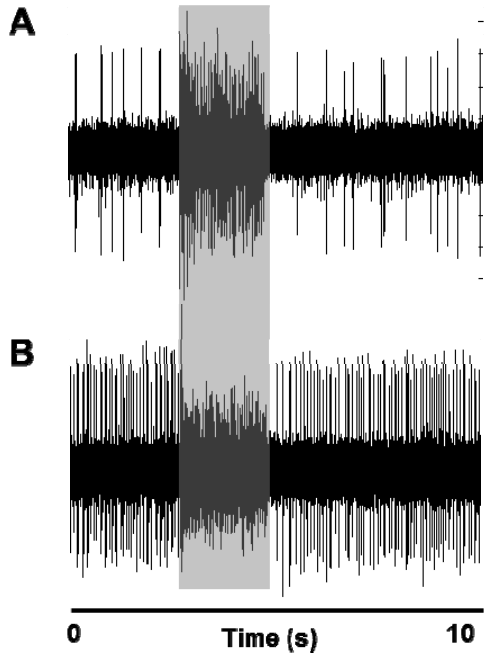

Figure 2. Blue light can both enhance and suppress firing rates of ganglion cells in the ChR2 with rd1 mouse retina. Gray bar indicates the time during blue light laser illumination (ON 2 sec/OFF 8 sec, 1~10mW/mm2, whole field). **A**, most of the recorded cell increased their firing rates during blue light illumination. **B**, A few cells showed the decreased firing rates during the illumination.

To make sure whether this OFF-like response arises from a remained inherent photoreceptor mediated response or not, we illuminated yellow light onto the retina instead. Yellow light did not induce any changes of firing activity of ganglion cells in the rd1/ChR2 mice, indicating that these OFF-like responses were not originated from a natural photoreceptor mediated circuit but from a putative ChR2 mediated inhibitory pathway (Figure 3A and B).

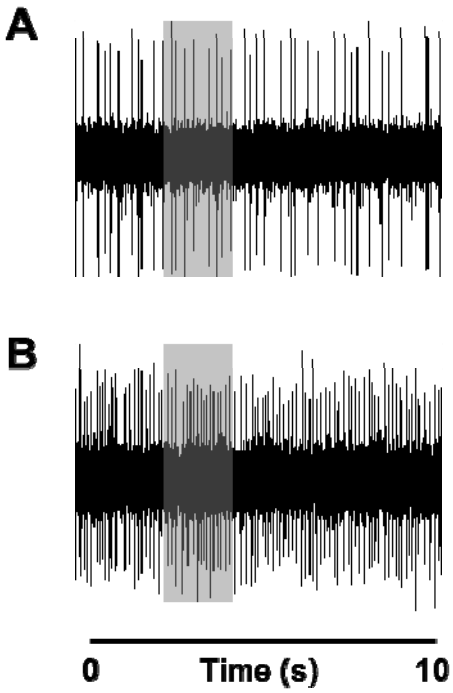

Figure 3. Yellow light did not elicit any firing rates of ganglion cells in the ChR2 with rd1 mouse retina. Gray bar indicates the time during blue light laser illumination (A and B) (ON 2 sec/OFF 8 sec, 1~10mW/mm2, whole field).

Retinal amacrine cells provide inhibition to the retina circuit by releasing neurotransmitter such as GABA or glycine to mediate ganglion cell surrounds or modulate spiking activity of ganglion cells. To test whether inhibitory inputs were required for this OFF-like response, we treated the reitna sample with picrotoxin, GABA inhibitory receptor antagonist when we were recording responses of the ganglion cells to blue light illumination. Blockade of GABA pathway in the retina changed the firing pattern of ganglion cells. A cell which showed a transient ON response followed by suppressed firing activity responded vigorously to the blue light illumination (Figure 4A). GABA treatment increased the response to the blue light stimuli, suggesting that blue light evoked inhibition could exist in rd1/ChR2 mice retina (Figure 4B).

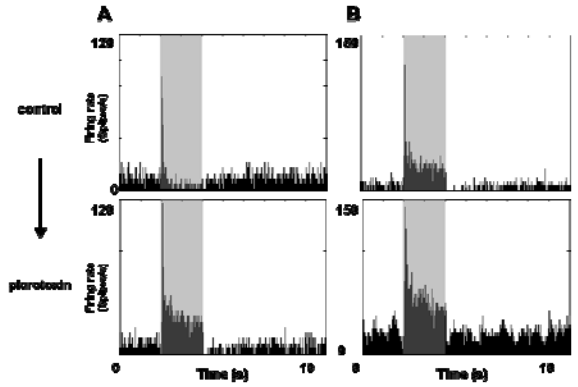

Figure 4. Blockade of GABA inhibition by picrotoxin treatment (100uM) in the ChR2 with rd1 mouse retina can increase the response of ganglion cells to the blue light illumination. Gray bar indicates the time during blue light laser illumination (ON 2 sec/OFF 8 sec, 1~10mW/mm2, whole field). **A**, This cell showed a transient increase of the firing rate followed by suppressed activities lower than spontaneous firing rates However, after picrotoxin treatment, this cell changed its firing pattern to sustained response. **B**, This cell showed a sustained response to blue light laser stimulation. The level of both evoked and spontaneous firing rates increased after picrotoxin treatment.

3 Conclusion

We showed that ChR2 mediated blue light responses in the retina can suppress the firing rate of ganglion cells in the rd1/ChR2 mouse retina via GABA inhibitory pathway. Ectopic expression of ChR2 in a few amacrine cells in the rd1/ChR2 mice might be a putative explanation of this phenomenon.

Previous study (Senthil et al., 2010) showed that ChR2 was exclusively expressed in ganglion cells not in other types of cell such as amacrine cells (Thyagarajan et al.,). However, ectopic expression of ChR2 in some GABAergic amacrine cells might be explained by mosaic expression of exo-gene in transgenic mouse line (Qi Lu et al.,). To make sure this suppressed activity is originated from amacrine cells, further studies are required.

Acknowledgement

This research was supported by National Agenda Project of the Korea Research Council of Fundamental Science & Technology(NAP-09-04) and the KIST Institutional Program(Project No. 2E24721)

References

[1] Baylor, D. (1996). How photons start vision. Proc. Natl. Acad. Sci. USA 93, 560e565.

[2] Richard H. Masland (2001) The fundamental plan of the retina. *Nature neuroscience, 4, 877 - 886*

[3] E J Chichilnisky. (2001). A simple white noise analysis of neuronal light responses. *Network : computation in neural systems*, 12, 119-213.

[4] Qi Lu, Elena Ivanova, Tushar H. Ganjawala, Zhuo-Hua Pan. (2013). Cre-mediated recombination efficiency and transgene expression patterns of three retinal bipolar cell-expressing Cre transgenic mouse lines. *Molecular Vision 19:1310-1321*

[5] Qi Lu, Elena Ivanova, Tushar H. Ganjawala, Zhuo-Hua Pan. (2013). Cre-mediated recombination efficiency and transgene expression patterns of three retinal bipolar cell-expressing Cre transgenic mouse lines. *Molecular Vision 19:1310-1321*

[6] Senthil Thyagarajan, Michiel van Wyk, Konrad Lehmann, Siegrid Lo¨wel, Guoping Feng, and Heinz Wa¨ssle Visual Function in Mice with Photoreceptor Degeneration and ransgenic Expression of Channelrhodopsin 2 in Ganglion Cells (2010) *The Journal of Neuroscience*, June 30, 30(26):8745–8758

[7] Lagali PS, Balya D, Awatramani GB,Mu¨nch TA, Kim DS, Busskamp V, Cepko CL, Roska B (2008) Light-activated channels targeted to ON bipolar cells restore visual function in retinal degeneration. *Nat Neurosci* 11:667–675.

[8] Bi A, Cui J, Ma YP, Olshevskaya E, Pu M, Dizhoor AM, Pan ZH (2006) Extopic expression of a microbial-type rhodopsin restores visual responses in mice with photoreceptor degeneration. *Neuron* 50:23–33.

Decoding of Motion Directions by Direction-Selective Retina Cells

Michele Fiscella[1]*, Felix Franke[1], Jan Müller[1], Ian L. Jones[1], Andreas Hierlemann[1]

1 Bio Engineering Laboratory, ETH Zurich, Basel, Switzerland
* Corresponding author. E-mail address: michele.fiscella@bsse.ethz.ch

Abstract
Computing the direction of a moving object is a basic task that animals must perform in order to survive. Population activity of neurons that respond exclusively to defined motion directions has been studied in different brain regions with the aim to understand how animals infer motion directions. Retinal ON-OFF direction-selective ganglion cells (oo-DSGCs) are the first neurons to encode motion directions in the visual system. We used a microelectronics-based microelectrode array for recording simultaneous extracellular activity from all known retinal oo-DSGCs and for decoding their activity. We stimulated oo-DSGCs with moving objects of different velocities and sizes and tested different decoding methods (linear, Bayesian) to infer motion directions. Our decoding results indicate that population activity is required for decoding motion directions (~ 9 degrees, RMSE) with low error, and that the direction-selective system is robust towards changes in light stimulus parameters.

1 Background / Aims

The retina extracts information on the direction of a moving object by relying on a certain type of neurons, known as ON-OFF direction-selective ganglion cells [1] (Fig. 1) (oo-DSGCs).

The mammalian retina contains four types of oo-DSGCs, and their concerted activity is likely to be combined in higher brain regions (thalamus, superior culliculus and visual cortex) to compute the direction of a moving object [2]. Our main goals are: (a) recording population activity from oo-DSGCs (b) investigating, which is the best strategy for decoding oo-DSGC population activity; (c) exploring how and what parameters of light stimuli influence the decoding performance.

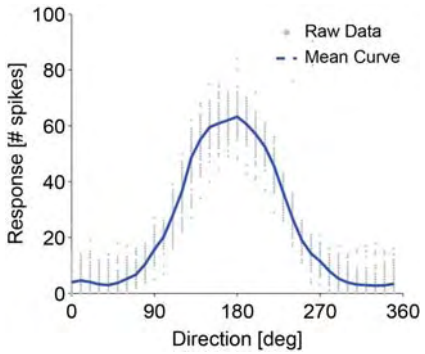

Fig. 1. Response of a single oo-DSGC to a rectangular bar moving along 36 directions, spaced 10° apart. Stimulus movement in every direction was repeated 100 times, and the bar moved at 1.6 mm/s. Gray dots show cell responses to a single sweep. The blue curve is the mean response.

2 Methods / Statistics

The eyes of New Zealand albino rabbits were dissected under dim red light conditions in Ames solution, and the retina was isolated for recording extracellular activity of the ganglion cell layer.

For extracellular recordings we used a microelectronics-based high-density microelectrode array (HD-MEA) [3]. The microelectrode array features 11,011 platinum electrodes with diameters of 7 µm and electrode center-to-center distances of 18 µm over an area of 2 * 1.75 mm^2. 126 electrodes can be arbitrarily selected for simultaneous recording. Extracellular action potentials were recorded at a sampling frequency of 20 kHz.

In order to isolate single-cell activity, spike sorting was carried out manually by using the software UltraMegaSort2000 [4] on non-overlapping groups of 5-7 electrodes.

3 Results

Dozens of direction-selective neurons have been recorded from the visual cortex, and their synchronous activity has been studied for decoding motion directions [5]. Nevertheless, only recently it was possible to record concerted activity from defined retinal populations by microelectronics-based high-density microelectrode arrays (HD-MEAs) (Fig. 2 A-B).

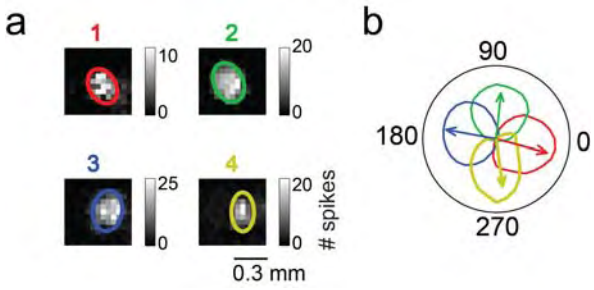

Fig. 2. (a) Overlapping receptive fields of four simultaneously recorded oo-DSGCs with different preferred directions. (b) Normalized direction-tuning curves and preferred directions of the cells shown in Fig. 2a.

We isolated light-induced extracellular activity from all known oo-DSGC types (Fig. 3) and explored the following issues: (1) what combination of cells performs best in decoding motion direction; (2) what decoding strategy is most accurate; (3) how do different stimulus parameters influence the decoding (e.g., velocity, size of moving object).

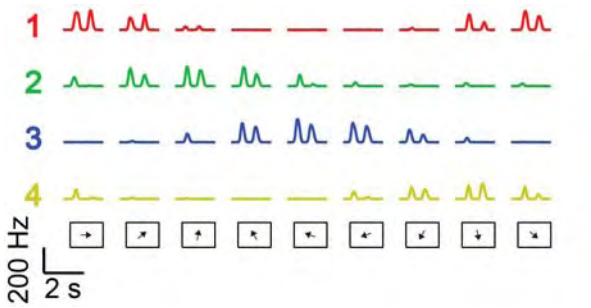

Fig. 3. Synchronously recorded responses of 4 oo-DSGCs to motion. Responses are colored according to the ganglion cell's preferred direction. Every row shows the activity of a single ganglion cell upon different directions of motion. Bottom arrows show directions of stimulus motion.

We found that the decoding of the simultaneous activity of all oo-DSGCs types improved the precision of direction estimation about 6-fold in comparison to using the signals of only a single oo-DSGCs (Fig. 4). In addition, population probabilistic decoders (i.e. Bayesian maximum-likelihood) performed significantly better than linear decoders (population vector, optimal linear estimator) [6]. Finally, the velocity of the moving object did not influence decoding precision, while an increase in the size of the moving object negatively affected direction estimation.

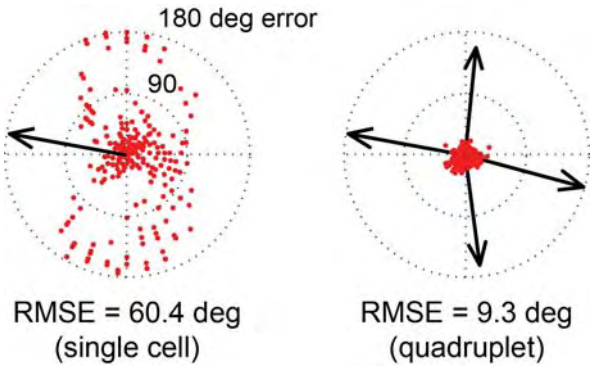

Fig. 4. Left: decoding results by using a single direction-selective cell. Right: decoding results obtained by a combination of four orthogonal direction-selective cells. Red dots indicate the decoding error along a defined direction of motion (max error = 180 degrees). RMSE = root-mean-square error.

4 Conclusion/Summary

The results described here show that the precision of direction estimation decoding can be improved by recording the simultaneous activity of all oo-DSGCs types. Furthermore, since we have access to the noise correlations in the comprehensive data set, our data can be used to test if noise correlations influence decoding performance.

Acknowledgement

This work was supported by the Advanced ERC Grant "NeuroCMOS" under contract number AdG 267351 and the SNSF Sinergia Project CRSII3_141801 Michele Fiscella acknowledges individual support through a Swiss SystemsX interdisciplinary PhD grant No. 2009_031.

References

[1] Barlow HB, Hill RM (1963) Selective sensitivity to direction of movement in ganglion cells of the rabbit retina. Science 139: 412-414.

[2] Cruz-Martin A, El-Danaf RN, Osakada F, Sriram B, Dhande OS, et al. (2014) A dedicated circuit links direction-selective retinal ganglion cells to the primary visual cortex. Nature 507: 358-361.

[3] Fiscella M, Farrow K, Jones IL, Jackel D, Muller J, et al. (2012) Recording from defined populations of retinal ganglion cells using a high-density CMOS-integrated microelectrode array with real-time switchable electrode selection. J Neurosci Methods 211: 103-113.

[4] Hill DN, Mehta SB, Kleinfeld D (2011) Quality metrics to accompany spike sorting of extracellular signals. J Neurosci 31: 8699-8705.

[5] Graf AB, Kohn A, Jazayeri M, Movshon JA (2011) Decoding the activity of neuronal populations in macaque primary visual cortex. Nat Neurosci 14: 239-245.

[6] Tanabe S (2013) Population codes in the visual cortex. Neurosci Res 76: 101-105.

High Resolution Large-Scale Recordings of Light Responses from Mouse Retinal Ganglion Cells

Gerrit Hilgen[1], Alessandro Maccione[2], Stefano Di Marco[2], Luca Berdondini[2], Evelyne Sernagor[1]

1Institute of Neuroscience, Medical Sciences, Newcastle University, Newcastle upon Tyne, UK
[2]Neuroscience and Brain Technologies, Istituto Italiano di Tecnologia , Genova, Italy

Abstract
We combined an innovative light-stimulation system with a CMOS-based 4096-electrode array to study light responses from mouse retinal ganglion cells at a pan-retinal level. Here we show for the first time a method to record light responses from thousands of ganglion cells simultaneously.

1 Background/Aims

The retina converts the visual scenery into neuronal signals. Retinal ganglion cells (RGCs), the output cells of the retina, receive all the visual information transduced by photoreceptors and processed by various layers of highly specialized retinal interneurons, encoding this information into trains of action potentials that are transmitted to the visual centres of the brain via the optic nerve. Relatively little is known about retinal strategies for encoding visual scenes. Multielectrode array (MEA) recording from the RGC layer is a commonly used approach to study retinal encoding. However, most commercially available systems are restricted in terms of coverage and spatial resolution. In order to achieve better knowledge about global encoding of visual scenes by the RGC layer, one should ideally record from the entire RGC layer at high spatiotemporal resolution.

2 Methods

Using the high-density large-scale CMOS-based Active Pixel Sensor (APS) MEA (Biocam, 3Brain, Landquart,CH) featuring 4,096 electrodes (42 µm spacing) arranged in a 64x64 configuration that covers an active area of 2.67x2.67 mm (7.12 mm^2) (Berdondini et al., 2009), we can record from nearly the entire RGC layer in the mouse retina (Maccione et al., 2014). Further, a new light-stimulation system consisting of two components was developed and combined with the APS device: 1) custom written control software (VisualStimulator) and 2) modified DLP Pico Projector (Texas Instruments) connected via an HDMI cable to the computer (Fig1.A). VisualStimulator sends display data and control signals through this connection back to the projector. Each frame onset of the display data is monitored and sent over a BNC cable directly into the Biocam where it is visualized and recorded using the Brainwave software (3Brain).

3 Results

Here we present for the first time light-evoked activity recorded simultaneously from thousands of individual RGCs (Fig. 1 B,C) at pan-retinal level in the neonatal and adult mouse retina using a set of stimuli classically used to characterize basic features of RGC receptive fields (RFs) (e.g. binary white noise, full field flashes, gratings, disks, annuli). Our recordings show how spatio-temporal RF features such as response duration, timing and direction selectivity sharpen with development.

4 Conclusions

The large scale of the array and the density of the electrodes give us unprecedented opportunities to decipher how the whole retina encodes visual stimuli, without variability caused by pooling data from multiple experiments. Preliminary results already show that light-evoked RGC responses obtained with the large-scale APS allow not only to characterise thousands of receptive fields simultaneously, but also to detect potential long range interactions across the retina, which may be of major significance in the encoding of complex natural scenes at the pan-retinal level.

The research is supported by the 7th Framework Programme for Research of the European Commission, under Grant agreement no 600847: RENVISION project of the Future and Emerging Technologies (FET) programme (ES, LB).

References

[1] Berdondini et al., 2009: “Active pixel sensor array for high spatio-temporal resolution electrophysiological recordings from single cell to large scale neuronal networks”, Lab On Chip, vol 9, pp. 2644–2651, 2009.

[2] Maccione et al., 2014: “Following the Ontogeny of Retinal Waves: Pan-Retinal Recordings of Population Dynamics in the Neonatal Mouse“.J Physiol. 2014 Apr 1;592(Pt 7):1545-63

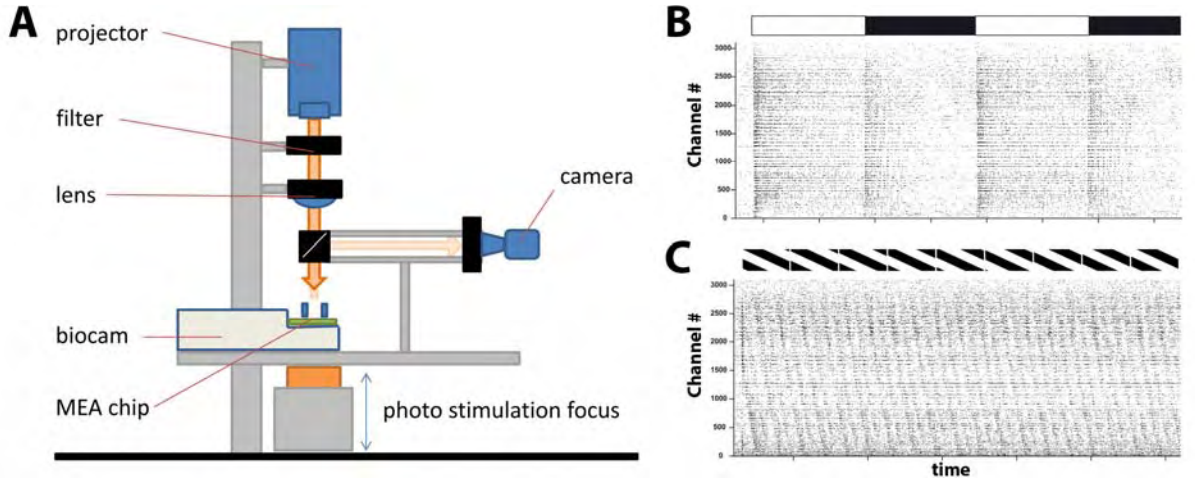

Fig.1: A) Diagram showing the Biocam combined with the Projector system. **B, C)** Raster plots of 3105 channels recorded from simultaneously, responding either to full field flashes (B) or to moving gratings (C).

Novel Insights into Visual Information Processing of Human Retina

Katja Reinhard[1], Marion Mutter[1], Michele Fiscella[2], Jan Müller[2], Felix Franke[2], Andreas Hierlemann[2], Thomas Münch[1*]

[1] Centre for Integrative Neuroscience, University of Tübingen, Tübingen, Germany
[2] ETH Zürich, D-BSSE, Basel, Switzerland
* Corresponding author. E-mail address: thomas.muench@cin.uni-tuebingen.de

1 Background/Aims

Retinal information processing has been studied extensively in animal models. Many specialized circuits providing information about direction selectivity, specific temporal and spatial aspects of a visual scene, colour, approaching movements etc. have been identified. It is often thought that such sophisticated image processing might be absent in human retina. However, except for a short communication by Weinstein et al. in 1971 [1], the retinal information processing in the human retina has not been studied with in-vitro methodology. Further, we believe that it is important to gain more knowledge about the human retina also to develop targeted treatment options against visual impairment. We thus aimed at studying human retina function at cell and system levels in-vitro.

2 Methods

Human retinas were donated by patients, who had to undergo a medically indicated enucleation of one eye. Pieces of these retinas were placed ganglion cell side-down on a 60-electrode multi-electrode array (Multichannel Systems, 200 µm electrode distance, 30 µm electrode diameter), and stimulated with various light stimuli. We recorded spikes produced by retinal ganglion cells (RGCs) in response to the light stimuli. In addition, we implemented a high-density MEA with 11’011 electrodes, and performed first successful measurements with human retina.

3 Results

In 8 out of 15 donated retinas we could measure abundant light responses. The recorded cells showed diverse properties: ON-, OFF- and ON-OFF-responses, different response latencies and transiencies. Further, we found that human RGCs are tuned to higher speeds and higher temporal frequencies compared to previously recorded mouse RGCs.

4 Conclusion/Summary

We show that it is possible to perform in-vitro electrophysiology with donated human retina. The recorded retinas showed light responses with diverse properties. The observed differences in speed tuning might be explained by the higher angular velocities to which human RGCs are exposed in the bigger human eye. Further, differences in temporal frequency tuning suggest species-specific kinetic differences of synaptic processing within the retinal circuitry. In conclusion, we show that it is possible to record light responses from human retina in-vitro, and that the human retina shows high diversity in its information processing, as it has been demonstrated for other species. In the future, the extensive use of high-density MEAs will allow further comprehensive characterization of human RGC types.

Acknowledgement

We would like to thank Prof. K. U. Bartz-Schmidt and the operating team of the University Eye Hospital Tübingen for the collaboration for the donation process.

References

[1] Weinstein GW, Hobson RR, Baker FH. Extracellular recordings form human retinal ganglion cells. Science 1971; 171(975): 1021–2.

Investigation of Functional Connectivity in Degenerative Retina Using MEA-STA System

Hyuk-June Moon[1], DongHoon Kang[1], JaeHong Park [1], SuJin Hyung[1], HyunJoon Shin[1], JunKyo Francis Suh [1*]

1 Center for Bionics, Biomedical Research Institute, KIST, Seoul, Korea
* Corresponding author. E-mail address: jkfsuh@kist.re.kr

Abstract
With the trend of population ageing, the number of people experiencing vision loss by retinal degeneration disease, such as age-related macular degeneration(AMD) and retinitis pigmentosa(RP), has increased dramatically. Recently, several electrical/optogenetics retinal prosthesis(implant) schemes that stimulate remaining cells in the retina instead of lost photoreceptors have been proposed. However, degenerated retinas may have distorted neural circuits and functional connectivity among remaining cells is hardly researched, which may be a critical key for the high level vision prosthesis. Therefore, we suggest a method using MEA and spike-triggered average stimulus analysis to investigate the functional connectivity among remaining cells in degenerative retina.

1 Introduction

In case of certain retinal degeneration disease, such as AMD and RP, retinal tissue except photoreceptors layer remains healthy and maintains its functions until the late stages of the disease. Recently, several electrical/optogenetics retinal prosthesis researches which aim to restore vision by stimulating remaining retinal cells have been conducted around the world [1][2].

For the high level vision restoration such as shape, letter recognition, retinal prosthesis has to understand and utilize retinal circuits composed of remaining cells. However, degenerated retinas may have distorted neural circuits caused by disease and functional connectivity among remaining cells has hardly been researched.

In this research, a retinal signal processing system which consists of MEA, optical stimulator and STA(Spike-triggered average) stimulus analysis method for investigating functional connectivity among retinal cells is proposed[3].

2 Methods

2.1 The MEA-STA system

The whole system is composed of 4 parts, stimulation control system, optical stimulator, MEA and signal analysis system(Fig.1). Stimulation control system could generate signals for various dynamic/static stimulation patterns. The whole process was controlled by customized code with MATLAB (Mathworks, U.S.A.) and PsychToolBox. Optical stimulation system translated the control signal to laser stimulus pattern with high spatial/temporal resolution and stimulated the retina tissue. LC-R 720(Holoeye, Germany) spatial light modulator(SLM) was used to modulate the pattern.

USB-MEA 256 system and 200-30 MEA plates (Multichannel systems, Germany) were used for retinal signal acquisition. The recorded data is analyzed with STA analysis programs coded on MATLAB.

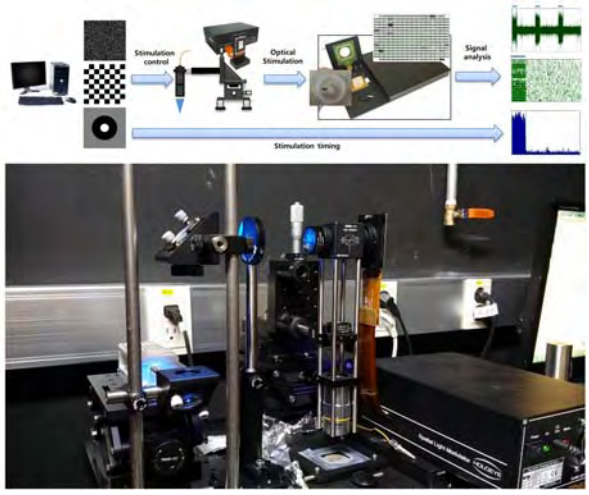

Fig. 1. Implementation of the retinal signal analysis system. (up) scheme of the system composed of stimulation controller, light stimulator and MEA. (down) picture of the implemented system.

2.2 Methods of experiments

To investigate functional connectivity with retinal ganglion cells, ChR2 gene had to be genetically targeted to specific cell type in the retina of C3H/HeN ($Pde6b^{rd1}$;rd1). In this study, however, we used blind ChR2 transgenic mouse(thy-1/rd1), instead of using gene-transfer methods, as a preliminary research tool to show a potential of the system. Retinas of the mouse were explanted and recorded on the MEA-STA

system while light-stimulated. Ames' medium, with O_2 95%, CO_2 5% aeration, was used for preparation and also circulated on MEA plate while recording neural signal. The whole procedure was executed in dark room.

To test the feasibility of the system, the whole field ON/OFF(2 sec : 8 sec) and binary random pattern stimulation(2x2/4x4) for STA analysis were performed on the system. The neuronal spike data acquired from the system was analysed to peri-stimulus time histogram(PSTH) and STA stimulus pattern, respectively.

3 Results

In the experiment with the whole field ON/OFF stimulation, the number of neural spikes on light ON phase was obviously higher then OFF phase in the ChR2-targeted mouse, whereas, the untreated rd1 control retina didn't show any difference between ON and OFF phase(Fig.2). Ganglion cells out of the stimulation area also didn't show any regular pattern. Spikes time stamp data of ganglion cells with random and uniformly distributed binary pattern stimulation was analysed with the STA method which provides an average stimulation pattern making the specific ganglion cell fire(Fig.3).

4 Conclusion

This system which modulates laser stimuli with high spatial/temporal resolution could stimulate specific regions of the target retina in expected time windows. After data analysis procedure, we could estimate from which region cells(or a cell) generated the retinal signal that made target RGC(retinal ganglion cells) fire. Furthermore, from the results of many RGCs, we could investigate functional connectivity of the retina.

This research showed the potential to figure out the function of the various cell types in retina and connectivity among them by combining with methods which can give light-activity to specific cell types, such as optogenetics.

Acknowledgement

This research was supported by National Agenda Project of the Korea Research Council of Fundamental Science & Technology(NAP-09-04) and the KIST Institutional Program (Project No. 2E24721).

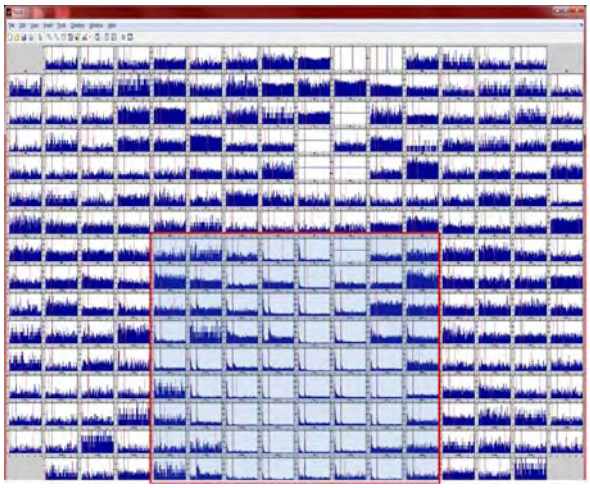

Fig. 2. Peri-stimulus time histogram(PSTH) matrix of the Thy-1/rd1 ChR2 TG mouse. The electrodes in the red square was stimulated(wide field) and ON responses were only shown in that area.

Fig. 3. Spike-triggered average(STA) stimulus(4x4) matrix of the Thy-1/rd1 ChR2 TG mouse. The light stimulation which covered the region around the electrode induced the RGCs near the electrode to fire.

References

[1] Dorn JD, et al. (2013). Argus II Study Group. The Detection of Motion by Blind Subjects with the Epiretinal 60-Electrode (Argus II) Retinal Prosthesis. *JAMA Ophthalmol*. 131(2):183-9

[2] Pamela S Lagali, Constance L Cepko & Botond Roska, et al. (2008). Light-activated channels targeted to ON bipolar cells restore visual function in retinal degeneration. *Nature neuroscience*, 11, 667-675.

[3] E J Chichilnisky. (2001). A simple white noise analysis of neuronal light responses. *Network : computation in neural systems*, 12, 119-213.

Pharmacology, Toxicology, and Drug Screening

Neurotoxicity Screening Using Multi-Well Microelectrode Array Plates: Lessons Learned and a Path Forward

Timothy J Shafer[1*]

1 Integrated Systems Toxicology Division, NHEERL, ORD, United States Environmental Protection Agency, RTP, NC USA
* Corresponding author. E-mail address: shafer.tim@epa.gov

Abstract
The large numbers of chemicals for which toxicity information is lacking has caused a paradigm shift in toxicity testing from descriptive, animal-based studies to predictive, in vitro approaches. Because neurotoxicity and developmental neurotoxicity can result from interactions of chemicals with a wide variety of different biological target molecules, in vitro, high-throughput testing approaches must be sensitive to effects mediated via many different pathways. Spontaneous activity of neuronal networks grown on microelectrode arrays (MEAs) is known to be sensitive to disruption by a drugs and chemicals acting via multiple ion channels, neurotransmitter receptors and other pathways. Recent improvements in the throughput of MEAs have made screening and prioritization of compounds for additional testing feasible, and several studies have demonstrated that chemical screening with MEAs has high sensitivity and selectivity and is reproducible across laboratories. However, other challenges remain, including improving the throughput of data analysis, automation of workflow, and incorporation of networks of human origin.

1 Introduction

1.1 The problem of too many chemicals.

In the 20th century, toxicology was largely a descriptive science, and characterization of the hazard (neurotoxicity, hepatotoxicity, renal toxicity, etc) and risk (hazard x exposure) of chemicals was done largely on a chemical by chemical basis, largely using animal based testing approaches. However, in vivo approaches are low throughput, and in many cases were not predictive of outcomes in humans. Because the synthesis of novel chemicals and their introduction into the marketplace has far outstripped characterization of their toxicity, it is estimated that there are ~80,000 chemicals in the environment for which adequate toxicity data are lacking, including neurotoxicity and developmental neurotoxicity data. A recent study reported that to date, there are only approximately 12 chemicals that are known to cause developmental neurotoxicity in humans, but that thousands of other chemicals also have potential to do so but to date have not been characterized.

In 2007, the United States National Research Council published a report on *Toxicity Testing in the 21st Century* [1]. This report highlighted the need for a new approach to chemical testing and recommended using in vitro testing approaches that are high-throughput and predictive of adverse outcomes in humans, as well as the use of human-derived cellular models and tissues. This created new challenges for the field of neurotoxicology in order to be able to screen and prioritization of chemicals for their potential to cause neurotoxicity and developmental neurotoxicity.

2 Testing approaches for neurotoxicty and developmental neurotoxicity.

2.1 Molecular, structural and functional approaches to neurotoxicity testing.

Several different types of approaches can be utilized for neurotoxicity testing, each with its own advantages and dis-advantages. Molecular and biochemical approaches, such as receptor binding assays, enzyme activity assays, and other biochemical endpoints have the advantage of being easily scalable to high-throughput or ultra high-throughput assays, as well as being able to identify potential receptor binding sites, allosteric interactions, and enzyme inhibition. However, these assays often times are performed using cellular components rather than whole cells or neuronal networks, and a large number of assays are needed to adequately cover the biological space that might be disrupted leading to neurotoxicity or developmental neurotoxicity. Morphological endpoints, such as high-content imaging, have the throughput necessary for screening and can provide information regarding a chemical's ability to alter the structure of neurons, but lack the ability to determine if that structure is associated with a meaningful change in function. By contrast, neurophysiological assays provide functional information, but until the advent of higher throughput MEAs, either were too focused on an individual end-

point (e.g. a single ion channel in high-throughput patch assays) or lacked the temporal resolution to provide the most meaningful physiological data (e.g. fura measurements of calcium signals).

2.2 Advances in the use of MEAs for neurotoxicity screening.

Over the past 5 years, there have been significant advances in the use of MEAs for neurotoxicity screening. The reproducibility of MEAs across different laboratories was demonstrated by Novellino and colleagues [2]. MEAs were shown to be highly sensitive and selective in separate studies by Defranchi and colleagues [3] and McConnell and colleagues [4] using sets of 20 and 30 chemicals, respectively. Interestingly, one class of compounds that was not detected well in both of these studies was agonists of the nicotinic acetylcholine receptor (nAChR). Over the past 2 years, my laboratory has examined a set of 92 unique compounds from the EPA's ToxCast program, and has confirmed the sensitivity and selectivity of these earlier experiments. One lesson learned from this work is that the first 20 minutes of recording can be a period of dramatic changes in activity (Figure 1) and that filtering out this period of time results in more stable baselines (Figure 2).

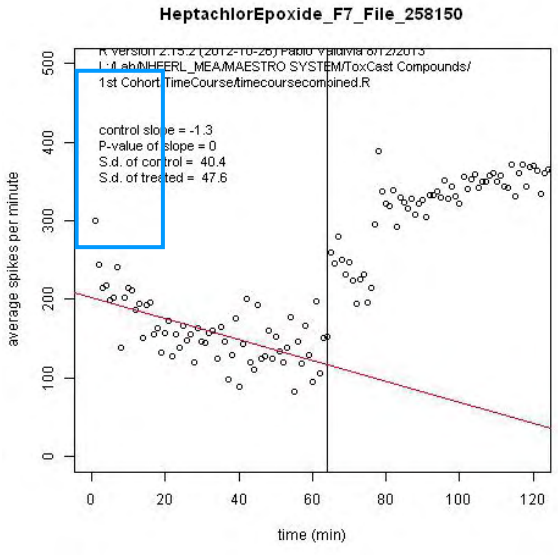

Fig. 1. Stability of baseline recordings. In the example shown above, the mean firing rate per minute is plotted vs time. Sixty minutes of control activity is plotted, followed by 60 minutes of activity in the presence of a test compound (Heptachlor in this recording). The red line is a linear regression of the first 60 minutes of activity. The blue box illustrates that during the first 20 min of recording, spike rate changes dramatically, and influences the slope of the regression line.

Further, this work also indicates that agonists of nAChR do not cause alterations of mean firing rate in primary cultures of cortical neurons. More recent work in my laboratory has applied MEAs to screening of nanoparticles for effects on network activity as well as different classes of flame retardants. Overall, this work demonstrates that it is possible to utilize MEAs to screen compounds for their ability to disrupt function of neuronal networks.

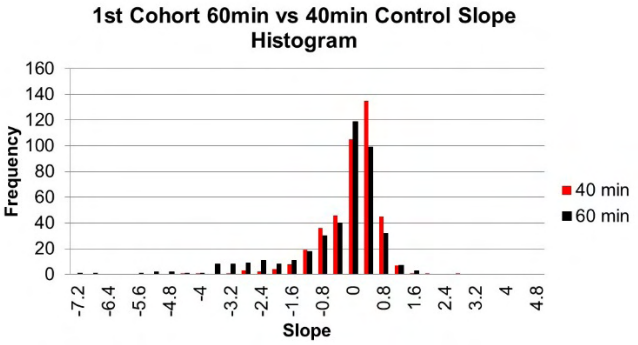

Fig 2. Histogram of slope values from control recordings for the entire 60 min of recording vs the final 40 minutes of recording. As is illustrated the final 40 min of recording histogram has a narrower distribution and a mean slope value of -0.23, while the entire 60 min has more very negative slope values and a mean slope value of -0.62. (n=450 wells.)

3 Future Needs.

3.1 Data analysis needs

The advent of multi-well MEA plates has greatly facilitated the collection of data on different compound effects on neuronal network function. Extraction of metrics such as the mean firing rate in a well and the number of electrodes that are recording activity are fast and easy. However, a greater challenge is a more rapid and efficient extraction of data on bursting parameters, correlation of activity, and other endpoints, which may also contain information regarding a compound's effects on network activity. Progress is being made on this front in the form of freely sharable scripts for R-programming and MATLAB. Once extraction of these endpoints is more streamlined, there will be a need to use infomatics approaches to organize and extract useful information about effects of hundreds or thousands of compounds that could potentially be tested in MEAs.

3.2 Human neuronal models are needed.

As outlined in the report from the NRC, one critical component for prediction of toxicity in humans is to, where possible, utilize human tissue or human cells. In the past, there were few sources of human neurons available to scientists, mostly consisting of either transformed cell lines or tissue from surgical resections [5], neither of which are ideal for various reasons. However, the advent of embryonic and inducible stem cell derived neurons offers a new opportunity to study activity in "normal" human neuronal networks in vitro. To date, however, there have been only a few publications utilizing these models in MEAs [6.7]; thus, a major goal is to expand the capability to use human stem cell derived neurons and standardize the culture methods necessary to successfully differentiate these cells into fully functional neuronal networks.

3.3 Utilizing MEAs for Developmental Neurotoxicity screening.

While MEAs are increasingly being used to screen compounds for potential acute neurotoxicity, their use in developmental neurotoxicity screening has lagged. Proof-of-concept papers have been published that indicate MEAs are also a sensitive approach for developmental neurotoxicity screening [6,7]. However, even small numbers (10-20) of compounds have yet to be tested under a developmental exposure paradigm. The increased availability of multi-well MEAs should facilitate progress in this area, and my laboratory is currently working to develop such approaches.

4 Conclusions

MEAs have been utilized for some time to characterize the neurotoxicity of individual chemicals and are known to be sensitive to effects of compounds acting via a wide varitety of receptors, channels and other targets. However, their use to screen larger numbers of compounds for potential neurotoxicity was limited by throughput. Multi-well MEA platforms have solved that problem and screening activity with MEAs is increasing. Increasing the ease and throughput of data analysis, greater utilization of human-derived neuronal networks, and incorporation of developmental exposure paradigms are challenges that, once addressed, will further the use of this technology for neurotoxicity testing.

Acknowledgement

I greatly appreciate the support of the student contractors, research support scientists, and my colleagues who have contributed to this work in too many ways to enumerate.

References

[1] NRC. Toxicity Testing in the Twenty-First Century: A Vision and a Strategy. Washington, D.C: The National Academies Press, 2007.

[2] Novellino A, Palosaari P, Scelfo B, Price A, Whelan M, Sobanski, T, Gross GW, Gramowski A, Schroeder O, Shafer T, Johnstone A, Chiappalone M, Martinoia S, Tedesco MTB, Pittaluga E, D'Angelo P. Successful assessment of the in vitro electrophysiology from neuronal network coupled to micro electrode array based for neurotoxicology tests of neuroactive chemicals. Frontiers in Neuroengineering Apr 27; 4:4, 2011.

[3] Defranchi E, Novellino A, Whelan M, Vogel S, Ramirez T, van Ravenzwaay B, Landsiedel R. Feasibility assessment of mirco-electrode chip assay as a method of detecting neurotoxicity in vitro. Frontiers in Neuroengineering. 2011. 4(6): 1-12.

[4] McConnell ER, McClain MA, Ross J, LeFew WR and Shafer TJ. Evaluation of multi-well microelectrode arrays for neurotoxicity screening using a chemical training set. Neurotoxicology 33, 1048-57, 2012.

[5] Breier, J. Radio, N. Mundy, WR and Shafer, TJ. Development of a high-throughput assay for assessing anti-proliferative compounds using human neuroprogenitor cells. Tox. Sci. 105, 119-133, 2008.

[6] Heikkilä, J., Ylä-Outinen, L., Tanskanen, J. M., Lappalainen, R. S., Skottman, H., Suuronen, R., Mikkonen, J. E., Hyttinen, J. A., and Narkilahti, S. (2009). Human embryonic stem cell-derived neuronal cells form spontaneously active neuronal networks in vitro. Exp. Neurol. 218, 109–116.

[7] Ylä-Outinen, L., Heikkilä, J., Skottman, H., Suuronen, R., Äänismaa, R., and Narkilhati, S. (2010). Human cellbased micro electrode array platform for studying neurotoxicity. Front. Neuroengineering 3:111.

[8] Hogberg, HT, Sobanski T, Novellino A, Whelan M, Weiss DG, Bal-Price AK. Application of micro-electrode arrays (MEAs) as an emerging technology for developmental neurotoxicity: evaluation of domoic acid-induced effects in primary cultures of rat cortical neurons. Neurotoxicology. 2011. 32, 158-168.

[9] Robinette B, Harrill J, Mundy, WR and Shafer TJ. In vitro assessment of developmental neurotoxicity: use of microelectrode arrays to measure functional changes in neuronal network ontogeny. Frontiers in Neuroengineering. Jan 20, 4:1, 2011.

Cytotoxicity of the Antimalarial Drug Mefloquine and Novel Protection by Quinolinic Acid

Katelyn E. Holmes*, David Smith, Guenter W. Gross

Center for Network Neuroscience, Department of Biological Sciences, University of North Texas, Denton, TX 76203
* Corresponding author: katelynholmes@my.unt.edu

Abstract
Mefloquine Hydrochloride has been used for many decades to prevent malaria. Many mefloquine users have reported adverse side effects such as depression, general anxiety disorder, psychoses, convulsions, seizures, tinnitus, and movement disorders. However, there are no quantitative data on mefloquine toxicity in the literature, and no direct toxic effects on neurons have been published. We report that mefloquine inhibits spontaneous network activity in the nanomolar range with an EC50 of 421.2 nM. Further studies have identified Quinolinic Acid as a protection shifting the neurotoxicity of mefloquine to much higher concentrations. Endogenous concentrations of Quinolinic Acid might be an explanation for the varying side effects experienced by mefloquine users.

1 Backround / Aims

Mefloquine Hydrochloride (Larium), a 4-quinolinemethanol derivative, is an antimalarial agent that has been used for the past 40 years. Numerous reports of neurological side effects have recently led the FDA to issue a strong warning, which lead the US Army to discontinue its use in 2013. Mefloquine is still used widely throughout the world because it is very effective in preventing against all five species of Plasmodium that contribute to malaria including *Plasmodium falciparum* which has been developing a resistance to anti malarial agents [5]. Despite serious side effects, such as depression, general anxiety disorder, psychoses, convulsions, seizures, tinnitus, and movement disorders there are no quantitative data on mefloquine toxicity in the literature. No explanation has yet been given for the observation that not all users report such side effects [1].

Quinolinic acid (QA) is synthesized from L-tryptophan in the kynurenine pathway and is produced by microglia and resident macrophages [2]. QA increases during times of immune responses and aids in breakdown of toxins [2]. There have been multiple studies on the endogenous concentrations of QA and current literature is quite variable. It is known that some of the highest levels of QA (up to 20 uM) reside in immuno-compromised individuals. These levels are restricted to the brain tissue, while CSF levels remain at ~3.5 uM [8].

2 Methods / Statistics

We have used primary cultures derived from embryonic mouse cortical tissue, growing on MEAs, to investigate mefloquine toxicity and potential blockers of such toxicity. Mefloquine is only slightly soluble in water, and stock solutions were prepared in dimethyl sulfoxide (DMSO). The maximum DMSO volume in the medium bath did not exceed 1% of the total bath volume. Concurrent DMSO controls confirmed slight excitation at 1.5% with minor activity suppression at 3% and major loss at 8%.

Mefloquine dissolved in DMSO was applied with a micropipette to achieve concentrations ranging from 200-1000 nM. The network activity was continuously monitored and displayed as 1min total or average activity. Successive additions were delayed until the network activity formed a temporally stable (horizontal) plateau (usually about 30 min). All experiments received 40 uM bicuculline ~ 60 min prior to the addition of mefloquine. Experiments with quinolinic acid were conducted using the same procedure but were adjusted for the testable application of QA applied (25-200 uM).

3 Results

Mefloquine is functionally toxic by suppres-sing spontaneous network activity in a concen-tration-dependent manner. Fig. 1 depicts the typical stepwise activity suppression in response to mefloquine additions.

The normal IC50 to mefloquine is 421.2+/-12.0 nanoM (n=6). The activity suppression is only minimally reversible with two medium changes after a normal 4 hr dose-response experiment. At 1 microM, mefloquine becomes clearly cytotoxic within 10 min after compound application. All spontaneous activity is lost within one min after application and cannot be retrieved by 2 medium changes. Both neurons and glia show clear signs of cell stress, necrosis, and extensive membrane blebbing. This is followed by total cell death of almost all network components.

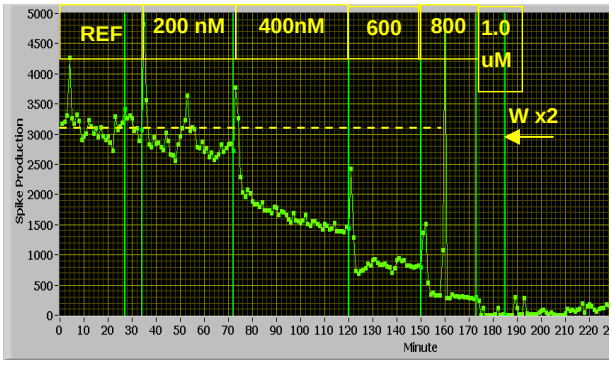

Fig. 1- Stepwise decrease of activity with increasing concentrations of mefloquine. Two medium changes (W) reveal that activity cannot be revived after 3 hr exposures.

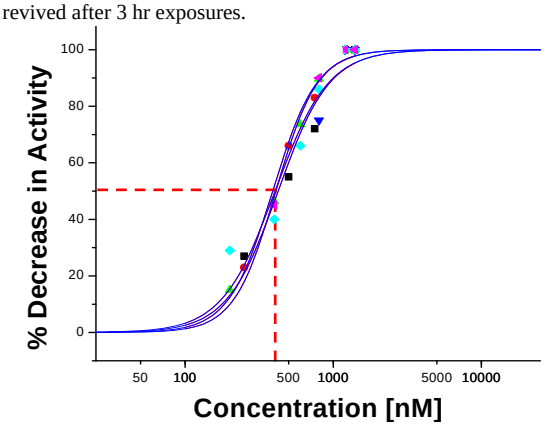

Fig. 2- Mefloquine concentration response curves (n=6). IC_{50}: 421+/- 13 nM.

Table 1- Mefloquine IC50 data.

Exp.	Date	Units*	IC50 [uM]
KH04	10/21/13	84	438.3
KH05	10/28/13	60	421.7
KH15	1/30/14	48	437.3
KH16	1/31/14	52	416.8
KH18	2/15/14	34	404.6
KH19	2/18/14	35	408.6
	average		421+/-13

NOTE: Units in Tabel 1 refers to discriminated neuronal signatures based on template matching, > 2:1 SNRs, and threshold crossing.

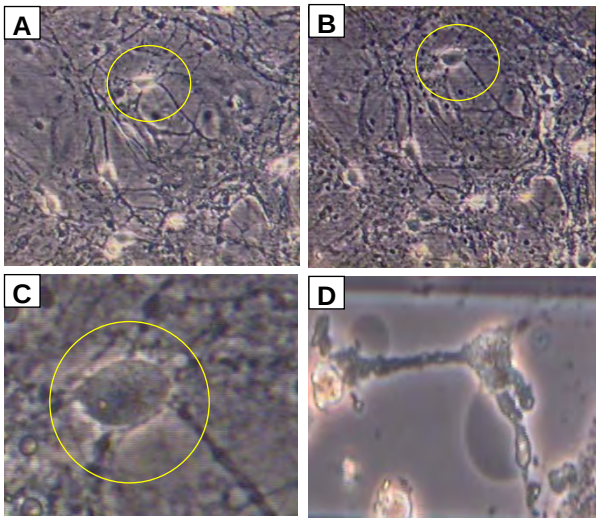

Fig. 3. Gradual destruction of network components by 1 microM mefloquine within 30 min of application. Both neurons and glia are affected. Circle shows swelling of neuron during this time period. (D) Blebbing of another neuron after 50 min exposure.

Protection by Quinolinic Acid

As a possible answer to the variable side effects experienced by mefloquine users, we have found that the ubiquitous metabolite, quinolinic acid (QA), is protective and shifts the IC_{50} to higher concentrations. In the presence of 100 uM QA, the mefloquine IC_{50} is 1.06 +/- 0.07 microM, a 2.5-fold increase (n=5). With the addition of 25 uM QA 30 min before the application of mefloquine, the IC_{50} is shifted from 420.7 to 645.7 nanoM (n=1).

Blebbing of neurons after a one time appli-cation of mefloquine is shifted from 1 micoM to 3 microM in 30 minutes with the protection of QA. Although this compound has been linked to axonal degeneration and excitotoxicity [2] , such responses have not been seen in cultured networks until QA concentrations reach 300 micoM (n=5).

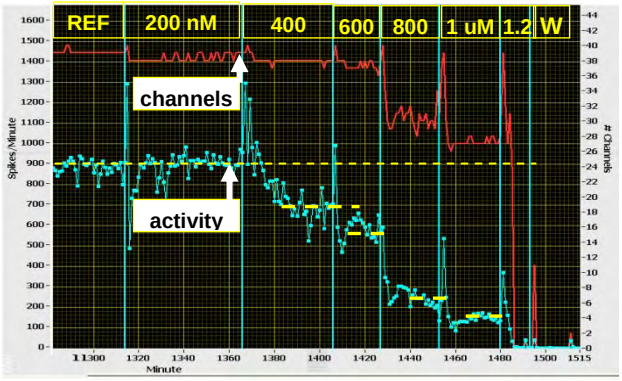

Fig. 4- Step wise decrease of activity with mefloquine and the protection of 25 uM QA

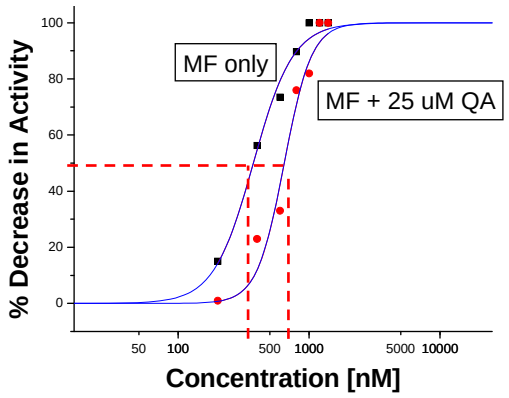

Fig. 5. Shift of CRC's in presence of 25 uM QA from 421 uM to 646 uM.

Table 2- Mefloquine IC50 in the presence of 100 uM QA

Exp.	Date	# Un.	IC50
07	11/11	73	940.4
25	3/22	89	1162.1
28	3/28	60	1044.37
29	3/31	55	1000
32	4/11	50	1026.6

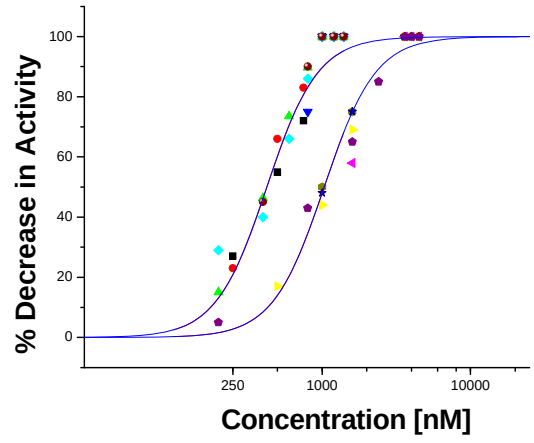

Fig. 6- Major CRC shift in the presence of 100 uM QA. IC50 values change from 421.7+/-13 nM to 1.06 +/- 0.07 uM with 30 min pre-application of QA.

4 Conclusion/Summary

Mefloquine appears to cause network activity suppression through at least two mechanisms. The rapid (1-2min) responses suggest binding to plasma membrane receptors. However, the slower development of necrosis and massive membrane blebbing reflects major subcellular disruption. Blebbing occurs when the membrane separates from the underlying cytoskeleton [9].

Levels of endogenous quinolinic acid vary as the compound has the ability to accumulate within the CNS [2], although normal levels are reported to remain in the nanomolar range. However, in vitro experiments with cerebellar granular cells have shown that QA has a protecting effect when applied in concentrations up to 2.5 microM [4]. At these concentrations, no cell death was seen. Protection was assumed to involve amelioration of glutamate induced apoptosis [4]. This study hypothesised that QA is not neurotoxic but serves as a protecting agent.

Mefloquine has been shown to have a high affinity for the adenosine A2A receptor where it acts as an antagonists [6]. These properties have made mefloquine a good candidate for Parkinson's disease symptom management. Literature also supports that QA acts on the same adenosine A2A receptors [7]. Our findings demonstrate mefloquine functional toxicity and cytotoxicity in the nanomolar range. A clear protective effect by quinolinic acid is also evident, as mefloquine EC50 values are shifted to substantially higher concentrations. In addition the reported neurotoxicity of quinolinic acid already in the nanomolar range is not supported by our experiments. QA does not become cytotoxic until concentrations reach 300 uM (n=5).

We suggest that the highly variable responses reported by mefloquine users are at least partially caused by different endogenous concentrations of quinolinic acid.

References

[1] Aschenbrenner, D (2013) Antimalarial Drug Can Produce Neurologic or Psychiatric Symptoms. American Journal of Nursing 11: 1.

[2] Guillemin, GJ (2012) Quinolinic acid, the Inescapable Neurotoxin Febs. 279, 1355-1365

[3] Gopal, K. (2011) Assessment of Styrene Oxide Neurotoxicity Using *In Vitro* Auditory Cortex Networks Int. J. Occup Med Environ Health, 20 (2), 215-22

[4] Yoshitatsu S. (1997) Quinolinic acid protects rat cerebellar granule cells from glutamate-induced apoptosis. Neuroscience Letters 241;180–184.

[5] Nosten, F. (2000). Effects of artesunate-mefloquine combination on incidence of *Plasmodium falciparum* malaria and mefloquine resistance in western Thailand: a prospective study. The Lancet: 35 (9226): 297–302.

[6] Weise, S. (2003). Discovery of nonxanthine adenosine A_{2A} receptor antagonists for the treatment of Parkinson's disease. *Neurology 61(11): S101-S106*

[7] Behan, W. (2002) Enhanced neuronal damage by co-administration of quinolinic acid and free radicals, and protection by adenosine A_{2A} receptor antagonist. British Journal of Pharmacology 135(36): 1435–1442.

[8] Heyes, M. (2001) Elevated cerebral spinal fluid quinolinic acid levels are associated with region-specific cerebral volume loss in HIV infection. Brain 124: 1033-1042.

[9] Yi, Y. (2012) Integrin-mediated Membrane Blebbing Is Dependent on Sodium-Proton Exchanger 1 and Sodium-Calcium Exchanger 1 Activity. *J. Biol. Chem. 2012, 287:10316-10324*

Norepinephrine Modulates Bursting Activity Differently During Development

Lui Yoshida[1*], Kiyoshi Kotani[1], Yasuhiko Jimbo[1]

1 The University of Tokyo, Tokyo, Japan
* Corresponding author. E-mail address: yoshida@neuron.t.u-tokyo.ac.jp

Abstract
To evaluate norepinephrine (NE) effect on cultured neuronal network during development, spontaneous activities with NE applications were measured in 14 DIV (2 WIV), 22 DIV (3 WIV), and 28 DIV (4 WIV). NE suppressed the number of spikes and bursts regardless of development stages whereas NE did not supress the mean length of bursts, the mean number of spikes in bursts, and the active electrodes in bursts in 2-3 WIV cultures but in 4 WIV ones. These results suggest that NE modulate bursting activity differently during development.

1 Background

Network bursts are thought to be essential for information processing, but recent studies indicated that network bursts were hallmark of pathological condition [1] and altered its properties during development [2]. Norepinephrine (NE) modulates neuronal activity such as awareness [3] and signal processing [4] and is considered to have anti-epileptic effect [5]. However, little is known about NE effect at the network level in detail. Therefore this study focused on NE effect on network bursts during development.

2 Method

2.1 Cell culture

Hippocampal neurons from new-born Wistar rat P4-6 were cultured on MEA which held a square grid pattern of 64 electrodes for 14 DIV (days *in vitro*) (2 WIV (weeks *in vitro*)) (N_{2WIV}=3), 22 DIV (3 WIV) (N_{3WIV}=3), and 28 DIV (4 WIV) (N_{4WIV}=5).

2.2 Extracellular potential measurement

Spontaneous activity of each culture was measured for 75 minutes. To evaluate dose dependency, NE was applied four times every 15 minutes and the final concentration of NE was increased in increments of 10 μM. The data for 800 seconds during each condition of NE concentration was used for analysis. Each condition was named as S, N1, N2, N3, and N4.

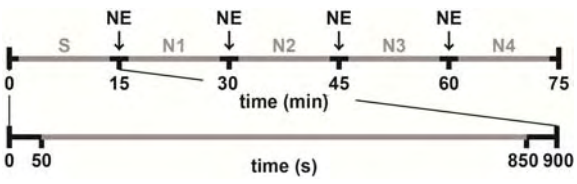

Fig. 1. Experiment protocol. NE was applied four times every 15 minutes. Each condition was named as S, N1, N2, N3, and N4.

2.3 Analysis

Spikes were detected with five standard deviation threshold. The number of spikes and spike rate were calculated for each condition

Network bursts were detected with Pelt's method [2]. The number of bursts and burst properties such as length of bursts and number of spikes and active electrodes in bursts were calculated for each condition.

3 Results and discussion

Spike analysis

The spike rates and the numbers of spikes of 2-4WIV cultures were decreased after the NE applications (Fig. 2 (a-b)). After the second NE application, the time course of the number of spikes did not change markedly at all developmental stages.

These results show that NE has suppressant effect on activity regardless of the developmental stages and the saturating concentration of the effect is 20μM.

Network burst analysis

The numbers of bursts were decreased after the NE applications at all developmental stages (Fig. 3 (a)). However, the length of bursts and the number of spikes and the active electrode in bursts were not changed in 2-3WIV cultures, but those of 4 WIV ones were decreased after the NE applications (Fig. 3 (b-d)).

According to that network burst is wide-spread synchronized activity which has a similarity to epileptic activity, the burst suppression effect of NE would be related to anti-epileptic effect. The observation of the effect suggests that details of anti-epileptic effect could be elucidated *in vitro*. Downes showed that the cultured neuronal network changed its network topology during development [6]. From this point of view, the different effect of NE on the burst properties between 2-3 WIV and 4 WIV cultures would have relation with the change of the network topology.

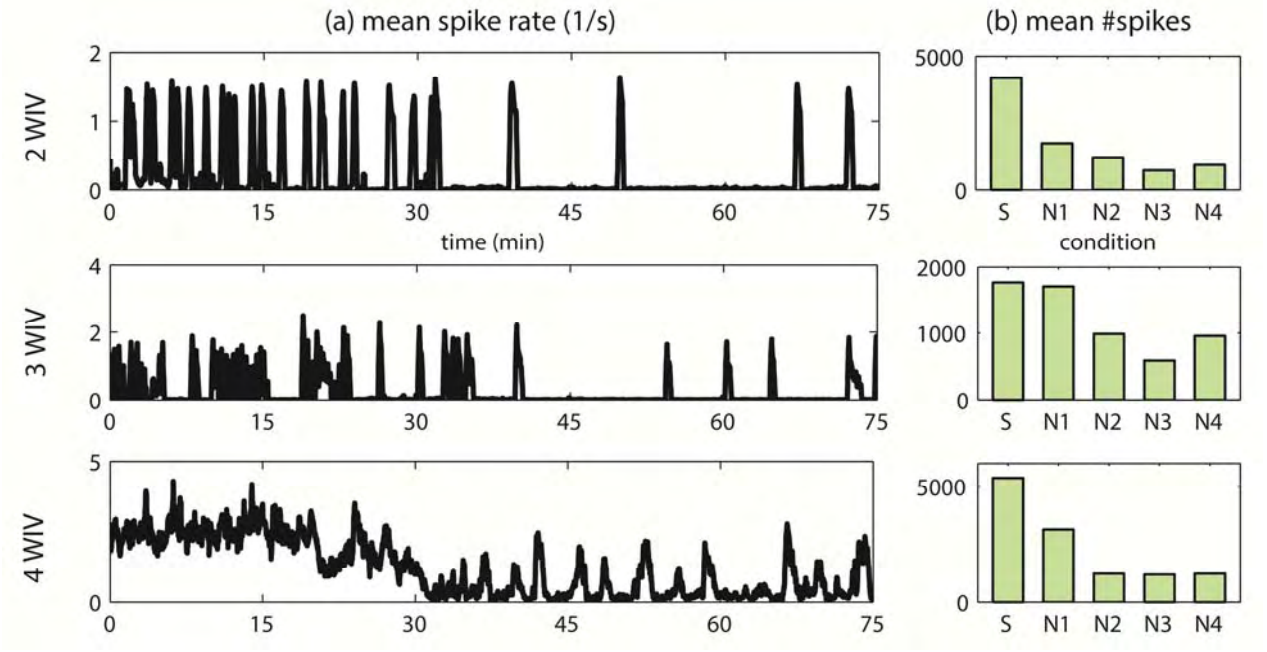

Fig. 2. Spike analysis. (a) Mean spike rate of representative cultures. (b) Mean number of spikes of all cultures (N_{2WIV}=3, N_{3WIV}=3, N_{4WIV}=5). The spike rate and the number of spikes were decreased after the second NE application in 2 WIV (upper), 3 WIV (middle), and 4 WIV (lower).

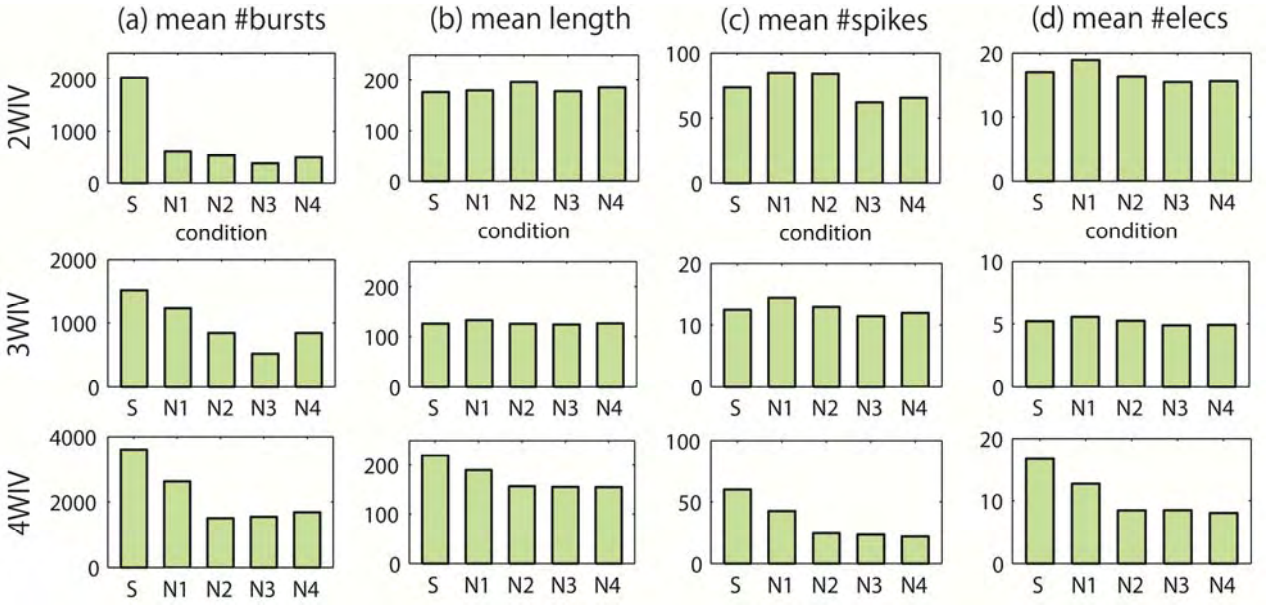

Fig. 3. Network burst analysis. (a) Mean number of bursts. (b) Mean length of bursts. (c) Mean number of spikes in bursts. (d) Mean number of active electrodes in bursts. The number of bursts was decreased after NE application in 2 WIV (upper), 3 WIV (middle), and 4 WIV (lower). Mean length of bursts and mean number of spikes and active electrodes in bursts of 2-3 WIV cultures were not remarkably changed, but those in 4 WIV ones were decreased after NE applications.

Acknowledgement

This work was supported in part by Grants-in-Aid for Scientific Research (23240065) and JSPS Fellows (12J07412)

References

[1] Wagenaar, D. A., Madhavan, R., Pine, J., Potter, S. M. (2005). Controlling bursting in cortical cultures with closed-loop multi-electrode stimulation. *The Journal of neuroscience*, *25*(3), 680-688.

[2] van Pelt, J., Wolters, P. S., Corner, M. A., Rutten, W. L., & Ramakers, G. J. (2004). Long-term characterization of firing dynamics of spontaneous bursts in cultured neural networks. *Biomedical Engineering, IEEE Transactions on*, *51*(11), 2051-2062.

[3] Aston-Jones, G., Bloom, F. E. (1981). Activity of norepinephrine-containing locus coeruleus neurons in behaving rats anticipates fluctuations in the sleep-waking cycle. *The Journal of Neuroscience*, *1*(8), 876-886.

[4] Hasselmo, M. E., Linster, C., Patil, M., Ma, D., & Cekic, M. (1997). Noradrenergic suppression of synaptic transmission may influence cortical signal-to-noise ratio. *Journal of Neurophysiology*, *77*(6), 3326-3339.

[5] Krahl, S. E., Clark, K. B., Smith, D. C., & Browning, R. A. (1998). Locus coeruleus lesions suppress the seizure‐attenuating effects of vagus nerve stimulation. *Epilepsia*, *39*(7), 709-714.

[6] Downes, J. H., Hammond, M. W., Xydas, D., Spencer, M. C., Becerra, V. M., Warwick, K., Whalley, B. J., Nasuto, S. J. (2012). Emergence of a small-world functional network in cultured neurons. *PLoS computational biology*, *8*(5), e1002522.

Microelectrode Array Recording and Ca^{2+} Imaging in Hippocampal Cultures Enzymatically Treated with Hyaluronidase

Mukhina Irina[1,2*], Vedunova Maria[1,2], Mitrosina Elena[1,2], Sakharnova Tatiana[1,2], Zakharov Yury[1], Pimashkin Alexey[1], Dityatev Alexander[1,3]

1 N.I. Lobachevsky State University of Nizhny Novgorod, Nizhny Novgorod, Russia
2 Nizhny Novgorod State Medical Academy, Nizhny Novgorod, Russia
3 German Center for Neurodegenerative Diseases (DZNE), Magdeburg, Germany
* Corresponding author. E-mail address: mukhinaiv@mail.ru

Abstract

Microelectrode array recording were used for estimation of network activity in hippocampal cultures after destruction of the hyaluronic acid containing perineuronal nets (PNNs), surrounding cell bodies and the proximal dendrites. The extracellular matrix (ECM) plays an important role in use-dependent synaptic plasticity. Hyaluronic acid (HA) is the backbone of the neural ECM, which has been shown to modulate AMPA receptor mobility, paired-pulse depression, L-type voltage-dependent Ca^{2+} channel (L-VDCC) activity, long-term potentiation and contextual fear conditioning. To investigate the role of HA in the development of spontaneous neuronal network activity, we used microelectrode array recording and Ca^{2+} imaging in hippocampal cultures enzymatically treated with hyaluronidase (Hyase). Our results suggest that changes in the expression of hyaluronic acid can be epileptogenic and involve changes in Ca^{2+} oscillations. Spontaneous recover of the hyaluronic acid containing perineuronal nets after destruction correlated with reduction of neuronal “superbursts” and neuronal and astrocytic Ca^{2+} “superoscillations.”

1 Introduction

The extracellular matrix (ECM) plays an important role in use-dependent synaptic plasticity. Hyaluronic acid (HA) is the backbone of the neural ECM, which has been shown to modulate AMPA receptor mobility, paired-pulse depression, L-type voltage-dependent Ca2+ channel (L-VDCC) activity, long-term potentiation and contextual fear conditioning [1]. To investigate the role of HA in the development of spontaneous neuronal network activity, we used microelectrode array recording and Ca2+ imaging in hippocampal cultures enzymatically treated with hyaluronidase (Hyase).

2 Methods

Hippocampal cells were dissociated from embryonic mice (on embryonic day 18) and plated with an initial density of approximately 9000 cells/mm2 on microelectrode arrays (MEA, Multichannel Systems, Germany). After 24 hrs, the plating medium was replaced by a medium containing Neurobasal medium with 2% B27, 1 mM L-glutamine and 0.4% fetal calf serum without any antibiotics or antimycotics. Glial growth was not suppressed because glial cells are essential for long-term culture maintenance. Experiments were performed when the cultures reached the 17th day in vitro (DIV) and finished at the 34th DIV. Individual burst detection was based on threshold estimation of the basal spike rate activity [2]. Experiments were done when the cultures were 16 days in vitro (DIV). Local application of drugs to the culture was performed using a feeder. Hyaluronidase (from Streptomyces hyalurolyticus, Sigma; 75 U/ml) was added on 17th day in vitro. Glutamat transmission were blocked by adding 10 mcM CNQX, 10 mcM CPP, and L-type voltage-dependent Ca^{2+} channel (L-VDCC) blocker 10 mcM diltiazem to the extracellular solution. All reagents were purchased from Sigma or Tocris. A confocal laser scanning microscope, Zeiss LSM 510 (Germany), with a WPlan-Apochromat 20×/1.0 objective was used to investigate the spontaneous activity of the neuronal and astrocytic network. Cytosolic Ca^{2+} was visualized via Oregon Green 488 BAPTA-1AM (OGB-1) (0.4 μM; Invitrogen) excitation with the 488 nm line of Argon laser radiation and emission detection with a 500–530 nm filter. Astrocytes were visualized with specific indicator sulphorodamine SR101 (10 μM; Invitrogen SR101), which was excited by 543 nm radiation from a He–Ne laser and detected with the use of a 650–710 nm filter for emission. Time series of 256 × 256-pixel images with a 420 μm × 420 μm field of view were recorded at a rate of 4 Hz.

Statistical analysis of the bursting activity characteristics was performed by ANOVA tests ($p<0.05$).

3 Results

Our findings revealed that Hyase destructed the ECM of perineuronal nets (PNNs), surrounding cell

bodies and the proximal dendrites of neurons, and induced a slow development of seizure-like activity. The increase of mean burst frequency, but the decrease in inter-burst intervals and mean burst duration were observed like in our previous experiments [3]. The treatment transformed normal network spiking bursts into long-lasting “superbursts” and caused the appearance of neuronal and astrocytic Ca^{2+} “superoscillations.”

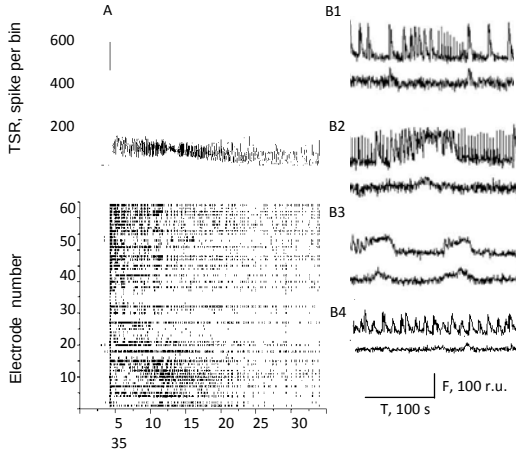

Fig. 1. (**A**) Example of raster plot of electrical spiking activity over 64 electrodes (upper rows) and total spike rate diagram (lower row) in primary hippocampal cultures. Hippocampal neuronal network activity in Hyase-treated cultures 9 days after Hyase treatment; (**B**). Examples of hyaluronidase-induced Ca^{2+} “superoscillations” in the neuronal (uppercurves) and glial (lower curves) networks in dissociated hippocampal cultures: (**B1**) Spontaneous Ca^{2+} oscillation recordings from control (20DIV); (**B2**) 3^{d} day (20DIV) after Hyase application; (**B3**) 9th day (26DIV) after Hyase application, the neuronal Ca^{2+} superoscillations are shorter but the astrocytic oscillations are longer compared to DIV20; (**B4**) 16th day (30DIV) after Hyase application.

Seizure-like activity in Hyase-treated cultures persisted for at least 9 days and could be suppressed by an L-VDCC blocker but not by an NMDA receptor antagonist. These results suggest that changes in the expression of hyaluronic acid can be epileptogenic and involve changes in Ca^{2+} oscillations. Spontaneous recover of the hyaluronic acid containing perineuronal nets after destruction on 16th day correlated with reduction of neuronal “superbursts” and neuronal and astrocytic Ca^{2+} “superoscillations”.

4 Conclusions

These results suggest that changes in the expression of hyaluronic acid can be epileptogenic in the early stage of brain development and that hyaluronidase treatment hippocampal cultures grown on microelectrode array in vitro provides a robust model for the dissection of the underlying mechanisms.

Acknowledgement

The research was supported by The Ministry of Education and Science of Russia, Grant for Leading Scientists (No11.G34.31.0012).

References

[1] Kochlamazashvili G., Henneberger C., Bukalo O., Dvoretskova E., Senkov O., Lievens P.M., et al. (2010). The extracellular matrixmolecule hyaluronic acid regulates hippocampal synaptic plasticity by modulating postsynaptic L-type Ca^{2+} channels. *Neuron* 67, 116–128.

[2] Pimashkin A., Kastalskiy I., Simonov A., Koryagina E., Mukhina I. and Kazantsev V. (2011) Spiking signatures of spontaneous activity bursts in hippocampal cultures. *Front. Comput. Neurosci*. 5:46

[3] Vedunova M., Sakharnova T., Mitroshina E., Perminova M., Pimashkin A., Zakharov Yu, Dityatev A. and Mukhina I. (2013) Seizure-like activity in hyaluronidase-treated dissociated hippocampal cultures. *Front. Cell. Neurosci*. 149:8.

Cortical Networks Respond with Major Activity Changes to Sildenafil Citrate (Viagra)

Nicole K Calderon[1,2], Daniel Ledee[1,2], Kamakshi Gopal[1,2], Guenter W. Gross[2,3]

1 Department of Speech and Hearing Sciences
2 Center for Network Neuroscience
3 Department of Biological Sciences
University of North Texas, Denton, TX 76203
* Corresponding author. E-mail address: NicoleCalderon@my.unt.edu

1 Background

Sildenafil citrate (Viagra), a drug within the class of phosphodiesterase type 5 inhibitors, is commonly used to treat disorders such as: erectile dysfunction, pulmonary arterial hypertension, and benign prostatic hyperplasia. Viagra has recently been cited as a possible cause of sudden sensorineural hearing loss and tinnitus [1]. This study shows Viagra causes hypersynchrony of auditory neurons, and presents a novel method for quantifying the neuromodulatory effects of Viagra.

2 Methods

Mouse embryos (Balb-C/ICR, day E16) were extracted from the dame after CO_2 narcosis and cervical dislocation. Auditory cortex tissue were mechanically minced, enzymatically dissociated, triturated, and mixed with Dulbecco's Modified Minimal Essential Medium (DMEM). Horse serum (10%) and fetal bovine serum (4%) were supplemented to the DMEM. The cell suspension was then placed onto the microelectrode arrays (MEAs) and incubated at 37°C in a 10% CO_2, 90% air atmosphere to create a neuronal networks. After 3 to 4 weeks of growth, the networks were used to quantify the drug-induced changes via multichannel extracellular recording. The standard culturing process, as well as the fabrication, preparation, and recording techniques of microelectrode arrays have been previously described [2,3].

Based on the daily clinical dose of 100 mg sildenafil citrate (approximately 2.7 µM), we evaluated network responses at 1.4 (n=3) and 2.7 µM (n=4), and also at the supra-dosage concentrations of 5.4 µM (n=4) and 10 µM (n=3).

3 Results

Typical response profiles consist of a substantial increase in spike activity 5-7 minutes after drug application followed by a relaxation to activity plateau with values always higher than reference.

At the clinical dose (2.7 µM), network spike rate per minute peaked to 215 - 250% above reference in 8 - 24 minutes (n=4). Subsequent spike activity plateau values were an average 84% above reference 1 hour after application. Similar patterns were seen at 1.4 µM, 5.4 µM, and 10 µM.

Spike patterns organized into highly coordinated bursting after the application of Viagra and continued throughout the plateau phase of the response (Figures 1 and 2).

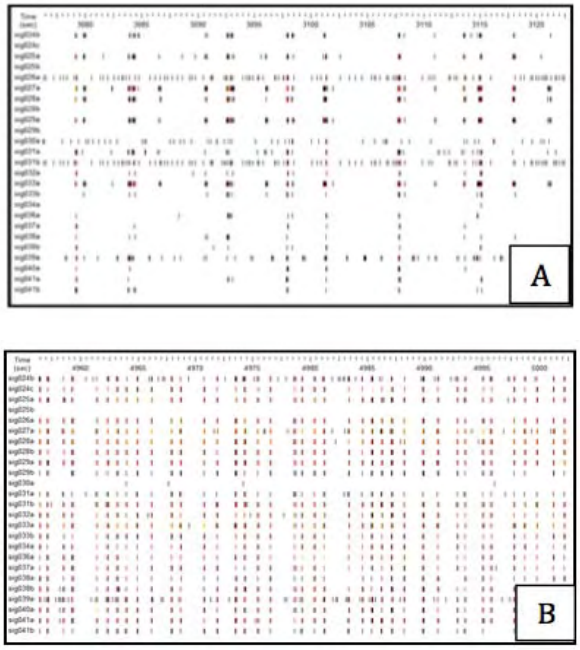

Fig. 1. Raster plot (spike sequence) from 62 active units (50 second window) before and after a 2.7µM dose. The figure compares spontaneous activity before drug application (A) and the coordinated bursting 50 minutes after drug application (B).

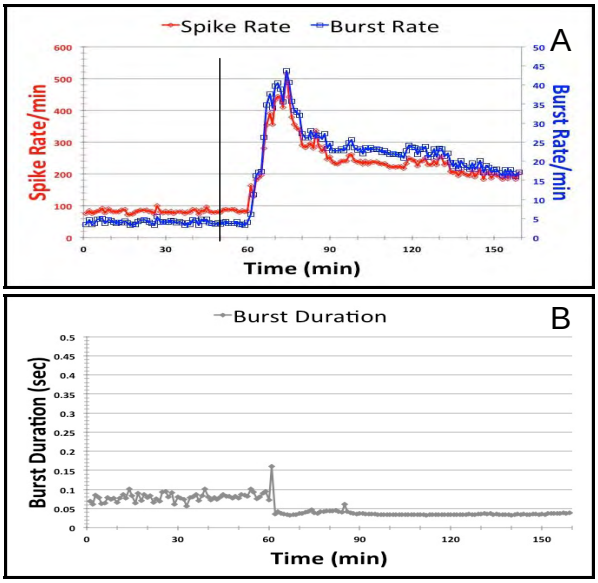

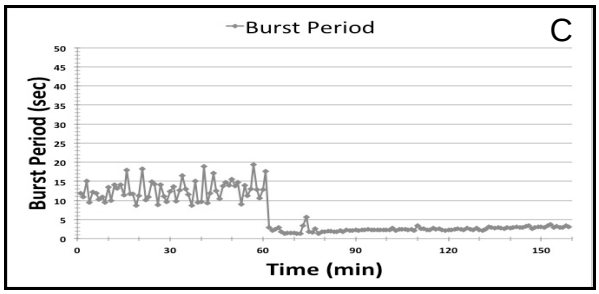

Fig. 2. (A) Typical neuronal network response to Viagra showing the change in spike rate and burst rate after the application of Viagra. Vertical line indicates the application of a 10 µM dose of Viagra. Active units: 62. Tissue: Auditory cortex. (B) Burst duration decreases after the application of Viagra. (C) Burst period decreases after the application of Viagra. B and C show clear reductions in minute-to-minute fluctuations, reflecting a pattern regularization that is also seen in cultures exposed to tinnitus-inducing drugs.

The level of dose was shown to affect the slope, or the rate at which the network reached peak spike activity (Figure 3.), and the percent increase in burst activity with regards to the reference activity one hour after dose application.

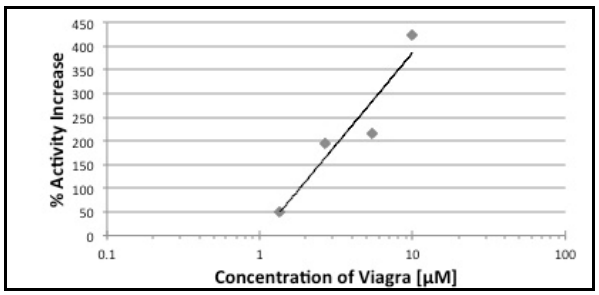

Fig. 3. Percent increase in plateau spike activity one hour after the application of Viagra at different concentrations.

4 Conclusion

This study provides preliminary evidence that Viagra has a direct excitatory effect on cortical neurons. The average 5-7 minute delay in the response is indicative of secondary messenger or metabolic mechanisms and does not support involvement of plasma membrane receptors. The changes to temporally highly regular and coordinated bursting may support previous reports of Viagra causing tinnitus. Even at a typical clinical dose of 2.7 µM, bursting patterns within the network became highly coordinated - which has been suggested to be a correlate of tinnitus [4].

References

[1] Mukherjee B and Shivakumar MT. A case of sensorineural deafness following ingestion of sildenafil. Journal of Laryngology & Otology, 2007; 121:395-397.

[2] Gross GW (2011) Multielectrode Arrays. Scholarpedia, 6(3): 5749.

[3] Gopal, K.V., Gross G.W. Auditory cortical neurons *in vitro*: cell culture and multichannel extracellular recording. Acta Otolaryngol, 1996; 116: 690-696.

[4] Wu C, Gopal K, Gross GW, Lukas TJ, Moore EJ. An *in vitro* model for testing drugs to treat tinnitus. European Journal of Pharmacology, 2011; 667:188-194

Role of Tachykinin1 and αCGRP on Modulating Inflammatory Sensitization of TRPV1

Sakthikumar Mathivanan, Christoph Jakob Wolf, Isabel Devesa, Clotilde Ferrandiz Huertas, Antonio Ferrer-Montiel*

Instituto de Biología Molecular y Celular, Universidad Miguel Hernandez de Elche, Alicante, Spain
*Corresponding author. E-mail address: aferrer@umh.es

Abstract
TRPV1, a polymodal non-selective cation channel, acts as a major integrator of painful stimuli, is predominantly expressed in dorsal root ganglion (DRG) neurons (1). Upon tissue damage there is a release of inflammatory mediators that sensitize TRPV1 channels leading to enhanced nociceptor excitability and thermal hyperalgesia. Acute inflammatory sensitization of TRPV1 involves both the modification of channel gating properties by phosphorylation (2), and the recruitment of channels to the neuronal surface, a mechanism that occurs through SNARE-dependent exocytosis (3). We have used Multi electrode array (MEA) technique to characterize TRPV1 mediated neuronal firing from neonatal rat DRG neurons. This technique helps to study inflammatory mediators induced sensitization of neuronal excitability through activation of TRPV1 in a network of cultured nociceptors. Further studies are required to examine the molecular mechanisms behind inflammatory sensitization of TRPV1 mediated neuronal excitability on different sub populations of nociceptors and the role of tachykinin1 and α-CGRP neuropeptides expressed in TRPV1 carrying vesicles, on modulating inflammatory sensitization of TRPV1 will be studied.

1 Backround / Aims

To characterize inflammatory sensitization of TRPV1 by ATP, a pro-algesic agent that modifies channel gating, also augments the recruitment of new channels to the neuronal surface. The approach involves monitoring the nociceptor excitability evoked by ATP using multielectrode arrays.

2 Methods / Statistics

Primary DRG sensory neurons were isolated from neonatal rats (P2-P6). Cells were suspended 150µls of complete medium from which 30µls of medium containing cells were seeded on five arrays of 60ThinMEA200/30iR-ITO-gr (Multichannel Systems GmbH), and electrical activity of primary sensory neurons was recorded by MC_Rack software 4.3.0 at 25 kHz sampling rate. TRPV1-mediated neuronal firing activity was evoked by three repetitive 15s-applications of capsaicin at 500nM, using continuous perfusion system (2 mL/min flux). 10 µM ATP was perfused between the second and the third pulse for 8min Data were analyzed using MC_Rack spike sorter and Neuroexplorer Software (Next Technologies, USA). An evoked spike was defined when the amplitude of the neuronal electrical activity overcame a threshold set at -20µV. The recorded signals were then processed to extract mean spike frequency.

3 Results

Neuronal firing mediated by TRPV1in MEA chambers was observed when activated by capsaicin which exhibits a good signal to noise ratio. Also desensitization of TRPV1 mediated neuronal firing was observed upon repeated applications of capsaicin. Sensitization of TRPV1-evoked neuronal firing was notably increased in ATP treated nociceptors compared to control group.

4 Conclusion/Summary

These results indicate that, using MEA technique TRPV1 mediated neuronal activity can be studied in cultured nociceptors, which was clearly supported by desensitization of neuronal spikes and its sensitization by ATP. Further experiments will help to study the modulation of TRPV1 activity by different inflammatory mediators and the role of genes involved.

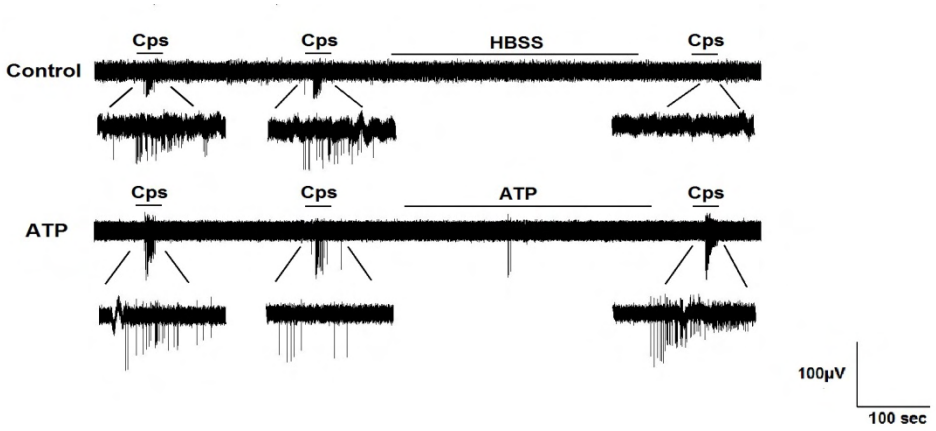

Figure 1: Multielectrode array recordings in rat cultured DRGs. Representative images illustrating sensitization of capsaicin-evoked extracellular electrical signals (500nM, 15s) induced by short incubation with by ATP (10µM) or HBSS buffer between the second and the third pulse of capsaicin in neonatal rat cultured DRGs.

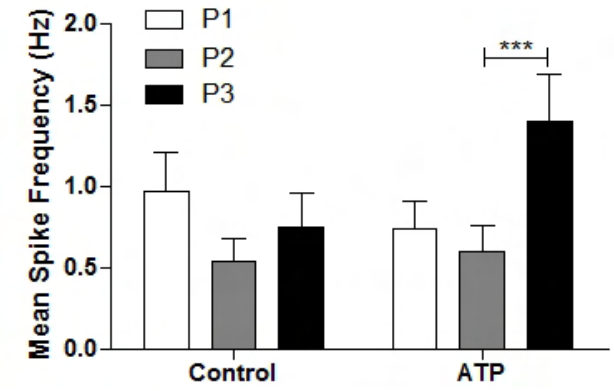

Figure 2: ATP induced inflammatory sensitization of TRPV1 mediated neuronal firing in nenonatal rat DRG neurons. DRG neurons from neonatal rats were used for studying ATP induced potentiation of TRPV1 mediated neuronal firing. Three repetitive pulses of capsaicin at 500nM concentration were given for the continuous protocol. Effect of ATP 10µM mediated potentiation of TRPV1 mediated neuronal firing activity was determined by comparison of all the three pulses (P1, P2, P3) in each groups and represented as Mean spike frequency (Hz). Data are expressed as mean ± SEM. Number of cultures ≥3. ATP induced potentiation of TRPV1 mediated neuronal firing was significantly increased (***- P<0.001) – One way ANOVA repeated measures with Bonferroni's post hoc test, whereas in control groups no such Potentiation was observed.

Acknowledgement

This work was supported by grants from el Ministerio de Economía y Competitividad (BFU2012-39092-C02-01, CONSOLIDER-INGENIO 2010 CSD2008-00005) and la Generalitat Valenciana (PROMETEO/2010/046). S.M. was a recipient of a Santiago Grisolia Fellowship form la Generalitat Valenciana. The authors declare no competing financial interests.

References

[1] Planells-Cases R, Valente P, Ferrer-Montiel A, Qin F and Szallasi A (2011) Complex Regulation of TRPV1 and Related Thermo TRPS: Implications for Therapeutic Intervention. *Transient Receptor Potential Channels, Advances in Experimental Medicine and Biology*, vol: 704,491-515

[2] Morenilla-Palao C, Planells-Cases R, Garcia–Sanz N and Ferrer-Montiel A (2004) Regulated Exocytosis Contributes to Protein Kinase C Potentiation of Vanilloid Receptor Activity. *J.Bio Chem.* vol: 279, No. 24, 25665–25672.

[3] Camprubi-Robles M, Planells-Cases R and Ferrer-Montiel A (2009) Differential contribution of SNARE-dependent exocytosis to inflammatory potentiation of TRPV1 in nociceptors. *The FASEB Journal*.vol: 23 no.11, 3722-3733.

Pharmacological Studies of Synaptic Communication in Maturing Human Pluripotent Stem Cell Derived Neural Networks

Meeri Mäkinen[1], Laura Ylä-Outinen[1], Dimitriy Fayuk[1], Susanna Narkilahti[1*]

1 NeuroGroup, BioMediTech, University of Tampere, Tampere, Finland.
* Corresponding author. E-mail address: susanna.narkilahti@uta.fi

Abstract
Human pluripotent stem cell (hPSC) derived neural networks develop spontaneous network activity. However, the mechanisms and connections of this activity remain elusive. We studied the cell communication in neuronal networks of human origin by pharmacologically manipulating the networks while observing their activity with MEA and calcium imaging.

1 Background & Aim

Spontaneous synchronous network activity develops in the networks formed by human pluripotent stem cell (hPSC) derived neurons *in vitro* [1-5]. During embryogenesis, the developing brain expresses a similar form of spontaneous synchronous network activity [6]. During this period, neural cells integrate into the existing networks of the developing brain [7, 8]. Thus, it is likely that the same occurs *in vitro*. However, the cellular composition and the intercellular connections in spontaneously active neuronal networks remain unclear.

Our aim was to understand how cells communicate during the activity formation in hPSC derived neuronal networks *in vitro*.

2 Methods

Cells

hPSCs were differentiated to neurons as described earlier [9]. The cells were differentiated in suspension for 8 weeks after which they were plated down for adherent culturing. The cultures were studied at different time points after plating.

Network activity measurements

Cells were plated onto 6-well MEA dishes (Multi Channel Systems MCS GmbH) for MEA measurements, onto cover slips for calcium imaging and onto thinMEAs (Multi Channel Systems MCS GmbH) for combined MEA measurements and calcium imaging. Fura-2 or Fluo4 (both from Life Technologies, Molecular Probes) was used in imaging experiments.

Pharmacology

The participation of gap junctions on network activity was studied using gap junction blocker carbenoxolone. The participation and development of inhibitory GABAergic communication system was studied by applying GABA and $GABA_A$ receptor antagonist Bicuculline. Glutamatergic signalling was studied by applying a mixture of competitive glutamate receptor antagonists (CNQX and D-AP5) and glutamate. All pharmacological reagents were purchased from Sigma-Aldrich.

3 Results

The participation of gap junctions, glutamate and GABA into the generation of the early network activity was suggested. The amount of gap junctional coupling and GABA mediated signalling seemed to change during neuronal network maturation. In addition networks were found to contain sub networks responding differently to the treatments.

4 Conclusions

The activity in hPSC derived neuronal networks is mediated by mechanisms similar to those occurring during the early brain development. The described pharmacological protocols were promising for studying differences in cellular composition and functional connections.

Acknowledgement

The personnel of IBT are acknowledged for support in stem cell research. This study was funded by TEKES - the Finnish Funding Agency for Technology and Innovation.

References

[1] Kiiski H., Äänismaa R., Tenhunen J., Hagman S., Ylä-Outinen L., Aho A., Yli-Hankala A., Bendel S., Skottman H., Narkilahti S. (2013). Healthy human CSF promotes glial differentiation of hESC-derived neural cells while retaining spontaneous activity in existing neuronal networks. *Biology Open*, 13, 605-612.
[2] Mäkinen M., Joki T., Ylä-Outinen L., Skottman H., Narkilahti S., Äänismaa R. (2013). Fluorescent probes as a tool for cell

population tracking in spontaneously active neural networks derived from human pluripotent stem cells. *Journal of Neuroscience Methods*, 215, 88-96.

[3] Kreutzer J., Ylä-Outinen L., Kärnä P., Kaarela T., Mikkonen J., Skottman H., Narkilahti S., Kallio P. (2012). Structured PDMS Chambers for Enhanced Human Neuronal Cell Activity on MEA Platforms. *Journal of Bionic Engineering*, 9, 1-10.

[4] Ylä-Outinen L., Heikkilä J., Skottman H., Suuronen R., Äänismaa R., Narkilahti S. (2010). Human cell-based micro electrode array platform for studying neurotoxicity. *Frontiers in Neuroengineering*, 3, 111.

[5] Heikkilä T.J., Ylä-Outinen L., Tanskanen J.M., Lappalainen RS., Skottman H., Suuronen R., Mikkonen J.E., Hyttinen J.A., Narkilahti S. (2009). Human embryonic stem cell-derived neuronal cells form spontaneously active neuronal networks in vitro. *Experimental Neurology*, 218, 109-116.

[6] Voigt T., Opitz T., de Lima A.D. (2001). Synchronous oscillatory activity in immature cortical network is driven by GABAergic preplate neurons. *The Journal of Neuroscience*, 21, 8895-8905.

[7] Jäderstad J., Jäderstad LM., Li .J, Chintawar S., Salto C., Pandolfo M., Ourednik V., Teng Y.D., Sidman R.L., Arenas E., Snyder E.Y, Herlenius E. (2010). Communication via gap junctions underlies early functional and beneficial interactions between grafted neural stem cells and the host. *Proceedings of the National Academy of Sciences of the United States of America*, 107, 5184-5189.

[8] Stephens CL., Toda H., Palmer TD., DeMarse TB., Ormerod BK. (2012). Adult neural progenitor cells reactivate superbursting in mature neural networks. *Experimental Neurology*, 234, 20-30.

[9] Lappalainen R.S., Salomäki M., Ylä-Outinen L., Heikkilä T.J., Hyttinen J.A., Pihlajamäki H., Suuronen R., Skottman H., Narkilahti S. (2010). Similarly derived and cultured hESC lines show variation in their developmental potential towards neuronal cells in long-term culture. *Regenerative Medicine, 5, 749-762*.

Automated Cytocentering™ Patch Clamp Recordings of Primary and iPSC-derived Cells Open New Paths in Basic and Applied Ion Channel Research

Dirck Lassen[1,2], Olaf Scheel[1*], Stefanie Frech[1], Thomas Knott[1], Peter van Stiphout[2]

1 Cytocentrics Bioscience GmbH, Joachim-Jungius-Str. 9, 18059 Rostock, Germany
2 Cytocentrics BV, High Tech Campus 9, 5656 AE Eindhoven, The Netherlands
* Corresponding author. E-mail address: o.scheel@cytocentrics.com

Abstract

In recent years, automated patch clamp has been established as a standard tool for drug discovery and safety pharmacology. Several high and medium throughput platforms offer seal and recording quality sufficient for generating routine results when using recombinant cell lines. However, when primary cells or induced pluripotent stem cell (iPSC)-derived cells are used, most planar systems are stretched to their limits: Low seal quality does not provide for a proper voltage clamp necessary for identifying several ion channels in these cells with a high signal to noise ratio. Special non-physiological buffer compositions are often required to allow for seal formation and stable whole-cell recordings. These may interfere with the channels' regulation leading to non-physiological channel characteristics such as altered activation and inactivation kinetics or non-physiological shape and duration of action potentials. Moreover, most automated systems require a high cell amount, a fact that frequently is a hindrance when native cells are investigated. By integration a traditional glass pipette into a microfluidic chip all these limitation are overcome and the benefits of an automated device were successfully combined with the quality and flexibility of conventional manual patch clamp.

1 Cytocentering Patch Clamp

1.1 The Patch Pipette in a Microfluidic Chip

Contrary to common approaches for automated patch clamp recordings - comprising a planar substrate with one or more apertures per recording chamber – the Cytocentering™ method features a dedicated patch pipette, which is surrounded by a second concentric Cytocentering™ channel and both are embedded in a microfluidic quartz covered CytoPatch™ chip. This unique design makes it possible to emulate the manual patch clamp process, i.e. starting to form a seal only if a cell is in close proximity to the pipette tip, resulting in stable gigaohm seals (without the addition of fluoride in the intracellular buffer). Only 150 nl cell suspension is consumed during a single cell catch process. With its additional features such as the continuous bi-directional and fast perfusion system, temperature control as well as the flexible and interactive AssayDesigner software, the CytoPatch™ 2 offers flexibility and data quality en par with the manual patch clamp for research on primary cells or iPSC-derived cells.

2 The Applications

2.1 Measurements of Rat Dorsal Root Ganglion Neurons (DRG) and iPSC-derived Human Cardiomyocytes

To demonstrate these capabilities, we present current and voltage-clamp recordings of freshly dissociated rat dorsal root ganglion neurons (DRG) and of iPSC-derived human cardiomyocytes (Cor.4U® cells kindly provided by Axiogenesis). Moreover, the CytoPatch™ chip offers intracellular buffer exchange, and the Cytocentering™ channel can be used to apply mechanical force onto the patched cell to activate mechano-sensitive channels, as demonstrated by whole-cell voltage-clamp recordings of Piezo channels in Neuro2A cells.

This shows that Cytocentering patch clamp offers unmatched assay flexibility and data quality, surpassing conventional manual patch clamp rigs in features and ease of use.

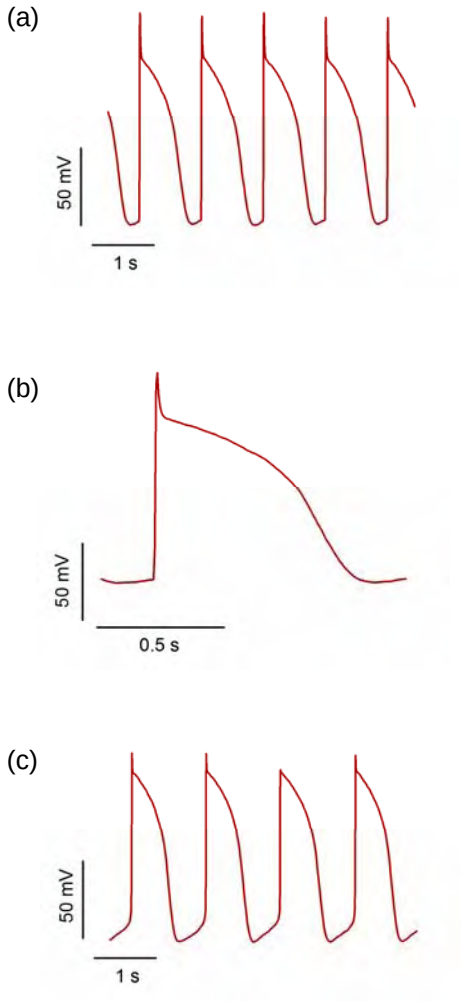

Fig. 1: Action potentials in Cor.4U iPSC derived cardio-myocytes
a) Paced action potentials (400 pA for 10 ms, 1 Hz)
b) Single trace from (a) in high magnification
c) Spontaneous action potentials

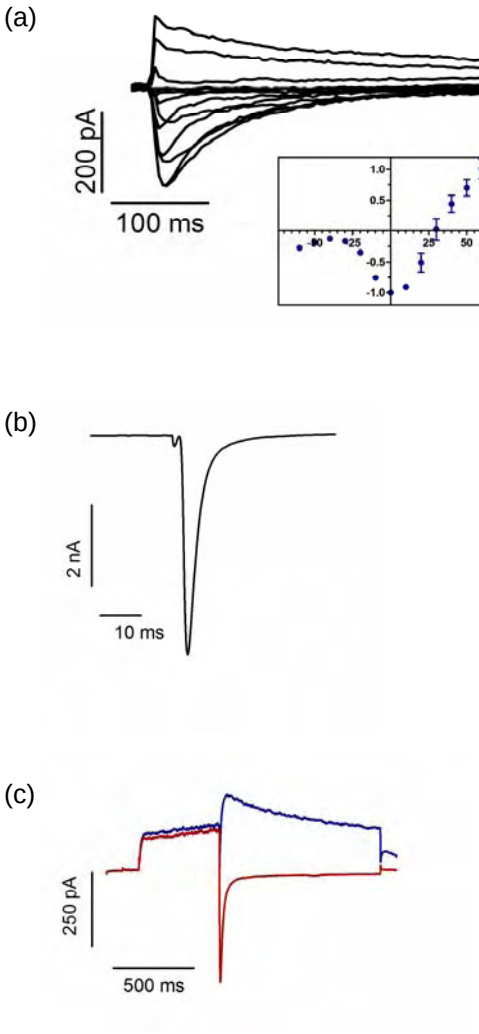

Fig. 2: Voltage clamp recordings of Cor.4U® cells
a) Overlay of whole cell calcium currents in response to a double pulse protocol with a voltage step to –40 mV followed by voltage steps ranging from –60 mV to +60 mV in 10 mV increments. Insert: current voltage relationship of the peak currents elicited by this protocol. Axes: normalised current vs. step voltage (mv); (n=10 cells). Outward currents mediated by K+ channels.
b) Voltage-gated sodium channel activated by a voltage step to 0 mV
c) hERG-like K+ current activated by a depolarising voltage step to +40 mV followed by a step to –40 mV (blue trace) or –120 mV (red trace)

Acknowledgement

We thank Axiogenesis AG for their generous supply of Cor.4U cells to support this study.

Ostreopsis cf. *Ovata* Toxicity Evaluation by Using Microelectrode Array Based Platform

Susanna Alloisio[1,2], Valentina Giussani[3], Marika Zanin[1], Valentina Asnaghi[3], Mariachiara Chiantore[3], Antonio Novellino[1,2]

(1) ETT S.p.A., via Sestri 37, 16154 Genoa (Italy)
(2) Institute of Biophysics, National Research Council, via De Marini 6, 16149 Genoa (Italy).
(3) DiSTAV, University of Genoa, Corso Europa 26,16132 Genoa (Italy)

Abstract
Harmful benthic microalgae blooms are an emerging phenomenon causing health and economic concern, especially in tourist areas. This is the case of the Mediterranean Sea, where *Ostreopsis cf. ovata* blooms occur in summer, with increasing regularity. Ostreopsis species produce a number of palytoxin-like compounds, termed ovatoxins, along with trace amounts of putative palytoxin as the causative agents of the *O. ovata* -related human intoxications. So far, any risk assessment for ovatoxins as well as establishment of their molecular target have not yet been elucidated. In order to improve our knowledge about the neurotoxic potential of the O. cf. ovata we performed electrophysiological measurements on neuronal networks coupled to microelectrode arrays (MEAs). Toxicity of sonicated cells and filtrate growth medium at the end of stationary algae growth phase was evaluated. The integrated analysis of specific parameters related to the spontaneous electrical activity showed that sonicated cells treatment was the most effective with maximal inhibition around 70% gained from 2 cells/ml concentration. Differently, a maximal inhibition around 20% was obtained with the filtrated growth medium from 7 cells/ml concentration.
The results show that the platform based on microelectrode arrays is a fast and highly sensitive screening system for detecting and evaluating the neurotoxicity of environmental biotoxins.

1 Background / Aims

In Mediterranean countries new public health risks have started being recurrent since *Ostreopsis cf. ovata*, a benthic dinoflagellate widespread in tropical seas, has colonized several areas of the Italian, Spanish, Greek, French, Tunisian and Algerian coasts.

Ostreopsis species produce palytoxin (PTX) and a number of palytoxin-like compounds, termed ovatoxins, the causative agents of the *O. cf. ovata*-related human intoxications by inhalation and irritations by contact. Due to its ubiquitous molecular target, the sodium-potassium pump protein, PTX is considered one of the most toxic molecules occurring in nature, provoking severe and sometimes lethal intoxications in humans. Toxicity report are usually referred to the *O. ovata* cells concentrations determined in seawater, but these data are not per se predictive for human risk, since dinoflagellates do not always produce the same amount of toxins. Furthermore, *O. cf. ovata* cell debris can be present in the marine aerosol and their contribution to the effects on human health cannot be excluded.

In order to improve our knowledge about the toxicity of this dinoflagellate species on mammalian cells, we performed electrophysiological measurements on neuronal networks coupled to microelectrode arrays as a fast and sensitive biotoxicological screening assays. The neurophysiological activity patterns in terms of spike and burst firing were evaluated.

2 Methods / Statistics

Ostreopsis cf. ovata. Laboratory cultures of *O. cf. ovata* were obtained starting from preliminary wild-cell isolation from environmental samples collected along Genoa coast, Italy. Algae were cultured in sterilized plastic flasks maintained at 20 ± 0.5 °C in a 16:8 h light:dark period (light intensity 6.000-10.000 lux). Toxicity of sonicated cells and filtrate growth medium at the end of stationary algae growth phase was evaluated.

Primary neuron cultures. The primary cultures of cortical neurons were prepared from foetal day 18 rats. The cells were seeded on 60-electrode PEDOT-CNT MEA chips with internal reference (Multi Channel Systems, Reutlingen, Germany) pre-coated with poly-D-lysine (0.1 mg/ml) and laminin and (0.02 mg/ml) as 50µl droplets (1500–2000 cells/mm2).

Experimental layout and data analysis. Experiments were carried from 20 to 30 days in vitro (DIV). Each preparation was tested at least three times and using neuronal networks from different neuronal isolations. All analyses were conducted on binned data with bin size of 60s. Data from experimental episodes were averaged for the last 15min over the 20-min time window of recording for each concentration. The network Mean Firing Rate (MFR), Mean Burst Rate (MBR), percentage of spikes in Burst (% Spikes_B), Mean Burst Duration (MBD) and Mean Interspike In-

terval in Burst (MISI_B) were extracted as descriptors of the network electrical activity using NeuroExplorer software(Nex Technologies). To obtain the estimated IC50 values, the normalized dose–response curves of single chemicals were interpolated by a four-parameter logistic function and analysed using SigmaPlot8 (Jandel Scientific).

3 Results

To evaluate if exposure to the *O. cf. ovata*-derived preparations was affecting the neuronal spontaneous electrical activity in primary cultures of rat cortical neurons, the mean firing rate and its bursting behaviour were studied. For each parameter the concentration-response curves based on the mean normalized values were obtained. The integrated analysis of specific parameters related to the spontaneous electrical activity showed that sonicated *O. cf. ovata* cells was the most effective with maximal inhibition around 70% gained from 2 cells/ml concentration. Differently, only a maximal inhibition around 20% was obtained with the filtrated growth medium from 7 cells/ml concentration.

4 Conclusion/Summary

The different samples administered to the neuronal cultures on MEAs have confirmed that the mixture of algal toxins causes a rapid and irreversible blockade of spontaneous electrical. The mechanism involves not only the reduction of the frequency of discharge, but especially its temporal disorganization, as demonstrated by the decline in the number, length and density of the bursts. The preparation more effective in the blocking of the electrical activity is the sonicated one containing the intracellular stores, while the filtrate one has a specific effect on the electrical pattern and this would indicate a specific molecular target of the toxins naturally release in the medium.

In conclusion the results show that the platform based on neural networks coupled to microelectrode arrays is a highly sensitive screening system for evaluating the toxicity of environmental biotoxins.

Biphasic Response of Neuronal Networks to Sodium Valproic Acid (NaVPA)

Matthias Nissen[1], Sebastian Bühler[2], Marco Stubbe[1], Werner Baumann[1] and Jan Gimsa[1*]

1 University of Rostock, Biophysics
Gertrudenstraße 11a, 18057 Rostock, Germany
2 Leibniz-Institut für Nutztierbiologie (FBN)
Wilhelm-Stahl-Allee 2, 18196 Dummerstorf, Germany
* Corresponding author. E-mail address: jan.gimsa@uni-rostock.de

Abstract
Sodium valproic acid (NaVPA) is known as a common drug for the treatment of epilepsy. However, it may have adverse effects in the embryonic development. Thus, NaVPA is a drug for *in vitro* developmental neurotoxicity test systems. Here we investigated the reaction of neuronal networks on the acute exposure to different concentrations of NaVPA.

1 Material and Methods

Neuronal cortex cells derived from mouse embryos were dissected 18 days after gestation and sowed on substrate-coated multi-electrode arrays (MEA). After two weeks of incubation under cell culture conditions, the cells developed spontaneous electric active networks and maintained a stable electric activity up to six weeks. Before starting the measurements of the electric activity, the cell culture medium was removed and the cells were equilibrated for 10 minutes in an extracellular buffer (ECB: NaCl 137 mM, KCl 5 mM, $CaCl_2$ 3 mM $MgCl_2$ 0.1 mM, Glucose 10 mM, Glycin 0.01 mM, Hepes 5 mM). In a first step, the electric activity was measured for 15 min and the obtained data was defined as “control”. Further measurements were conducted as described before but with a factor-of-three concentration series of NaVPA ranging from 0.03 mM to 65.61 mM NaVPA. All measured data were fitted using an equation for biphasic kinetics with OriginLab 8.1 software [1].

2 Results

The different concentrations of NaVPA were plotted against the mean firing rate of the channels (Fig. 1, Mean +/- SE). While the electric activity of the neuronal cortical mouse cells showed an increase at lower NaVPA concentrations (from 0.09 to 0.27 mM), a decrease was observed at higher concentrations (> 0.27 mM). This results correlate with *in vivo* findings from Bigss *et al.* in rats, who showed a biphasic influence of VPA on the GABA concentration [2]. The authors found a minimal GABA concentration at 200 mg/kg NaVPA which corresponds to 1.38 mM/l *in vitro*. GABA as inhibitory neurotransmitter could very well explain the recorded data.

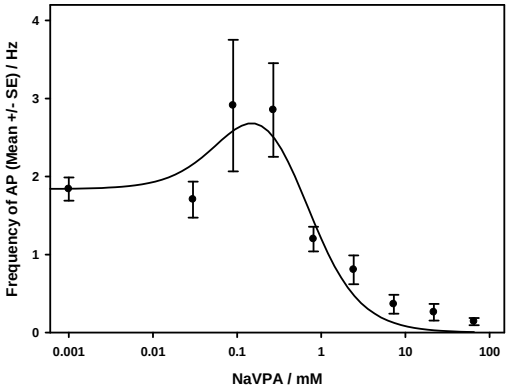

Fig. 1. Frequency of the recorded action potentials (Mean +/- SE) for different concentrations of NaVPA. NaVPA shows a biphasic kinetic with a maximum between 0.03 mM and 0.27 mM. Please note that control data (0 mM) were plotted at 0.001 mM.

3 Discussion

NaVPA is an important drug in the treatment of epilepsy, but it has adverse side effects in embryological development. Different concentrations of NaVPA in the ECB lead to a biphasic change in the in vitro neuronal activity of networks grown from primary mouse neurons. Further in vitro studies are necessary on the GABA activity concentration and the mechanism of the biphasic change in GABA concentration.

References

[1] Buehler S.M., Stubbe M., Gimsa U., Baumann W., and Gimsa J. (2011). A Decrease of Intracellular ATP Is Compensated by Increased Respiration and Acidification at Sub-Lethal Parathion Concentrations in Murine Embryonic Neuronal Cells: Measurements in Metabolic Cell-Culture Chips. *Toxicology Letters*, 207 (2): 182–90.

[2] Biggs C. S., Pearce B. R., Fowler L. J., and Whitton P. S. (1992). The Effect of Sodium Valproate on Extracellular GABA and Other Amino Acids in the Rat Ventral Hippocampus: An *in Vivo* Microdialysis Study. *Brain Research* 594 (1), 138–42.

Thymoquinone Protects Cultured Hippocampal and Human Induced Pluripotent Stem Cells-Derived Neurons Against α-Synuclein-Induced Synapse Damage

Alhebshi Amani, Odawara Aoi, Gotoh Masao, Suzuki Ikuro*

Graduate School of Bionics, Tokyo University of Technology, Tokyo, Japan
* Corresponding author. E-mail addresses: s.ikurou@gmail.com, isuzuki@bs.teu.ac.jp.

Abstract
Thymoquinone (TQ) is the major active component of the medicinal plant *Nigella Sativa* seed's oil known as The Black Seed. This natural antioxidant has recently received considerable attention for its potent protective properties and has demonstrated several neuropharmacological attributes. Using cultured rat primary hippocampal and human induced pluripotent stem cells (hiPSC)-derived neurons, the present study aims to investigate whether TQ could provide protective effects against alpha-synuclein (αSN)-induced synaptic toxicity, a presynaptic protein that is implicated in Parkinson's disease, dementia with Lewy Body and other neurodegenerative diseases.

1 Introduction

Synapse degeneration is a common feature in patients with neurodegenerative diseases who exhibit dementia, including those with Parkinson's disease (PD), Alzheimer's disease (AD), and dementia with Lewy bodies (DLB) [1]. These patients display an accumulation of proteins, including α-synuclein (αSN) aggregates, in cortical and subcortical regions of the brain [2]. Evidence indicates that this pathology occurs in response to aggregates of αSN that accumulate at presynaptic terminals and trigger synapse degeneration [3].

Thymoquinone (TQ) is extracted from the plant Nigella sativa, and the most abundant, account for most of the pharmacological properties of the plant. Because dementia in patients with PD and AD is closely associated with synaptic abnormalities, the protective effect of TQ against αSN-induced synapse damage in cultured rat hippocampal and human induced pluripotent stem cell (hiPSC)-derived neurons was determined by quantifying the level of synaptophysin using immunostaining and determining synaptic activity using the fluorescent dye FM1-43. To further clarify our results, we investigated the effect of αSN on spontaneous spiking activity in hiPSC-derived neurons using a multielectrode array (MEA) system.

2 Materials and Methods

2.1 Immunostaining

Embryonic wistar rat hippocampal neurons and hiPSC-derived neurons were treated with αSN (1μM) with or without TQ (100nM) for 72h. The levels of synaptophysin were measured by immunostaining. Treated cells were fixed and immunostained with the primary antibodies anti-MAP2, anti-β-tubulin III and anti-synaptophysin at 4◦C overnight. The cells were then washed and incubated with secondary antibodies (anti-mouse Alexa Fluor 488, anti-rabbit Alexa Fluor568 and Hoechst 33258). Fluorescence was measured using a microplate reader at excitation and emission wavelengths of 485 nm and 535 nm, respectively. Immunostained specimens were viewed using an inverted fluorescence microscope, and images were captured using an electron multiplying CCD camera.

2.2 FM 1-43 assay

The fluorescent styryl dye FM1-43 is readily incorporated into synaptic vesicles and determines synaptic activity as previously described [4]. On the day of the experiment, the culture medium was removed; treated neurons were incubated with 1μg/ml FM1-43 for 5 min, washed thrice in ice-cold PBS, and suspended in PBS. Fluorescence was measured using a microplate reader at excitation and emission wavelengths of 480 nm and 612 nm, respectively.

2.3 Multielectrode arrays

In this experiment, we used hiPSC-derived neurons (iCell Neurons, Cellular Dynamics international). The effects of αSN and TQ on the action potential of hiPSC-derived neurons were studied using an MEA system (Alpha MED Scientific, Japan). MEA probes (MED-P515A, Alpha MED Scientific) were comprised 50μm × 50 μm 64 electrodes spaced 150 μm

apart and arranged in an 8 × 8 grid. Recordings were obtained for10 min at six times per days using Mobius software (Alpha MED Scientific). Firing analyses were performed for number of firings which obtained at 64 electrodes.

3 Results

3.1 Effect of TQ on αSN-induced synapse damage

In the present study, treatment of hippocampal neurons with αSN induced a 25% reduction in synaptophysin. However, the co-administration with TQ (100nM) protected neurons against αSN-induced synapse damage and restored the synaptophysin level to 98% of the control value. Moreover, the addition of αSN to hiPSC-derived neurons induced a 20% reduction in synaptophysin levels. However, the co-administration with TQ protected the neurons against αSN-induced synapse damage and enhanced the synaptophysin level by 6% compared with controls.

3.2 Effect of TQ on αSN-induced inhibition of synaptic vesicle recycling

The addition of αSN reduced FM1-43 uptake by 50% compared with that of controls. However, co-administration of αSN and TQ restored the uptake of FM1-43 by 40% compared with αSN-treated cells, and thus maintained synaptic activities in hippocampal neurons. Addition of αSN to hiPSC-derived neurons induced a 25% reduction in FM1-43 uptake compared with controls. However, the co-administration with TQ (100nM) restored the uptake of FM1-43 by 20% compared with αSN-treated neurons, and thus maintained synaptic activities.

3.3 Effect of TQ on the electrophysiological activity of αSN-treated neurons

We investigated neural activity by in vitro extracellular electrophysiological recording of the temporal electrical activity of cultured hiPSC-derived neurons using MEA. The addition of αSN (2μM) induced more than 80% reduction in spontaneous firing activity at 11 days after exposure. However, when co-administered with TQ (100nM), the cells maintained approximately 85% of their baseline firing activity 11 days after exposure (Fig.1).

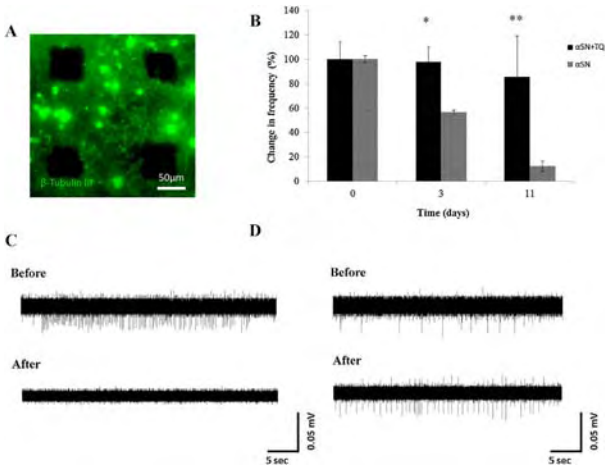

Fig.1. Protective effects of TQ against αSN-induced inhibition of spontaneous firing activity. (A) A fluorescence image of fixed hiPSC-derived neurons (19 DIV) cultured on the microelectrode probe of the multielectrode array (MEA) system after incubation with αSN and TQ. The neuronal marker β-tubulin III is shown in green. (B) Time course of the effect of TQ on spontaneous firing frequency when administered with αSN showing the reversal of the effect of αSN on the firing frequency of hiPSC-derived neurons by TQ. (100% represents baseline values before exposure to αSN) ± SD, n = 1 (*P < 0.0002, **P < 0.004 vs. αSN). (C) The waveforms show typically spontaneous firings before and after 11 days of αSN administration. (D) The waveforms before and after 11 days of αSN and TQadministration.

4 Conclusion

In conclusion, our results suggest that TQ has potential therapeutic value for treating PD, DLB, and other neurodegenerative disorders.

Acknowledgement

This work was supported by the Japan Society for the Promotion of Science (JSPS) Grant Number 24700485 and the Saudi Arabian Ministry of Higher Education.

References

[1] J.E. Galvin, K. Uryu, V.M. Lee, J.Q. Trojanowski, (1999): Axon pathology in Parkinson'sdisease and lewy body dementia hippocampus contains alpha-, beta-, andgamma-synuclein, Proc. Natl. Acad. Sci. U. S. A. 96 ,13450-13455.

[2] C. Pacheco, L.G. Aguayo, C. Opazo, (2012): An extracellular mechanism that can explainthe neurotoxic effects of α-synuclein aggregates in the brain, Front. Physiol.297, 3389–3399.

[3] A.G. Kazantsev, A.M. Kolchinsky, (2008) : Central role of alpha-synuclein oligomersin neurodegeneration in Parkinson disease, Arch. Neurol. 65, 1577–1581.

[4] M.A. Cousin, P.J. Robinson, (1999): Mechanisms of synaptic vesicle recycling illumi-nated by fluorescent dyes, J. Neurochem. 73, 2227–2239.

Exciting New Easy-to-Use Hybrid Measurement System for Extracellular Potential And Impedance Recording in a 96-Well Format

David Guinot[1*], Leo Doerr[1], Sonja Stoelzle-Feix[1], Ulrich Thomas[1], Matthias Beckler[1], Michael George[1], Niels Fertig[1]

1 Nanion Technologies GmbH, Munich, Germany
* Corresponding author. E-mail address: david.guinot@nanion.de

Abstract
Cardiac safety assessment is a vital part of drug development since late withdrawals of compound candidates due to heart liability issues such as ventricular arrhythmia are very costly. The CardioExcyte 96 is a new pharmacological tool for drug safety screening allowing reliable high throughput label-free measurements of short- and long-term compound effects. It allows to monitor both, the extracellular field potential (EFP) and the impedance of a cell monolayer, with an outstanding time resolution of 1ms. Due to the development of stem-cell derived cardiomyocytes as a model standard for cardio-vascular risk assessment this combination will most probably be the prospective choice for in-vitro diagnostics in the future.

1 Background / Aims

For in-vitro diagnostics, stem cell-derived cardiomyocytes are emerging as a powerful new tool in safety evaluations and drug screening. A new trend in the industry utilizes induced pluripotent stem cells (iPSCs) for functional assays to identify cardiac pathologies and their genetic underpinnings (such as Long QT Syndrome (LQTS)), in addition to cardiotoxicity profiling of pharmaceutical compounds. Until now, label-free large-scale screening platforms for cardio-vascular risk were not available on the market.

2 Methods / Statistics

We present a new screening platform – the CardioExcyte 96, a hybrid instrument that combines impedance readout (a correlate of cell contractility) with field potential recordings of the compound signal that is generated by cellular action potentials (Fig. 1). These electrophysiological measurements are label-free and have an unparalleled temporal resolution of 1 ms. This screening tool is capable of combining the impedance readout of compound affected cell-contractility and MEA-type measurements of an action potential, thereby redressing the lack of easy-to-use high throughput in-vitro assays. In comparison to MEA, a simpler and cost efficient electrode technique based on a 96-well plate format is developed which allows to monitor both, the extracellular field potential (EFP) and the impedance (Fig.2). The CardioExcyte 96 is placed inside the incubator ensuring a physiological cell environment. Approximately 2-3 days after seeding cardiomyocytes, the monolayer formed a network and is starting to beat synchronized so that a compound screening can be conducted. For cardio-vascular risk assessment an entire experiment from seeding cells to data analysis can be performed within less than one week.

Fig. 1. Left:CardioExcyte 96 with inserted 96-Well sensor plate. Right: Sensor design of the 96-well sensor plate can be used for EFP and impedance measurements.

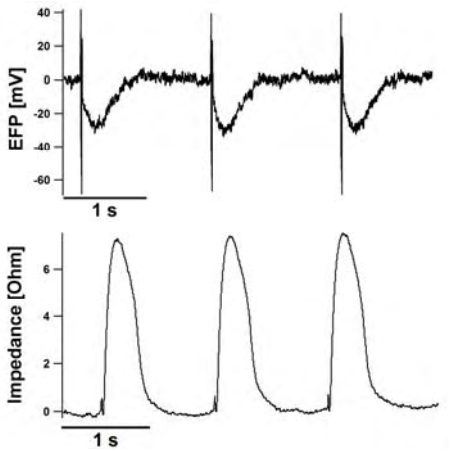

Fig. 2. Representative extracellular potential and impedance recording of stem-cell derived cardiomyocytes on the CardioExcyte 96.

3 Results

Several commercially available stem-cell derived cardiomyocytes have been analysed. Below, we introduce the EFP and impedance signal.

As seen in a representative readout (Fig. 3), the EFP reflects the characteristic regions of the capacitive coupling with neighbouring cells (1), the influx of sodium ions (2) and inward directed calcium currents (3) leading to a depolarisation of the membrane potential as well as the repolarisation phase (4) [1, 2].

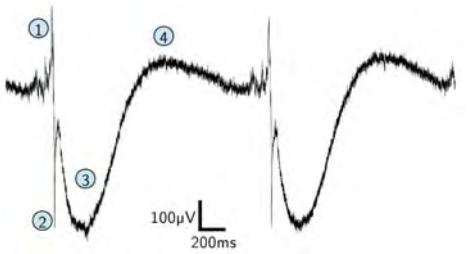

Fig. 3. Representative EFP-readout with its characteristic regions, the capacitive coupling with neighbouring cells (1), influx of sodium ions (2), inward current of calcium ions (3) and the repolarisation phase (4).

The action potential induced cell contraction can be analysed using the impedance signal.

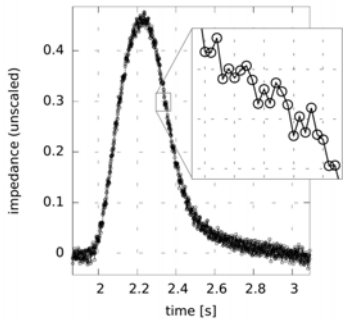

Fig. 4. Representative impedance readout with 1ms sampling-rate.

Drug induced effects of several reference compounds on the measured wave form in the EFP and impedance recording mode were analysed. As an example, the effect of Blebbistatin is shown in a representative measurement (Fig. 5).

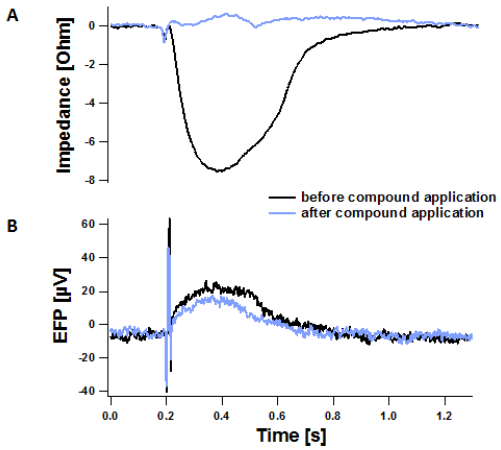

Fig. 5. Effect of Blebbistatin (6 µM) on the impedance amplitude (A) and the EFP (B). Traces before and after the compound addition are compared.

Blebbistatin blocked the impedance signal at a concentration of 6 µM whereby the EFP signal stayed unaffected according to its mode of action as an inhibitor of myosin II.

To facilitate the Ease-of-Use and the efficiency of the CardioExcyte96, a specialized software package for rapid data handling and real-time analysis was developed, based on novel algorithms that allow for a comprehensive investigation of the cellular beat signal. The software offers dose response curve or single point screening analysis based on beating parameters.

As an example, the concentration dependent effect and the IC50 calculation (41.6 nM) of Dofetilide on the impedance amplitude are summarised in Figure 6.

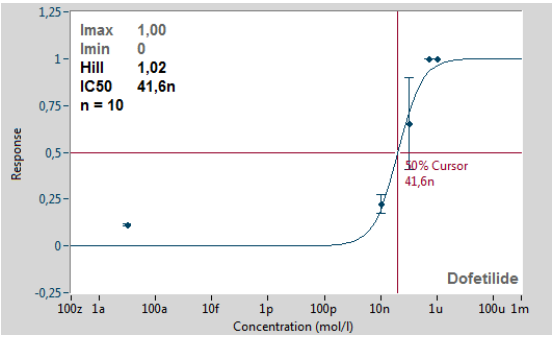

Fig. 6. Dose response curve and IC50 analysis of Dofetilide on the impedance amplitude.

4 Conclusion/Summary

The CardioExcyte 96 allows combining MEA-like extracellular potential measurements and impedance measurements with an ultrafast time resolution of 1 ms. The CardioExcyte 96 sensor plate is based on a 96-well format with a single electrode structure for high-throughput and cost efficient cardio-vascular drug screening. The CardioExcyte 96 allows predicting cardiotoxicity of pharmaceutical compounds.

Acknowledgement

We thank Axiogenesis and CDI for the collaboration and for providing us the cardiomyocytes Cor.4U and iCells.

References

[1] Christoph Sprössler et al. “Electrical recordings from rat cardiac muscle cells using field-effect transistors”. In: Physical Review E 60.2 (1999), pp. 2171–2176. ISSN: 1063-651X.

[2] Ian L. Jones et al. “The potential of microelectrode arrays and microelectronics for biomedical research and diagnostics”. In: Analytical and Bioanalytical Chemistry 399.7 (2011), pp. 2313–2329. ISSN:1618-2642.

Electrical Stimulation of Neuronal Cultures as a New Method for Neuropharmacological and Neurotoxicological Evaluation

Marika Zanin[2], Enrico Defranchi[1], Susanna Alloisio[2,3], Antonio Novellino[2,3], Sergio Martinoia[1].

1 DIBRIS, University of Genoa, Genoa (Italy).
2 Alternative Toxicity Services, ETT s.p.a., Genoa (Italy).
3 Institute of Biophysics, National Research Council, Genoa (Italy).

Abstract
In vitro neuronal networks coupled to micro electrode arrays represent a simplified model for investigating neurons activity in response to external manipulation and it has been proposed as a tool for in vitro neurotoxicity assessment. In this study we tested a new protocol based on electrical stimulation coupled to pharmacological stimulation to overcame the variability of spontaneous activity in order to improve the reliability, the informative content and to take advantage also by the reduced time needed to perform the test.

1 Backround / Aims

Ex vivo/in vitro neuronal networks respond to classical agonists of the various receptors as well as to specific pharmacological substances in a manner that is comparable to those observed in the brain, thus constituting a promising in vitro tool for neuropharmacology and neurotoxicity testing (Defranchi et al., 2011, Novellino et al., 2011). Here we propose a new method, based on the application of electrical stimulation, for detecting electrophysiological activity changes, related to the administration of chemical substances as a valuable tool to evaluate pharmacological effects leading to an improvement in term of time required and informative content. The final objective of the introduction of electrical stimulation is to increase the deterministic aspect of the network response by reducing the intrinsic variability of spontaneous activity.

2 Methods / Statistics

Due to the peculiarities of the system in use (micro-electrode arrays), the stimulation occurs on the extracellular matrix and, although it is applied through a single electrode, given the high connectivity among the neurons constituting the network, the stimulation spreads and affects many neurons and as a consequence many recording sites. The stimulus consists of a biphasic pulse with duration of 250 μs per phase and peak-to-peak amplitude of 1.5 volt. Trains of stimuli (120 pulses) at 0.2Hz are delivered, sequentially, from three separate sites (electrodes). The experimental protocol consists of 18 steps, each lasting 10 minutes for a total of 3 effective hours of recording, for a range of effective concentrations of chemical spanning from 100pM to 100□M.

The substances used for chemical stimulation were:

- **Bicuculline:** is a competitive antagonist for GABAA receptors. More specifically, works by blocking the inhibitory action of GABA ionotropic excitatory synaptic transmission causing an epileptic a behavior .
- **APV** ((2R)-amino-5-phosphonovaleric acid): is a selective competitive antagonist for ionotropic glutamate receptor. It acts by masking the ligand (glutamate) binding site of NMDA receptors causing inhibition of excitatory synaptic transmission.
- **Fluoxetine:** selective serotonin reuptake inhibitor (SSRI) in central neurons, thus prolonging the presence of serotonin in the synaptic cleft.
- **Muscimol:** it is a potent selective agonist of the GABAA. The stimulation of the GABAA receptor causes the opening of channel permeable to Cl- and is able to induce a hyperpolarization of the postsynaptic membrane.
- **Verapamil:** it is a L-type voltage-dependent Calcium channel blocker of the phenylalkylamine class..

3 Results

In order to evaluate the results of the proposed method, we compared the mean firing frequency rate changes (MFR) during spontaneous activity with the pPSTH (population Post Stimulus Time Histogram) that account for the global evoked response (total number of evoked spikes in a defined window) by the entire neuronal network. In such a way, two dose-response curves were obtained, showing the effect of

the administered substance on each of these two parameters.

With respect to the basal levels before administration, the dose response curves for MRF and pPSTH presented essentially two different trends with the concentration increase. From one side, Bicuculline and resulted with an increase in the MRF and pPSTH values, reaching a saturation plateau at concentration higher than 100nM. . On the other hand, in the cases of Muscimol, Fluoxetine and APV, the initial levels of the network activity had progressively reduced with a sharp transition around 1uM.

Results obtained with different pharmacological conditions showed good agreement between the two parameters considered (MRF and pPSTH).

4 Conclusion/Summary

The new protocol aims to increase the deterministic aspect of the network response without overstimulation or plastic changes in the network. The stimulation pattern adopted was choose based on previously study (Bologna et al., 2010) showing that in case of low frequency electrical stimulation, neuronal networks manifest a consistent difference in terms of increased burst activity and spreading of synchronous activity across the network compared to control non stimulated cultures, so the overall effect is the electrical network stabilization.

The analysis of the results with the coupled pharmacological and electrical stimulation reveals a similar behaviour of the two parameters considered during the different phases, while better highlighting specific physiological effects such as residual evoked activity in absence of spontaneous network activity, or increased evoked response following spontaneous administration.

In conclusion the result obtained suggest the innovative protocol as a possible complementary testing strategy for neurotoxicological and neuropharmacological assessment , but with an advance in term of time required for chemical testing respect to other protocols based on perturbation of spontaneous electrical activity after pharmacological administration and a more reliable data due to a decrease of the of the variability of spontaneous activity.

Acknowledgement

This works is partially supported by ESSENCE project (4th EuroTRansBio programme) and Neurotox project (6th EuroTRansBio programme).

References

[1] Bologna LL, Nieus T, Tedesco M, Chiappalone M, Benfenati F, Martinoia S. Low-frequency stimulation enhances burst activity in cortical cultures during development. Neuroscience. 2010 Feb 3;165(3):692-704.

[2] Defranchi E, Novellino A, Whelan M, Vogel S, Ramirez T, van Ravenzwaay B, et al. Feasibility assessment of microelectrode chip assay as a method of detecting neurotoxicity in vitro. Front Neuroeng 2011;4(6):1–12.

[3] Novellino A, Scelfo B, Palosaari T, Price A, Sobanski T, Shafer T, et al. Development of micro-electrode array based tests for neurotoxicity: assessment of interlaboratory reproducibility with neuroactive chemicals. Front Neuroeng 2011;4(4):1–14.

Real-time Monitoring of Lesion Healing by Impedance Spectrometry on Chip

Heinz D. Wanzenboeck[1], Andreas Exler[1], Johann Mika[1], Emmerich Bertagnolli[1]
Elisabeth Engleder[2], Michale Wirth[2], Franz Gabor[2]

1 Vienna University of Technology, Institute for Solid State Electronics,
Floragase 7/1-E362, A-1040 Vienna, AUSTRIA
2 University of Vienna, Department of Pharmaceutical Technology and Biopharmaceutics
Althanstrasse 14, A-1090 Vienna, AUSTRIA
* Corresponding author. E-mail address: Heinz.Wanzenboeck@tuwien.ac.at

Abstract
An impedance-analyzer-system was developed and used for long-time impedance measurements of living epithelial tissue. For the measurement of impedance spectra the CaCo2-cellline was used. As measurement platform a microelectrode array of planar interdigitated electrodes (IDES) was developed. This setup provides low signal-to-noise ratio and allows long-time measurement using a specific software for long-time measurement. Successful permeability measurements with Bromelain as permeation enhancer as well as measurements of the regenerative properties of the CaCo2-cellmonolayer could be demonstrated. With this impedance spectroscopy system non-invasive in-vitro investigations could be performed and will in future allow addressing a wide range of pharmaceutical and medical cytological issues such as drug uptake and regeneration properties.

1 Background

Impaired wound healing leads to infection and tissue necrosis. This has been a strong motivation for the search and identification of new wound healing agents. For a screening of potential candidates a fast and reliable methodology to test the wound healing capabilities of substances has been frequently demanded. While in-vivo tests and clinical studies are essential for approval of new drugs, a fast ex vivo screening method is required for the plethora of newly designed therapeutic substances.

In this work we present a microelectronic system for automatic impedance monitoring of wound healing of an epithelial layer. Impedance spectroscopy has already been successfully employed for monitoring of fibroblast behaviour, for toxicological screening and to monitor the mortality of living cells [1,2]. Using a reproducible cell culture of epithelial cells, the healing process of an mechanically inflicted wound may be monitored in real-time and fully automatically. Such a cell culture based model systems will provide a deeper understanding of how these compounds exert their activities in biological systems and contributes to the future discovery of wound healing agents.

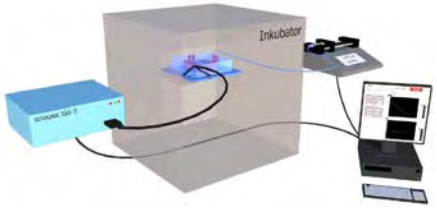

Fig.1 Schematic setup of impedance-analyzer-system

2 Methods

In this work we present an impedance-analyzer-system (Fig.1) for long-time impedance measurements of living epithelial tissue. The cells used for this study are the CaCo2-cellline which has metabolic properties comparable to the human small intestine epithelial cell walls. Combining the CaCo2-cells with the measurement system mentioned above allows to investigating important biological problems such as drug intake and regeneration properties.

The use of microstructural and planar interdigitated electrodes (IDES) provides low signal-to-noise ratio and allows long-time measurement. The contact pad is adapted to the Multichannel System MEA60 biochip standard. Each sensor chip (Fig 2) holds 4 separated culture wells with noble metal IDES on glass. The impedance-analyzer-system contains a specific software solution for continuous online-monitoring in real-time. By implementing a microfluidic media supply made of biocompatible materials the system can be extended.

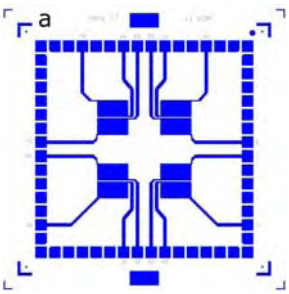

Fig.2 Schematic image of IDES Sensor with 8-electrode pairs

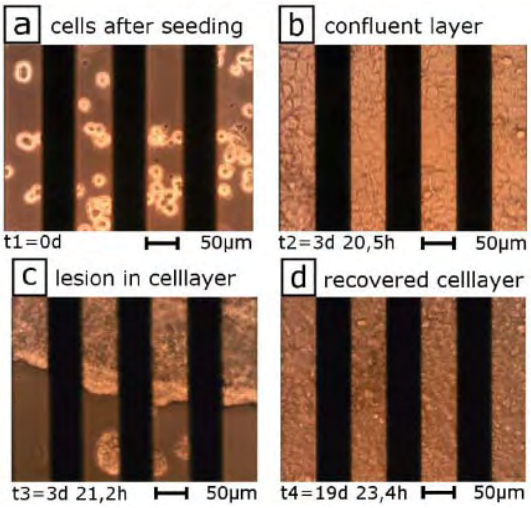

Fig. 3 Optical microscope images of the Caco-2 cell culture grown on the interdigitated electrodes.

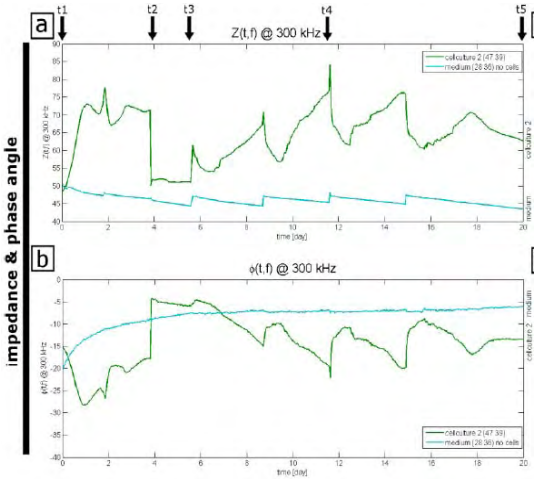

Fig. 4. Time-dependent development of the impedance at 300kHz of a Caco-2 cell culture. The graphs show (a) the absolute value of Impedance, (b) the value of the phase

3 Results

The improved 8-electrode pair-design (Fig 2) provides a better spatial resolution of culture-specific proliferation variations and a higher cell-cell contact resolution. This provides for a better monitoring of intestinal drug intake. The functionality of the microfluidic supplying device and its control-software has been demonstrated. A lesion was mechanically inflicted to a confluent cell layer and the healing procedure (Fig. 3) was imaged and monitored by impedance spectroscopy. Impedance measurements allowed to track the regenerative process of the CaCo2-cell monolayer (Fig.3). Both impedance and phase at 300 kHz show a significant change when a scratch was administered (t2). The wound healing process until t4 is imaged showing the gradual increase in impedance towards the value before t2.

4 Conclusion

The measurement of impedance spectra of cell cultures allows to address a wide range of pharmaceutical and medical cytological issues. As (f. e. on living cell cultures) most conventional analyses are based on qualitative optical results impedance spectroscopy offers an excellent instrument for non-invasive in-vitro investigations. With the improved impedance-analyzer-system not only a good quantitative diagnostic instrument has been implemented but it is also provided for a system which enables reproducible results in the biological distribution.

References

[1] I. Giaever und C. R. Keese, „Monitoring fibroblast behavior in tissue culture with an applied electric field,“ Proceedings of the Mational Academy of Sciences, Nr. 81, pp. 3761-3764, 1984.

[2] J. H. Luong, M. Habibi-Rezaei, J. Meghrous, C. Xiao, K. B. Male und A. Kamen, „Monitoring Motility, Spreading, and Mortality of Adherent Insect Cells Using an Impedance Sensor,“ Analytical Chemistry, Nr. 73, pp. 1844-1848, 2001

Acknowledgement

We thank the Center for Micro- and Nanostructuring for providing the fabrication facility.

Functional Phenotypic Compound Screening with Primary Brain-Region Specific Cell Cultures

Alexandra Voss[1*], Corina Ehnert[1], Konstantin Jügelt[1], Anna-Maria Pielka[1], Angela Podßun[1], Olaf H.-U. Schröder[1]

1 NeuroProof GmbH, Rostock, Germany
* Corresponding author. E-mail address: alexandra.voss@neuroproof.com

Abstract
Recently, an analysis revealed the phenotypic approaches to be the more successful strategy for small-molecule and therefore are reconsidered and reintroduced as a complementary strategy of a target-based approach for drug discovery (Swinney and Anthony, Nat Rev Drug Discov. 2011). Phenotypic screening with neuronal cell cultures on microelectrode arrays (MEAs) is an elegant and efficient way to discover and characterize neuro-active compounds in preclinical drug development. Dissociated neuronal cell cultures derived from specific areas of the brain offer a reliable tool for analyzing brain region specific effects. Despite lacking a genetically defined, layered or 'cell nucleus' topology, primary neuronal cultures share many features with the tissues from which they are obtained, including cell phenotypes, receptor and ion channel complements, intrinsic electrical membrane properties, synaptic development and plasticity. The electrophysiological properties of compounds can be evaluated using their ability to induce activity changes in primary neuronal networks grown on MEA neurochips. Such network cultures remain spontaneously active and pharmacologically responsive for several months. Numerous research groups demonstrated the inter-culture repeatability of the networks and the feasibility to study functional and morphological properties of specific brain areas. Additionally, compounds induce brain region-specific effects in the network activity changes of dissociated cell cultures which were also relevant for the in vivo situation.

1 Background/Aims

Phenotypic screening with neuronal cell cultures on micro electrode arrays (MEAs) is an elegant and efficient way to discover and specify neuroactive compounds in preclinical development. Dissociated neuronal cell cultures derived from specific areas of the brain offer a reliable tool for analyzing brain region specific effects. Despite lacking a genetically defined, layered or ‘cell nucleus’ topology, primary neuronal cultures share many features with the tissues from which they are obtained, including cell phenotypes, receptor and ion channel complements, intrinsic electrical membrane properties, synaptic development and plasticity.

The electrophysiological properties of compounds can be evaluated using their ability to induce activity changes in primary neuronal networks grown on MEA neurochips. Such network cultures remain spontaneously active and pharmacologically responsive for several months. Numerous research groups demonstrated the inter-culture repeatability of the networks and the feasibility to study functional and morphological properties of specific brain areas. Additionally, compounds induce brain region-specific effects in the network activity changes of dissociated cell cultures which were also relevant for the in vivo situation.

2 Methods/Statistics

We further enhanced the MEA technology platform by establishing functional fingerprints in a multiparametric approach to describe the native, spontaneous activity of neuronal networks or induced pharmaceutical changes. With the pattern analysis tool NPWaveX it is possible to compute several hundred parameters from spike trains. We routinely compute 204 parameters to analyze spike train properties describing general activity, synchronicity, regularity of bursting patterns and burst structure. The NeuroProof platform allows assessing and quantifying any modifications of electrophysiological signaling patterns in a neuronal network. Hence we have a very sensitive measure for the assessment of compound effects on network activity. Appling additional methods like pattern recognition and similarity analysis of the activity profiles of compounds and drug candidates enables a phenotypic description of functional changes evoked by compounds and/or challenge agents. Our classification technology platform can be trained with functional fingerprints of reference compounds. For primary neurons, more than 100 fingerprints are available in the NeuroProof database for frontal cortex and those for the other tissue cultures are continuously growing in number of screened compounds. These databases serve to functionally compare the pharmacological response between different tissue cultures.

This enables the pattern recognition and similarity analysis of the activity profiles of compounds and

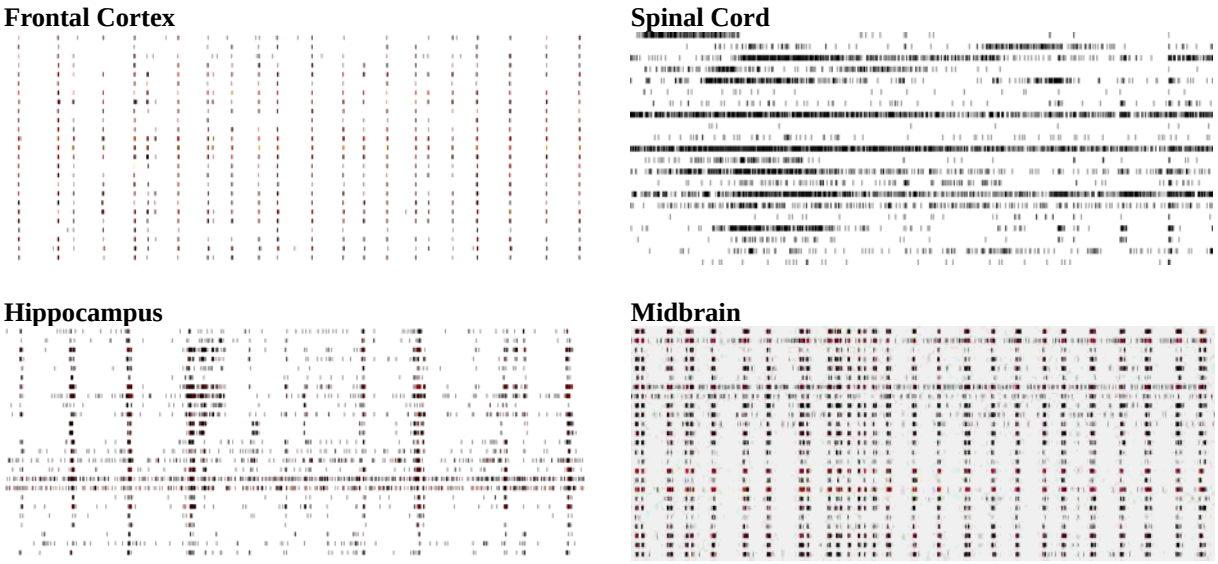

Fig. 1. Network spike train patterns of brain-region specific primary cell cultures derived from embryonic murine tissue of the frontal cortex, spinal cord (with dorsal root ganglia), hippocampus, and midbrain (co-cultured with frontal cortex). Plotted are 60 s of 25 neurons of spontaneous network activity at 28 days *in vitro*.

drug candidates. Thereby the effect of new drug candidates on the CNS pharmacology and possible neurotoxic effects can be predicted early on in drug discovery by studying phenotypic changes in a functional network; those possess the temporal resolution of cell-assembly cooperation. Thus it is possible to estimate the mode of action and considerably accelerate the preclinical development of CNS drugs.

3 Results

We routinely culture primary mixed neuron/glia cultures from different brain tissues such as frontal cortex, hippocampus, midbrain, and spinal cord on MEAs, where they differentiate for 4 weeks in vitro. We show that each of these brain-region specific cell cultures generates their own unique spontaneous network spike train activity pattern (Figure 1) which can be differentiated by classification using cross validation analysis. The four phenotypic cultures showed a self-recognition of 85–96%. Feature selection methods on the 204 parameters determine the best describing 15 parameters for each brain-region specific culture type.

In multiple examples at the GABA, glutamate and other receptor subtypes we exhibit the brain-region specific responses induced by compounds in those cultures.

We further demonstrate that the complex micro circuitry in network activity in matured cortical cultures are very similar to the in vivo situation in their functional outcome by means of their activity structure regarding the levels of activity strength, synchronicity, oscillatory behavior and spike train structure (burst structure).

4 Conclusion/Summary

In conclusion, functional screenings with neuronal networks derived from primary tissue cultures have the advantage that a multitude of targets, known and unknown, can be addressed and compared to each other (=phenotypic screening). With this phenotypic approach compounds can be selected which have a similar induced network activity, but have new not yet discovered mode of actions with similar therapeutic options. The technology supplements brain slice and patch clamp methods and provides new complementary insights to accelerate drug discovery.

References

[1] Swinney DC, Anthony J.: How were new medicines discovered? Nat Rev Drug Discov. 2011 Jun 24;10(7):507-19.

MEA technology - a New Player in Diabetes Research

Sven Schönecker[1], Peter Krippeit-Drews[2], Gisela Drews[2], Karl-Heinz Boven[3], Elke Guenther[1], Udo Kraushaar[1*]

1 NMI Natural and Medical Sciences Instute at the University of Tübingen, Dept. Electrophysiology, Reutlingen, Germany
2 University of Tübingen, Institute of Pharmacy, Dept. Pharmacology, Tübingen, Germany
3 Multi Channel Systems, Reutlingen, Germany
*Corresponding author. Email adress: udo.kraushaar@nmi.de

Background and Aims
The increase in postprandial blood glucose concentration leads to glucose-induced electrical activity of pancreatic beta-cells resulting in insulin secretion. This electrical activity manifests in glucose concentration-dependent oscillations which can easily be recorded by microelectrode arrays (MEA). Until now the number of experiments was limited to one at the time. To increase the throughput to an extent suitable for drug development we developed a MEA-based parallelized recording system for freshly dissected islets of Langerhans called BetaScreen.
In addition, to understand mechanisms leading to beta-cell dysfunction (e.g. during the development of type-2 diabetes mellitus; T2DM) as well as to investigate other long-term effects, a noninvasive MEA-based long-term culture of intact islets of Langerhans is required. Thus, we developed for the first time such a culture protocol in which the glucose-dependent oscillatory activity is conserved over weeks of culture within intact islets.

1 Methods

Intact murine islets of Langerhans were either used acutely or directly cultivated on MEA chips for several weeks. Electrical oscillatory activity was repetitively recorded at 37°C as field potentials and quantified as fraction of plateau phase (FOPP = percentage of time with burst activity). Insulin secretion was detected by radioimmunoassay.

2 Results

The current prototype recording chamber of the BetaScreen device allows to record electrical oscillations from up to five intact islets of Langerhans simultaneously. Positioning of the islets is realized by suction of the islets onto the electrodes. First validation experiments including glucose concentration-response curves and application of ion channel modulators indicate that the physiology is not altered by this holding method.

Furthermore, we demonstrate that glucose concentration-dependent electrical oscillations from intact mouse islets of Langerhans are preserved for up to 34 days in vitro (DIV). The glucose-dependent FOPP dynamics were conserved within 34 days in culture and comparable with those obtained from acute islets. (FOPP 32 ± 3 % (n = 8; DIV6/7) and 36 ± 2 % (n = 7; DIV34) at 10 mM glucose and 70 ± 6 % (n = 8; DIV6/7) and 72 ± 5 % (n = 7; DIV34) in 15 mM glucose, respectively). Furthermore we could show that insulin secretion is intact throughout the entire cultivation time. Our current investigations focus on the induction of oxidative stress by H2O2 in order to mimic the development of T2DM.

3 Conclusion

The development of the BetaScreen opens the door for large-scale investigations of beta-cell electrical activity for both academic and industrial purposes. Furthermore we developed an *in vitro* model to investigate functional behavior of individual islets for more than one month. This paves the way for the development of an *in vitro* disease model to e.g. investigate the onset and development of T2DM.

Neuron and Network Properties

Analysis of (Sub)-Cellular Neuron Properties

Glutamate Mediated Astrocytic Filtering of Neuronal Activity

Gilad Wallach[1], Yael Hanein[1]

1 School of Electrical Engineering, Faculty of Engineering, Tel Aviv University, Tel Aviv, Israel
* Corresponding author. E-mail address: giladwa1@gmail.com

Abstract
Neuron-astrocyte communication is an important regulatory mechanism in various brain functions. The complexity and role of this communication are not yet fully understood and several recent models have been proposed as possible mechanisms. We demonstrate, for the first time, the existence of a frequency dependent, glutamate-mediated signaling mechanism between neurons and astrocytes. The electrical activity of neuron-glia cultures on multi electrode arrays was mapped using Ca^{2+} imaging while neurons were selectively activated with underlying micro-electrodes. By modifying the stimulation frequency and number of spikes, we revealed a clear onset of astrocytic activation at neuron firing rates around 3 Hz. Astrocytic activation by neurons, as evidenced by astrocytic intracellular Ca^{2+} transients, was abolished with glutamate receptor blockers, validating the glutamate-dependence of this neuron-to-astrocyte pathway. The frequency dependent neuro-astrocyte communication presented here may play an important, task specific role in brain function.

1 Background

Evidence obtained during the last few years established the important role of astrocytes in information processing in the brain. The "tripartite synapse" concept [1,2] is gaining acceptance, and is replacing the original bipartite synaptic view. This concept builds on expansive experimental evidence which shows that astrocytes display a form of excitability based on elevations of their intracellular Ca^{2+} concentrations ($[Ca^{2+}]_i$) in response to synaptically released neurotransmitters [3–5].

The study of astrocyte-neuron communication is complicated by its bidirectional nature. Glutamate transmission is a typical example: just like neurons, astrocytes express efficient glutamate transporters that clear glutamate from the synaptic cleft and glutamate receptors (metabotropic); they also release glutamate in a process that may be similar to neurons [1,6]. Experimental evidence generally supports the idea that astrocytes are more than simple passive (linear) readout of the synaptic activity but process it in an integrated and complex fashion, encoding the input neuron activity as a nonlinear response in their Ca^{2+} dynamics [6,7]. However, how exactly astrocytes integrate and process synaptic information is still unclear. Thus, additional studies are needed to reveal the complex nature of neuron-to-astrocyte communication and the properties of astrocytic $[Ca^{2+}]_i$ signals evoked by synaptic activity.

To explore neuronal modulation of astrocytic activity on a network level we used neuron-glia mixed cultures. We applied direct electrical stimulation with micro electrodes to selectively activate neurons according to a specific protocol, while optically reading neuronal and astrocytic activation using a calcium imaging technique [8]. Using this technique we show that astrocytes exhibit elevations of their $[Ca^{2+}]_i$ level in response to synchronized neuronal activity, but more interestingly we discovered that the response is frequency dependent with high response at physiologically relevant frequencies (i.e. gamma waves). The results presented in this investigation indicate the existence of a buffer-like encoding process underlying neuro-glia pathway.

2 Methods

Dissociated cortical cultures were prepared from surgically removed cortices of E18 Sprague Dawley rat embryos as described before [8]. Calcium imaging was performed in open air environment using Oregon-Green BAPTA-I dye. Electrical stimulations consisted of rectangular and biphasic 400 µs-long current pulses of 25-35 µA applied to cell cultures by an extracellular multi-electrode array (MEA). Recording were performed with different pharmacological antagonists in order to supress synapse efficacy (APV, CNQX, MPEP, LY367385).

3 Results

Mixed neuro-glia cultures from rat cortices on micro electrode array (MEA) substrates were used as a model experimental system to study neuro-glia communication. Optical recordings of intracellular Ca^{2+} levels were performed between 14 and 27 days in vitro (DIV) [8].

We explored astrocytic activation in response to neuronal activity. To maximize neuronal activation we used nine stmiulating electrodes and applied a stimulation protocol consisting of 30 s current pulse trains at varying frequencies ranging from 0.2 to 70 Hz. Fig.1A displays the Ca^{2+} responses of selected neu-

rons and astrocytes (*red* and *green* curves accordingly). Strong changes in astrocytic Ca^{2+} are observed in repsonse to stimulated neuronal activity. The central result in this work is that the astrocytic responses are highly dependent on neuronal activity frequency: globally, astrocyte tends to respond only when the stimulation frequency becomes large enough. A similar effect was observed in 9 experiments, from 7 different cultures. It should be noted that, whatever the stimulation frequency, the responsive astrocytes were uniformly distributed around the stimulating electrode. Since the astrocyte response does not depend on the distance to the electrode, the possibility of direct electrical stimulation, from the electrode to the astrocyte, is unlikely. A candidate molecule to support the above-described neuron-astrocyte communication is glutamate [4,9–13]. To explore the role of glutamate as the biological transmitter underlying the neuron-astrocyte activity, we applied mGluR1 and mGluR5 antagonists (LY367385 and MPEP respectively). Figure 1B shows that in those conditions, the neuronal Ca^{2+} traces are unchanged and faithfully follows electrical stimulation. However astrocytic activity is completely abolished as a result of blocking mGluRs. These experiments yield two important conclusions. First, in our experimental conditions, calcium dynamics in the neuron somata does not appear to be significantly dependent on mGluR group I receptors. More importantly, these experiments indicate that the neuron-astrocyte communication evidenced here is mediated by glutamate activation of astrocytic mGluR group I receptors.

To further test the above indication the stimulation frequency is indeed the significant parameter affecting astrocyte response, we applied an alternative stimulation protocol, in which we varied the frequency of the electrical stimulation but kept the number of stimulations constant (the stimulation duration was inversely related to its frequency). In addition, the order with which the stimulation frequencies were applied to the MEA was chosen at random, so as to avoid artifactual responses such as cell fatigue or dye poisoning. The goal of this alternative stimulation protocol was to distinguish an astrocyte response that would depend on the stimulation frequency from a response that depends on the number of neuronal spikes in an accumulative manner. Figure 2A shows that astrocytic calcium activity in response to neuronal stimulation is indeed frequency dependent since in response to this alternative protocol, the astrocyte still tend to respond only to the largest stimulation frequencies. Furthermore, as with the stimulation protocol of Figure 2, the application of mGluR1 and mGluR5 antagonists abolished astrocyte calcium activity in response to neuronal activation (Figure 2B). To quantify the above results, we computed the single-cell responsiveness of an astrocyte as the increase of the calcium signal of this astrocyte that is specifically triggered by the stimulation. Figure 2C displays the distributions of the single-cell responsivenesses of all the activated astrocytes in the experiment of Figure 2A. For low stimulation frequencies, the single-cell reponsivenesses are essentially peaked around a very low mean value. When the stimulation frequency increases, the distributions of single-cell responsivenesses get much broader, thus revealing increasing cell-to-cell variations in the response, but the average value of the distribution increases rapidly. Figure 2D shows the evolution of the average value of the single-cell responsivenesses distribution (referred to as the *population average*, see *Methods*) as a function of the stimulation frequency (each data point on the figure shows the population average of a single experiment). In control conditions (empty *grey* circles), the population responsiveness is very low below a frequency threshold and increases rapidly above this threshold. This sigmoid-like response thus defines an onset frequency that varies from cell to cell and between experiments, as a result of network and intrinsic cell parameters. The average responsiveness over the experiences (black circles in Figure 2D, total of n=284 cells) displays a sigmoid shape (dashed line) with an onset frequency of 2.8±1.02 Hz (95% confidence level). Figure 2D also shows the population responsiveness in the presence of mGluR group I antagonists (n=239) (*empty green squares*). In agreement with the traces in panel B, blocking mGluR receptors suppresses population responsiveness throughout the frequency range. Linear fit of the average population responsiveness (*full blue squares*) yields a roughly zero slope (*dashed blue line*) thus confirming the absence of astrocyte response over the whole frequency range. Taken together, these results show that astrocytic activation in response to neuronal activity is nonlinear with a sharp frequency onset and mediated by glutamate and mGluR type I receptors.

4 Conclusions

The activation of intracellular calcium signaling in astrocytes by neuronal activity has been amply documented during the last twenty years. It is even at the origin of the recent renew of interest for astrocytes and neuron-glia interactions [14]. However, how the temporal pattern of astrocyte calcium response varies with the properties of the neuronal stimulation is still poorly understood. Here, we provide unequivocal evidence that the astrocyte calcium response depends on the neuronal stimulation frequency in a nonlinear way and features a marked onset frequency (around 2-5 Hz) below which astrocytes do not respond to neuronal stimulation.

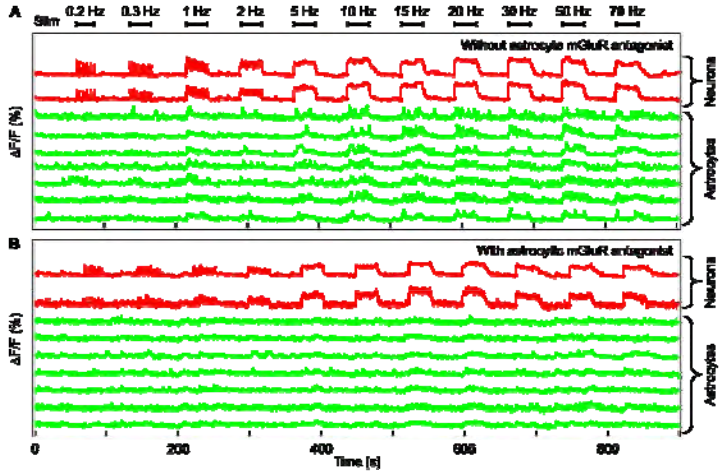

Figure 1. Astrocytic response to neuronal activity. A, Ca^{2+} traces of two selected neurons (in *red*), showing stimulated activity according to a multi-frequency protocol, and seven selected astrocytes (in *green*) in presence of neuronal AMPAR and NMDAR/kainate antagonists. **B,** Representative traces of same cells and stimulation protocol as in A, showing no $[Ca^{2+}]_i$ elevations in the presence of neuronal AMPAR and NMDAR/kainate antagonists, and astrocytic mGluR1 and mGluR5 antagonists. Culture was 17 DIV.

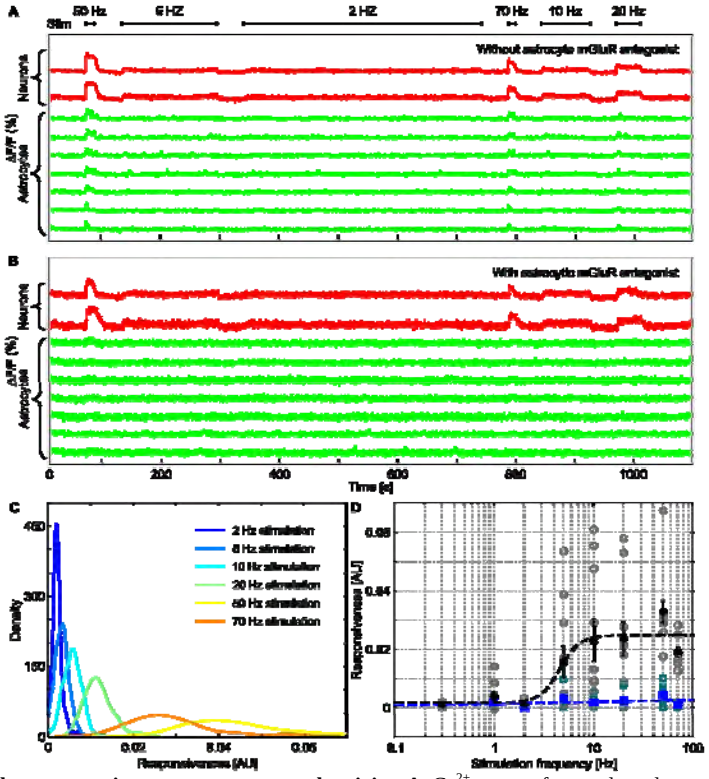

Figure 2. Frequency dependent astrocytic response to neuronal activity. A, Ca^{2+} traces of two selected neurons (in *red*), showing stimulated activity according to a random multi-frequency protocol, and seven selected astrocytes (in *green*) showing frequency dependent $[Ca^{2+}]_i$ elevations in response to neuronal activity. Experiments were performed in the presence of neuronal AMPAR and NMDAR/kainate antagonists. **B,** Ca^{2+} traces of same cells and stimulation protocol as in A, showing no astrocytic $[Ca^{2+}]_i$ elevations in the presence of neuronal AMPAR and NMDAR/kainate antagonists, and astrocytic mGluR1 and mGluR5 antagonists. **C,** Astrocytic distribution of the single-cell responsiveness of astrocytes shown in A. **D,** Astrocytic population responsiveness versus stimulation frequency. *Grey* empty circles are population responsivenesses for experiments performed with NMDAR & AMPAR but without (astrocytic) mGluR antagonists (n=284). Corresponding mean result, standard errors (*black* circles and bars), and sigmoid fit (*black dashed* line) are also illustrated. *Turquoise* empty squares are population responsivenesses obtained in the presence of both NMDAR & AMPAR and mGluR antagonists (n=239). Corresponding mean results and standard errors and linear fit are shown as *blue* squares (with bars and *dashed blue* line, respectively).

References

[1] Volterra A, Meldolesi J (2005) Astrocytes, from brain glue to communication elements: the revolution continues. Nat Rev Neurosci 6: 626–640. doi:10.1038/nrn1722.

[2] Araque A, Parpura V, Sanzgiri RP, Haydon PG (1999) Tripartite synapses: glia, the unacknowledged partner. Trends Neurosci 22: 208–215. doi:10.1016/S0166-2236(98)01349-6.

[3] Cornell-Bell A, Finkbeiner S, Cooper M, Smith S (1990) Glutamate induces calcium waves in cultured astrocytes: long-range glial signaling. Science (80-) 247: 470–473. doi:10.1126/science.1967852.

[4] Porter JT, McCarthy KD (1996) Hippocampal Astrocytes In Situ Respond to Glutamate Released from Synaptic Terminals. J Neurosci 16: 5073–5081.

[5] Araque A, Martin ED, Perea G, Arellano JI, Buno W (2002) Synaptically Released Acetylcholine Evokes Ca2+ Elevations in Astrocytes in Hippocampal Slices. J Neurosci 22: 2443–2450.

[6] De Pittà M, Volman V, Berry H, Parpura V, Volterra A, et al. (2012) Computational quest for understanding the role of astrocyte signaling in synaptic transmission and plasticity. Front Comput Neurosci 6: 98. doi:10.3389/fncom.2012.00098.

[7] Perea G, Navarrete M, Araque A (2009) Tripartite synapses: astrocytes process and control synaptic information. Trends Neurosci 32: 421–431. doi:10.1016/j.tins.2009.05.001.

[8] Herzog N, Shein-Idelson M, Hanein Y (2011) Optical validation of in vitro extra-cellular neuronal recordings. J Neural Eng 8: 056008. doi:10.1088/1741-2560/8/5/056008.

[9] Gurden H, Uchida N, Mainen ZF (2006) Sensory-evoked intrinsic optical signals in the olfactory bulb are coupled to glutamate release and uptake. Neuron 52: 335–345. doi:10.1016/j.neuron.2006.07.022.

[10] Pasti L, Volterra A, Pozzan T, Carmignoto G (1997) Intracellular Calcium Oscillations in Astrocytes: A Highly Plastic, Bidirectional Form of Communication between Neurons and Astrocytes In Situ. J Neurosci 17: 7817–7830.

[11] Perea G, Araque A (2005) Properties of synaptically evoked astrocyte calcium signal reveal synaptic information processing by astrocytes. J Neurosci 25: 2192–2203. doi:10.1523/JNEUROSCI.3965-04.2005.

[12] Schummers J, Yu H, Sur M (2008) Tuned responses of astrocytes and their influence on hemodynamic signals in the visual cortex. Science 320: 1638–1643. doi:10.1126/science.1156120.

[13] Wang X, Lou N, Xu Q, Tian G-F, Peng WG, et al. (2006) Astrocytic Ca2+ signaling evoked by sensory stimulation in vivo. Nat Neurosci 9: 816–823. doi:10.1038/nn1703.

[14] Agulhon C, Petravicz J, McMullen AB, Sweger EJ, Minton SK, et al. (2008) What Is the Role of Astrocyte Calcium in†Neurophysiology? Neuron 59: 932–946. doi:10.1016/j.neuron.2008.09.004.

Analysis of Related Molecules to Synchronized Burst Activity of Rat Cultured Cortical Networks

Daisuke Ito[1,2*], Kazutoshi Gohara[3]

1 Division of Functional Life Science, Faculty of Advanced Life Science, Hokkaido University, Sapporo, Japan
2 Research Fellow of the Japan Society for the Promotion of Science, Tokyo, Japan
3 Division of Applied Physics, Faculty of Engineering, Hokkaido University, Sapporo, Japan
* Corresponding author. E-mail address: ditoh@mail.sci.hokudai.ac.jp

Abstract
We investigated the network dynamics of cultured neurons and analyzed the related molecules to synchronized burst activity during long-term development. We measured spontaneous electrical activity of the networks for 1 month using multi-electrode arrays (MEAs). Over this culture period, the spontaneous spikes became synchronized bursts as the neuronal networks developed. The network showed an initial increase and subsequent saturation of the activity. Immunofluorescence staining of vesicular glutamate transporter 1 (VGluT1) and vesicular transporter of γ-aminobutyric acid (VGAT) revealed that both glutamatergic and GABAergic synapric boutons increased around the dendrites and somata over 1 month. In contrast, immunofluorescence staining of microtuble associated protein 2 (MAP2) and neurofilament 200 kD (NF200) revealed that the density of neurons decreased gradually and then remained constant. Gene expression analysis clarified that the transcription factor gene *Creb1* was consistently expressed during the culture period. However, *Arc* gene expression was not observed at 1-7 days *in vitro* (DIV), but the gene was expressed from 14 up to 28 DIV. The first expression of the *Arc* gene occurred at the same number of culture DIV as the generation of synchronized bursts under this culture condition.

1 Introduction

Synchronized burst is a remarkable phenomenon in the electrical activity of neuronal networks. Using multi-electrode arrays (MEAs) [1, 2], generation of synchronized bursts and the dynamics of burst activity were investigated [3-7]. Recently, it has been investigated that minute-to-hour time-scale changes in gene and protein expression during pharmacologically induced activity changes in synchronized bursts [8, 9]. However, the molecules involved in the generation and maintenance of synchronized bursts during long-term development (day-to-month time-scale) of cultured neuronal networks remain unclear.

Neuronal circuits regulate gene transcription depending on external inputs using a system called activity-dependent gene expression [10]. These genes contain many immediate-early genes such as *c-fos*, *Egr*, *Homar1a*, and *Arc* [11, 12]. In this study, we focused on neuron-specific gene/protein expression. We investigated the temporal relationship between the gene/protein expression and the generation of synchronized bursts during long-term development.

2 Methods

2.1 Cell culture

We cultured cortical cells derived from Wistar rats at embryonic day 17 using a Nerve-Cell Culture System (Sumitomo Bakelite Co., Tokyo, Japan) as described previously [13-18]. After dissociation procedure, the cell suspension was plated onto poly(ethyleneimine)-coated multi-electrode dish (MED) probe (Alpha ME Scientific, Osaka, Japan), which consisted of 64 planar microelectrodes (MED-p515A). We also plated the cell suspension onto a poly(ehyleneimine)-coated coverslips, which were inserted into 24-well cell culture plates. The cultures were incubated with the Neuron Cultured Medium (Sumitomo Bakelite Co.) in a humidified atmosphere containing 5% CO_2 and 95% air at 37℃. After 3 days of culture, half of the culture medium was replaced with fresh medium consisting of Dulbecco's modified Eagle's medium (DMEM; Life Technologies-Gibco, Carlsbad, CA) supplemented with 5% fetal bovine serum (FBS; Life Technologies-Gibco), 5% horse serum (Sigma-Aldrich, St. Louse, MO), 25 μg/mL insulin (Life Technologies-Gibco), 100 U/mL penicillin, and 100 μg/mL streptomycin (Life Technologies-Gibco). Then, half of culture medium was replaced twice a week.

2.2 Electrical activity recordings

Spontaneous electrical activity recordings were performed using a MED64 extracellular recording system (Alpha MED Scientific) at a sampling rate of 20 kHz with a software filter (MED Mobius; Alpha MED Scientific) set to 100-5000 Hz for 300s. All recordings were conducted in an incubator at 37℃. Activity was recorded approximately twice per week for approximately 1 month.

The amplitude of what we considered to be spike had to exceed a noise-based threshold within a win-

dow of 1 ms. Threshold determination was performed as described previously [13, 14]. Synchronized bursts were defined as described below. The time window was set to 100 ms and then the spikes (total for electrodes) in the window were counted. By shifting the window, a histogram of the change in firing rate across the threshold was obtained for each culture. Anything above the threshold was defined as a synchronized burst. The threshold was set to 100 spikes per window.

2.3 Immunocytochemistry

The primary antibodies were anti-microtuble associated protein 2 (MAP2) mouse IgG (Sigma-Aldrich), anti-neurofilament 200 kD (NF200) rabbit IgG (Sigma-Aldrich), anti-vesicular glutamate transporter 1 (VGluT1) rabbit IgG (Frontier Institute Co., Hokkaido, Japan), and anti-vesicular transporter of γ-aminobutyric acid (VGAT) guinea-pig IgG (Frontier Institute Co.). The secondary antibodies were Alexa Fluor 405-labeled anti-mouse IgG (Life Technologies – Molecular Probes), Alexa Fluor 488-labeled anti-guinea pig IgG, and Alexa Fluor 546-labeled anti-rabbit IgG.

The cultures were fixed with 4% formaldehyde in phosphate in phosphate-buffered saline (PBS: Life Technologies-Gibco) for 10 min. After permeabilization with 0.5% Triton X-100 in PBS for 30 min, the cultures were incubated with PBS containing 10% goat serum and Triton X-100 for 30 min. The permeabilized cultures were incubated with primary antibodies in PBS containing 10% goat serum overnight at 4℃ and were rinsed with PBS for 10 min three times. The cultures were then incubated with secondary antibodies (0.4% in PBS containing 10% goat serum) for 1h at room temperature and rinsed three additional times. In case of nucleus staining, the cultures were incubated with 1 μg/mL Hoechst33342 for 10 min at room temperature. Fluorescence images were acquired using a confocal laser-scanning unit (FV1000-D; Olympus, Tokyo, Japan) coupled to an IX-81 microscope (Olympus).

2.4 Quantitative image analysis

Volocity 5.5.1 visualization and quantification software (PerkinElmer, Waltham, MA) was used for quantitative analysis. Each VGluT1- and VGAT-immunopositive puncta was detected as a spherical object by setting brightness intensity threshold. After automatically separating objects that were touching, oversized and small objects were excluded. Objects area limits were set at 0.05-10 μm^3. Next, the number of objects was counted. The densities of the VGluT1- and VGAT-labeled terminals were defined as the number of VGluT1- and VGAT-immunopositive punctae per MAP2-immunopositive area. For quantification of the number of neurons, MAP2-immunopositive somata were counted manually. The cell nuclei were detected as circle objects. After slightly overlapped images were separated, the nuclei were counted automatically.

2.5 Gene expression analysis

For gene expression analysis, total RNA was firstly extracted using a PureLink RNA Mini Kit (Life-Technologies-invitrogen) from cultures at 1, 7, 14, 21, and 28 DIV. During this process, PureLink DNase (Life Technologies-invitrogen) was added to remove any genomic DNA contamination. The purified total RNA was quantified by measuring of OD_{260} absorbance using a spectrophotometer (DU730; Beckman Coulter, Tokyo, Japan). Total RNA was reverse-transcribed using SuperScript Ⅲ First-Strand Synthesis SuperMix and Oligo dT (Life Technologies-invitrogen). The synthesized cDNA was then amplified by polymerase-chain-reaction (PCR) using AmpliTaq Gold 360 Master Mix (Applied Biosystems, Foster City, CA) and a thermal cycler (S1000, Bio-Rad, Tokyo, Japan). Gene specific primers (*Gapdh, Creb1, Arc*) were designed and were made to order by Life Technologies-invitrogen. Next, electrophoresis of amplified genes was performed using the E-Gel iBase Power System and E-Gel EX agarose 2% (Life Technologies-invitrogen). UV light was used to illuminate the gel and gel images were captured with a digital camera. Gene expressions were evaluated by identifying specific bands.

3 Results and Discussion

3.1 Measurement of electrical activity

Figure 1A shows the developmental changes in network activity of rat cortical cells cultured for 1 month. The spontaneous spikes became synchronized bursts as the neuronal networks developed. To quantify the network activity, we calculated the network firing rate and synchronized burst rates. The network activity showed an initial increase and subsequent saturation of both rates during the 1-month culture period. These results suggest that network activity (firing rate and synchronized burst rate) became saturated at approximately 1 month after initial increase and remained saturated thereafter under this culture condition [13, 14].

3.2 Immunocytochemistry and quantitative analysis

To analyse the molecules related to the neuronal dynamics over the month, we performed immunofluorescence staining of synapse-specific proteins. We labeled glutamatergic and GABAergic synapses separately using antibodies against VGluT1 and VGAT, respectively (Fig. 1B). The densities and distributions of both types of synaptic terminal were measured simultaneously. Observations and subsequent measurements of immunofluorescence demonstrated that the densities of both types of antibody-labeled termi-

nal increased gradually from 7 to 21-28 DIV. The densities had not increased further at 35 DIV and tended to become saturated. Triple staining with VGluT1, VGAT, and MAP2 enabled analysis of the distribution of both types of synapse, and revealed that the densities of both types of synaptic terminal on somata were not significantly different, but that glutamatergic synapses predominated on the dendrites during long-term culture. In addition, the number of culture days to saturation from the initial increase corresponded to the electrical activity [13].

By contrast, the density of neurons labelled with MAP2 antibody decreased gradually over the cultured period (Fig. 1C). Then, the density of surviving neu-

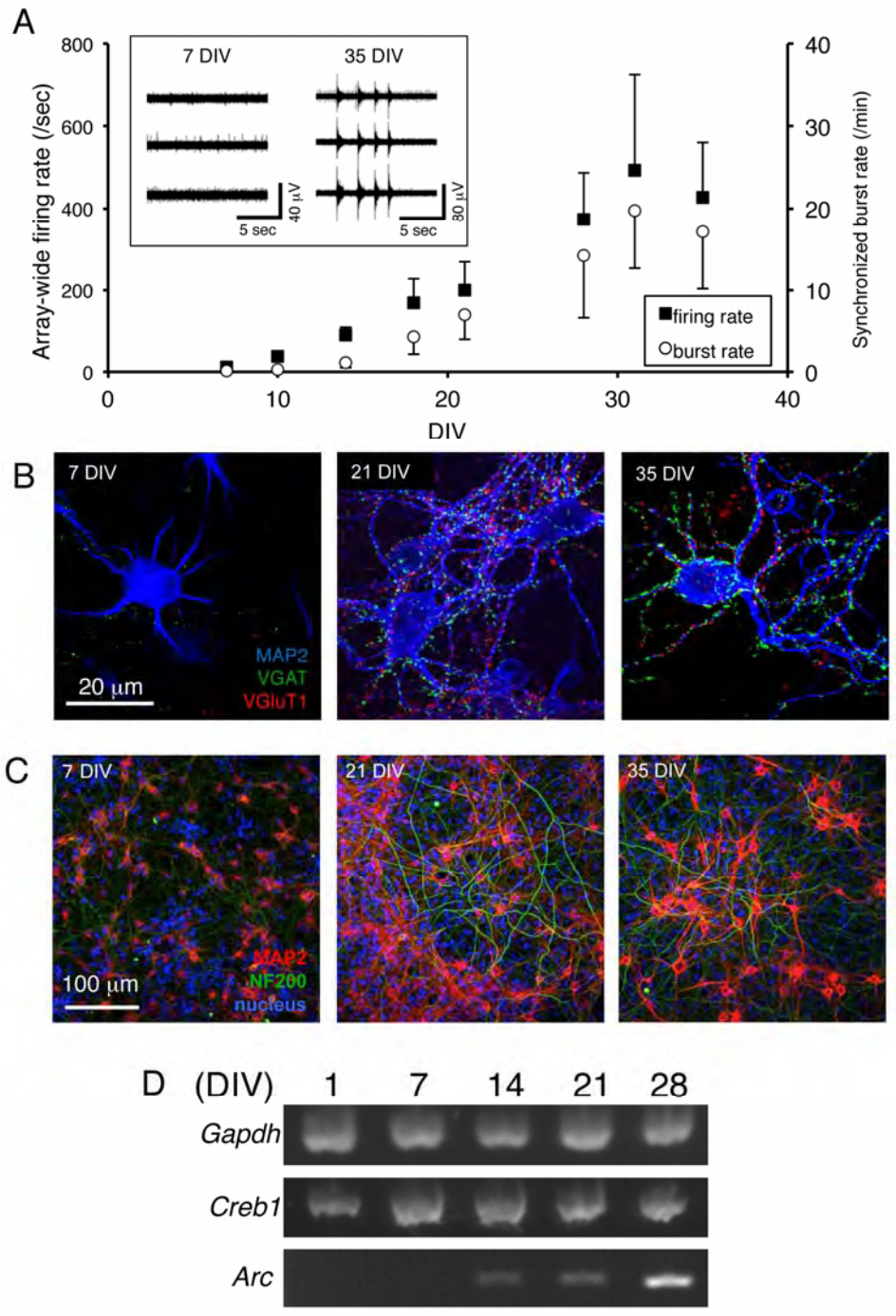

Fig. 1 (A) Changes in network activity during long-term development of cultured rat cortial neurons. The upper leht frame shows the extracellular potential traces recorded in each electrode. Firing rate data are shown as the mean +standard error of the mean (SEM), whereas the synchronized burst rate data are shown as the mean –SEM (for both n = 6). (B) Immunofluorescence micrographs of cultured cortical neurons. Blue color indicates MAP2. Green color indicates VGAT (marker of GABAergic synapses). Red color indicates VGluT1 (marker of glutamatergic synapses). (C) Immunofluorescence micrographs of cultured cortical neurons. Red color indicates MAP2 (marker of neuron somata and dendrites). Green color indicates NF200 (marker of neurites). Blue color indicates cell nulei stained with Hoechst33342. (D) Electrophoresis of *Gapdh, Creb1, and Arc* genes extracted from cultures every week during a 1-month cultured period. The genes were amplified by RT-PCR using gene-specific primers.

rons remained constant from 35 to 60 DIV, and the neurites labelled with NF200 covered the surface of the culture up to 60 DIV. These results indicate that cultured neuronal networks survived at least 2-month culture periods.

3.3 Gene expression analysis

To investigate gene expression during long-term development of cultured neuronal networks, we performed RT-PCR analysis. Figure 1D shows the results of electrophoresis of some target genes (*Gapdh, Creb1, and Arc*). Both specific bands for the housekeeping gene *Gapdh* and transcription factor gene *Creb1* were consistently detected from 1 DIV to 28 DIV. In contrast, the specific band for the immediate-early gene *Arc* was not identified at 1-7 DIV, but was identified from 14 DIV up to 28 DIV. These results indicate that the *Arc* gene began to be expressed from a certain point of neuronal development, although both *Gapdh* and *Greb1* were consistently expressed during long-term culture periods. Furthermore, the number of culture days to detect *Arc* gene expression was the same as the generation of synchronized burst during long-term culture periods in this culture condition.

In the developing brain, *Arc* gene expression increases markedly during the second and third postnatal weeks [11]. The tendency in time-course expression of the *Arc* gene is similar to our results. In addition, Arc protein expression is known to be essential for the consolidation of synaptic plasticity and long-term memory [12]. Therefore, the expression of the *Arc* gene from 14 DIV in this study suggests its role in network development and electrical activity. Based on these results, quantitative analysis of expression levels by real-time PCR is required to reveal this role in detail. Also, other molecules will need to be exhaustively investigated to elucidate the molecular mechanisms underlying the generation and maintenance of synchronized burst activity.

Acknowledgement

This work was supported in part by Grants-in-Aid for Scientific Research from the Japan Society of the Promotion of Science awarded to D.I. (Nos. 23700523, 24・3395, and 26750139) and to K.G. (Nos. 20240023 and 21650049).

References

[1] Gross, G.W., Rieske, E., Kreutzberg, G.W., Meyer, A. (1977) : A new fixed-array multi-microelectrode system designed for long-term monitoring of extracellular single unit neuronal activity *in vitro*. *Neurosci. Lett., 6, 101-105.*

[2] Pine, J. (1980): Recording action potentials from cultured neurons with extracellular microcircuit electrodes. *J. Neurosci. Meth., 2, 19-31.*

[3] Robinson, H.P.C., Kawahara, M., Jimbo, Y., Torimitsu, Y., Kuroda, Y., Kawana, A. (1993): Periodic synchronized bursting and intracellular calcium transients elicited by low magnesium in cultured cortical neurons. *J. Neurophysiol, 70, 1606-1616.*

[4] van Pelt, J., Wolters, P.S., Corner, M.A., Rutten, G.J.A., Ramarkers, G.J.A. (2004): Long-term characterization of firing dynamics of spontaneous bursts in cultured neural networks. *IEEE Trans. BioMed. Eng., 5, 2051-2062.*

[5] Chiappalone, M., Bove, M., Vato, A., Tedesco, M., Martinoia, S. (2006): Dissociated cortical networks show spontaneously correlated activity patterns during *in vitro* development. *Brain Res., 1093, 41-53.*

[6] Wagenaar, D.A., Pine, J., Potter, S.M. (2006): An extremely rich repertoire of bursting patterns during the development of cortical cultures. *BMC Neurosci., 7, art. 11.*

[7] Eytan, D., Marom, S. (2006): Dynamics and effective topology underlying synchronization in networks of cortical neurons. *J. Neurosci., 26, 8465-8476.*

[8] Arnold, F.J.L., Hofmann, F., Bengtson, C.P., Eittmann, M., Vanhoutte, P., Bading, H. (2005): Microelectrode array recordings of cultured hippocampal networks reveal a simple model for transcription and protein synthesis-dependent plasticity. *J. Physiol., 564.1, 3-19.*

[9] Pegoraro, S., Broccard, F.D., Ruaro, M.E., Bianchini, D., Avossa, D., Pastore, G., Bisson, G., Altafini, C., Torre, V. (2010): Sequential steps underlying neuronal plasticity induced by a transient exposure to gabazine. *J. Cell. Physiol., 222, 713-728.*

[10] Flavell, S.W., Greenberg, M.E. (2008): Signaling mechanisms linking neuronal activity to gene expression and plasticity of the nervous system. *Annu. Rev. Neurosci., 31, 563-590.*

[11] Lyford, G.L., Yamagata, K., Kaufmann, W.E., Barnes, C.A., Sanders, L.K., Copeland, D.J., Gilbert, D.J., Jenkins, N.A., Lanahan, A.A., Worley, P.F. (1995): Arc, growth factor and activity-regulated gene, encodes a novel cytoskeleton-associated protein that is enriched in neuronal dendrites. *Neuron, 14, 433-445.*

[12] Plath, N., Ohana, O., Dammermann, B., Errington, M.L., Schmitz, D., Gross, C., Mao, X., Engelsberg, A., Mahlke, C., Welz, H., Kobalz, U., Stawrakakis, A., Fernandez, E., Waltereit, R., Bick-Sander, A., Therstappen, E., Cooke, S.F., Blanquet, V., Wurst, W., Salmen, B., Bosl, M.R., Lipp, H-P., Grant, S.G.N., Bliss, T.V.P., Kuhl, D. (2006): Arc/Arg3.1 is essential for the consolidation of synaptic plasticity and memories. *Neuron, 52, 437-444.*

[13] Ito, D., Komatsu, T., Gohara, K. (2013): Measurement of saturation processes in glutamatergic and GABAergic synapse densities during long-term development of cultured rat cortical networks. *Brain Res., 1534, 22-32.*

[14] Ito, D., Tamate, H., Nagayama, M., Uchida, T., Kudoh, S.N., Gohara, K. (2010): Minimum neuron density for synchronized bursts in a rat cortical culture on multi-electrode arrays. *Neuroscience, 171, 50-61.*

[15] Nomura, M., Ito, D., Tamate, H., Gohara, K., Aoyagi, T. (2009): Estimation of functional connectivity that causes burst-like population activities. *Forma, 24, 11-16.*

[16] Yamaguchi, M., Ikeda, K., Suzuki, M., Kiyohara, A., Kudoh, S.N., Shimizu, K., Taira, T., Ito, D., Uchida, T., Gohara, K. (2011): Cell patterning using a template of microstructured organosilane layer fabricated by vacuum ultraviolet light lithography. *Langmuir, 27, 12521-12532.*

[17] Uchida, T., Suzuki, S., Hirano, Y., Ito, D., Nagayama, M., Gohara, K. (2012): Xenon-induced inhibition of synchronized bursts in a rat cortical neuronal network. *Neuroscience, 214, 149-158.*

[18] Suzuki, M., Ikeda, K., Yamaguchi, M., Kudoh, S.N., Yokoyama, K., Satoh, R., Ito, D., Nagayama, M., Uchida, T., Gohara, K. (2013): Neuronal cell patterning on a multi-electrode array for a network analysis platform. *Biomaterials, 34, 5210-5217.*

Functional Connectivity Estimate from Spontaneous and Stimulus Evoked Activities in Dissociated Cultured Neurons on a High-Density CMOS Microelectrode Array

Takeshi Mita[1], Douglas J. Bakkum[2], Urs Frey[3], Andreas Hierlemann[2], Ryohei Kanzaki[1], Hirokazu Takahashi[1*]

1 The University of Tokyo, Tokyo, Japan
2 ETH Zurich, Basel, Switzerland
3 RIKEN Quantitative Biology Center, Kobe, Japan
* Corresponding author. E-mail address: takahashi@i.u-tokyo.ac.jp

Abstract
Functional connectivity of a neural circuit is commonly characterized through a statistical analysis of ongoing spontaneous activity. However, little attention has been paid to the accuracy of connectivity estimations. In the present study, in primary dissociated cultures of neurons grown over a high-density CMOS microelectrode array, we compared functional connectivity patterns derived from spontaneous activity to those from stimulus-evoked activity. By single-axon stimulation, a single neuron was directly evoked and a number of post-synaptic neuronal activations could be identified. We showed that the conditional firing probability (CFP), derived from spontaneous activity, overestimated connection strengths by a factor of 10 as compared to the CFP estimates from stimulus-evoked activity. Furthermore, tetanic-stimulus-induced plasticity in CFP exhibited a consistent trend only in the estimates from stimulus-evoked activity, but not in those from spontaneous activity. These results may have implications for improved methods to estimate functional connectivity.

1 Background / Aims

Correlation-based analyses have been commonly used to estimate functional connectivity from spatio-temporal patterns of spontaneous activity. However, when bursts are dominant, as is often the case in a dissociated neuronal culture, it would be difficult to adequately estimate connectivity between pairs of neurons.

To overcome this difficulty, we attempted to characterize stimulus-evoked activity patterns upon single-axon activation. We tested whether functional connectivity patterns derived from spontaneous activity differed from those derived from stimulus-evoked activity. Additionally, we tested whether tetanic-stimulus-induced plasticity in connectivity patterns depended on estimation methods.

2 Methods / Statistics

Dissociated cells from E18 rat cortex were plated on high-density CMOS microelectrode arrays [1] with 11,011 electrodes in a 2.0×1.75 mm^2 area. The numbers of cells seeded on chip #1, #2 and #3 were 20,000, 43,000 and 34,000; the cells were cultured for 41, 12, and 41 days in vitro.

Action potentials from putative cell bodies were extracted and characterized. An adequate stimulation electrode was selected such that an arbitrary single neuron was directly activated through axonal microstimulation (Fig. 1) [2].

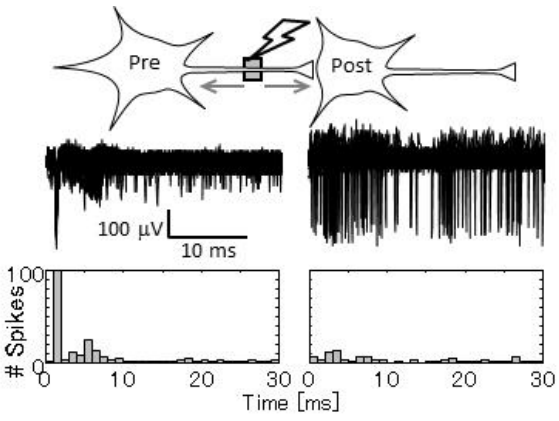

Fig. 1. Directly evoked spikes and synaptically evoked spikes. Top: Schematic of neurons and stimulation electrode (gray box). Middle: Directly evoked spikes and synaptically evoked spikes; traces for 100 trials were overlaid. Bottom: Histograms of evoked spikes

Conditional firing probability (CFP) [3] is a probability distribution of time delays of spikes of a neuron with respect to spikes of another neuron (Fig. 2). The difference between CFP at the first bin and the mean firing rate, δCFP, was used in the analyses. Tetanic-stimulation-induced plasticity in δCFP was defined as ΔCFP. The numbers of pairs analyzed were 53, 56 and 18 for chip #1, #2 and #3.

Spontaneous activity was recorded for 30 minutes, and stimulus evoked activity was recorded 100 times every 3 seconds. For tetanic stimulation, sets of 10 pulses at 20-Hz were delivered 20 times in total with 5-sec intervals at the stimulation electrode [4].

3 Results

Figure 3(A) compares δCFP of spontaneous activity (spontaneous δCFP) to δCFP of stimulus-evoked activity (stimulus-evoked δCFP), showing that spontaneous δCFP is not always highly correlated to stimulus-evoked δCFP (Spearman's rank correlation coefficient: chip #1, $r_s = 0.083$, $p = 0.55$; chip #2, $r_s = 0.40$, $p = 0.0025$; chip #3, $r_s = 0.55$, $p = 0.018$). Additionally, spontaneous δCFP was larger than stimulus-evoked δCFP by a factor of 10.

Figure 3(B) shows tetanic-stimulation-induced plasticity in stimulus-evoked δCFP, i.e., stimulus-evoked ΔCFP. There was a trend that pre-tetanus δCFP were significantly correlated to ΔCFP (chip #1 and #2 $r_s = -0.61$, $p < 0.001$; chip #3, $r_s = -0.64$, $p < 0.005$), suggesting that strong connectivity weakened after tetanic stimulation, and vice versa. On the other hand, as shown in Fig. 3(C), such a trend was not observed in stimulus-evoked δCFP and ΔCFP (chip #1, $r_s = -0.17$, $p = 0.23$; chip #2, $r_s = -0.33$, $p = 0.013$; chip #3, $r_s = -0.29$, $p < 0.24$).

4 Conclusion/Summary

We demonstrated that spontaneous δCFP is not always highly correlated to stimulus-evoked δCFP. Spontaneous δCFP is overestimated as compared to stimulus-evoked δCFP (Fig. 3A). This discrepancy is likely caused by the presence of bursts in spontaneous activity.

Second, we demonstrated that, following axonal tetanic stimulation, depression was observed in strong connections, while potentiation was observed in weak connections (Fig. 3B). This trend was not observed in spontaneous δCFP (Fig. 3C), possibly because of inadequate estimates of connectivity.

Our results may suggest that tetanic stimulation makes the post-synaptic connections more homogeneous. Further experiments are required to confirm the results.

Acknowledgement

This work was partially supported by KAKENHI (26630089, 23680050) and Denso Corp. (Kariya, Japan).

References

[1] Frey, U. et al. (2010): Switch-matrix-based high-density microelectrode array in CMOS technology. *IEEE J. Solid-State Circuits, 45, 2, 467–482*

[2] Bakkum, D.J. et al. (2013): Tracking axonal action potential propagation on a high-density microelectrode array across hundreds of sites. *Nature Comm, 4, Art no 2181*.

[3] le Feber, J. et al. (2007): Conditional firing probabilities in cultured neuronal networks: a stable underlying structure in widely varying spontaneous activity patterns. *J. Neural Eng., 4, 2, 54–67*

[4] Jimbo, Y. et al. (1999): Simultaneous Induction of Pathway-Specific Potentiation and Depression in Networks of Cortical Neurons. *Biophysical Journal, 76, 2, 670–678*

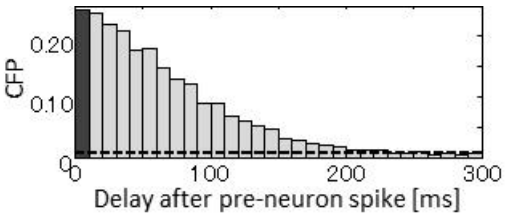

Fig. 2. Conditional firing probability (CFP). Dotted line represents the mean firing rate. The darker bar is the first bin used in the analysis.

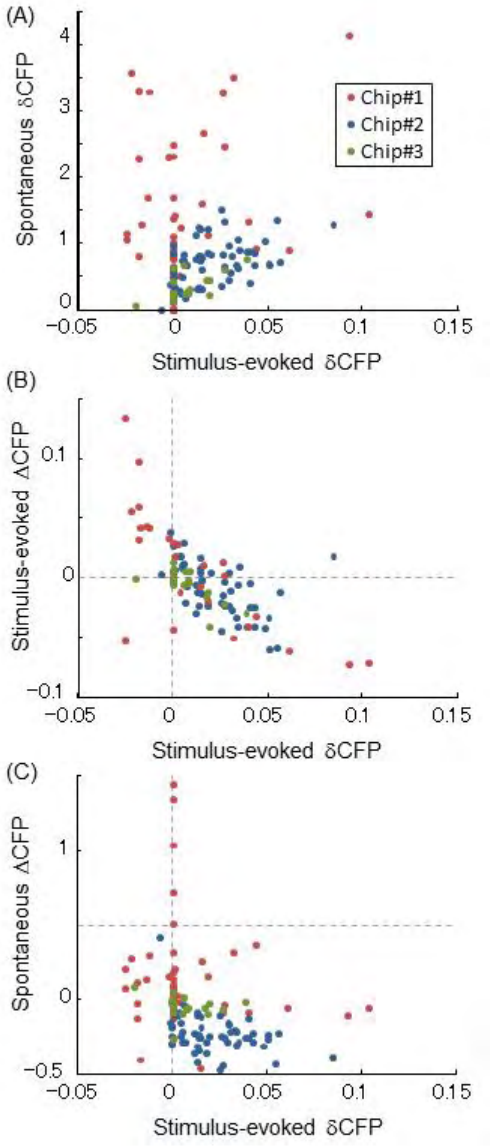

Fig. 3. (A) Spontaneous δCFP and stimulus-evoked δCFP. (B) Tetanic-stimulation-induced plasticity (ΔCFP) of stimulus-evoked δCFP. (C) ΔCFP of spontaneous δCFP. Colors indicate a test sample: red, chip #1; blue, chip #2; green, chip #3.

Frequency Multiplications Accompanied by Sudden Synchrony Leaps and Ultrafast Neuronal Plasticity

Hagar Marmari[1*], Roni Vardi[1*], Amir Goldental[2] and Ido Kanter[1,2+]

1 Gonda Interdisciplinary Brain Research Center and the Goodman Faculty of Life Sciences, Bar-Ilan University, Ramat-Gan, Israel
2 Department of Physics, Bar-Ilan University, Ramat-Gan, Israel
* These authors contributed equally to this work
+ Corresponding author. E-mail address: ido.kanter@biu.ac.il

Abstract
A classical view of neural coding relies on the underlying mechanism for temporal firing synchrony among functional groups of neurons; however, the underlying mechanism remains an enigma. Here we experimentally demonstrate a mechanism where time-lags among neuronal spikes leap from tens of milliseconds to nearly zero-lag synchrony. This mechanism also allows for sudden leaps out of synchrony, hence forming short epochs of synchrony. The underlying biological mechanisms are the unavoidable increase of the neuronal response latency to ongoing stimulations and temporal or spatial summation. These sudden leaps in and out of synchrony may be accompanied by multiplications of the neuronal firing frequency, functioning as reliable information-bearing indicators, which may bridge between the two principal neuronal coding paradigms. In addition, frequency multiplications alone result in sudden leaps in the neuronal response latency, which demonstrate a new form of ultrafast neuronal plasticity.

1 Introduction

One of the major challenges of modern neuroscience is to elucidate the brain mechanisms that underlie firing synchrony among neurons. Such spike correlations with differing degrees of temporal precision have been observed in various sensory cortical areas, in particular in the visual [1, 2], auditory [3, 4], somatosensory [4], and frontal [5] areas. Several mechanisms have been suggested, including the slow and limited increase in neuronal response latency per evoked spike [6]. On a neuronal circuit level its accumulative effect serves as a non-uniform gradual stretching of the effective neuronal circuit delay loops. Consequently, small mismatches of only few milliseconds among firing times of neurons can vanish in a very slow gradual process consisting of hundreds of evoked spikes per neuron [7, 8].

The phenomenon of sudden leaps from firing mismatches of several tens of milliseconds to nearly zero-lag synchronization (ZLS) is counterintuitive. Since the dynamical variations in neuronal features, e.g., the increase in neuronal response latencies per evoked spike, are extremely small, one might expect only very slow variations in firing timings. Moreover, relative changes among firing times of neurons require dynamic relaxation of the entire neuronal circuit to achieve synchronization. Hence, sudden leaps, in and out of synchrony, seem unexpected.

In the present study, based on [8, 9], we propose an experimentally corroborated mechanism allowing leaps in and out of synchrony. We demonstrate that the underlying biological mechanism to sudden leaps in and out of synchrony is the unavoidable increase of the neuronal response latency to ongoing stimulations [6, 10-14], which imposes a non-uniform stretching of the neuronal circuit delay loops. In addition we demonstrate ultrafast neuronal plasticity, sudden leaps in the response latency in response to sudden frequency changes.

2 Methods

2.1 Culture Preparation, Measurements and Stimulation, Cell Selection and Data Analysis

As described in previous publications [7-9, 14].

2.2 Stimulation Control

A node response was defined as a spike occurring within a typical time window of 2–10 ms following the electrical stimulation [15]. The activity of all source and target electrodes was collected, and entailed stimuli were delivered in accordance to the circuit connectivity.

Conditioned stimulations were enforced on the circuit neurons embedded within a large-scale network of cortical cells in vitro, according to the circuit connectivity. Initially, each delay was defined as the expected time between the evoked spikes of two linked neurons; e.g., conditioned to a spike recorded in the target electrode assigned to neuron A, a spike will be detected in the target electrode of neuron B after τ_{AB} ms. For this end, conditioned to a spike recorded in the target electrode of neuron A, a stimulus will be applied after τ_{AB}-$L_B(0)$ ms to the source elec-

trode of neuron B, where $L_B(0)$ is the initial response latency of neuron B.

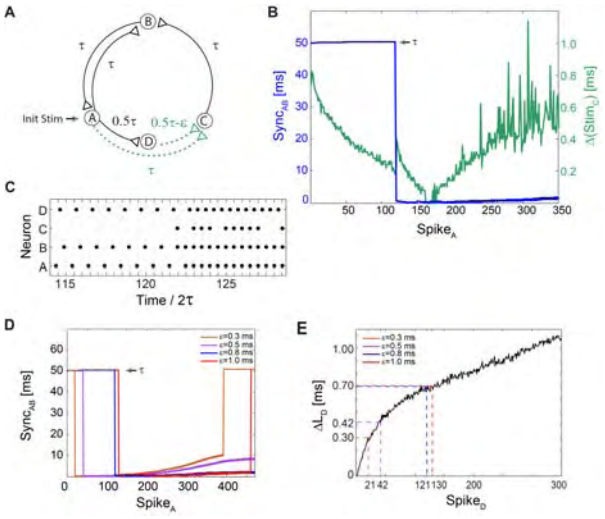

Fig. 1. (A) Schematic of a neuronal circuit consisting of four neurons and weak/strong stimulations represented by dashed/full lines. An initial stimulation is given to neuron A. (B) $\Delta(Stim_C)$ as a function of the spikes of neuron A ($Spike_A$). $\Delta(Stim_C)$ is initially set to $\varepsilon\approx0.8$ ms (green) with $\tau=50$ ms and $T_{TS}\approx0.23$. $Sync_{AB}$ (blue) indicates a sudden leap from $\tau=50$ ms to nearly ZLS. (C) Spike trains of the four neurons. A sudden leap to $Sync_{AB}\approx0$ occurs at time/2τ=122.5 ($Spike_A$=121) immediately following a single evoked spike of neuron C. It is accompanied by a doubled firing frequency, from ~10 Hz to ~20 Hz. $Sync_{AB}\approx0$ is robust to response failures of neuron C, e.g. time/2τ=124.5. (D) $Sync_{AB}$ as a function of $Spike_A$, for various ε, where the data for ε=0.8 (blue) is the same as in (B) and (C). The number of spikes to a leap to synchrony increases with ε. (E) ΔL_D for repeated stimulations at 10 Hz. Adapted from [8].

In cases where missed evoked spikes caused a termination of the neuronal circuit activity, stimulation was given to neuron A after a period of 100 ms, to restart the circuit's activity.

Strong stimulations, (−800 mV, 200 μs), resulting in a reliable neural response, were given to all circuit neurons excluding neuron C (Fig. 1) and E (Fig. 2). Weak stimulations (Fig. 1: −450 mV, 40 μs. Fig. 2: −700 mV, 60 μs) were given to neuron C (Fig. 1) or E (Fig. 2), so that an evoked spike is expected only if the time-lag between two consecutive weak stimulations is short enough. In cases where the time-lag between two consecutive stimulations was shorter than 20 μs (from the end of the first stimulation to the beginning of the consecutive one), a unified strong stimulation was applied, to overcome technical limitations. The weak stimulations were defined for each neuron separately, due to differences in their threshold.

T_{TS} (TS stands for temporal summation) is the maximal time-lag between two weak stimulations which typically results in an evoked spike. This quantity was empirically estimated by gradually changing the time-lag between two weak stimulations, and found to differ between neurons.

3 Results

3.1 Leap to Synchrony Accompanied by a Doubled Firing Frequency

We first demonstrate leaps to synchrony using a neuronal circuit consisting of four neurons and conditioned stimulations divided into weak/strong stimulations (Fig. 1A). All delays (denoted on connecting lines between neurons in Fig. 1A) were selected to initially include the response latency of the target neuron (see Methods). For τ=50 ms, neurons A and B initially fire alternately, in and out of phase, at a frequency of ~10 Hz (Fig. 1B). Neuron D fires ~τ/2 ms laggard to neuron A (Fig. 1C) and the time-gap between two weak stimulations arriving at neuron C, $\Delta(Stim_C)$, is initially ε (Fig. 1A,B). The experimentally estimated maximal time-gap between stimulations of neuron C which generates an evoked spike (temporal summation) is denoted by T_{TS}, thus for $\Delta(Stim_C) > T_{TS}\approx0.24$ ms neuron C typically does not fire. As a result of the increase in the response latency of neuron D, $\Delta(Stim_C)$ is reduced (green line, Fig. 1B) sufficiently so that neuron C starts firing [$\Delta(Stim_C)\leq T_{TS}$] (Fig. 1C). The circuit now consists of two delay loops, ~2τ (A-B-A) and ~3τ (A-C-B-A). Since the greatest common divisor (GCD) of the circuit delay loops is GCD(2,3)=1, ZLS between neurons A and B is theoretically expected [16] after a very short transient, τ (Fig. 1C). This phenomenon is quantitatively measured by the time-lag between spikes of neurons A and B, $Sync_{AB}$. The emergence of ZLS is clearly demonstrated by the leap to $Sync_{AB}\approx0$ ms (blue line, Fig. 1B), which is accompanied by a sudden frequency multiplication from ~10 to ~20 Hz (Fig. 1C). Note that the sudden multiplication in frequency, by itself, shortens $Sync_{AB}$ from 100 to 50 ms, however, it cannot lead to ZLS. The sudden emergence of $Sync_{AB}\approx0$ ms requires only a single firing of neuron C, and is then maintained by the mutual firing of neurons A and B, independently of the firing of neuron C (Fig. 1C). For a given T_{TS}, the number of evoked spikes of neuron D until the leap to synchrony, n, increases with ε (Fig. 1D). Quantitatively, using the experimental response latency profile of neuron D, L_D, one can find n fulfilling the equality:

$$\Delta L_D(n)\approx\varepsilon-T_{TS} \qquad (1)$$

where $\Delta L_D(n)$ stands for the increase in response latency of neuron D after n evoked spikes (Fig. 1E). Note that neuron D is laggard to neuron A, thus the number of evoked spikes of neuron A until the leap to synchrony increases with ε as well, in accordance with Equation (1) (Fig. 1D). Since T_{TS} varies between neurons and even within the same neuron over different trials, deviations from this equation are expected (e.g., ΔL_D for ε=0.8 ms and ε=1 ms are almost the same, Fig. 1D,E). A slow gradual increase in $Sync_{AB}$ after a leap to synchrony (Fig. 1D) is theoretically attributed to the difference in the increase of neuronal response latencies $|\Delta L_A(n)-\Delta L_B(n)|$ and the leap out of synchrony (Fig. 1D) is a consequence of a response failure of neurons A and/or B.

Similar results were observed for a different circuit, demonstrating a jump to synchrony accompanied by tripled firing frequency (not shown).

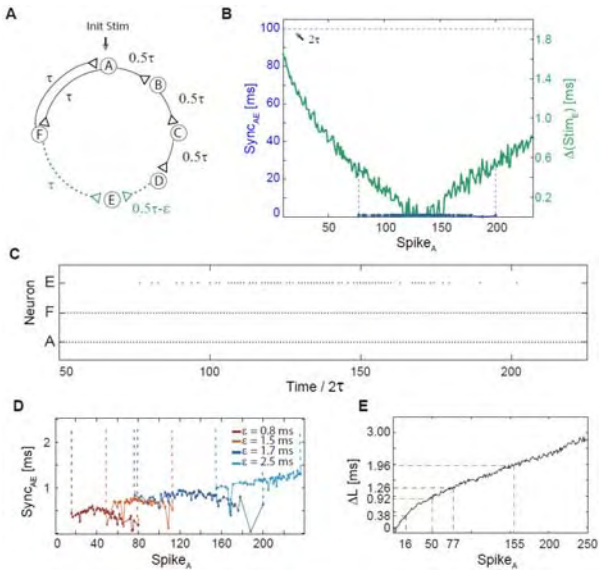

Fig. 2 (A) Schematic of a neuronal circuit consisting of six neurons and weak/strong stimulations represented by dashed/full lines. (B) Experimental measurements of $\Delta(Stim_E)$, similar to $\Delta(Stim_C)$ in Fig. 1B, with $\varepsilon \approx 1.7$ ms, $\tau=50$ ms and $T_{TS} \approx 0.5$ ms. The time delay between neurons A and E, ~2τ, is denoted by the dashed horizontal black line. The firing region of neuron E (blue dots), which is at nearly ZLS with the firing of neuron A, $Sync_{AE} \approx 0$, starts at $Spike_A=77$. The temporary firing of E terminates after $Spike_A \approx 200$. (C) Spike trains of neurons A, F and E, indicating a steady firing frequency (~10 Hz) of the neuronal circuit independent of the firing of neuron E, where an epoch of synchrony, $Sync_{AE} \approx 0$, begins at time/2τ=77. (D) The number of spikes prior to the firing of neuron E increases with ε. The mild increase in the firing mismatch, $Sync_{AE}$, is attributed to the additional increase by ε of the initial 2τ delay loop. The data for ε=1.7 ms (blue) is the same as in (B) and (C). (E) The number of spikes per neuron (e.g. $Spike_A$) until the leap to synchrony increases with ε. Adapted from [8].

3.2 Epochs of Synchrony not Accompanied by a Change in Frequency

A mechanism to leap out of synchrony as well as the interrelation between the sudden leap to synchrony and the firing frequency can be demonstrated by a circuit (Fig. 2A) consisting solely of a 2τ-delay loop, hence neurons A and F fire alternately in ~τ ms time-lags. Nevertheless, neuron A affects neuron E by weak stimulations arriving from two comparable initial delay routes; ~2τ ms (A-F-E) and ~2τ −ε ms (A-B-C-D-E) (Fig. 2A). Initially, neuron E does not fire since $\varepsilon \approx 1.7$ ms > $T_{TS} \approx 0.5$ ms. Since the overall increase in the neuronal response latency of a chain is accumulative, proportional to the number of neurons it comprises [7], $\Delta(Stim_E)$ gradually decreases below T_{TS} (Fig. 2B) and neuron E suddenly starts to fire. Consequently, since neuron A fires every ~2τ ms and neuron E fires ~2τ ms laggard to A, $Sync_{AE} \approx 0$ (Fig. 2B,C). As $\Delta(Stim_E)$ decreases, the response of neuron E becomes more reliable (Fig. 2B,C) and a leap out of synchrony is observed when $\Delta(Stim_E)$ again exceeds ~T_{TS} (Fig. 2B). Since neuron E's firing does not close a new neuronal loop, the leaps in and out of synchrony do not affect the firing frequency of the neuronal circuit (Fig. 2C). The number of spikes to synchrony increases with ε as well as the time-gap between neurons during synchronization, $Sync_{AE}$ (Fig. 2D,E).

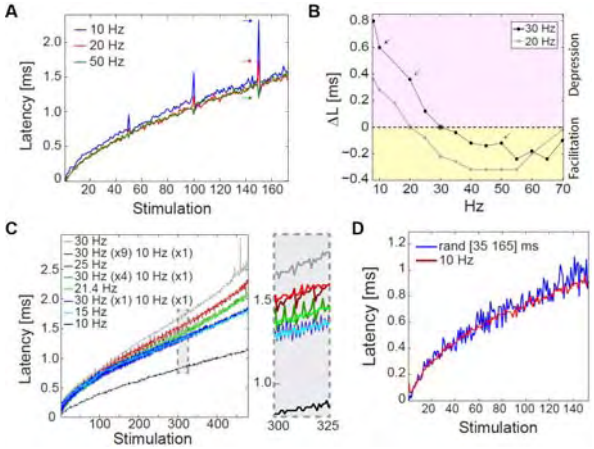

Fig. 3. (A) Experimental measurements of momentary changes in the neuronal response latency under stimulation at 30 Hz, where stimulations 50, 100, 150 were given at 10, 20 and 50 Hz. (B) A single neuron was stimulated at a frequency of 20 Hz (gray and 30 Hz (black), where at stimulation 150 a different frequency in the range of [8, 70] Hz was given, resulting in a latency leap ΔL=L(150)-L(149). (C) The neuronal response latency under stimulation at 10 Hz (black), 30 Hz (gray) and at 30 Hz where the frequency changed to 10 Hz every m=2 (dark blue), 5 (dark green), 10 (dark red) stimulations, and respectively at periodic stimulations 15 (light blue), 21.4 (light) and 25 (light red) Hz. The right panel shows a zoom-in of the gray area. (D) The neuronal response latency under stimulation at 10 Hz (red) and at random time-lags between stimulations in the range of [35, 165] ms (blue). Adapted from [9].

3.3 Firing Frequency Leap Accompanied by Facilitation and Depression (FAD)

A leap in the neuronal response latency appears when a leap to synchrony is accompanied by a change in frequency ($Spike_A=121$, Fig. 1B), however this latency leap does not appear when a leap to synchrony is not accompanied by a change in frequency ($Spike_A=77$, Fig. 2B). This phenomenon was replicated various times, always during a sudden change in frequency, regardless of the state of synchrony, and thus demanded investigation.

For a momentary increase/decrease in the stimulation frequency, facilitation/depression is observed through the latency of the neuronal response to the misplaced stimulations (Fig. 3A). FAD is measured by the momentary latency leap corresponding to the sudden change in the stimulation frequency (Fig. 3A). Typically the amplitude of FAD increases with the momentary frequency change; however, at moderate stimulation rates the effect of facilitation diminishes and might vanish (Fig. 3B).

The amplitude of FAD significantly varies with the timing of the misplaced stimulation and among neurons. Nevertheless, we find a robust and systematic global feature governing depression for a given neuron under a complex stimulation pattern. The profile of the neuronal response latency under a complex

stimulation pattern follows the profile of the neuronal response latency under a fixed stimulation rate, with the same average time-lag between stimulations (Fig. 3C). For instance, the neuronal response latency under alternating stimulations at 10 Hz (100 ms) and 30 Hz (~33.3 ms) follows the response latency profile under a fixed stimulation rate where the time-lag between stimulations is ~66.7 ms, equivalent to a stimulation rate of 15 Hz, which differs from the average frequency, 20 Hz (Fig. 3C). This systematic global feature of a neuron functioning as a precise time-integrator was found to be applicable even for random stimulation patterns (Fig. 3D).

4 Discussion

We proposed a mechanism which enables the emergence of a sudden leap to synchrony together with or independent of a leap in the firing frequency. This mechanism results in leaps from firing mismatches of several dozens of milliseconds to nearly ZLS, and can be accompanied by a sudden frequency multiplication of the neuronal firing rate, which allows for ultrafast neuronal plasticity. These sudden changes occur on a time scale such that even one ISI is sufficient to detect the transition without accumulatively estimating the ISI distribution. These fast and robust indicators might be used as reliable information carriers of time-dependent brain activity.

The proposed mechanism also allows for the simultaneous emergence of sudden leaps in rate and temporal synchrony, hence bridging between these two major schools of thought in neuroscience [1-4]. This mechanism requires recurrent neuronal circuits, and synchrony appears even among neurons which do not share a common drive. Sub-threshold stimulations serve as a switch that momentarily closes or opens a loop in the neuronal circuit (similar to [7, 14]). The state of the switch changes a global quantity of the network, the GCD of the entire circuit's loops, which determines the state of synchrony. These demonstrated prototypical examples call for a theoretical examination of more structured scenarios, including multiple leaps in and out of synchrony. In addition, a more realistic biological environment has to be examined containing synaptic noise and adaptation.

Acknowledgement

We would like to thank Moshe Abeles, Evi Kopelowitz and Shoshana Guberman for stimulating discussions. Fruitful computational assistance by Yair Sahar and Alexander Kalmanovich, technical assistance by Hana Arnon are acknowledged.

References

[1] R. Eckhorn, R. Bauer, W. Jordan, M. Brosch, W. Kruse, M. Munk, and H. Reitboeck, Biological cybernetics **60**, 121 (1988).
[2] C. M. Gray, P. König, A. K. Engel, and W. Singer, Nature **338**, 334 (1989).
[3] M. Ahissar, E. Ahissar, H. Bergman, and E. Vaadia, J. Neurophysiol. **67**, 203 (1992).
[4] M. A. Nicolelis, L. A. Baccala, R. Lin, and J. K. Chapin, Science **268**, 1353 (1995).
[5] E. Vaadia, I. Haalman, M. Abeles, H. Bergman, Y. Prut, H. Slovin, and A. Aertsen, Nature **373**, 515 (1995).
[6] R. Vardi, R. Timor, S. Marom, M. Abeles, and I. Kanter, Phys. Rev. E **87**, 012724 (2013).
[7] R. Vardi, S. Guberman, A. Goldental, and I. Kanter, Europhys. Lett. **103**, 66001 (2013).
[8] R. Vardi, A. Goldental, S. Guberman, A. Kalmanovich, H. Marmari, and I. Kanter, Front. Neural Circuits **7** (2013).
[9] R. Vardi, H. Marmari, and I. Kanter, Phys. Rev. E **89**, 042712 (2014).
[10] G. Aston-Jones, M. Segal, and F. E. Bloom, Brain research **195**, 215 (1980).
[11] R. De Col, K. Messlinger, and R. W. Carr, J. Physiol. **586** (2008).
[12] A. Gal, D. Eytan, A. Wallach, M. Sandler, J. Schiller, and S. Marom, J. Neurosci. **30**, 16332 (2010).
[13] A. Gal and S. Marom, Phys. Rev. E **88**, 062717 (2013).
[14] A. Goldental, S. Guberman, R. Vardi, and I. Kanter, Front. Comput. Neurosci. **8** (2014).
[15] D. A. Wagenaar, J. Pine, and S. M. Potter, J. Neurosci. Methods **138**, 27 (2004).
[16] I. Kanter, E. Kopelowitz, R. Vardi, M. Zigzag, W. Kinzel, M. Abeles, and D. Cohen, EPL (Europhysics Letters) **93**, 66001 (2011).

Simultaneous Intra- and Extracellular Recordings using a Combined High-Density Microelectrode Array and Patch-Clamp System

David Jäckel[1], Jan Müller[1], Thomas L. Russell[1], Milos Radivojevic[1], Felix Franke[1], Urs Frey[2], Douglas J. Bakkum[1] and Andreas Hierlemann[1]

1 ETH Zurich, Department of Biosystems Science and Engineering, Basel, Switzerland
2 RIKEN Quantitative Biology Center, Kobe, Japan.
* Corresponding author. E-mail address: jaeckeld@bsse.ethz.ch

Abstract
High-density microelectrode arrays represent a powerful tool to record from and to stimulate large numbers of neurons simultaneously. In this work, we combine a high-density microelectrode array system with intracellular whole-cell patch-clamp recordings, and show how this system can be used for different applications.

1 Introduction

Emerging high-density microelectrode arrays (HD-MEAs), based on complementary metal oxide semiconductor (CMOS), provide large numbers of readout channels and high spatiotemporal resolution. HD-MEAs can be used to record from and/or to stimulate large numbers of neurons simultaneously. Usually, extracellular recordings are used to detect action potentials (APs) or local field potentials. The whole-cell patch-clamp technique, in contrast, reveals also sub-threshold neuronal signals, such as post-synaptic potentials (PSPs). Patch clamping is, however, a challenging technique and limited to a few cells patched simultaneously.

In this work, we combine a HD-MEA system with intracellular patch-clamp recordings, and present fundamental applications of this system. One application is to use membrane potential (MP) measurements as a control for extracellular recording to better understand the relation between intra- and HD extracellular data [1], or for evaluating spike sorting algorithms [2]. Additionally, by monitoring the MP while the patched neuron is stimulated with HD-MEA electrodes, effects of HD-MEA stimulation can be investigated in great detail, overcoming the difficulties of stimulation artifacts. Finally, by combining HD-MEA recording and stimulation of many neurons in a neuronal network with recording of the intracellular signal of a specific individual patched neuron within that network, the presented system allows for extracting detailed information about synaptic inputs to the patched neuron.

2 Methods

The experimental set-up includes an upright microscope (Leica DM6000B), the HD-MEA system previously described in [3] (3150 electrodes/mm^2) and a patch clamp set-up (Multiclamp 700B amplifier). The HD-MEA system was extended with four analog-to-digital conversion channels, which synchronously acquire and stream the patch clamp signals with the HD-MEA data.

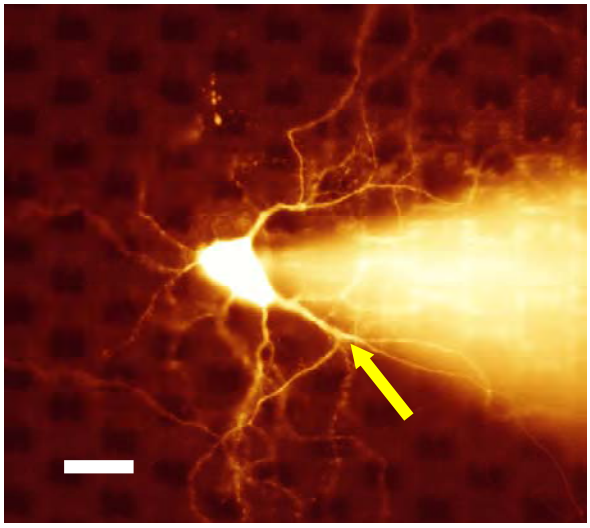

Fig. 1. Fluorescence image of a patched neuron on the HD-MEA. The cell is filled with a dye, and the MEA electrodes are visible as black squares. Scale bar: 20 µm

The microscope is mounted on a motorized XY stage (Scientifica UMS), allowing for precisely storing the microscope position for every acquired image. Custom image alignment software (MATLAB) enables the experimenter to load an image with the correct XY-coordinates respective to the HD-MEA immediately after acquisition. This feature is particularly important to select electrodes underneath the patched neuron for recording and stimulation.

Cortical neurons were dissociated and cultured on the HD-MEAs according to protocols described in [4]. The intracellular solution used for whole-cell patch clamping was mixed with a fluorescent dye (Alexa 594), and each neuron was imaged at the end of an experiment.

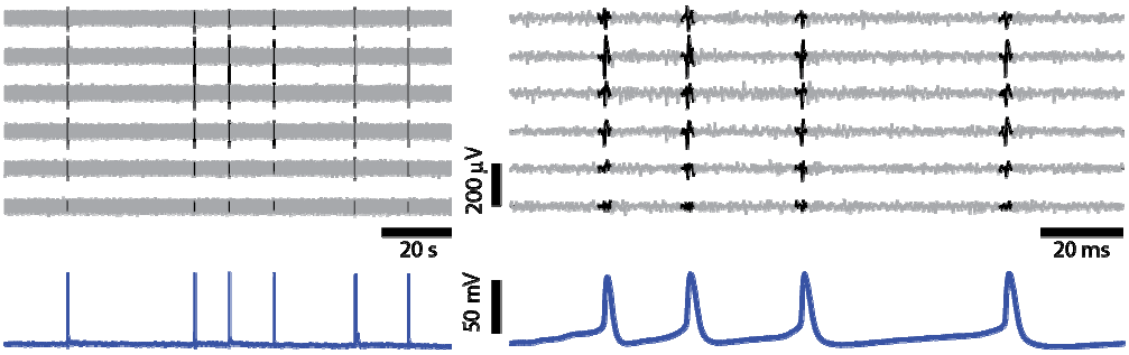

Fig. 2. Simultaneous extracellular (*top*, black traces indicate identified spikes) and intracellular (*bottom*) recordings of a spontaneously spiking neuron. *Left*: Two minutes of data with six bursts; *right*: close-up on one individual burst.

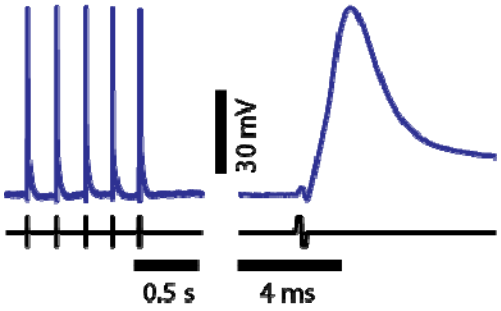

Fig. 3. APs (*top traces*) are evoked in the patched neuron of Fig.1 by applying voltage pulses of ± 300mV (*bottom traces*) at the electrode marked with a yellow arrow in Fig.1. *Left*: 5 sequentially evoked APs; *right*: close-up view of one AP.

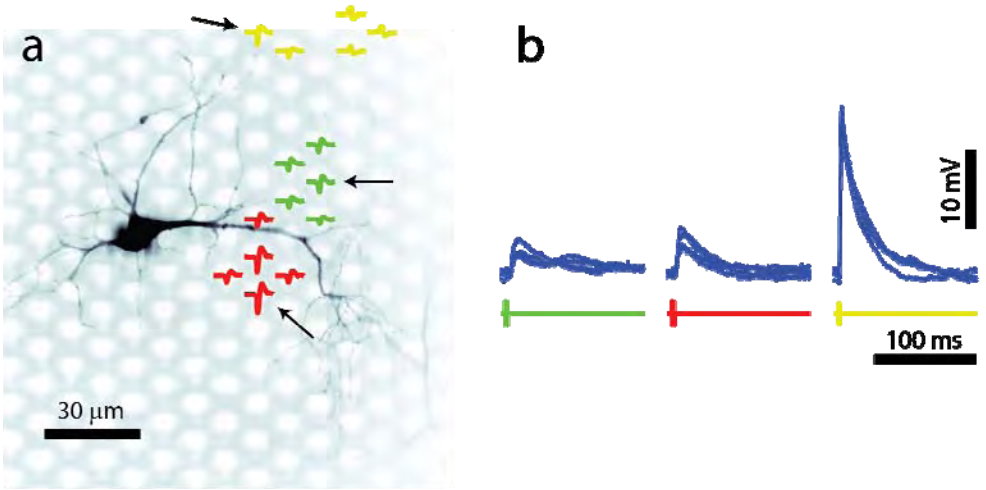

Fig. 4. Stimulating presynaptic neurons with the HD-MEA, while the postsynaptic membrane potential is measured. (a) Morphology (*black*) of patched (postsynaptic) neuron and spike-triggered average waveforms of three identified (presynaptic) neurons from HD-MEA recordings (*red, green and yellow*). The black arrows indicate the stimulation electrodes for the presynaptic neurons. b) PSPs recorded from the patched neuron, when each presynaptic neuron was stimulated four times with a biphasic voltage pulse (± 500mV); the coloured traces indicate the stimulus signals.

3 Results

We successfully patched cultured neurons on top of the HD-MEA (Fig.1). Spontaneous spiking activity was recorded with several electrodes close to the cell, while simultaneously acquiring the MP. Fig.2 shows how extracellular spiking events temporally match with the MP depolarizing phase.

We then monitored the MP of a neuron during extracellular stimulation with a HD-MEA electrode as shown in Fig.3. An AP was immediately initiated after each extracellular stimulus.

Finally, we measured PSPs in a patched neuron, generated by individual presynaptic input neurons. We stimulated electrodes, where significant spike amplitudes were previously recorded. Stimulating some electrodes (indicated by arrows in Fig.4) caused PSPs. The PSP amplitudes in Fig.4b suggest stable but relatively weak synaptic connections between the red, respectively the green and the patched neuron. The yellow neuron shows a much stronger PSP, which suggests a very strong synaptic connection to the patched neuron.

4 Discussion

We have shown different experiments that exploit the combination of intra- and extracellular recordings. Whereas the experiments in Fig. 2 and Fig. 3 use the MP recording mainly as a control measurement, the experiment shown in Fig. 4 optimally combines both techniques to extract additional information (i.e. synaptic strengths).

For a patched neuron, the presented system provides the possibility of precisely measuring the synaptic input strength of many presynaptic partners. At the same time, the temporally precise spiking activity of the presynaptic cells can be recorded and, if desired, manipulated by applying extracellular stimulation with the HD-MEA. Owing to all these features, the system represents a promising tool to study synaptic function and synaptic plasticity of neurons at unprecedented resolution in terms of presynaptic inputs.

Acknowledgements

We would like to thank Yan Sun for her contributions to the signal acquisition module and Alexander Stettler, Jörg Rothe, Marta Lewandowska and Ian Jones for their help with the experimental setup and cell culture preparations. Tamas Szkira and Pascal Pflimlin are expressly acknowledged for helping with the patch clamp experiments.

This work was supported by the Advanced ERC Grant “NeuroCMOS” under contract number AdG 267351. M. Radivojevic and D. J. Bakkum received funding support from the Swiss National Foundation through an Ambizione Grant (PZ00P3_132245).

References

[1] D. A. Henze, Z. Borhegyi, J. Csicsvari, A. Mamiya, K. D. Harris, and G. Buzsaki, “Intracellular Features Predicted by Extracellular Recordings in the Hippocampus In Vivo,” *J Neurophysiol*, vol. 84, no. 1, pp. 390–400, 2000.

[2] K. D. Harris, D. A. Henze, J. Csicsvari, H. Hirase, and G. Buzsáki, “Accuracy of tetrode spike separation as determined by simultaneous intracellular and extracellular measurements.,” *Journal of neurophysiology*, vol. 84, no. 1, pp. 401–14, Jul. 2000.

[3] U. Frey, J. Sedivy, F. Heer, R. Pedron, M. Ballini, J. Mueller, D. Bakkum, S. Hafizovic, F. D. Faraci, F. Greve, K.-U. Kirstein, and A. Hierlemann, “Switch-Matrix-Based High-Density Microelectrode Array in CMOS Technology,” *Solid-State Circuits, IEEE Journal of*, vol. 45, no. 2, pp. 467–482, 2010.

[4] D. J. Bakkum, U. Frey, M. Radivojevic, T. L. Russell, J. Müller, M. Fiscella, H. Takahashi, and A. Hierlemann, “Tracking axonal action potential propagation on a high-density microelectrode array across hundreds of sites.,” *Nature communications*, vol. 4, p. 2181, 2013.

An MEA-Based Model for Rapid Acceleration Injury to Neuronal Networks and Studies of Recovery

David C. Smith, Guenter W. Gross

Department of Biological Sciences, Center for Network Neuroscience
University of North Texas, Denton, TX 76203
* Corresponding author. -mail address: davidsmith14@my.unt.edu

Abstract
The complex pathology of TBI requires research on all levels: from studies of holistic brain injury to cellular and even synaptic disruption. In many cases, physical evidence does not exist, as standard CTI or MRI scans are not sensitive enough. Diffuse brain injury ranges from axonal damage after minor head injury to inflammatory responses and calpain-mediated cytoskeletal changes [1]. Although networks in vitro do not represent brain tissue in situ, the highly controlled environment and multifactorial readout provides quantitative injury data for establishing reliable damage thresholds, recovery profiles, and biochemical enhancement of recovery. Although the exact impact forces for specific responses may differ between in vitro and in situ, the recovery from cellular damage as well as the efficacy of potential interventions can be quantified in vitro and should be scalable to animal models.

1 Methods

Neuronal cell cultures were derived from frontal cortex tissue of mouse embryos (E 16) with standard procedures [1]. Culture ages at time of selection for experiments ranged from 20 to 70 days (mean 38). During recording, networks were maintained in a closed stainless steel chamber with a medium volume of 5 ml. The chamber was connected to a medium circulation system (total volume 35 ml) powered by a peristaltic pump at a flow rate of 0.4 ml/min. pH was maintained by a 10 ml/min stream of 10% CO2 in air in the medium supply flask [2]. Care was taken to eliminate all bubbles from the system.

The prototype ballistic pendulum system is shown in Fig. 1 and consists of a weighted striker arm and target pendulum holding the chamber and network. Disconnect time from amplifiers was usually 4 min. Because arm vibrations prevented the use of accelerometers, g-forces were estimated from the height reached by the target arm (h) caused by the peak kinetic energy upon impact (½ mv^2 = mgh, where v is the maximum velocity reached immediately after impact).

$V_{max} = [2gh]^{1/2}$ and $a = (V_{max} - Vo) / t_{max} - t_o$ t_{max} is considered the impact time, presently estimated to be 2 to 5 ms:

$$\mathbf{a = (2gh)^{1/2} / t}$$

For a 40 cm height and an impact interval of 2 ms, a = 143 g 's

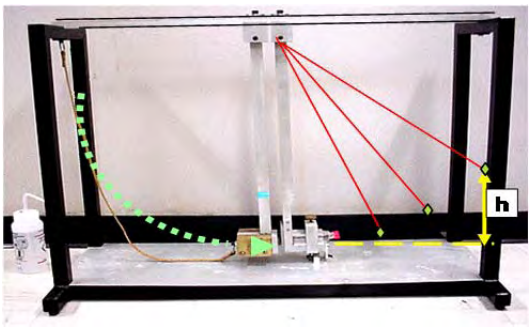

Fig. 1. Prototype ballistic pendulum apparatus Right arm: target with network in recording chamber; left arm striker.

2 Results

2.1 Single impacts

Single impacts at ~150 g reduce spontaneous activity for 10-20 min with a variable recovery time to within 10-15% of reference activity. Most networks have shown subsequent further loss of spike generation without loss of channels (Fig.2). This suggests adhesion and cell-electrode coupling are not compromised and that network spike generating mechanisms are affected.

EXP #	Phase 1 depression	Phase 2 % recov.	Time to max recov.
DS025	73%/23 min	90	160 min
DS027	72%/20 min	90	105 min
DS032	83%/11min	85	195 min
DS037	75%/20 min	92	200 min
DS038	71%/9 min	92	110 min

Table 1. Summary of Single 150 g Impact Data.

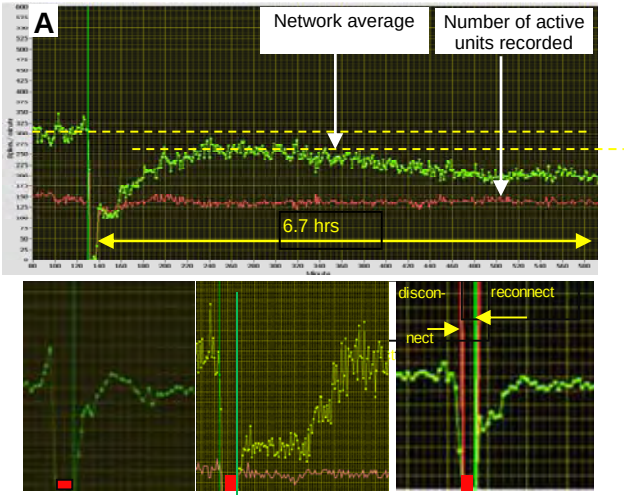

Fig. 2. Response profiles of single 150 g impacts from 4 different networks. Disconnect and reconnect dead time was generally 4 min (red squares).

2.2 Multiple impacts

The magnitude of activity suppression for multiple impacts at 100-150 g is a function of number of impacts and time between impacts. Presently, a period of sixty minutes between impacts produces a compounding response severity leading to more pronounced activity suppression. Figure 3 shows three successive impacts spaced by 85 and 65 minutes, respectively. Whereas response 1 and 2 are similar, the third response is comparatively massive. The insert to the figure shows a long-range (18 hrs) activity suppression despite a temporary recovery to 85% of baseline. The network was monitored for a total of 25 hrs following the third impact. Activity remained at 65 percent suppression with no spontaneous recovery.

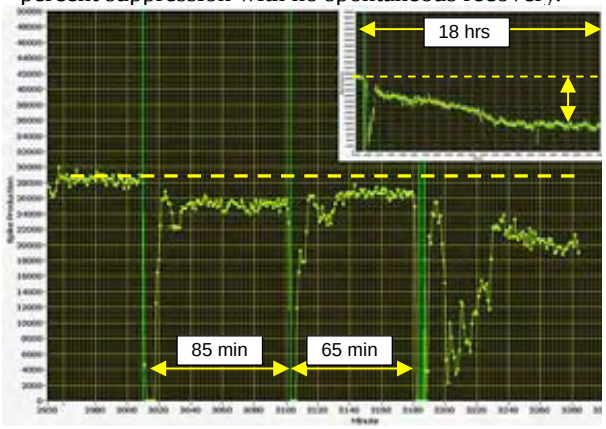

Fig. 3. Three successive impacts at approximately the same g-forces spaced by 85 and 65 min showing compounding damage after impact number 3. An 18- hour recording (insert) shows a gradual 65% decrease in activity with no recovery over a total monitoring period of 25 hrs.

2.3 System limitations

The present design causes minor MEA shifting relative to the stainless steel chamber and MEA breakage at higher g-forces. Shearing of chamber set screws has also been observed. Single impact cell death appears to require greater than 200 g's. In addition, pendulum arms have excessive vibration.

3. Discussion

Combining a ballistic pendulum with MEA technology allows quantitative comparisons of spontaneous activity before and within 4 min after rapid acceleration injury (RAI). With the present system, continual long term multichannel monitoring can be extended to more than 20 days, providing an efficient test bed for quantitative recovery analyses and pharmacological interventions. Single impact responses are consistent with in-vivo TBI studies on focal cortical compression in which the initial 20 minutes were characterized by activity depression [3].

Although g-forces are presently approximate, a clear difference can be observed between single and multiple impacts at the same magnitude. Rapid successive impacts are associated with greater activity suppression, a phenomenon also seen in vivo [4]. We anticipate that a reengineered system will allow higher g-forces for investigation of immediate cell death and quantitative exploration of direct impact injury to neurons and glia.

Acknowledgments

This research was made possible in part by UNT grant GA9365 and the Charles Bowen memorial endowment to the CNNS. David Smith was supported by the Howard Hughes Medical Institute. The authors thank Ahmet Ors for his dedicated MEA fabrication and Nicole Calderon for her volunteer effort in cell culture.

References

[1] Gross, G.W. and Pancrazio, J.P.P. (2007) Neuronal network biosensors. In: Smart biosensor technology (G.K. Knopf and A.S. Bassi, eds), Taylor and Francis Publishers, CRC Press. pp 177-201.

[2] Meyer, J.M., Wolf, B., and Gross, G.W. (2009) Magnetic stimulation and depression of mammalian networks in primary neuronal cell cultures. IEEE Biomedical Engineering. Vol 56, No.5, 1-12.

[3] Ding, MC., Wang, Q., Lo, EH., Stanley, GB. (2011) Cortical excitation and Inhibition following focal traumatic brain injury. J. Neurosci.31(40) doi : 10.1523/JNEUROSCI.3572-11.2011

[4] Giza C. C., Hovda D. A. (2001). The neurometabolic cascade of concussion. J. Athl. Train. 36, 228–235

Exploring the Role of Microtubule-Associated Protein Tau (Mapt) in Synaptic Plasticity

Torsten Bullmann[1,2 *], Tanja Treutlein[2], Jens T. Stieler[2], Max Holzer[2], Thomas Arendt[2], Urs Frey[1]

1 RIKEN Quantitative Biology Center, Kobe, Japan
2 Paul Flechsig Institute, Leipzig University, Leipzig, Germany
* Corresponding author. E-mail address: torsten.bullmann@riken.jp

Abstract
During hibernation transient tau phosphorylation is associated with reversible synapse regression, but the mechanism is largely unknown. Here we show that cooling of cell cultures induces a tau phosphorylation pattern similar as during hibernation. Therefore, we will combine high-density CMOS-based MEA (HDMEA) recordings, life imaging, and genetic methods to investigate synapse dynamics during reversible cooling and assess the role of tau. The HDMEA has the advantage of recording multi-units at high spatial resolution, which drastically improves accuracy of spike sorting used to obtain spike sequences of individual neurons.

1 Backround / Aims

Micro-electrode arrays (MEAs) are able to record from a large numbers of neurons simultaneously and stable over a long time. They have been used for studying synaptic plasticity as well as network connectivity. Recently, we proposed a hypothesis that phosphorylation of the microtubule associated protein tau (Mapt) regulates neuronal plasticity in hibernation and represents a “master switch”, regulating synaptic gain in neuronal networks [1]. Mapt has numerous Threonine and Serine residues which are highly phosphorylated in Alzheimer's disease (Fig. 1A), causing translocation of Mapt to sub-synaptic sites, synaptic impairment and cognitive decline long before formation of tau aggregates and neurodegeneration occurs. We previously observed a similar phosphorylation in hibernating animals, associated with synapse regression and other forms of structural plasticity, but remarkably, this process is reversible upon rewarming. This phosphorylation can be induced by hypothermia, hypo-metabolism, or hibernation-specific regulation of enzyme kinetics [2]. Using MEA recordings subjected to cooling [4] we will explore the role of Mapt phosphorylation in synaptic plasticity and network activity. As a prerequisite for these experiments, the pattern and dynamics of Mapt phosphorylation by cooling of cell cultures was investigated.

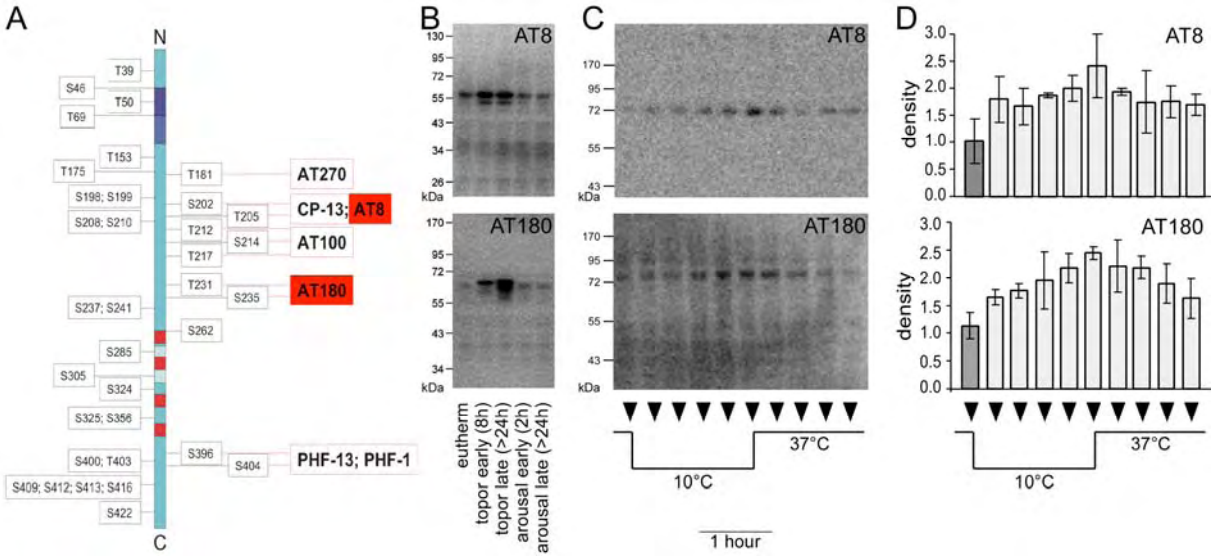

Fig. 1. Phosphorylation of Microtubule associated protein tau (Mapt) during cooling of cell cultures mimics the dynamics during hibernation. A. Mapt can be phosphorylated at several Threonine (pT) and Serine (pS) residues, particular relevant for Alzheimer’s disease are the epitopes formed by pS202/pT205 and pT231/pS235 which can be detected by the monoclonal antibodies AT8 and AT180, respectively [5]. – B. Transient phosphorylation at both epitopes during hibernation in hamsters [2]. – C. Fast phosphorylation and dephosphorylation at both epitopes during cooling of cell cultures expressing Mapt. – Time-course of Mapt phosphorylation. N=3 for each time point.

2 Methods / Statistics

Neuro2A cells (N2A, mouse neuroblastoma cell line) stable transfected with Mapt were plated in 6-well plates and cultured in Leibowitz L15 medium, which buffers pH in ambient air. Temperature was changed from 37°C to 10°C and back. Samples were taken every 20 minutes and phosphorylation of Mapt was assessed by western blots as previously described and compared with neocortex samples taken during hibernation cycle of Golden hamsters. Densitometry for the Alzheimer's disease related epitopes pS202/pT205 (AT8) and pT231/pS235 (AT180) show mean and s.e.m. for triplicates.

3 Results

Hypothermia leads to a sustained phosphorylation of Mapt on both pS202/pT205 and pT231/pS235 epitopes and upon rewarming returned to the basal levels present before cooling (Fig. 1C, D). This clearly shows that the ubiquitous Mapt kinases cdk5, GSK3beta, MAPK are sufficient for phosphorlyation and that this process is readily reversed by protein phosphatase PP2A. The tau phosphorylation pattern in hypothermia resembles that observed during torpor of hibernating hamsters (Fig. 1B), even though in vivo further kinase regulation occurs.

4 Conclusion / Summary

We could show that it is possible to mimic hibernation conditions in cell cultures by cooling. Now we use standard MEAs and high-density CMOS-based MEAs (HDMEA, Fig. 2A) [3] to record from neuronal cultures prepared from Mapt knockout and wild-type mice. The HDMEA allow the recording of spike trains from single neurons and multi-units and due to its high spatial resolution, drastically improves accuracy of spike sorting used to obtain individuals spike sequences. We aim to detect Synfire chains (Fig. 2B) and participation of individual neurons will be used to obtain a graph of neuronal connectivity (Fig. 2C) [6] to address the following questions:

• Is the functional connectivity preserved under hypothermia conditions similar to hibernation?

• What is the relationship between functional and morphological connectivity?

• What is the role of Mapt?

References

[1] Arendt T, Bullmann T (2013) Neuronal plasticity in hibernation and the proposed role of the microtubule-associated protein tau as a "master switch" regulating synaptic gain in neuronal networks. Am J Physiol Regul Integr Comp Physiol 305(5):R478-89.

[2] Bullmann T, Stieler J, Holzer M, Härtig W, Arendt T (2008) Hibernation, famine et hypothermie - Modeles pour la maladie d'Alzeimer. [Hibernation, Starvation and Hypothermia – Models for Alzheimer's Disease] Alzheimer Actualites. 196: 8-11.

[3] Frey U, Sedivy J, Heer F, Pedron R, Ballini M, Mueller J, Bakkum D, Hafizovic S, Faraci FD, Greve F, Kirstein KU, Hierlemann A (2010) Switch-matrix-based High-density Microelectrode Array in CMOS Technology. IEEE Journal of Solid-State Circuits 45(2): 467–482.

[4] Rubinsky L, Raichman N, Lavee J, Frenk H, Ben-Jacob E (2008) Spatio-temporal motifs 'remembered' in neuronal networks following profound hypothermia. Neural Netw 21(9):1232-7.

[5] Stieler JT, Bullmann T, Kohl F, Tøien Ø, Brückner MK, Härtig W, Barnes BM, Arendt T (2011) The physiological link between metabolic rate depression and tau phosphorylation in mammalian hibernation. PLoS One. 2011 Jan 18;6(1):e14530.

[6] Sun JJ, Kilb W, Luhmann HJ (2010) Self-organization of repetitive spike patterns in developing neuronal networks in vitro. Eur J Neurosci 32(8):1289-99.

[7] Hierlemann A, Frey U, Hafizovic S, Heer F. (2011) Growing Cells Atop Microelectronic Chips: Interfacing Electrogenic Cells In Vitro With CMOS-Based Microelectrode Arrays. Proc IEEE 99(2):252–284.

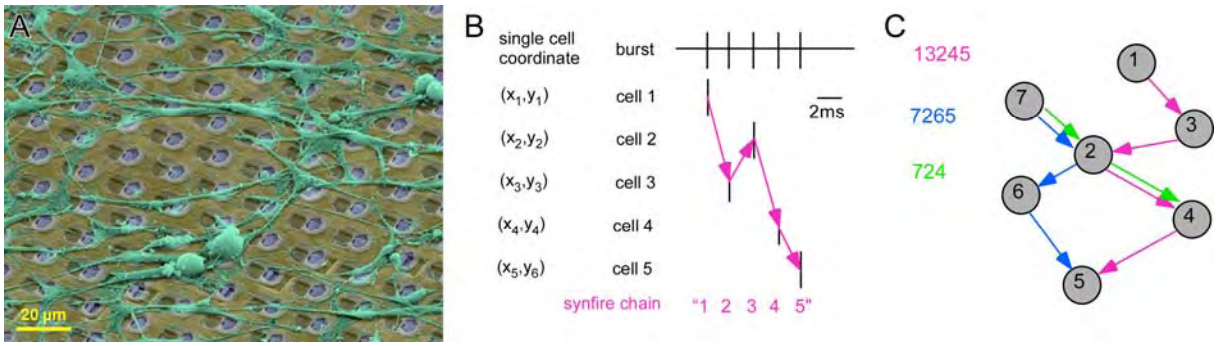

Fig. 2. Proposed experiments for the analysis of synaptic plasticity in culture. A. Colored scanning electron microscope picture of cultured dorsal root ganglion neurons on high-density CMOS- based multi-electrode array [7]. – B. A synfire chain (12345) encompassing individual neurons identified by their recording location during a burst. – C. Because individual neurons can participate on different synfire chains (e.g. also 7265 and 724) each synfire chain constitutes a path on the graph representing the functional neural network. The functional network structure can thereby inferred from the sampled synfire chains. Furthermore, individual neurons can be characterized as hubs participating in many synfire chains (2), starting (1,7) or stopping (5) synfire chains [6].

3D Finite Element Modeling of Single Neurons and the Microelectrode Array Microenvironment

Douglas J. Bakkum[1*], Milos Radivojevic[1], David Jäckel[1], Felix Franke[1], Thomas L. Russell[1], Urs Frey[2], Hirokazu Takahashi[3], Andreas Hierlemann[1]

1 ETH Zurich, Basel, Switzerland
2 RIKEN Quantitative Biology Center, Kobe, Japan
3 The University of Tokyo, Tokyo, Japan
* Corresponding author. E-mail address: douglas.bakkum@bsse.ethz.ch

Abstract
How action potentials within a neuron give rise to the extracellular voltage signal has been a subject of theory for many decades, but supporting experimental evidence has so far been sparse. Acquiring high spatial resolution experimental data in combination with computational modeling of the (bio)physics governing neuron-electrode interfaces would help to improve our interpretations of extracellular electrophysiology. In preliminary work, we used a high-density microelectrode array (MEA) to record the extracellular signals of single neurons at hundreds of electrode sites, conducted live-cell imaging in order to accurately model the neuron's geometry, and attempted to reproduce the experimental data using the COMSOL Multiphysics modeling tool.

1 Background / Aims

(Copied from the Abstract.) How action potentials within a neuron give rise to the extracellular voltage signal has been a subject of theory for many decades, but supporting experimental evidence has so far been sparse. Acquiring high spatial resolution experimental data in combination with computational modeling of the (bio)physics governing neuron-electrode interfaces would help to improve our interpretations of extracellular electrophysiology. In preliminary work, we used a high-density microelectrode array (MEA) to record the extracellular signals of single neurons at hundreds of electrode sites, conducted live-cell imaging in order to accurately model the neuron's geometry, and attempted to reproduce the experimental data using the COMSOL Multiphysics modeling tool.

2 Methods / Statistics

Cortical networks were grown for many weeks over high-density CMOS-based MEAs (11,011 electrodes; 17.8 μm pitch), from which 126 electrodes could be read out (or stimulated) at one time. Cells from embryonic Wistar rat cortices were grown in DMEM containing 10% serum. For culturing and MEA details, see [1] and [2], respectively. For live-cell imaging, cells were sparsely transfected with DsRedExpress (Addgene plasmid 22909 from the Callaway lab) using Lipofectamine 2000. Positive-first biphasic voltage pulses at distal axon locations induced antidromic action potentials.

Modeling was performed using COMSOL Multiphysics version 4.3 using the default time-dependent solver and the 'electric currents' physics node (i.e. Maxwell's equations). Intracellular and extracellular spaces had uniform electrical conductivity (1.4 S/m) and relative permittivity (80). The cell membrane was modeled using the 'contact impedance' node (i.e. thin-film approximation) with a membrane capacitance equal to 1 μF/cm^2. Hodgkin-Huxley equations were implemented in a 'boundary ODE' node in order to compute membrane conductivity. Applying a normal current density to the far end of the axon induced antidromic action potentials.

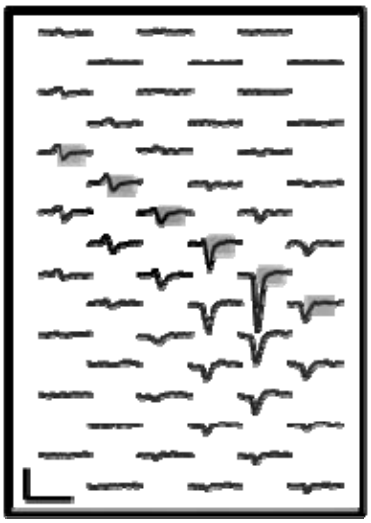

Fig. 1. Experimental data from a live-imaged neuron expressing red fluorescent protein. The neuron's (gray background image) axon extends towards the bottom right corner. Voltage traces recorded from neighboring electrodes are averages from 10 spontaneous spikes. The diagonal gray boxes show the dimensions of a subset of these electrodes. Scale bars: 2 ms and 100 μV.

3 Results

In recordings, we detected action potentials propagating through soma, axons, and dendrites that pro-

duced unexpected extracellular signals. Existing work typically considers the soma and dendrites to be the largest contributors to the extracellular voltage signal, with the axon's contribution considered negligible and, at times, excluded from analysis. Our experimental data show that the axon was in fact a large contributor, with the largest extracellular voltage signal arising near the axon initial segment in 8 out of 8 neurons imaged (Fig. 1). To begin investigating this discrepancy, we developed a custom COMSOL model to reconstruct a neuron's morphology and the local microenvironment, incorporated Hodgkin-Huxley ion channels into the cell membrane, and successfully simulated propagating action potentials (Fig. 2).

4 Conclusion / Summary

COMSOL's generic 3D finite element modeling environment is able to incorporate contributions from the local microenvironment, including the MEA surface and (ground) electrode layout. Work is ongoing, but we anticipate that such a tool will help expand our knowledge about a number of topics including: optimal design of electrodes and stimulation parameters both in vivo and in vitro; signal amplification effects of PDMS micro-tunnels; the role of endogenous electric fields and ephaptic interactions; and the biophysics of action potentials.

Acknowledgement

Supported by the Swiss National Science Foundation Ambizione Grant PZ00P3_132245, FP7 of the European Community through the ERC Advanced Grant 267351 'NeuroCMOS', and a KAKENHI Grant 23680050.

References

[1] Bakkum, D. J. et al. (2013) Tracking axonal action potential propagation on a high-density microelectrode array across hundreds of sites. *Nature Commun. 4:2181*

[2] Frey, U. et al. (2010) Switch-matrix-based high-density microelectrode array in CMOS technology. *IEEE J. Solid-St. Circ. 45, 467–482*

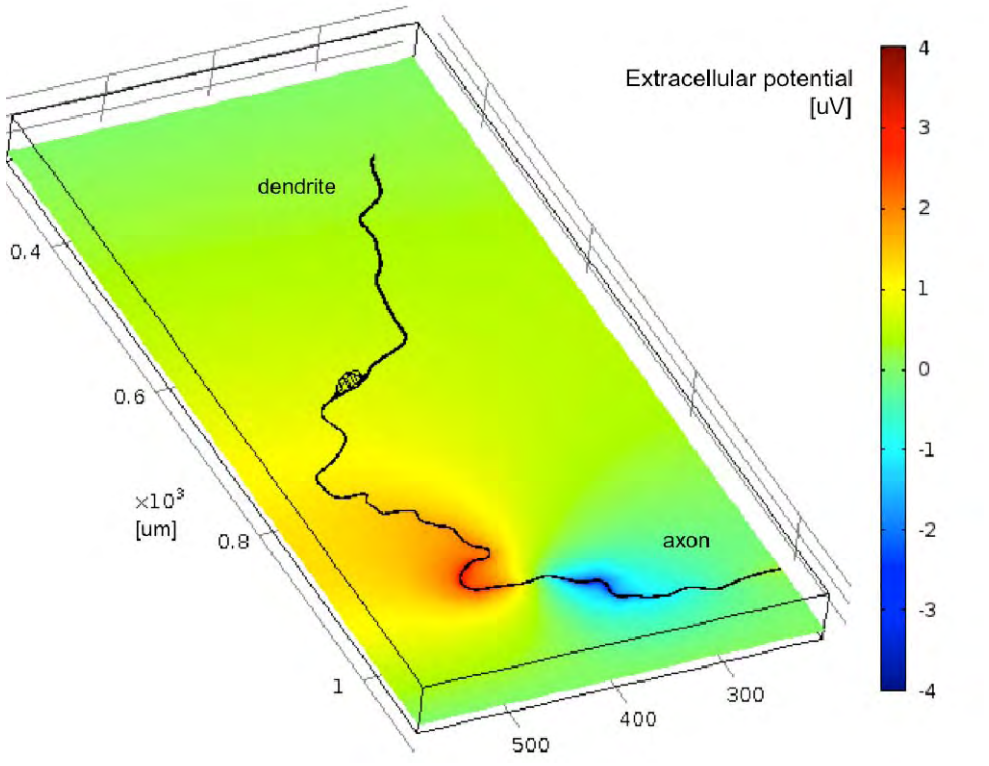

Fig. 2. 3D finite element model of the neuron from Fig. 1 and the biphasic (red to blue color) extracellular voltage produced by an antidromically propagating action potential. The array surface was modeled as an insulator.

Multi-Parameter Analysis Platform for Neuronal Growth, Differentiation and Communication

L. Micholt[1], D. Braeken[1*]

1 Life Science Technologies, imec, Kapeldreef 75, 3001 Heverlee, Belgium
* Corresponding author. E-mail address: dries.braeken@imec.be

Abstract
Investigation of neuronal growth, differentiation, and communication is of large interest not only to understand the underlying mechanisms of the neural system but also to develop new therapeutic solutions for neurodegenerative disorders. Controlled and simplified in vitro environments can help to address several challenges independently. Here, we present a multi-faceted approach to study neuronal guiding *in vitro* making use of silicon micro-fabrication. Topographical, soluble and electrical cues are used to study and interface with hippocampal neurons. We found that neuronal behavior is directional depending on spatial frequency of topography, and that this cue is synergistically enhanced by soluble attractants and repellents of neuronal growth. Further we found correlation of single neuron electrical stimulation with neuronal communication of neighboring cells.

1 Introduction

Neuronal guiding is a multi-faceted process essential for linking neurons into functional networks underlying the workings of the neural system. Many questions still remain how neurons act on complex environments. In vitro investigation of simultaneous multi-parameter cues can help us to understand behavior of neuronal growth, differentiation and communication.

2 Fabrication of silicon pillar array chips

In this study, using a novel silicon micro-fabricated analysis platform, we investigate the response of embryonic hippocampal neurons to superimposed topographic and soluble chemical cues, and neuronal network response to single-cell electrical stimulation. To achieve this, we used two silicon-based platforms: the first platform consisted of a nano-gradient of pillar arrays to induce stepwise increased frequencies of topographic cues presented to the neurons (Fig. 1) [1]. This silicon pillar matrix was combined with a microfluidic compartment to apply chemical gradients over the cells, resulting in a multi-parameter cell analysis platform [2]. A CMOS-based multi-electrode array chip combined with fluorescent calcium imaging was used to investigate the impact of electrical stimulation of single neurons in dense neuronal networks [3].

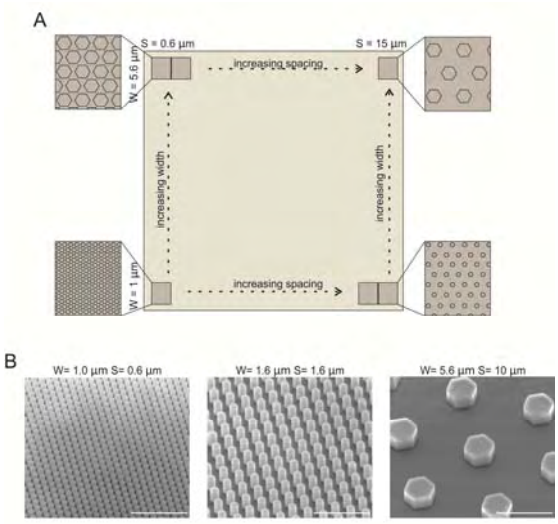

Fig. 1. Nano-gradient silicon pillar array to study neuronal growth and differentiation. A. Design of the pillar array. B. Scanning micrographs of some of the silicon pillar arrays.

3 Multi-cue interaction of neuronal outgrowth

We find that an optimal spatial frequency of topographic cues exists, maximizing the precision of the neurite extension. This optimal frequency can help neurites navigate through a topographically complex environment whilst providing strong directionality and cytoskeletal interactions (Figure 2). We also demonstrate that this cue synergistically enhances attractive and suppresses repulsive guidance by the soluble cue Netrin-1, and eliminates the repulsive guidance by the chemorepellent Semaphorin3A. Electrical stimulation of single cells in intensely interconnected neuronal networks shows the correlation between distance and impact of the electrical stimulation in reference to the point of stimulation.

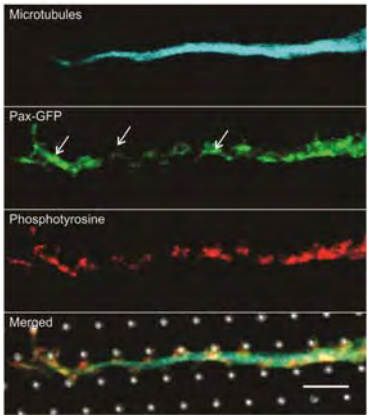

Fig. 2. Pillar arrays induce cytoskeletal interactions through involvement of paxillin in the signal transduction pathway.

4 Conclusion

These results suggest that topographic, chemical, and electrical cues applied on single cell level reveal strong interaction of neurons with their environment and the need of multi-parameter analysis platforms for deeper understanding of neuronal development.

References

[1] Micholt L. et al., PLoS ONE, (8)6, 2013.
[2] Kundu A. *et al.*, Lab Chip (6)13, 2013.
[3] Huys R. et al., Lab chip (12)7, 2012.

Characterizing the Human Embryonic Stem Cell – derived Neural Cultures: the Effect of Astrocytes on Network Properties

Marja Pajunen[1*], Tanja Paavilainen[1], Dmitriy Fayuk[1], Laura Ylä-Outinen[1], Susanna Narkilahti[1]

1 BioMediTech, University of Tampere, Finland
* Corresponding author. E-mail address: marja.peltola@uta.fi

Abstract

During the last decade the neuron centric research of central nervous system (CNS) has started to focus also on the role of astrocytes which are now seen as more dynamic cells than earlier. Human embryonic stem cell (hESC)-derived neural cells are potential source for studying the role of astrocytes in human neuronal networks. Microelectrode arrays (MEA) can be used to study the functional development of neuronal networks. In this study the functional development and maturation of two different hESC-derived neural cultures, neuronal enriched and astrocyte enriched, were characterized using MEA. Our results suggest that there are differences in the development of electrical activity in networks with different amounts of astrocytes.

1 Background

Central nervous system (CNS) has two main types of cells: neurons and glial cells (including oligodendrocytes and astrocytes). Traditionally, neurons have been considered to be more dynamic cells and astrocytes more static cells. However, lately new more dynamic roles have also been suggested to astrocytes. Thus, in addition to their traditional role as structural and nutritional supporters, astrocytes are now considered to be involved in the regulation of synaptic function and information processing [1]. Nowadays astrocytes, more detailed their dysfunctions, are considered to play a role also in some neurological disorders (e.g. epilepsy) [2]. Thus, it's important to study the role of the astrocytes more carefully also *in vitro*. In this study we used human embryonic stem cell (hESC)-derived neural cells. We studied the development and maturation of the electrical activity of neuron and astrocyte enriched cultures on MEA.

2 Materials and Methods

2.1 HESC-derived neuronal cells

The cells for the experiment were derived from hESCs (line Regea 08/023) [3]. Briefly, embryonic stem cell colonies were cut and allowed to form spheres in neural differentiation medium for 8 or 15 weeks. The formed neurospheres were cut to small pieces and plated onto MEAs (Multichannel Systems, MCS, Germany) [4] and cell culture well plates. In addition to the functional characterization with MEAs, the cultures were characterized using gene expression analysis and immunocytochemical staining.

2.2 MEA measurements

Before cell plating, the MEA-plates (60-6wellMEA200/30iR-Ti) were coated with PEI and laminin [4]. The functional development of the network was followed by MEA measurements (with 2100MEA system, MCS) twice a week for 10 minutes. The MEA data was analyzed using MATLAB protocol (MathWorks, Natick, MA, USA) designed in-house [5] and NeuroExplorer (NexTechnologies, Madison, AL, USA).

3 Results

We used two different populations, one differentiated for 8 weeks containing low amount of astrocytes (neuron enriched) and another culture differentiated for 15 weeks which contained more astrocytes (astrocyte enriched). According to the preliminary data, there seems to be a difference in the development of electrical activity in networks with different amounts of astrocytes. The neuron enriched cultures were more active compared to the astrocyte enriched cultures, demonstrated by the higher amount of spikes per active electrode in all measurement timepoints (Fig. 1 and Fig. 2A). Moreover, the burst dynamics of the neuron enriched and astrocyte enriched cultures differed. The neuron enriched cultures had more burst associated spikes compared to the astrocyte enriched cultures (Fig. 2B). To verify the amount of astrocytes in the neuronal and astrocytic cultures more detailed data analysis of protein and gene expression are ongoing. In addition more MEA data is currently being analyzed.

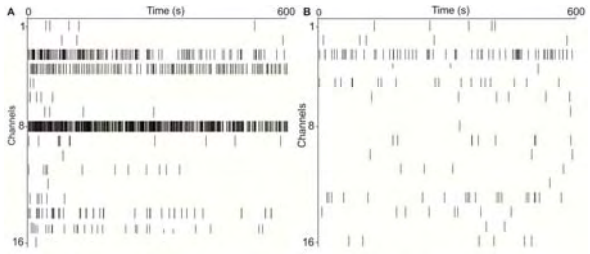

Figure 1. Raster blots of the spiking activity of neuron enriched **(A)** and astrocyte enriched cultures **(B)**. The X-axis represents the time 600s; the y-axis represents the channels 1-16. The spikes are marked as rasters.

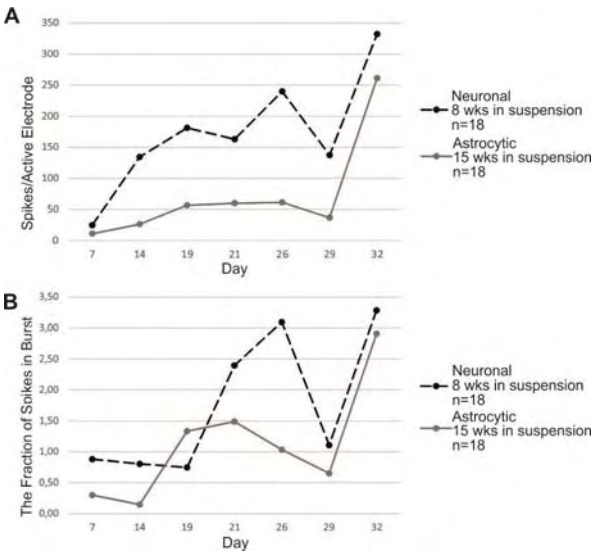

Figure 2. Spikes per active electrode for neuronal and astrocytic cultures **(A)**. The amount of spikes in burst relative to the amount of spikes not associated in bursts **(B)**.

4 Conclusions

According to our preliminary data, it seems that the amount of astrocytes affects both to the development and maturation of neural networks. Therefore it's important to characterize the role of astrocytes in the functional neural networks *in vitro*. To verify the significance of astrocytes in these networks more data will be analyzed in the future.

Acknowledgement

This research has been supported by the 3DNeuroN project in the European Union's Seventh Framework Programme, Future and Emerging Technologies, grant agreement n°296590.

References

[1] Theodosis, D.T., Poulain, D.A. & Oliet, S.H. (2008). Activity-dependent structural and functional plasticity of astrocyte-neuron interactions. *Physiological Reviews*, vol. 88, no. 3, pp. 983-1008.

[2] Steinhauser, C., Seifert, G. & Bedner, P. (2012): Astrocyte dysfunction in temporal lobe epilepsy: K+ channels and gap junction coupling. *Glia*, vol. 60, no. 8, pp. 1192-1202.

[3] Lappalainen, R.S., Salomäki, M., Ylä-Outinen, L., Heikkilä, T.J., Hyttinen, J.A., Pihlajamäki, H., Suuronen, R., Skottman, H. & Narkilahti, S. 2010, "Similarly derived and cultured hESC lines show variation in their developmental potential towards neuronal cells in long-term culture", Regenerative medicine, vol. 5, no. 5, pp. 749-762.

[4] Heikkilä, T.J., Ylä-Outinen, L., Tanskanen, J.M., Lappalainen, R.S., Skottman, H., Suuronen, R., Mikkonen, J.E., Hyttinen, J.A. & Narkilahti, S. (2009).Human embryonic stem cell-derived neuronal cells form spontaneously active neuronal networks in vitro). *Experimental neurology*, vol. 218, no. 1, pp. 109-116.

[5] Kapucu, F.E., Tanskanen, J.M., Mikkonen, J.E., Ylä-Outinen, L., Narkilahti, S. & Hyttinen, J.A. 2012, "Burst analysis tool for developing neuronal networks exhibiting highly varying action potential dynamics", *Frontiers in computational neuroscience*, vol. 6, pp. 38.

Neuronal Migration and Activity in Mature Primary Cultures on a High-Density CMOS Array

Hirokazu Takahashi[1*], Takeshi Mita[1], Satoru Okawa[1], Ryohei Kanzaki[1], Urs Frey[2], Andreas Hierlemann[3], Douglas Bakkum[3]

1 The University of Tokyo, Tokyo, Japan
2 RIKEN Quantitative Biology Centre, Kobe, Japan
3 ETH Zurich, Basel, Switzerland
* Corresponding author. E-mail address: takahashi@i.u-tokyo.ac.jp

Abstract
Neurons migrate even in a mature brain. We tested in primary dissociated cultures of neuronal cells whether and how neural activity changes with migration. In a mature culture of neurons, a high-density CMOS microelectrode array was used to continuously monitor neural migration and activity for more than two weeks. We found that neurons moved 2.0 ± 1.0 μm a day and that the moving distance was negatively correlated to their firing rate, suggesting that neurons featuring low firing rates tend to migrate actively. Thus, migration is likely to play a critical role for individual neurons to establish their connections and functions in a neuronal network.

1 Introduction

Neurons migrate even in a mature brain. For example, new-born neurons migrate towards existing, already matured neural networks in order to participate in neural computation. Such migration may play a critical role for individual neurons to establish their connections and functions in a network. However, long-term characterization of both neuronal migration and activities at a single-neuron level has been technically too challenging to address yet.

Cutting-edge CMOS microelectrode array technology may help to enable high-density recordings in *in vitro* neuronal cultures [1]. The CMOS array enables non-invasive, chronic measurement of neuronal activity and provides subcellular spatial resolution. Thus, the electrical imaging of neural activity can be used to track day-to-day locations of cell bodies during chronic experiments. We tested in primary dissociated cultures of neuronal cells, whether and how neural activity changed with cell migration.

2 Material and Methods

Cells from E18 rat cortices, dissociated in trypsin, were grown in DMEM with 10% horse serum on top of the CMOS arrays. A thin layer of polyethyleneimine and a 15 μl drop of Laminin were used for cell adhesion.

The CMOS microelectrode array has been described in detail elsewhere (Fig. 1a) [1]. The array has 11,011 Pt electrodes with 7 μm diameter within a 2.0×1.75 mm^2 area. The pitch between the electrodes is 18 μm, which is comparable to the size of cell bodies of neurons. Thus, action potential (AP) signals from a cell body can be captured by multiple recording sites (Fig. 1b). The sampling rate was 20 kHz.

Electrophysiological data were gathered in 2 samples of matured cultures, ranging from 26 days-in-vitro (DIV) to 42 DIV. AP signals were measured from each electrode, so that a spatial map of AP amplitudes was obtained. In this AP map, cell bodies were localized at local maxima that met the following empirical criteria: (i) a negative peak was measured; and (ii) the presumable AP was measured by three or more electrodes.

After the recording, test cultures were immunostained to compare the spatial map of AP amplitude with the anatomical structure of the neuronal circuits. After the recording experiments, the test culture was immunostained with mouse anti-MAP2 (microtubule associated protein-2, a neuron-specific marker protein) antibody, then with anti-mouse Alexa 488-labeled IgG.

3 Results

AP waveforms were collected from 1 min spontaneous activity at each recording site, and the peak amplitudes of averaged AP waveforms were spatially mapped (Fig. 2a). Upon comparison of this AP map to the immunostaining image, it was found that APs measured in the proximity of cell bodies exhibited a large, negative peak, which could be recorded at several electrodes (Fig. 2b). The electrode featuring the maximum amplitude of such AP signals was taken as the putative location of the cell bodies. On the other hand, when an AP signal was measured only at a single site, the signal source was most likely an axon (Fig. 2c); these signals were excluded from our analyses.

The putative locations of cell bodies were then tracked for 16 days (Fig. 3). This chronic measurement revealed that the cell bodies in a mature culture

migrated a distance of 50 ± 24 µm, i.e, 3.1 ± 1.5 µm a day.

Importantly, the distance of neuron migration was negatively correlated to the firing rate on the first day of measurement, i.e., at 26 DIV [sample #1, Pearson product-moment correlation coefficient r = -0.44 (t-test, $p < 0.05$); sample #2, r = -0.15 (t-test, $p < 0.05$)] (Fig. 4). This result suggests that while exhibiting a low firing rate, such neurons tend to migrate actively.

4 Discussion

Our results provide the evidence for a possible correlation between neuronal migration and their activity: the lower the neuronal activity, the more the neuron migrates. However, the causal relationships, or the mechanisms still remain elusive. First, low-firing neurons are likely to have fewer connections to other neurons and hence may have fewer restraints for migration, i.e., tension from neurites. On the other hand, actively firing neurons presumably are enmeshed in a more complex web of neurites, in which a balanced tension may inhibit migration. Second, there is a possibility that neurons actively migrate to explore an optimal location in terms of their homeostatic properties. Provided that individual neurons have their own optimal firing rate to establish certain roles in the neural network, low-firing neurons may follow an exploratory strategy of migration. Further experiments are required to reveal critical parameters of migration.

5 Conclusion

We have found that neurons grown *in vitro* move 3.1 ± 1.5 µm a day on average, and that low-firing-rate neurons tend to migrate more actively. These results suggest that migration may play a role for individual neurons to establish their connections and functions in a neuronal network.

Acknowledgement

This study was supported in part by Denso Corp. (Kariya, Japan) and KAKENHI (23680050).

References

[1] Bakkum et al. (2013): Tracking axonal action potential propagation on a high-density microelectrode array across hundreds of sites. *Nature Comm, 4, Art no 2181.*

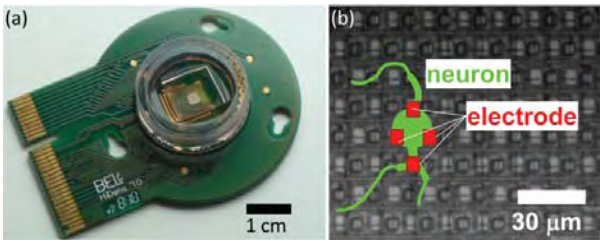

Fig. 1. High-density CMOS electrode array: (a) packaged chip; (b) magnification of the array surface. Typical size of a neuron is depicted with respect to the grid of electrodes.

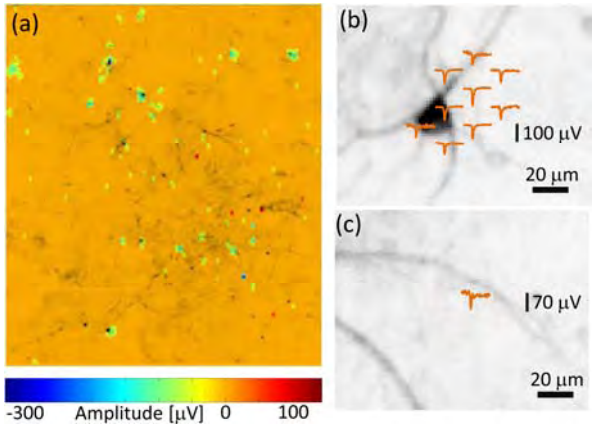

Fig. 2. Localization of cell bodies based on neuronal signals. (a) Superposition of immunostaining image and AP map. The peak amplitude of the averaged AP waveform is color-coded. (b) AP waveforms detected around a cell body of a neuron. (c) AP waveform excluded from the analyses.

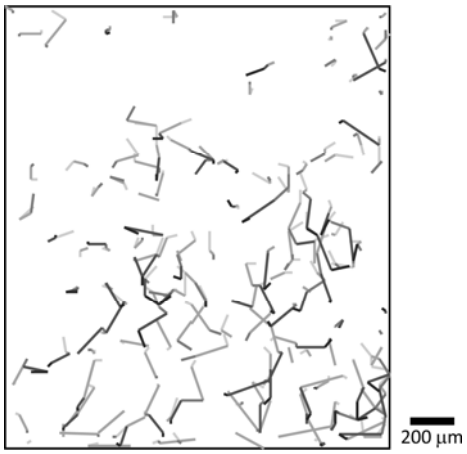

Fig. 3. Migration trajectories of putative cell bodies of neurons. Gray levels correspond to DIV: the lightest to DIV 26; the darkest to DIV 42.

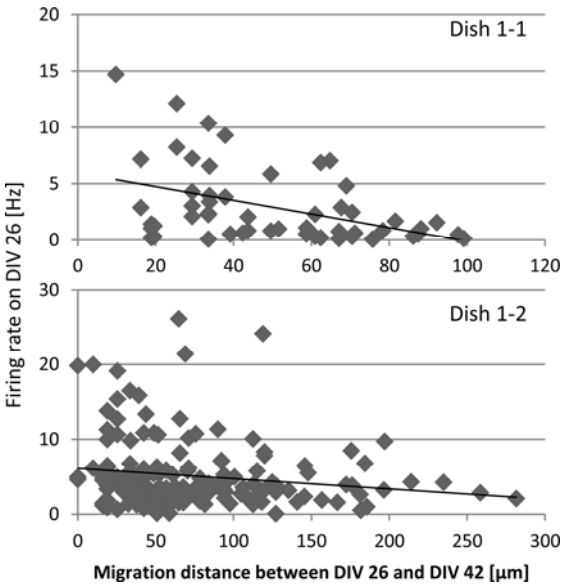

Fig. 4. Correlations between migration distance and firing rates of neurons. Results of 2 independent dishes are shown.

Simultaneous Microelectrode Array Recording and Intracellular Ca^{2+} Imaging of Human Pluripotent Stem Cell–Derived Neural Cultures

Fayuk Dmitriy [1*], Paavilainen Tanja [1], Meeri Mäkinen [1], Pajunen Marja [1], Heikkilä Juha [1], Narkilahti Susanna [1]

1 BioMediTech, University of Tampere, Tampere, Finland
* Corresponding author. E-mail address: dmitriy.fayuk@uta.fi

Abstract
In vitro neuronal networks can be formed using human pluripotent stem cells (hPSCs). Recording of electrical activity with microelectrode arrays (MEA) is commonly used approach to study functional properties of these kinds of networks while Ca^{2+} imaging can be used for characterization of single cell functionality. Therefore, we combined these two approaches to collect more information from the same network and search for correlation between single cell and network functions. We demonstrate here that simultaneous use of MEA recordings and intracellular Ca^{2+} imaging is a feasible tool, however, more experiments are needed to optimize protocols and prove the usability of the combined method. To this date, we did not find correlation between electrical activity recorded with MEA and Ca^{2+} transients in cell bodies nearby the "active" electrodes. Use of Ca^{2+} imaging with higher spatial resolution to detect also Ca^{2+} signaling in neurites is suggested.

1 Background

Human pluripotent stem cells can be differentiated into neural cell types, both neurons and glia, and they are able to form functional networks *in vitro* [1, 2]. Coordinated interactions among groups of neurons in these networks are believed to mimic processes *in vivo*. Therefore, experimental investigation of such network dynamics can gain us a better insight into basic mechanisms of neural network functioning in the brain. Over the past two decades, calcium imaging and microelectrode array (MEA) recording have emerged as essential tools for this purpose. A major advantage of MEAs is that they provide a view of the large-scale activity of a neural population with sub-millisecond temporal resolution [3]. However, MEAs cannot reveal what particular neurons are active in the networks. In contrast, calcium imaging in many cases is capable of identifying single cell activity even in the group of neurons. Here, we present our experiments where we combined MEA and calcium imaging measurements.

2 Methods

2.1 Human pluripotent stem cell (hPSC)-derived neuronal networks

The differentiation of hPSCs into neural cell types was conducted in neurosphere culture [1]. Briefly, hPSC colonies were manually cut and thereafter allowed to form aggregates in neural differentiation medium (7-8 weeks of differentiation). Neural cells were maturated by plating small pieces (Ø 50 µm) of aggregates on polyethylenimine (PEI) and laminin coated MEA dishes (60ThinMEA 200/30, Multichannel Systems, MCS, Germany).

2.2 MEA measurements and Ca^{2+} imaging

The functional development of the networks was followed with MEA recordings 2 times a week after plating. Combined MEA and Ca^{2+} imaging recordings were made two weeks after plating when network electrical activity demonstrated more mature patterns (spike trains). For fluorescent imaging (Fig. 1) of intracellular Ca^{2+} signals, the neural cultures were loaded with fluo-4 AM (Molecular Probes) and were imaged every 0.5 s using system consisted of Olympus IX61 inverted microscope, Andor iXon 885 EMCCD camera and Till Photonics Polychrom V monochromator. To study correlation between Ca^{2+} and electrical signals only the areas surrounding the MEA electrodes which reported regular electrical activity were imaged.

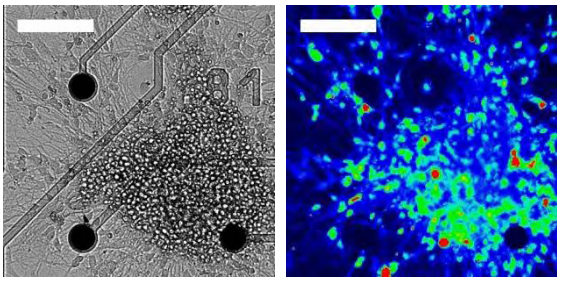

Fig. 1. Images of hPSC-derived network on MEA: in transmitted light (left) and as pseudo-colored fluorescence intensity of fluo-4 (right). Scale bar is 100 µm.

3 Results

The hPSC-derived networks demonstrated spontaneous electrical activity in MEA recordings detected as spike trains starting from week two after plating. In addition, spontaneous intracellular Ca^{2+} signaling was revealed in Ca^{2+} imaging experiments. During simul-

taneous employment of these two techniques, however, the MEA signals were complicated with periodical paired artifacts that temporarily and spatially strictly correlated with illumination used for excitation of fluo-4. High pass filtering (200 Hz) removed most of the artifact and subsequent spike sorting allowed us to separate residual artificial signals from cell activity signals (Fig 2). Strict periodicity of paired artificial "spikes" correlating with illumination parameters (2 Hz frequency, 50 ms duration) proved sorting algorithm.

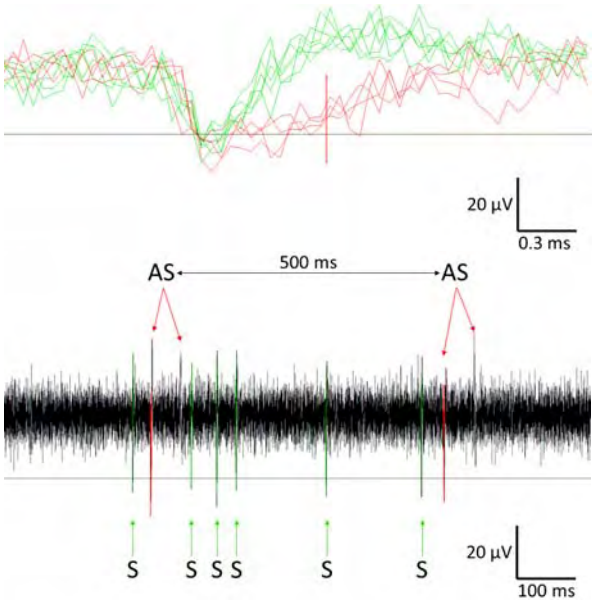

Fig. 2. **Spike sorting separated artificial residual spikes (AS, in red) from native cell activity spikes (S, in green).**

Despite the electrical and Ca^{2+} signals were detected in the same network regions we did not find temporal correlation between electrical activity recorded from particular MEA electrodes and Ca^{2+} transients in the neurons located near those "active" electrodes.

4 Conclusion

Simultaneous use of MEA measurements and Ca^{2+} imaging is a feasible approach and it promises to provide us more detailed information about particular neurons involved in the generation of electrical activity in the network. So far we did not, however, find correlation between electrical activity recorded by particular electrode and Ca^{2+} signals in the nearby neurons. We suggest that spike trains detected in our networks were produced by action potential trains in neuronal processes lying in close proximity to the electrodes rather than in nearby cell bodies. Ca^{2+} transients in those processes were not detected because of the low intensity of fluorescent signals in very thin structures against a bright background of cell body groups and aggregates. More experiments with focus on Ca^{2+} signaling in neurites are needed to check this hypothesis. New experiments can also clarify why Ca^{2+} transients detected in neuronal cell bodies nearby MEA electrodes did not correlate with electrical signals.

Acknowledgement

This research has been supported by the 3DNeuroN project in the European Union's Seventh Framework Programme, Future and Emerging Technologies, grant agreement n°296590. Finnish Funding Agency for Innovation (Human Spare Parts Project)

References

[1] Lappalainen R, Salomäki M, Ylä-Outinen L, Heikkilä TJ, et al. (2010) Regen. Med. 5:749–762.
[2] Heikkilä TJ, Ylä-Outinen L, Tanskanen JM, et al. (2009) Exp Neurol. 218(1):109–116.
[3] Wagenaar, D.A., Pine, J., Potter, S.M., 2006. An extremely rich repertoire of bursting patterns during the development of cortical cultures. BMC Neurosci. 7, 11.

Spontaneous and Evoked Activity in Patterned Multi-Cluster Neuronal Networks

Margarita Anisimova[1]*, Keiko Yokoyama[1,2], Daisuke Ito[2,3], Masaaki Suzuki[4], Tsutomu Uchida[1], Kazutoshi Gohara[1]

1 Division of Applied Physics, Faculty of Engineering, Hokkaido University, Sapporo, Japan
2 Research Fellow of the Japan Society for the Promotion of Science, Tokyo, Japan
3 Division of Functional Life Science, Faculty of Advanced Life Science, Hokkaido University, Sapporo, Japan
4 National Institute of Advanced Industrial Science and Technology (AIST), Sapporo, Japan
* Corresponding author. E-mail address: anisimova@ec.hokudai.ac.jp

Abstract
Since signal propagation in simple two-cluster cortical neuronal networks was demonstrated, there has been a fundamental question: How do the number and geometry of clusters and the connection between them affect the collective dynamics in networks? However the effect is still unclear. In order to answer this question, we investigated extracellular potential traces of multi-cluster neuronal networks. Spontaneous and evoked electrical activity analysis allowed us to find the initial bursting cluster as well as the signal propagation direction and passages in our neuronal networks.

1 Backround / Aims

Although synchronized burst activity is a remarkable phenomenon of electrical activity in neuronal networks [1,2], the signal propagation pathway remains unclear. Cell patterning techniques allow us to design the cell position and their connections. Recently, signal propagation among two neuronal clusters has been demonstrated [3]. However, propagation in multi-cluster networks is still not understood. In the present study, we investigate the signal propagation of spontaneous and evoked activity in multi-cluster networks.

2 Methods / Statistics

Cell Patterning: In order to construct isolated sub-networks, we applied our chemical patterning method [4], which modifies the cell adhesiveness of the poly-D-lysine to MEA by using a photolithographic method with vacuum ultraviolet light. In this study, we redesigned the pattern geometry. In addition, a mechanical manipulator was used to reshape certain cortical sub-networks as well as for pattern isolation.

Cell culture on MEAs: Cerebral cortices derived from Wistar rats at embryonic day 17 were dissociated on chemically-patterned multi-electrode dish (MED) probes. The cells were filled with a culture medium and cultured for 1 month in a CO_2 incubator [5].

Electrical signal recording: Data was recorded from sub-network clusters on the electrodes by using a MED64 (Alpha MED Scientific, Osaka, Japan) extracellular recording system at a sampling rate of 20 kHz. Spontaneous electrical activity was recorded each time before external stimulation in order to obtain a reference signal. External electrical stimulation with different signal parameters such as amplitude, shape, length and period was used.

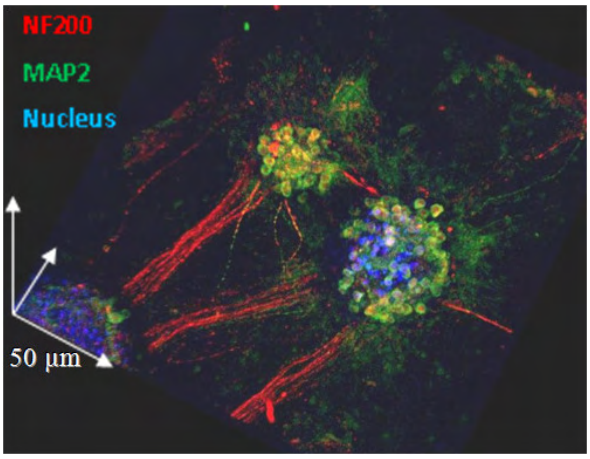

Fig. 1. The 3D fluorescent image of a neuronal cluster with axon connections (red). Green stands for dendrites and blue for the neuron's nucleus.

Fluorescent 3D imaging: After cultivation, the cells were fixed and stained with MAP2 and NF200 antibodies to identify neuronal cell bodies, dendrites and axons. The cell nuclei were stained with hoechst33342. Fluorescence was observed using confocal laser scanning microscopy (IX81/FV1000D, Olympus).

3 Results

Our chemical patterning method allowed us to successfully grow a number of clusters connected to each other by axon passages on gold electrodes and to record spontaneous and evoked synchronized burst activity. Fluorescence imaging (Fig. 1) confirmed that the connections between clusters are axons and

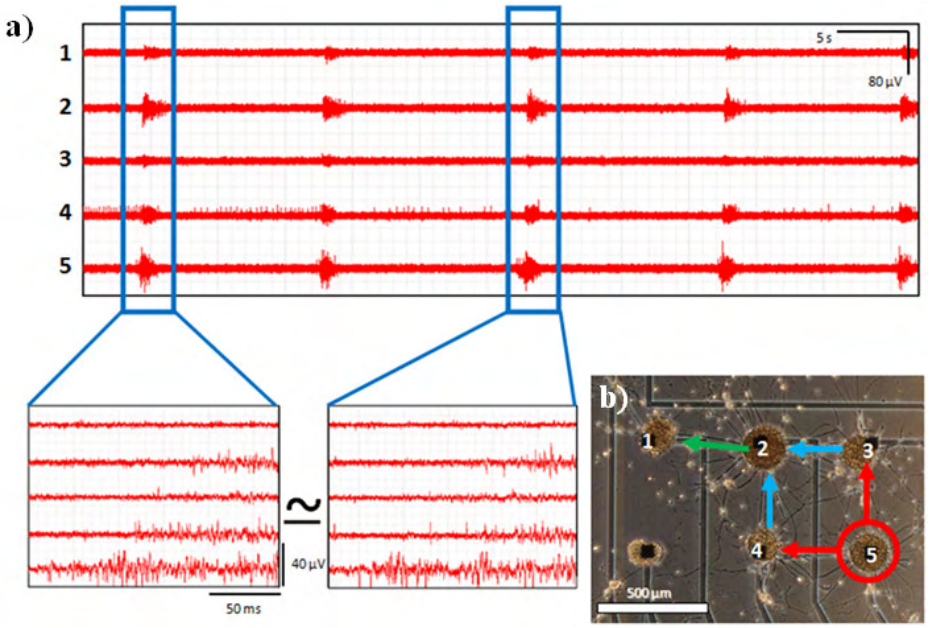

Fig. 2. a) Extracellular potential traces of multi-cluster neuronal networks. The clusters showed synchronized bursts. The Numbers correspond to the position of electrodes. **b)** The signal propagation passages. Red circle - initial burst cluster. Red arrows - first pass of signal propagation. Blue arrows - second pass of signal propagation. Green arrow - third pass of signal propagation.

not dendrites, which play a significant role in signal transfer within the neuronal network. By analysing the signal waveform in a sub-network, we were able to identify the propagation direction (Fig. 2a and b). Each network appeared to have one main initial synchronized burst cluster (e.g., #5 in Fig. 2b). This cluster, so-called Leader [6], remains the starting point in approximately 60 to 90% of synchronized activity firing (with respect to cluster number and size within one network). The Leader assigning mechanism is not yet fully understood, however, the data obtained from the series of experiments show the possibility that the axon connections between clusters play a significant role.

To support the above hypothesis, manual reshaping was introduced to the network. During the cutting procedure a multi-cluster network was isolated and some of the axon connections between clusters were removed. This interference not only resulted in significant changes in Leader assigning, but also caused a new type of signal waveform to appear.

In addition, the external stimulation with various pulse periods prompted a characteristic response pattern, obtained from each cluster within the network in both cases: before and after reshaping. Comparison of spontaneous and evoked activity suggests the existence of specific rest/response times for each cluster (data not shown). This phenomenon however needs to be studied more carefully before any conclusions can be made.

Also for reshaped networks we counted the number of cells within the clusters using 3D fluorescence imaging (blue neuron nucleus on Fig. 1) and studied its effect on electrical activity. We obtained different signal waveforms, such as single, double and triple responses, according to the cluster shape. Thus, for the signal waveform, the cluster geometry appears to be more substantial, than the number of cells.

4 Conclusion/Summary

In the present study, we investigated the collective dynamics of neuronal networks such as the spontaneous and evoked synchronised burst activity. We found that most initial bursts in the isolated neuronal networks start within one specific cluster, which we called the Leader. Mechanical manipulations of the network geometry (cutting or reshaping) caused a change of the Leader and of the waveform shape. Also, precise analysis of the extracellular potential traces of multi-cluster networks showed that the signal pathway remains unchanged if the burst starts from the same cluster.

References

[1] Maeda *et.al.* (1995), J. Neuroscience, 15(10), 6934-6845
[2] Idelson *et.al.* (2011), Front. Neuroeng., 4(10), 1-8
[3] Idelson *et.al.* (2010), PLoS ONE, 5(12), e14443
[4] Suzuki *et.al.* (2013), Biomaterials, 34(21), 5210-5217
[5] Ito *et al.* (2010), Neuroscience, 171(1), 50-61
[6] Ham *et al.* (2008), J. Comput. Neurosci., 24(3), 346-357

Evaluation of Action Potential Conduction Velocity for Myelination Research

Koji Sakai[1*], Kenta Shimba[1], Kiyoshi Kotani[1], Yasuhiko Jimbo[1]

1 The University of Tokyo, Tokyo, Japan
* Corresponding author. E-mail address: sakai@neuron.t.u-tokyo.ac.jp

Abstract
Remyelination is a potent therapeutic strategy for myelin disorders such as multiple sclerosis. However, little is known about the effect of myelination on the change of action potential conduction velocity. In this study, we aim to develop a neuron-oligodendrocyte co-culture device which enables us detect the propagation of action potentials with multi electrodes. Myelination was observed by immunocytochemistry in neuron and oligodendrocyte co-culture, and propagations of action potential were detected in spontaneous activity by using microchannel structure and a spike sorting method. These results suggest that the structure and culture environment in this device are suitable for investigating the change of action potential conduction velocity in myelination process.

1 Background and Aim

Remyelination is a potent therapeutic strategy for myelin disorders such as multiple sclerosis [1]. Earlier studies have not achieved myelin repair and restoration of motor function completely. However, it is difficult to investigate the effect of myelination on the change of action potential conduction velocity in animal study. Then, the aim of our study is to develop a neuron-oligodendrocyte co-culture device which enables us evaluate the change of action potential conduction velocity in myelination process. In order to achieve this purpose, two fundamental experiments were performed in this study. First, to evaluate action potential conduction velocity, a culture device to detect the propagation of action potentials with multi electrodes was developed. Second, to confirm myelin formation in our co-culture environment, neurons and oligodendrocytes were co-cultured in the device.

2 Methods and Statistics

The culture device consists of a microelectrode array (MEA) and a micro chamber fabricated by photolithography techniques (Fig. 1). The chamber has two soma compartments and four microchannels in which axons outgrowth. Each microchannel is located on a line of eight electrodes. Mouse cortical neurons were cultured in soma compartments of the device. Oligodendrocyte precursor cells were seeded and Triiodothyronine was added to culture medium 18 days after seeding neurons [2]. Spontaneous activity was recorded for 20 minutes from neurons without seeding oligodendrocyte. Spike train was detected at the fourth electrode from the left side. To detect the propagation of action potentials, spike sorting was performed. The data recorded from third, fourth, fifth and sixth electrodes around spike timings were used for spike sorting.

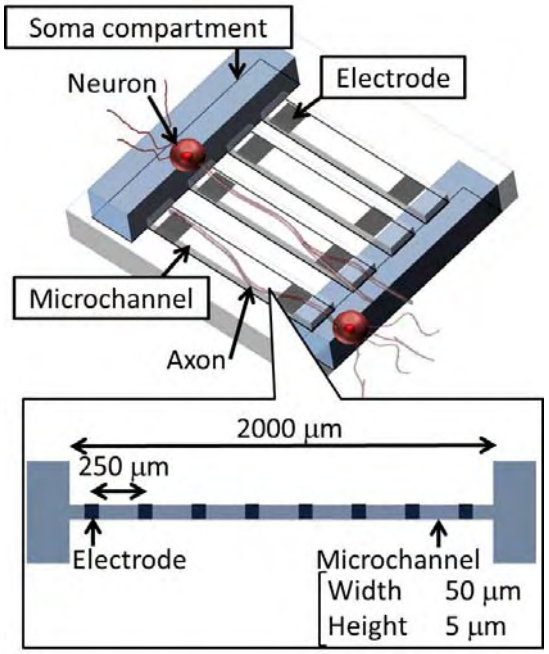

Fig. 1. The schematic of culture device. The lower panel shows magnified view of a microchannel.

3 Results

Fig. 2 are immunofluorescent images of neuron and oligodendrocyte co-cultured in the device at 45 days in vitro. Myelin segments were formed (Fig. 2A, white arrows) and neurites grew into the microchannel. These results suggest that the co-culture environment for myelination was able to be maintained in the device.

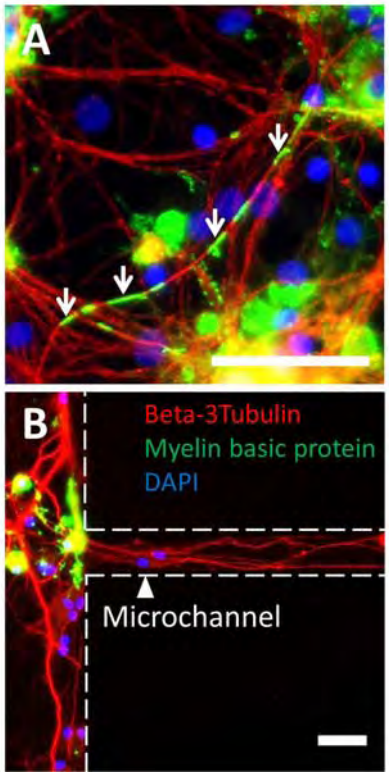

Fig. 2. Immunofluorescent images of neuron-oligodendrocyte co-culture. (A) Myelin sheaths in the soma compartment are indicated by white arrows. (B) Neurites entered a microchannel. Neurites entered a microchannel. Neurites and myelin sheaths were stained by antibodies against Beta 3 Tubulin (red) and Myelin basic protein (green), respectively. Scale bar indicates 50 μm.

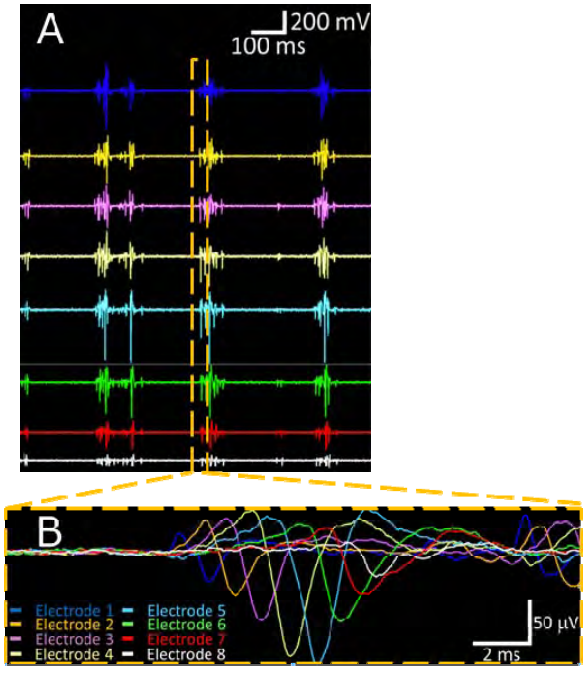

Fig. 3. Spontaneous activity recorded from eight electrodes underneath a microchannel. The synchronized activity between eight electrodes (A) and a propagation of action potentials along these electrodes (B) were observed at 17 days in vitro.

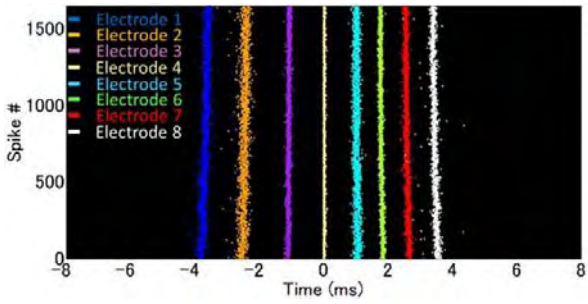

Fig. 4. Delay times of conduction between electrodes. Peak times of eight electrodes around spike timings of the fourth electrode were plotted at 17 days in vitro. The vertical axis indicates spike number in a cluster. The horizontal axis indicates time triggered by spike timing of the fourth electrode.

As shown in Fig. 3, propagations of action potentials were observed along eight electrodes repeatedly. Delay times of conduction between adjacent electrodes were almost constant (about 1 ms). To evaluate the temporal change and the difference according to the part of axon in delay time of conduction, peak time of eight electrodes around spike timing in a cluster were plotted (Fig. 4). Delay times of conduction were almost constant for 20 minutes and delay times were different according to the set of electrodes. These results suggest that propagations of action potentials was detected from recording data by using the spike sorting method and that the device enable us to detect the difference of action potential conduction velocity according to the part of axon .

4 Conclusion

Myelination was observed by immunocytochemistry in neuron and oligodendrocyte co-culture, and propagations of action potential were detected in spontaneous activity by using the microchannel structure and the spike sorting method. These results suggest that the microchannel structure and culture environment in this device are suitable for investigating the change of action potential conduction velocity in myelination process.

Acknowledgement

We gratefully acknowledge the partial financial support provided by the Japan Society for the Promotion of Science (JSPS) via a Grant-in-Aid for science research (2324006).

References

[1] A. Chang, W. W. Tourtelliotte, R. Rudick and B. D. Trapp: “Premyelinating oligodendrocytes in chronic lesions of multiple sclerosis.”, *N. Engl. J. Med.*, Vol. 346, No. 3, pp. 165-173 (2002)

[2] Y. Pang, B. Zheng, S. L. Kimberly, Z. Cai, P. G. Rhodes and R. C. Lin: “Neuron-oligodendrocyte myelination co-culture derived from embryonic rat spinal cord and cerebral cortex.“, *Brain Behav.*, Vol. 2, No. 1, pp. 53-67

Electrophysiological Characterization of Individual Neurons in Sparse Cortical Cultures

Weir Keiko, Blanquie Oriane, Kilb Werner, Luhmann Heiko J.* and Sinning Anne

Institute of Physiology, University Medical Center Mainz, Mainz (Germany)
*Corresponding author: E-mail address: Luhmann@uni-mainz.de

Abstract
We used a 120-channel multielectrode array (MEA) to analyze spike waveforms and bursting patterns generated spontaneously in primary cortical cultures. We aimed to find a spike parameter that would distinguish between inhibitory and excitatory neuronal populations. Immunohistochemistry confirmed the presence of GABAergic neurons in our culture system. However, none of the 15 spike waveform or bursting properties analyzed identified two distinct populations. Our data indicates that parameters used to differentiate excitatory and inhibitory neurons *in vivo* might not be applicable to *in vitro* preparations, which could be due to a different expression profile of ion channels *in vitro*.

1 Backround / Aims

Multielectrode arrays are a powerful tool for simultaneously recording activity from a large population of neurons. However, a careful characterization of the spike waveforms and bursting patterns is crucial for using these arrays in any experimental procedure. It is generally assumed that extracellular signals from distinct cell types have a unique electrical signature and that there is a correlation between waveform properties and the spatial distribution of the recording electrode and the source neuron [1-4]. Yet, a thorough analysis and direct evidence for these correlations *in vitro* is lacking.

Here, we analyzed recordings of spontaneous electric activity from cortical neurons cultured on 120-channel arrays at different densities. Our goal was to use spike waveform and bursting properties to identify a parameter that distinguishes inhibitory and excitatory populations in this cell culture system. We also sought to establish a sparse cortical culture model that would enable optical identification and characterization of single neurons to be correlated with extracellular recordings.

2 Methods / Statistics

Dissociated cortical neurons from newborn C57BL/6 mice were cultured with a low and medium cell density (ca. 1000 and 1500 cells/mm^2) on 120-channel multielectrode arrays (Multichannel Systems) as described previously [5]. One-third of culture medium was exchanged after 7 days *in vitro* (DIV). Recordings were performed after 14-16 DIV at 32°C with a sampling rate of 50 kHz and high-pass filtered at 200 Hz on a MEA2100 System (Multichannel Systems). Electrodes on MEAs are 30 µm in diameter and are arranged in a 12 by 12 grid with 100 µm interelectrode distances. Spikes were detected based on a threshold set to 7x the SD of the noise level of each recording electrode in MC Rack (Multichannel Systems) and recorded for a period of 10 minutes in medium as well as in artificial cerebrospinal fluid that resembled the ionic composition of the culture medium. Spikes recorded in MC Rack were sorted and spike times and averaged spike waveforms were analyzed for 15 different parameters in a custom Matlab routine. Immunohistochemical stainings for GAD67 and NeuN were performed in sister cultures to confirm the presence of GABAergic interneurons in our culture system.

3 Results

In order to identify a spike waveform parameter or a bursting property that distinguishes glutamatergic excitatory and GABAergic inhibitory neurons, all detected neurons were analyzed for 15 different parameters of neuronal activity. To ensure that spike waveform and spike bursting properties were similar in our lower density culture system to those recorded at a higher culture density, activity from medium density cultures was also recorded as a control. 91 neurons from 7 low density cultures were recorded, and 364 neurons from 8 medium density cultures were recorded for at least 10 minutes. Fig 1A and B illustrate a typical raster plot and the corresponding peristimulus time histogram from a low density culture and a medium density culture respectively. As described previously, low density cultures have a lower firing frequency, but do not have major differences in firing patterns [7].

Averaged spike waveforms were analyzed for voltage amplitude, trough-to-peak time, spike half-width and asymmetry. A cluster plot of asymmetry versus trough-to-peak time revealed no clusters in both culture densities (Fig 1C,D). Voltage amplitude and spike half-width also did not reveal any distinct clusters.

In addition, 11 bursting parameters were analyzed, including the average number of spikes in a

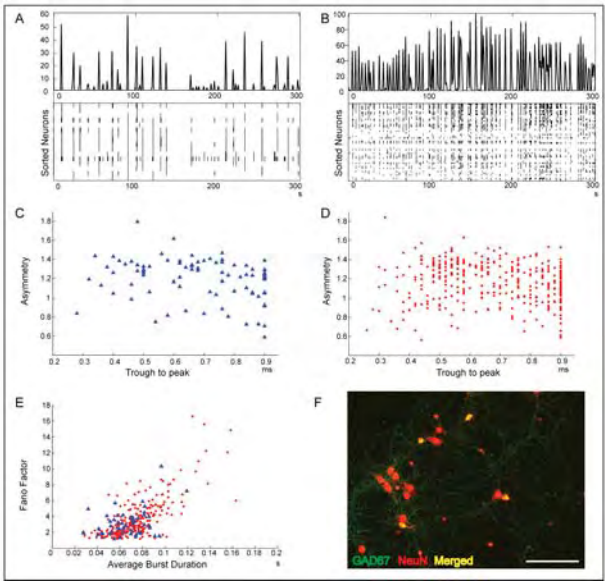

burst (defined by an inter-spike interval of less than 50 ms), intra-burst rate (burst duration / number of spikes), the fano factor (analyzed within an 800 ms window), the average burst duration, and the covariance of the inter-spike interval. None of the properties analyzed resulted in clustering. As an example, fano factor is plotted against averaged burst duration for 49 neurons from low density cultures and 257 neurons from medium density cultures in Fig 1E. Parallel double immunohistochemical stainings for GAD67 and NeuN were performed in sister cultures and revealed that GABAergic interneurons were present in our cell culture system (Fig 1F).

4 Conclusion/Summary

Here, we have attempted to use averaged spike waveforms as well as spike times of single neurons to identify a parameter or a combination of parameters that distinguishes two populations of neurons in our cortical culture system. Our results indicate that none of the spiking parameters could identify two distinguishable populations, even though an immunohistochemical staining confirmed the presence of interneurons in our culture system. Previous *in vivo* and *in vitro* studies have claimed to be able to identify interneurons using similar spike properties [1-4]. Our negative results may be due to a different developmental time course of the neurons *in vitro* [6]. Our low density culture system will allow for future experiments to visually confirm the identity of single neurons using a transgenic mouse models and simultaneously record their electrical activity.

Acknowledgement

We would like to thank Simone Dahms-Praetorius and Beate Krumm for their excellent technical assistance. The work was supported by funding from the DAAD to KW, DFG (SFB 1080) to HJL and the Ministerium für Bildung, Wissenschaft, Weiterbildung und Kultur/Rheinland-Pfalz to AS.

References

[1] Reyes-Puerta, V., Sun, J.J., Kim, S., Kilb, W., Luhmann, H.J. (2014): Laminar and Columnar Structure of Sensory-Evoked Multineuronal Spike Sequences in Adult Rat Barrel Cortex In Vivo. Cereb. Cortex: bhu007v1-bhu007.

[2] Becchetti A1, Gullo F, Bruno G, Dossi E, Lecchi M, Wanke E. (2012): Exact distinction of excitatory and inhibitory neu rons in neural networks: a study with GFP-GAD67 neurons optically and electrophysiologically recognized on multielec trode arrays. Front Neural Circuit, 6: doi: 10.3389.

[3] McCormick, D.A., Connors, B.W., Lighthall, J.W., Prince, D.A. (1985) Comparative electrophysiology of pyramidal and sparsely spiny stellate neurons of the neocortex. J. Neurophy siology, 54: 782-806.

[4] Henze, D.A., Borhegyi, Z., Csicsvari, J., Mamiya, A., Harris, K., Buzsaki, G. (2000) Intracellular Features Predicted by Extracellular Recordings in the Hippocampus In Vivo. J Neurophysiology 84: 390-400.

[5] Sun, J.-J., Kilb, W. and Luhmann, H. J. (2010): Self-organization of repetitive spike patterns in developing neuronal networks in vitro. European Journal of Neuroscience, 32: 1289–1299.

[6] Rowan, M., Tranquil, E., Christie, J. (2014): Distinct Kv Channel Subtypes Contribute to Differences in Spike Signaling Properties in the Axon Initial Segment and Presynaptic Boutons of Cerebellar Interneurons. J. Neuroscience, 34: 6611-6623.

[7] Biffi, E., Regalia, G., Menegon, A., Ferrigno, G., Pedrocchi, A. (2013): The Influence of Neuronal Density and Maturation on Network Activity of Hippocampal Cell Cultures: A Methodological Study. PLoS ONE 8(12): e83899.

Axon-Isolating Channels on a High Density Micro-electrode Array

Marta K. Lewandowska[1*], Douglas J. Bakkum[1], Andreas Hierlemann[1]

1 Department of Biosystems Science and Engineering, ETH Zürich, Basel Switzerland
* Corresponding author e-mail address: martal@bsse.ethz.ch

Abstract
A simple microfluidic device to supplement our high density CMOS MEA is used to better study axonal function. Axons grown through narrow channels over more than 50 closely spaced electrodes and the size of their spikes is enhanced by the structures such that single trials can be examined. Electrical interactions between axons are observed. Stimulation facilitates measuring propagation velocities and observing high frequency effects.

1 Introduction

Improved resolution of MEAs enables the study of single cells and even subcellular processes. In order to better interface with the axon, channels that isolate axons but connect two culture chambers have been added on top of our MEA. A number of groups have either built their own low density MEAs with channels on top [1],[2] or have attached commercial [3] or custom [4] channel devices on top of MCS MEAs. Our construction is unique in that individual soma can be identified and paired with their axons, and single spikes can be elicited by the on-chip stimulation and observed propagating across multiple sites.

2 Methods

Our MEA is fabricated in CMOS technology and features 11,011 Pt electrodes with a pitch of 17 µm and 126 reconfigurable readout and stimulation channels.[5] The axonal device is made of polydimethylsiloxane (PDMS) using a custom SU-8 mould. The two chambers are open on both ends and covered channels are 7 µm high, 12 µm wide, and 950 µm long; see Figure 1. Cortical cells from rat embryos (day 18-19) are dissociated and plated into the culture chambers.

3 Results

From observations of spontaneous spiking, a soma can often be matched to its axon in a channel using spike timing alone. The channels enhance the size of the axonal spike, which is otherwise hidden in the noise, from 10s of microvolts to 100s of microvolts andn up to 1 mV. Although the channels do not appear to distort the propagating spikes and simple spike shapes are observed, complex, highly reproducible waveform shapes are also seen, which could be the result of electrical coupling between axons.

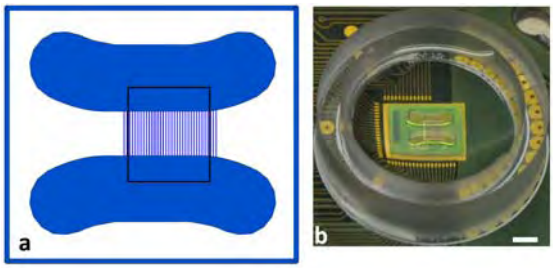

Figure 1: Layout of the microfluidic channel device and packaging on the chip. **a.** Layout of chambers, channels on the MEA (box is 1.7 x 2.0 mm^2) and **b.** packaging of MEA chip (glued and wire-bonded to PCB) with PDMS device sealed on top. Scale bar is 2 mm.

Stimulations in the channels show that axons from several different soma typically grown into a single channel, while stimulations of soma show that a relatively high proportion of axons branch before entering the channels. High frequency stimulations of soma (30-50 Hz) result in changes to the propagating spike: its width broadening and height decreasing until subsequently leading to failures; see Figure 2.

4 Conclusion

A device for studying axon information processing has been presented. It enables the tracking of individual action potentials from a single soma and through a long part of its axon with unprecedented time and spatial resolution. Interactions between axons are observed, as are failures along axons following high frequency stimulation.

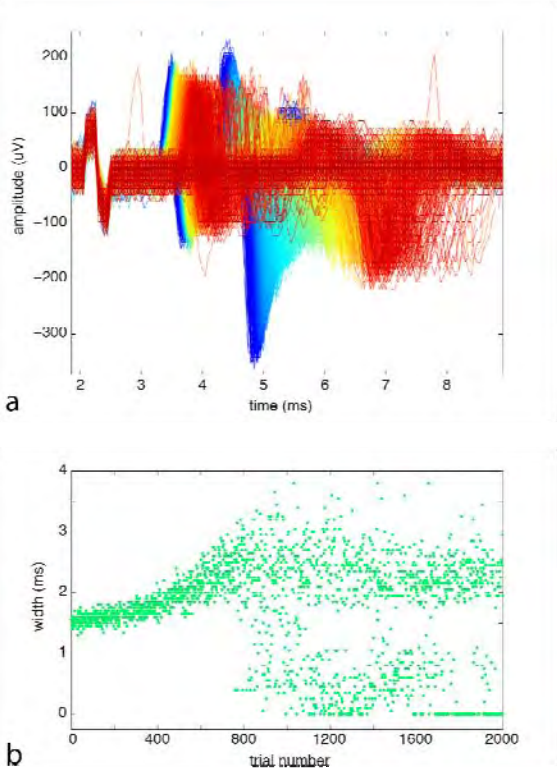

Figure 2: High frequency stimulation at the soma results in transmission failures along the axon. **a.** 50 Hz stimulation was repeated 2000 times with the results shown changing from blue to red (left to right). The latency of the spike increases, the width increases, and the height (negative peak) decreases until failures result. **b.** Peak width as a function of trial number showing the failures that result after 700 stimulations.

Acknowledgements

This work was supported by the Swiss National Science Foundation Ambizione Grant PZ00P3_132245 and the FP7 of the European Community through the ERC Advanced Grant 267351 'NeuroCMOS'.

References

[1] Wheeler, B. C.; Brewer, G. J., *Proceedings of the IEEE* **2010,** *98* (3), 398-406.

[2] Claverol-Tinturé, E.; Ghirardi, M.; Fiumara, F.; Rosell, X.; Cabestany, J., *Journal of neural engineering* **2005,** *2* (2), L1.

[3] Kanagasabapathi, T. T.; Massobrio, P.; Barone, R. A.; Tedesco, M.; Martinoia, S.; Wadman, W. J.; Decré, M. M., *Journal of neural engineering* **2012,** *9* (3), 036010.

[4] Brewer, G. J.; Boehler, M. D.; Leondopulos, S.; Pan, L.; Alagapan, S.; DeMarse, T. B.; Wheeler, B. C., *Frontiers in neural circuits* **2013,** *7*.

[5] Frey, U.; Sedivy, J.; Heer, F.; Pedron, R.; Ballini, M.; Mueller, J.; Bakkum, D.; Hafizovic, S.; Faraci, F. D.; Greve, F., *Solid-State Circuits, IEEE Journal of* **2010,** *45* (2), 467-482.

Pathomechanisms of Acquired Autoimmune Encephalitis Disorders Associated with Epilepsy and Anti-NMDA Receptors and Anti-LGI1 Autoantibodies

Elsen G. E.[1], Wolking S.[1], Maljevic S.[1], Wandinger K.P.[2], Lerche H.[1], Dihné M.[3]

1 Hertie Institute for Clinical Brain Research, Department of Neurology and Epileptology, University of Tübingen, Germany;
2 Institute for Clinical Chemistry and Department of Neurology, University Hospital Schleswig-Holstein, Lübeck, Germany
3 Department of Neurology, St. Lukas Klinik, Solingen, Germany

Background/Aims
Epilepsy is a common neurological disorder and in many patients the cause of seizures remains unknown. In recent years the identification of autoantibodies in cerebrospinal fluid (CSF) and serum of epilepsy patients has been reported as a possible link to the underlying etiology and pathogenesis. Currently, the antibodies most relevant to epileptology target ion channels and associated proteins, such as NMDARs and LGI1 protein, which is known to form complexes with VGKCs and AMPARs. Anti-NMDAR-encephalitis is a recently discovered autoimmune disorder caused by antibodies against the NMDARs and is characterized by a severe encephalopathy with psychosis, epileptic seizures and autonomic disturbances. LGI1 autoantibodies have been identified in patients with autoimmune limbic encephalitis, which is characterized by loss of memory, psychological disturbances and epileptic seizures. The overall goal of this project is to lead to a rapid prediction of the pathological role of the antibodies in the prognosis of the autoimmune epileptic disorders and identify pharmacological strategies for the reversal of the effects.

1 Methods

To better understand the pathological mechanisms of antibodies in autoimmune epilepsies and design more rapid therapeutical strategies, we first obtained in vitro neuronal networks from dissociated murine hippocampal neurons. Then, the effects of pure pathological CSF (pCSF) from anti-NMDAR and anti-LGI1 autoimmune epilepsy patients or CSF from normal controls (hCSF) were recorded using multielectrode arrays (MEAs). Signals from all 60 electrodes were simultaneously sampled at 25 kHz, visualized and stored using the software MC_Rack provided by Multi Channel Systems. Spike and burst detection was performed off-line by custom built software (Result, Düsseldorf, Germany).

2 Results

We first describe the effects of pCSF from an anti-NMDAR encephalitis patient on in vitro neuronal network activity (ivNNA). pCSF taken during the initial weeks after disease onset suppressed global ivNNA in contrast to pCSF sampled after clinical recovery and decrease of NMDAR antibody titers. The synchrony of pCSF-affected ivNNA remained unaltered during the course of the disease. In order to further verify effects of pCSFon ivNNA, 6 additional CSF samples from anti-NMDAR encephalitis patients and 2 CSF samples form anti-LGI1 encephalitis patients were tested on MEAs. pCSF of anti-NMDAR and anti-LGI1 encephalitis patients showed a decrease of global network activity compared to hCSF controls, while network synchrony was not significantly affected.

3 Conclusion/Summary

We are in the process of conducting pharmacological experiments using synaptic modulators of NMDARs, VGKCs and AMPARs and known therapeutic antiepileptic agents to recapitulate the effects of autoantibodies on ivNNA and to determine which synaptic transmission pathway is affected by the pathological antibodies and aim to reverse the pathological effects. Furthermore, we are generating functional human ivNNA to provide a more adequate model system to test the functional effect of pCSF changes. This will be the first study to compare the functional effects of antibodies from several forms of CNS encephalitis patients on murine or human neuronal networks, and could represent a step in the direction of identifying a unique in vitro diagnostic test for autoimmune disorders in general.

Effects of Epilepsy-Associated Ion Channel Mutations on Neuronal Network Activity

Snezana Maljevic[1], Yvonne Füll[1], Heidi Löffler[1], Filip Rosa[1], Yuanyuan Liu[1], Holger Lerche[1]

1 Dept. of Neurology and Epileptology, Herti Institute for Clinical Brain Research, University of Tübingen, Tübingen, Germany

Background/Aims
Epilepsy is a common neurological disorder underlined by diverse factors, with the genetic component contributing to approximately 40% of all cases. Among the affected genes, the ones encoding ion channels are the most represented. Two voltage-gated channels residing at axon initial segments of principal neurons in brain have been linked to neonatal (K_V7.2, gene *KCNQ2*) or neonatal-infantile (Na_V1.2; gene *SCN2A*) benign epilepsy seizures. We use murine primary hippocampal cultures to analyze the effects of different disease-causing mutations found in these channels on the network activity *in vitro* via micro-electrode arrays (MEA) technique.

1 Methods

Effects of two mutations affecting K_V7.2 channels were studied in primary neuronal cultures obtained from E17 +/- *kcnq2* mice. For this purpose, we tagged WT and mutant K_V7.2 with green fluorescent protein (GFP), cloned them into a lentiviral vector and infected neurons plated on MEA chips. The transduction efficiency was >80% and the neuronal network activity was recorded at different time points after infection. To analyze the impact of a *SCN2A* mutation, E17 primary hippocampal cultures, derived from mice carrying an epilepsy-causing mutation inserted at the homologous place in the mouse *scn2a* gene, have been plated on MEA chips and the activity of WT, +/mut and mut/mut neurons analyzed at different days after plating.

2 Results

Compared to the WT cultures, *kcnq2* +/- neurons showed enhanced excitability, i.e. increased number of spikes and peak firing rate. The same was observed when the mutant K_V7.2 channels were expressed, whereas infection of cultures with the WT channel reduced the network activity, revealing its rescuing effect. Neuronal network activity of cultures obtained from *SCN2A* knock-in mouse is being assessed in undergoing experiments.

3 Conclusion/Summary

MEA technique can successfully be applied to analyze activity of neuronal networks obtained from genetically modified mice. Even more, the lentiviral transduction system used in this study, with its high efficiency and low toxicity, can enable analysis of large number of mutations related to different diseases characterized by hyperexcitability. Thus far obtained results indicate increased *in vitro* activity of neuronal networks expressing epilepsy-related mutations. Such networks may present a useful tool for drug screening..

Neuron and Network Properties

Signal Analysis and Statistics

Paired Spiking Is an Ubiquitous Response Property in Network Activity

Aurel Vasile Martiniuc[1*], Rouhollah Habibey[2], Asiyeh Golabchi[2], Victor Bocos-Bintintan[3], Alois Knoll[1], Axel Blau[2]

1 Computer Science Department VI, Technical University Munich, Garching, Germany
2 Dept. of Neuroscience and Brain Technologies (NBT), Fondazione Istituto Italiano di Tecnologia (IIT), Genoa, Italy
3 Faculty of Environmental Science & Engineering, Babes- Bolyai University, Cluj-Napoca, Romania
* Corresponding author. E-mail address: martiniv@in.tum.de

Abstract

In paired spiking (PS), a neuron generates two action potentials within a time window of 2-5 milliseconds followed by a refractory period up to several hundred milliseconds. Regardless of the neuroscientific context, whether in cultured neural networks or in intact brain architectures, in spontaneous activity or in response to stimuli, PS has been found in any type of spike trains. Recent evidence shows that PS forms spatiotemporal patterns and participates in establishing functional and effective connectivity in networks of cultured neurons of different types [1]. Another prominent example is PS participation in neural communication at the retinogeniculate synapse *in vivo* [2]. However, little is known on the richness and robustness of its function and its coding mechanisms at both single cell and network level. Here, we show that PS activity forms robust activity patterns with most frequently occurring inter-paired spike intervals (mfoIPSIs) of 1 sec. Its shape within the recorded spike trains of retinal ganglion cells (RGCs) is furthermore preserved between local sites and at network level under different stimuli conditions. Furthermore, PS carries information on the stimulus that was applied to the receptive field of the recorded RGCs. However, the information density differs for different cell types. This suggests that PS may change its contribution to information transmission relative to the type of the recorded cell according to its morphological, physiological and structure-function classification.

1 Backround

Ursey *et al.* explained how PS enhancement may shape the neural response *in vivo* [2]. Recent findings show that a key role within the concept of sparse coding efficiency is played by PS activity. Both *in vivo* and *in vitro*, PS preserves information from one stage to the next in both stimulated and spontaneous activity [1], [3]. Presumably, it represents an ubiquitous response property of different types of neurons in different species. Here, we analyzed extracellularly recorded activity from different types of RGCs, using different stimuli, and discuss PS involvement in shaping retinal spike trains and its role in information processing. Additionally, in simulations [4], we quantify the PS-related information being transmitted to a modeled postsynaptic neuron.

2 Methods

We analyzed extracellularly recorded stimulated neural activity from different isolated retinal slices from mice and rabbits using multielectrode arrays (Multichannelsystems). For mouse retinal whole mounts, we repeatedly applied light pulses of 1.5 s duration by LEDs emitting at different wavelengths [5]. The second stimulus consisted in moving grating bars at different directions over the rabbit retinal slices, which allowed us to calculate the direction selectivity index (DSi) [4]. In this case, we used an Integrate and Fire model to simulate the postsynaptic counterpart for each recorded RGC [4]. For both stimuli, we extracted the PS activity within the recorded spike trains. We then quantified the information content that PS carried about the stimulus with respect to that of the overall spike activity [1]. However, we only considered the relative percentage by dividing the mutual information (MI) carried by PS-related activity by that carried by the entire spike train [1].

3 Results

Recently it has been shown that PS develops activity patterns in spontaneous neural activity of cultured neural networks [1]. Our results indicated that spatiotemporal PS patterns are robust in all trials. We found that the number of mfoIPSIs from individually recorded RGCs could reach 250 while at network level numbers up to 600 were counted. The highest number of PS for a trial at individual recording sites was ≤1500 while the number of PS at network level was ≤2500 (Fig. 1 c and d). The inter-paired-spike interval (IPSI) distribution at both single site and network level shows that the mfoIPSI was steady at 1 sec. for all trials (Fig. 1 a and b). The information processing function had different shapes for different cell types. Thus, the mean amount of information about the stimulus that was carried by PS related activity was varying from 5% up to 60% (Fig. 2b). However, at net-

work level, it was fluctuating less between 20% and 30% (Fig. 2c).

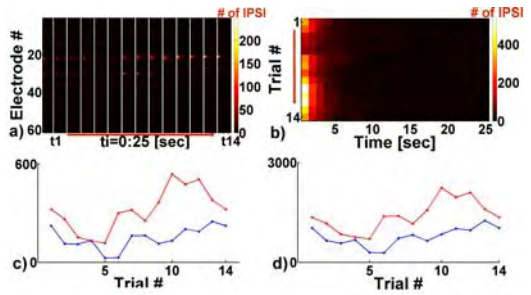

Fig. 1. IPSI distribution at individual sites a) and network level b). c) Number of repetitions of mfoIPSI at network level (red) and at individual sites (blue). d) Number of PS at network level (red) and highest number of PS at individual sites (blue).

Fig.2a depicts the evolution of PS-related information for each trial at individual channels showing a rather robust shape for each channel at different trials.

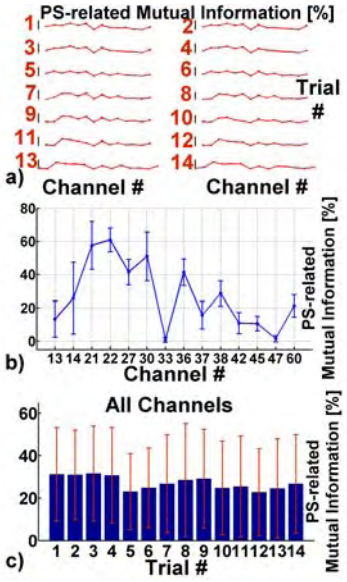

Fig. 2. a) PS-related information carried by each channel (X axis) as depicted in b), for each trial (Y axis). Vertical bars represent 100%. Mean PS-related information carried by each channel for all trials (b) and for each trial by all channels (c).

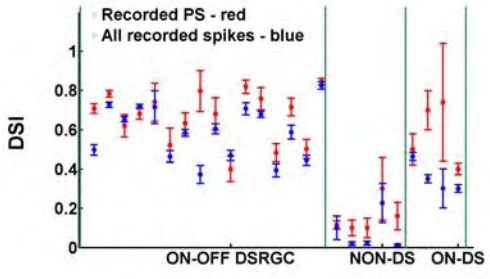

Fig. 3. DSi for PS (red) and for the entire spiking activity (blue) for different RGCs separated by green vertical bars.

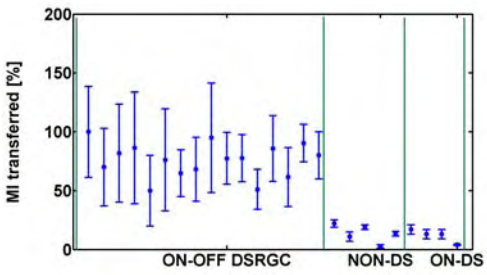

Fig. 4. Percentage of PS-related mutual information (MI) transferred to the modelled postsynaptic counterpart for each RGC. Lower values are for non directional cells (NON-DS) and for ON-DSRGCs (ON-DS).

Applying a drifting grating bar stimulus we found that PS-related information that had been transferred to the modeled counterpart neuron in the lateral geniculate nucleus (LGN) was between 50% and 98% for ON-OFF DSRGCs and much below 50% for other types of RGCs (Fig. 4). However, the DSi was always higher for PS than for the entire recorded spiking activity for all cells (Fig. 3).

4 Conclusion

Our findings show that PS shapes the neural activity in recorded RGCs under stimulus condition. While PS forms robust spatiotemporal patterns for all types of cells, its shape varies with cell type. Interestingly, the information carried by PS varied with cell type as well. For instance, for ON-OFF DSRCs, PS activity carries most of the information regarding the stimulus direction. This finding is sustained by morphological and functional explanations. For example, ON-OFF DSRGCs perform one-to-one connectivity with their LGN counterparts. Thus, PS from a single cell becomes crucial, while in ON-DSRGCs multiple cells send convergent inputs toward their counterparts in the accessory optic system (AOS). Presumably, the information is enriched as a consequence of heterosynaptic mechanisms. The latter mechanism holds true at higher brain areas and suggests that PS changes its shape from mono- to polysynaptic contributions.

References

[1] Martiniuc , A.V., Blau, A. and Knoll, A. Paired spiking activity robustly shapes spontaneous activity. (submitted)

[2] Usrey, W.M., Reppas, J.B. & Reid, R.C. Paired-spike interactions and synaptic efficacy of retinal inputs to the thalamus. Nature 395(6700), 384-387. (1998).

[3] Sincich, L. C., Horton, J. C. & Sharpee, T.O. Preserving information in neural transmission. The Journal of Neuroscience 29(19):6207– 6216, 6207. (2009).

[4] Martiniuc AV, Zeck G, Stürzl W, Knoll A. Sharpening of directional selectivity from neural output of rabbit retina. J. Comput. Neurosci. 30(2):409-26. (2011).

[5] Blau, A., Murr, A., Wolff, S., Sernagor, E., Medini, P., Iurilli, G., Ziegler, C. and Benfenati, F. Flexible, all-polymermicroelectrode arraysf or the capture of cardiac and neuronal signals. Biomaterials 32 : 1778-1786. (2011).

Cultured Cortical Neurons Can Separate Source Signals from Mixture Inputs

Takuya Isomura[1,2*], Kiyoshi Kotani[3], Yasuhiko Jimbo[3]

1 Department of Human and Engineered Environmental Studies, Graduate School of Frontier Sciences, The University of Tokyo, Tokyo, Japan
2 Japan Society for the Promotion of Science (JSPS), Tokyo, Japan
3 Department of Precision Engineering, School of Engineering, The University of Tokyo, Tokyo, Japan
* Corresponding author. E-mail address: isomura@neuron.t.u-tokyo.ac.jp

Abstract
Blind source separation such as independent component analysis (ICA) is essential for information processing in neural systems. Using microelectrode array (MEA) system, we demonstrated that cultured neurons can separate source signals from the mixture inputs. After training, evoked response specialized a side of 2 hidden signal sources, indicating that these neurons came to decode a signal from a hidden signal source.

1 Introduction

Blind source separation such as cocktail party effect [1] is essential for information processing in neural systems, which has been modelled as independent component analysis (ICA) in theoretical neuroscience [2]. In computational studies, ICA has been represented by the non-linear firing rate neuron model [2] and the spiking neuron model [3]; however, there has been little experimental evidence of blind source separation in actual neural networks. Here, using microelectrode array (MEA) system [4], we demonstrated that cultured neurons can separate source signals from the mixture inputs.

2 Methods

Cortical cells were taken out from E19 rat embryos and dissociated. 5×10^5 cells were seeded on MEA dishes and cultivated 18-80 days. We induced into the neurons electrical pulse trains $s_1(t)$, …, $s_{32}(t)$ with 1 s interval and 256 s length from 32 electrodes of MEA [4]. The trains were constructed from two independent binary signal sources $\mathbf{u}(t) = (u_1(t), u_2(t))$, $u_1(t), u_2(t) \in \{0, 1\}$. At each time period, $s_1(t)$, …, $s_{16}(t)$ were randomly selected by $u_1(t)$ with a probability of 3/4 or $u_2(t)$ with that of 1/4 at each time periods, while $s_{17}(t)$, …, $s_{32}(t)$ were randomly selected by $u_1(t)$ with a probability of 1/4 or $u_2(t)$ with that of 3/4. A cycle was constructed from the stimulating time with these trains and 244 s resting time. 111 cycles of stimulation were induced into each culture. Evoked responses to the input trains were recorded from 64 electrodes of MEA. The valleys of extracellular potentials lower than $\mu - 5\sigma$ were defined as spikes, where μ and σ represent the mean and the standard deviation of the potential recorded at each electrode. The number of evoked spikes of neuron i during 100 ms after each stimulation was defined as $x_i(t)$. We calculated Kullback-Leibler divergence (KLD) [5], the distance between two distributions, between $P(x_i \mid \mathbf{u}=(1,0))$ and $P(x_i \mid \mathbf{u}=(0,1))$, which is represented as

$$\begin{aligned} &D_{KL}(P(x_i \mid \mathbf{u}=(1,0)) \,||\, P(x_i \mid \mathbf{u}=(0,1))) \\ &= \sum_{k=0}^{\infty} P(x_i = k \mid \mathbf{u}=(1,0)) \log \frac{P(x_i = k \mid \mathbf{u}=(1,0))}{P(x_i = k \mid \mathbf{u}=(0,1))} \\ &= \lambda_{i1} \log (\lambda_{i1} / \lambda_{i2}) - \lambda_{i1} + \lambda_{i2}, \end{aligned} \quad (1)$$

where we assumed that conditional probabilities $P(x_i \mid \mathbf{u}=(0,1))$ and $P(x_i \mid \mathbf{u}=(0,1))$ obeyed Poisson distribution. $P(x_i \mid \mathbf{u}=(0,1))$ and $P(x_i \mid \mathbf{u}=(0,1))$ were parameterized by the intensities of evoked activity λ_{i1} and λ_{i2}, respectively. Estimated values of λ_{i1} and λ_{i2} were obtained using maximum likelihood estimation. Note that we evaluated KLDs of neurons near to non-stimulated electrodes.

3 Results

Figure 1A shows examples of the raster plots of evoked response at 9 electrodes in a culture before- (left panels) and after (right panels) the training period. These 9 electrodes were picked up from electrodes at which the changes in the neural activity were observed. Red and blue dots show evoked spikes when the state of hidden signal sources were $\mathbf{u}$ = (1, 0) and $\mathbf{u}$ = (0, 1), respectively. After training, neurons near to stimulated electrodes $s_1(t)$, …, $s_{16}(t)$ (top panels) tended to increase their evoked activity when $\mathbf{u}$ = (1, 0), while neurons near to $s_{17}(t)$, …, $s_{32}(t)$ (middle panels) were more activated when $\mathbf{u}$ = (0, 1). Neurons near to non-stimulated electrodes (bottom panels) showed various changes. Then we focused on the changes in activities of neurons near to non-stimulated electrodes.

Adaptation to signal sources was evaluated using the difference in expectations of KLDs before- and after the training period. Figure 1B shows the change in the mean KLDs. Dots indicate the mean KLDs averaged with all recorded neurons near to non-stimulated electrodes in each culture. A gray line indi-

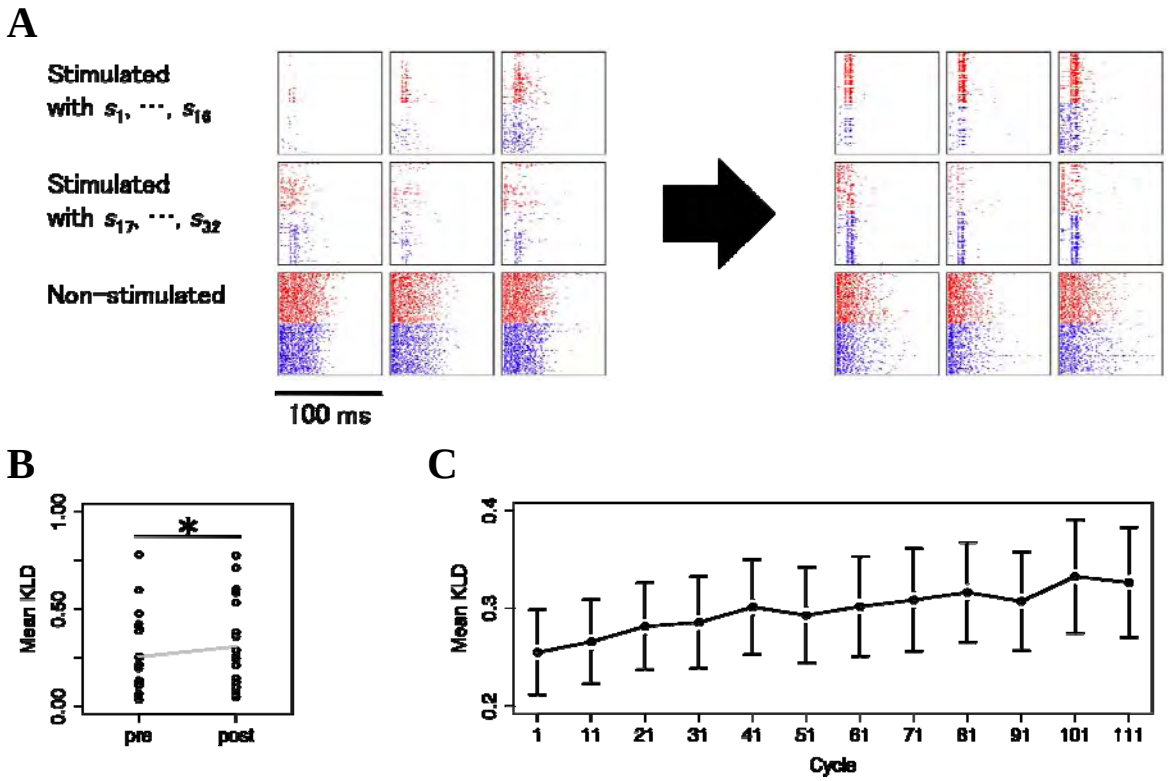

Fig. 1. Alternation in the neural activity. (A) The raster plots of evoked responses at 9 electrodes in a culture. (B) The change in the mean KLDs calculated using neurons near to non-stimulated electrodes. $n = 21$, *, $p < 0.05$ with paired t-test. (C) The transition of the mean KLD. Bars are standard errors.

cates the mean KLD averaged with all samples ($n = 21$) pre- and post-training. We observed increases of the mean KLDs after training ($n = 21$, *, $p < 0.05$ with paired t-test). Figure 1C shows the transition of the mean KLD averaged with all samples. Bars indicate standard errors. As inducing the training stimulation, the mean KLD gradually increased, indicating that evoked response shifted to specialize a side of 2 hidden signal sources. The result suggests that the cultured neurons came to decode a signal from a hidden signal source.

4 Discussion

Previous studies on cultured neural networks have revealed properties of learning and memory, e.g., pathway-specific synaptic plasticity induced by local tetanic stimulation [6], supervised learning [7], and pattern recognition [8]; however, the neural basis of blind source separation has been rarely examined using actual neurons. We found that neural responses shifted to specialize a side of 2 hidden signal sources, and that KLDs of neurons near to non-stimulated electrodes increased after training while inputs were the mixture of sources. The result suggests that even in dissociated cultures of cortical neurons, neural circuits have the ability of blind source separation.

Acknowledgement

This work was supported by Grants-in-Aid for Science Research (23240065; the Japanese ministry of Education, Culture, Sports, Science and Technology).

References

[1] Bronkhorst, A. W. (2000). The cocktail party phenomenon: A review of research on speech intelligibility in multiple-talker conditions. Acta Acustica united with Acustica, 86(1), 117-128.

[2] Bell, A. J., & Sejnowski, T. J. (1997). The "independent components" of natural scenes are edge filters. Vision research, 37(23), 3327-3338.

[3] Clopath, C., Büsing, L., Vasilaki, E., & Gerstner, W. (2010). Connectivity reflects coding: a model of voltage-based STDP with homeostasis. Nature neuroscience, 13(3), 344-352.

[4] Jimbo, Y., Kasai, N., Torimitsu, K., Tateno, T., & Robinson, H. P. (2003). A system for MEA-based multisite stimulation. Biomedical Engineering, IEEE Transactions on, 50(2), 241-248.

[5] Bishop, C. M. (2006). Pattern recognition and machine learning. New York: springer.

[6] Jimbo, Y., Tateno, T., & Robinson, H. P. C. (1999). Simultaneous induction of pathway-specific potentiation and depression in networks of cortical neurons. Biophysical Journal, 76(2), 670-678.

[7] Shahaf, G., & Marom, S. (2001). Learning in networks of cortical neurons. The Journal of Neuroscience, 21(22), 8782-8788.

[8] Ruaro, M. E., Bonifazi, P., & Torre, V. (2005). Toward the neurocomputer: image processing and pattern recognition with neuronal cultures. Biomedical Engineering, IEEE Transactions on, 52(3), 371-383.

High-Throughput, High-Performance, Low-Latency Spike-Sorting Hardware Platform

Dragas Jelena*, Jäckel David, Franke Felix, Hierlemann Andreas

ETH Zurich, Department of Biosystems Science and Engineering, 4058 Basel, Switzerland
* Corresponding author. E-mail address: jelena.dragas@bsse.ethz.ch

Abstract
The ever-growing number of simultaneously recorded electrode signals in HDMEA-based neural recording systems imposes high demands on data-storage units. In on-line personal-computer-based neural signal processing systems, the processing latency is determined by the communication delay between the electrode array and the personal computer (host machine). Processing signals on a dedicated hardware allows for extraction of the relevant data (spike times/spike waveforms) prior to storing, hence, significantly reducing the data storage requirements. The simplified data communication protocols between the electrodes and the signal processing platform, as compared to the ones between the electrodes and the PC, allow for low data latencies, suitable for closed-loop experiments. Here we present a spike-sorting hardware platform, capable of processing recordings containing both single and overlapping neural spikes with an error of 0.04, taking into account errors due to false positive and false negative spikes. The latency is 2.75ms, well in the range required for neural synapse manipulation in closed-loop experiments.

1 Background

The number of electrodes in today's state-of-the-art high-density multi-electrode arrays (HDMEAs) is on the order of thousands. Consequently, the amount of memory needed to store the recorded data for later processing is in the range of terabytes. Performing the processing on-line by extracting only the spike times and spike waveforms from the recordings decreases the storage requirements. On-line spike processing is also required for so-called "closed-loop" experiments. Here, the recorded neural cells in the network are stimulated based on the most recent network activity. The latency between the activity occurrence and the stimulation should be in the range of a few milliseconds [1]. However, performing on-line spike sorting on a personal computer cannot guarantee a short enough latency. Here, the latency is usually in the range of a few tens of milliseconds due to the complex data communication between the recording device and the software running on the personal computer. Further, HDMEA recordings usually target high-density neural networks, which leads to recordings of signals from different cells on the same electrodes – spike overlaps.

In this work, we present an FPGA-based hardware platform running an optimized Bayes-optimal template matching (BOTM) algorithm [2]. The hardware performs template matching in real time and features pair-wise spike-overlap decomposition.

2 Method

The hardware architecture is based on parallel filtering operations, which are multiplexed (folded) in time in order to save hardware resources and to allow for processing of more neuronal signals at a time. The spike templates are calculated off-line (see [2] for more details) on a host machine and loaded into the FPGA periodically to adapt the processing to the changing recording environment. The template loading does not interrupt the normal algorithm operation. Figure 1 shows the impact of architecture folding on hardware resource utilization. Typically, each neuron is simultaneously recorded by several surrounding electrodes while using HDMEAs.

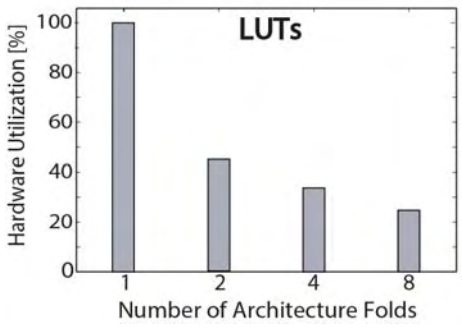

Fig. 1. Hardware utilization as a function of architecture folds. The number of neurons in each architecture is 64. The utilization is represented in the number of look-up tables (LUTs) of a Virtex 6 device. The values are normalized by the one-fold system hardware utilization in which 5 electrodes (Ne=5) are considered per each neuron ($180 \cdot 10^3$ LUTs).

The figure shows results for the case that 5 electrodes are considered per individual neuron. The results imply that a medium-size Virtex 6 FPGA device can process around 250 neurons simultaneously.

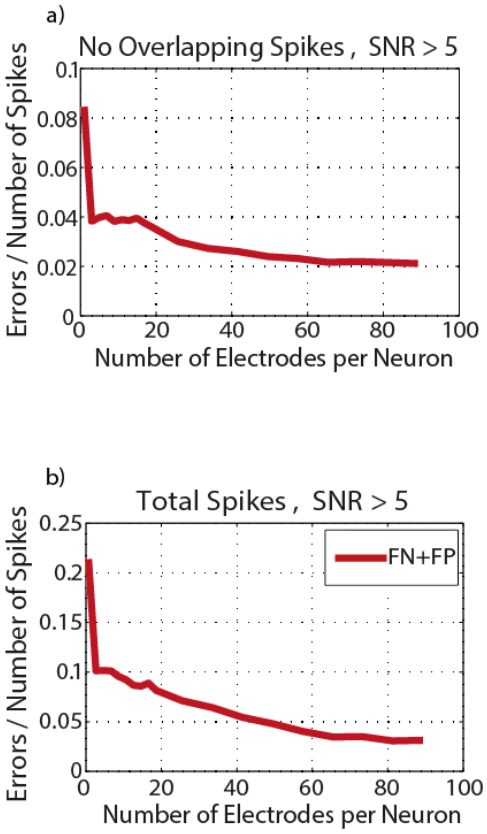

Fig. 2. Hardware spike-sorter performance assessment. Error rate as a function of the number of electrodes per neuron (Ne). The results represent average error rates for around 1000 processed neurons.

3 Results and Conclusion

The spike-sorting performance was evaluated on semi-realistic retinal ganglion data. Figure 2 shows results for a cell density of 2887 cells/mm2. The considered neurons have an SNR > 5. SNR of a neuron with a multi-electrode template, ξ, is calculated as SNR= $max(|\xi|)/\sigma$ (σ being the standard deviation of the noise on an electrode, on which the template ξ has the maximal absolute value).

The error rate is calculated as: E=(FN+FP)/Ns. FP represents the number of spikes that were falsely detected (“false positives”), FN the number of spikes present in the recordings that have not been detected (“false negatives”), and Ns represents the true number of spikes in the data.

The hardware spike-sorting platform provides an error rate as low as 0.02 for non-overlapping spikes and 0.04 for all spikes in the recording. The pair-wise overlap decomposition brings the processing latency to 2.75ms, well within the range needed for neural synapse manipulation. The folded architecture design enables several hundred neurons to be processed simultaneously.

Acknowledgement

This work was financially supported by the European Community through the ERC Advanced Grant 267351, “NeuroCMOS”.

References

[1] G.-Q. Bi, M.-M. Poo, “Synaptic modification by correlated activity: Hebb’s postulate revisited,” A. Review of Neurosci., pp. 139–166, 2001.

[2] F. Franke, “Real-time analysis of extracellular multi-electrode recordings,” PhD Thesis, Technische Universität Berlin, 2011. Available at: http://opus.kobv.de/tuberlin/volltexte/2012/3387.

CARMEN, HDF5 and NDF: Reproducible Research on MEA Signals from Mouse and Ferret Retina.

L. S. Smith[1*], S. J. Eglen[2], E. Sernagor[3]

1 Computing Science and Mathematics, University of Stirling, Stirling FK9 4LA, Scotland UK
2 DAMTP, Centre for Mathematical Sciences, University of Cambridge, Cambridge CB3 0WA, England, UK
3 Institute of Neuroscience, Faculty of Medical Sciences, University of Newcastle, Newcastle upon Tyne NE2 4HH, England, UK
* Corresponding author. E-mail address: l.s.smith@cs.stir.ac.uk

Abstract
CARMEN is a portal based collaborative facility for neuroscientists (and in particular electrophysiologists) to share data and tools for working on data. Here it is applied to retinal datasets, enabling reuse of existing data.

1 Background

The CARMEN Virtual Laboratory [1] is a collaborative online facility for neuroscientists. Data can be uploaded to (and downloaded from) the repository, and shared with other neuroscientists. Services which process the uploaded datasets to produce new data, and workflows composed from these services can operate on datasets. Extensive metadata can be attached to the data, and a search facility allows data and services to be located in the repository. Fine-grained security of access is available. The system is currently targeted towards electrophysiology data, predominantly MEA and EEG data. A novel internal data format (Neural Data Format: NDF [2]) was developed: by using services to translate to this format, services and workflows can cope with the many different formats that recorded data from different equipment may have. While NDF is open, it is not based on the HDF5 standard, and this has restricted its usage. The HDF5 working group of the INCF Electrophysiology Task force is developing a new standard based on HDF5, but in the meantime, a major study enabling reproducible research on MEA signals from mouse and ferret retina using an HDF5 format has been undertaken [3], and a service to translate this HDF5 format to NDF created.

2 Methods

In this study, datasets originating from 12 different laboratories were used: this entailed writing functions (using R) to parse the different data formats, in order to create datasets in a single (HDF5) based format: HDF5 was used to enable future-proofing of access to the data. The MEAs used had from 60 to 4,096 electrodes, and recordings varied from 2 to 450 minutes. The data was stored as a set of objects in the root of the HDF5 tree, and the metadata in the /meta/ group of the tree. Initial processing of the dataset in CARMEN uses the HDF5 to NDF service: this allows many different services (which can be written in Matlab, Python, R, C/C++ or Java) to be run on the data, and these services can be concatenated to form workflows. For this specific task, two new services were created: a burst detection service, and a graphing service, which plots durations of multiple input files.

A generic HDF5 to NDF converter is not yet possible: this requires a generic HDF5 specification for neural recordings, and this is under development by the INCF Task Force. Once an HDF5 standard is at a sufficiently mature level, a generic HDF5 to NDF converter will be deployed.

3 Summary

The repository allows re-analysis of the original data either directly on CARMEN, using its services, or by downloading the datasets to researchers' own systems. The repository provides public datasets of MEA data, and will, we hope, encourage future researchers to share data. By using an open standard, datasets should remain universally readable. The datasets and services are now publicly available: prospective users should first register with the CARMEN portal. We hope that others sets of datasets will become available in the near future.

Acknowledgement

We acknowledge the contribution of the UK Research Councils (EPSRC grant EP/E002331/1 and BBSRC grant BB/I001042/1) towards this work.

References

[1] https://www.portal.carmen.org.uk.
[2] http://www.carmen.org.uk/standards/CarmenDataSpecs.pdf
[3] S. J. Eglen, M. Weeks, M. Jessop, J. Simonotto, T. Jackson, E. Sernagor, A data repository and analysis framework for spontaneous neural activity recordings in the developing retina, *GigaScience* 3: 3, 2014 http://www.gigasciencejournal.com/content/3/1/3

Post Stimulus Activity Patterns Reflect Stimulus Responses

Jelle Dijkstra[1] and Joost le Feber[1,2*]

[1] Biomedical Signals and Systems, University of Twente, Enschede, the Netherlands
[2] Clinical Neurophysiology, University of Twente, Enschede, the Netherlands
* Corresponding author. E-mail address: j.lefeber@utwente.nl

Abstract
We developed a small-scale computational network using standard neuron and synapse models and spike-timing-dependent plasticity. Such networks develop a balance between intrinsic activity and connectivity. In this balance, the spontaneous activity patterns support the current connectivity. Stimulation disturbs the equilibrium, and leads to changes in synaptic weights, affecting the shape of the burst patterns after stimulation. To quantify this change, we used a correlation-based similarity measure between a network burst and a stimulus response. The average similarity between the stimulus responses and the post-stimulus bursts was significantly higher than the average similarity to the pre-stimulus bursts. This implies that stimulus induced activity, that does not fit the current equilibrium between activity and connectivity, appears in the spontaneous activity after stimulation.

1 Introduction

Cultured neuronal networks on MEAs become spontaneously active after approximately 1 week of culturing. Activity patterns depend on the connectivity of the network, and, vice versa, connectivity is affected by activity patterns. We hypothesize that the activity and connectivity form an equilibrium where the intrinsic activity maintains the current connectivity. Stimuli, that induce activity patterns that do not fit with this equilibrium may drive the network to a new equilibrium that does incorporate this new pattern. If this is true, stimulus responses should differ significantly from pre stimulation activity patterns, and become more similar to post stimulation patterns.

We performed a modeling study to verify this hypothesis in a small scale computational network. Then we validated our findings in cultured networks.

2 Methods

2.1 Modeling

We modeled a network with a total of 100 neurons [1], of which 80 were excitatory and 20 inhibitory. On average, every neuron was connected to 50% of the other neurons with synapses by [2]. The axons were modeled as randomly chosen delays (1-10ms). A spike-timing-dependent plasticity model with additive increase and multiplicative decrease similar to [3] was included as the only form of long-term plasticity. Networks were activated by normally distributed noise added to the membrane potentials of all neurons.

After reaching a stable weight distribution, we stimulated a network by simultaneously making a set of three neurons fire an action potential, usually sufficient to cause a network wide response. We used three distinct initial networks and four disjoint sets of neurons each, leading to 12 simulations. The networks were stimulated for 2h with an inter-stimulus-interval of 8s. Three hours of spontaneous activity was measured before and after stimulation.

2.2 Experimental data

We did 9 experiments on 4 cultures. Each had a 60 min pre- and post-stimulus recording, separated by 2 hours of single electrode stimulation at 0.125 Hz.

2.3 Data analysis

We measured changes in the relative weights of the synapses, which were limited to the unit interval, by the Euclidean distance between two weight matrices. $ED_0(t')$ denoted the Euclidean distance between the weight matrix at t=t' with the weight matrix at t=0.

During phases of no stimulation, network bursts were extracted using the algorithm by [4] and categorized as pre- and post-stimulus bursts. Both bursts and stimulus responses are denoted as synchronous bursting events (SBEs) and their similarity was calculated using the algorithm by [5], which was adapted such that similarity was bounded within the unit interval.

3 Results

All models reached a stable equilibrium between activity and connectivity within2 days of simulated time. Beyond that point synaptic weights showed independent fluctuations around a stable mean.

Figure 1 shows the change in synaptic weights during the stimulation protocol, averaged over all simulations. Before stimulation at t=3h, ED_0 increases slightly due to individual fluctuations of the weights.

Stimulation causes significant weight changes. After the stimulation, the weights return towards their original distribution after circa 20h (not shown). Figure 2 shows the similarities between all the synchronous bursting events in one of the simulations.

Similarities among the stimulus responses, located in the center of the matrix, was high compared with the other similarities. In addition, the stimulus re-

sponse stabilized after approximately one fourth of the stimulation.

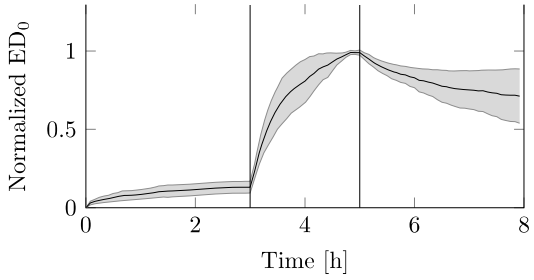

Fig. 1. Development of ED_0 due to stimulation was normalised per simulation by its maximum and averaged over all simulations. Vertical bars indicate stimulation phase. Shaded areas depict the unbiased sample estimate of the standard deviation.

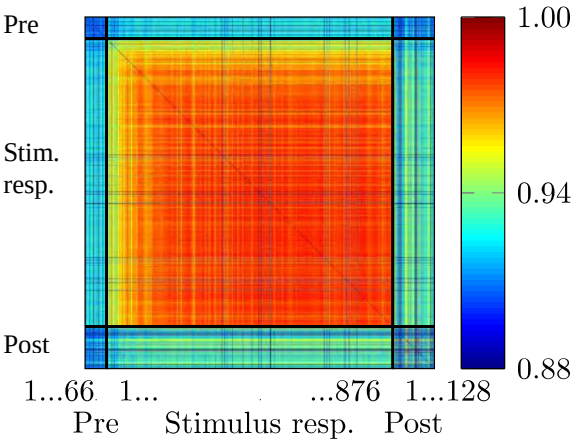

Fig. 2. Similarities between all the synchronous bursting events in one of the simulations categorized as pre-stimulus bursts (Pre), stimulus responses and post-stimulus bursts (Post).

Figure 3 shows the average similarity between a stimulus response and all pre- / post-stimulus bursts for one of the simulations. Both similarities are similar at first, and the last 400 stimulus responses become more similar to the post-stimulus bursts than to the pre-stimulus bursts.

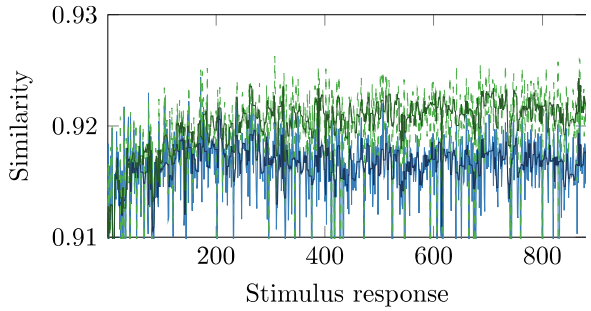

Fig. 3. Average similarity of a stimulus response with all pre-stimulus bursts (blue, bottom) and post-stimulus bursts (top, green) in one of the simulations.

For every simulation, the average similarity between all stimulus responses and all pre- / post-stimulus bursts was calculated, yielding a total of 12 similarity pairs. The average similarity of the stimulus responses to the post-stimulus bursts was significantly higher than to the pre-stimulus bursts (one-sided Wilcoxon signed rank, p=0.0007).

In 7 of 9 experiments we were able to obtain persistent stimulus responses. Figure 4 shows that averaged over all experiments, a stimulus response has a higher similarity with the bursts after stimulation than before, but the difference is not significant.

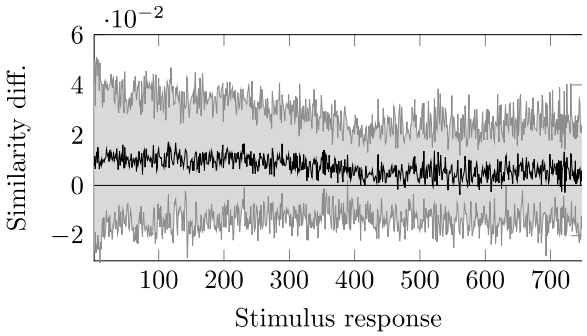

Fig. 4. Similarity of a stimulus response with all bursts after stimulation minus the similarity with all bursts before stimulation, averaged over all successful experiments. Shaded areas depict the unbiased sample estimate of the standard deviation.

4 Discussion

Our network does not use any global activity regulation mechanisms, yet a stable equilibrium can be obtained due to a multiplicative decrease in the STDP model. Stimulation, however, alters the synaptic weights, such that spontaneous activity patterns after stimulation have higher similarity to the stimulus responses than the patterns before stimulation.

Our results show that a neuronal network can establish a balance between activity and connectivity, and stimulation can disturb this balance. After stimulation, traces of the stimulus response are present in the spontaneous network activity patterns.

Experiments showed the same trend, i.e. the stimulus responses had on average a higher similarity with the bursts after stimulation than before, but this difference was not significant. Interestingly and in contrast to the simulations, the differences were higher for the early than for the late responses. This may be related to the sometimes decreasing responses to electrical stimulation in living networks due to adaptation of the cells or deterioration of the stimulated cells, or the electrode cell contact.

References

[1] Izhikevich, E., *Simple model of spiking neurons.* IEEE trans Neural networks, 2003. **14**(6): p. 1569-1572.
[2] Markram, H., Y. Wang, and M. Tsodyks, *Differential signaling via the same axon of neocortical pyramidal neurons.* . Proc Natl Acad Sci USA 1998. **95**: p. 5323-5328.
[3] Van Rossum, M.C.W., G.Q. Bi, and G.G. Turrigiano, *Stable hebbian learning from spike timing-dependent plasticity.* J. Neurosci., 2000. **208812{8821**: p. 8812-8821.
[4] Eckmann, J.P., et al., *Leader neurons in population bursts of 2d living neural networks.* . New Journal of Physics, 2008. **10**.
[5] Sevev, R., et al., *Hidden neuronal correlations in cultured networks.* . Physical Review Letters, 2004. **92**(11).

Detecting Significant Changes in Oscillatory Power with Cluster-Based Permutation Testing

Ben van Lier[1,2 *], Andreas Hierlemann[2] and Frederic Knoflach[1]

1 F. Hoffmann - La Roche Ltd. Pharmaceutical Research and Early Development, Neuroscience, Basel, Switzerland
2 ETH Zürich, Department of Biosystems Science and Engineering, Basel, Switzerland.
* Corresponding author. E-mail address: ben.van_lier@roche.com

Abstract
Detecting significant changes in neuronal oscillatory activity is of great interest. Datasets created by MEA technology are large and complex. For these datasets, classic statistics are not suitable because of the multiple-comparison problem. To avoid the multiple-comparison problem and retain all information within a dataset, we use cluster-based permutation testing. Clusters consist of adjacent datapoints in time, space, and frequency. We simulated data for testing purposes and the statistics were done with the Matlab toolbox for EEG analysis named FieldTrip.

1 Background

Neural oscillations are the rhythmic, synchronous firing of groups of neurons that can be measured in the local field potential. Neural oscillations are extensively linked to memory function; therefore, detecting oscillatory activity with MEAs in acute slices or organotypic cultures is of great interest. Often, experimental designs hold different conditions under which the power of oscillations is expected to change. With MEA technology, there are three types of relevant information in the data: temporal (when), spectral (which frequencies), and spatial (which electrodes). Classic statistics (Neyman-Pearson approach) are of severely limited use in this case, because of the multiple-comparison problem.

2 Methods

2.1 Permutation testing

All testing was done with the Matlab toolbox for EEG analysis named FieldTrip[1]. Experiments should be based on several trials per condition. First, the difference is quantified (e.g. with a t statistic) between the trials of condition A and B. Then, the trials are put into a single set and drawn at random into subset 1 and 2. The difference is again quantified, and the process is repeated a large number of times. Each result is used to build the permutation distribution. We can then look up, where the originally observed statistic falls in this distribution and determine a p-value.

2.2 Clustering

We have *a priori* knowledge about the information in electrophysiological data. We know that two similar data points that are adjacent to each other in time, frequency or space are likely to originate from the same physiological signal. Therefore, they do not need to be considered separately and can be clustered together.

2.3 Cluster-based permutation testing

To do cluster-based permutation testing[2], we start with permutation testing like described in section 2.1. Every time a test statistic crosses a threshold, it is considered for clustering. When neighbors (in time/frequency/space) also cross the threshold, they form a cluster. The test statistics within a cluster are summed to find the cluster stat. There can be several separate clusters. We build the permutation distribution of the largest cluster stat. Lastly, all originally observed cluster stats are compared to this single distribution to find their respective p-values. This is a single test and therefore the multiple comparisons problem is avoided.

3 Results

MEA data was simulated for 100 channels in two conditions (300s each). First condition was random noise (1-100Hz at 1 RMS). Second condition was noise + signal (40-60 Hz at 1 RMS) in half of the channels and noise only for the other half. Data was divided in 30s trials, so 10 trials per condition. The analysis showed two significant clusters ($p=0.001$ and $p=0.018$), see Figure 1. Channels with signals that were not part of a spatial cluster were not indicated to be significant. These results are in line with expectations.

4 Conclusion

Cluster-based permutation testing provides a way of avoiding the multiple-comparison problem while

retaining all the relevant information. Therefore, it is a viable and flexible method to get the most out of MEA data. Next, we will apply this analysis method to data acquired with isolated brain slices on HiDens MEAs[3].

Acknowledgements

This project is a part of the EU Marie Curie Initial Training Networks (ITN) Biomedical engineering for cancer and brain disease diagnosis and therapy development: EngCaBra. Project no. PITN-GA-2010-264417. Authors would like to thank the Donders Institute at University of Nijmegen for providing the FieldTrip EEG analysis software (http://fieldtrip.fcdonders.nl).

References

[1] Oostenveld, R., Fries, P., Maris, E. & Schoffelen, J.-M. FieldTrip: open source software for advanced analysis of MEG, EEG, and invasive electrophysiological data. *Computational intelligence and neuroscience* **2011**, (2011).

[2] Maris, E. & Oostenveld, R. Nonparametric statistical testing of EEG-and MEG-data. *Journal of neuroscience methods* **164**, 177–190 (2007).

[3] Frey, U. *et al.* Switch-matrix-based high-density microelectrode array in CMOS technology. *Solid-State Circuits, IEEE Journal of* **45**, 467–482 (2010).

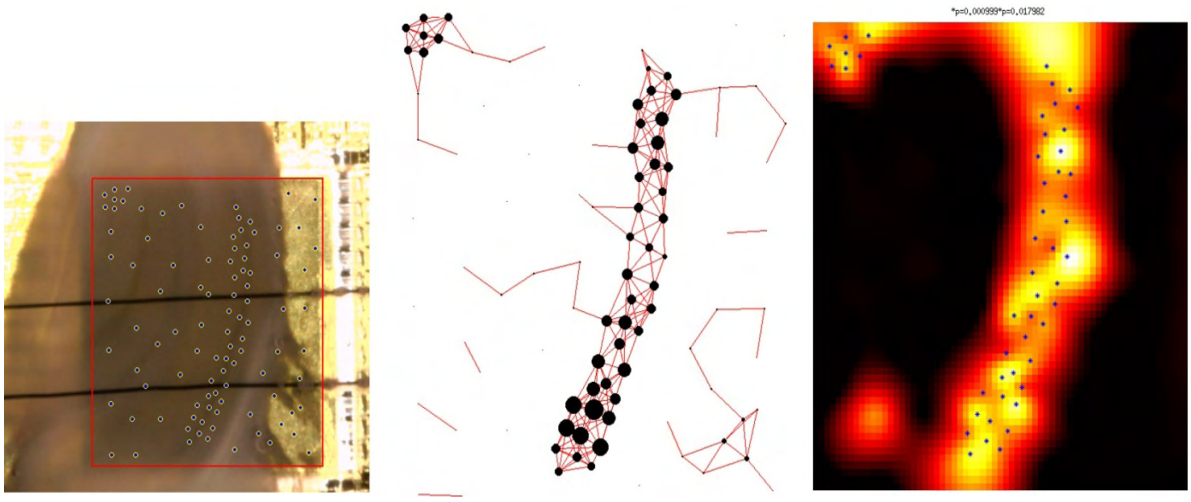

Fig 1. Cluster-based permutation testing on simulated data. *Left*: sample picture of an acute hippocampal slice on a HiDens MEA. Dots show a hypothetical electrode configuration. *Middle*: Cluster plot. The bigger the dot, the more (spatial) neighbors an electrode has. Here, any electrodes within a radius of 200 µm are considered neighbors. *Right*: Heat map showing a large and a small significant cluster. Hotter means a bigger difference between conditions. Dots represent electrodes that crossed the threshold along with their neighbors to form a cluster.

Topological Effects on Bursting and Reverberation Dynamics

Chun-Chung Chen[1*]

1 Institute of Physics, Academia Sinica, Taipei, Taiwan
* Corresponding author. E-mail address: cjj@phys.sinica.edu.tw

Abstract
Dynamical behavior of bursting and reverberation in a cultured network contains important information on its connectivity or topology. Since the structural properties of a network is usually harder to measure directly, it is desirable to recover this information through analysis of the measured dynamics of the network. To understand the relationship between structure and dynamics in a neuronal network, we modify an electrophysiological model of spiking neurons, capable of producing reverberatory bursts that closely resemble what have been observed in cultures, and apply it to networks of different topologies ranging from scale-free to random networks with narrow degree distribution. By varying parameters controlling the excitability of neurons and efficacy of synapses while preserving the time ratio between the bursting and resting states, we show that the two factors compensate each other well only for networks of narrow degree distribution. For these networks, the reverberation remains clearly evident for the entire parameter range considered. For networks of broad degree distribution such as scale-free networks, the mean burst period varies significantly with the parameters, while the reverberation, if exists, is only evident for a limit range of the parameter space.

1 Backround

Population bursts are coordinated neuronal activities that can last for seconds in cultures. They are important dynamic behavior of neuronal networks that are relevant in various neural functions and development [5]. Within these bursts, reverberation can occur as repeated peaking episodes of neural activity level that are separated by quiet intervals in the order of hundred milliseconds [2]. While these types of dynamic behavior of cultured neuronal networks can easily be obtained with MEA recording, sorting out their structural properties can still take up significant efforts event with recent advances in imagining technology [3]. To understand the mechanism behind the reverberatory population bursts, computer model of electrophysiological interactions and neural transmission has been successful constructed to produce dynamics *in silico* very similar to observation in vitro using physiologically meaningful parameters [7]. While the network considered in [7] is a simple random network with narrow degree distribution, recent study on evolution of core patterns in the dynamics of cultured neurons suggests that scale-free functional structures can emerge as the networks mature [6]. Also development in the theory of neuronal avalanches has suggested that critical states with a power law distribution of activity sizes can be optimal for information processing [1]. It is therefore of interest to know the impact of underlying network topologies, such as scale-free or random, can have on the bursting dynamics.

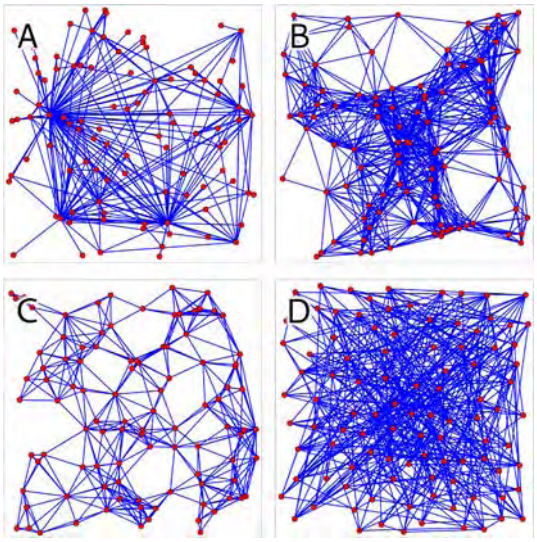

Fig. 1. Network topologies considered in the simulations.

2 Methods

In the current study, we modify and implement the neuronal network model as described in [7] and apply it to networks of different topologies, from scale-free networks generated using algorithm described in [4] to random network similar to that used in [7], as shown in Fig. 1. For a physiological realistic model, there are 30 parameters in the implementation, of which all but two, background current and mean synaptic weight, are fixed with reasonable values similar to those in [7]. The bursting and resting states of the networks are defined with a hysteretic criteria on the number of distinct spiking neurons within a 200ms time window. To compare different networks under

different conditions, we adopt a functional criteria requiring a 1-to-3 ratio between the time for the system to stay in the bursting and resting states. For a given background current, we adjust the mean synaptic weight of a network in the simulations until the 1-to-3 ratio is achieved. We then record the spike times for over a thousand bursts to find the mean burst duration and calculate the time histogram with 4ms-bin to characterize the reverberation.

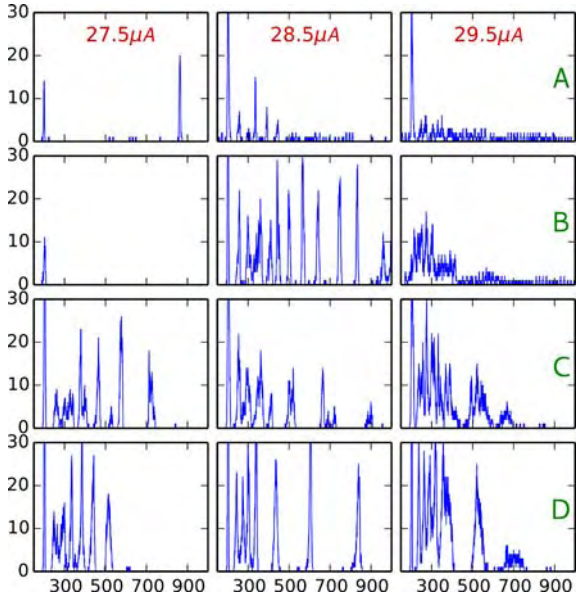

Fig. 2. Bursting behavior for networks shown in Fig. 1 different background current. The horizontal axes are in milliseconds while the vertical axes are in number of spikes within 4ms sliding bin.

3 Results

The bursting behavior are shown in Fig. 2, where the reverberation is most evident in network C, D for the entire current range and in network B for intermediate background current. The scale-free network A seldom goes quiet between peaks of activity level during a burst. Generally, we see less synchrony for the firing of spikes for higher background current (or correspondingly, lower mean synaptic weight).

The average burst durations for different networks as functions of background current are shown in Fig. 3. We see the burst durations vary strongly with background current for scale-free network A and network B, which has a broad degree distribution. On the other hand, the duration is more robust for networks C and D with narrower degree distributions.

For the two model parameters we choose to vary, background current controls the excitability of the neurons while the mean synaptic weight represents the efficacy of the synapses. We verify that to maintain a functional requirement of a network (the 1-to-3 duty ratio for the current study), an increase in background current should be compensated by a decrease in mean synaptic weight. However, such a variation can impact other functional characteristics of the network, such as, the burst duration and the reverberation behavior. Our result showed that they are related to the topology of the networks and tend to be stronger for scale-free or network with a broad degree distribution and milder for random network with a narrow degree distribution.

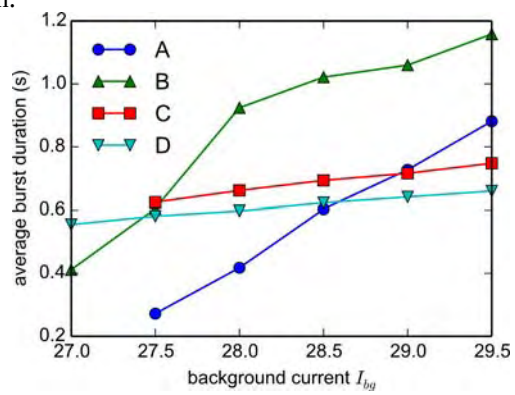

Fig. 3. Average burst duration as functions of background current for different networks.

4 Conclusions

In the current study, we show how the topology of a network can influence its dynamic properties. With typically many system factors or parameters involved in producing dynamics, one can imagine that there will be a right combination for a different network topology to produce similar dynamics. Under such a situation, we show that characters related to the topology of the network can be revealed by a variation to the operation condition and assess the change to its dynamic behavior. Furthermore, we also learn that the equivalence between neuronal excitability and synaptic efficacy can be better expected if the network has a narrow degree distribution. For networks with scale-free topology, one should not expect to counter the effect of heightened neuronal excitability by a medicine that reduces the efficacy of synaptic transmission.

References

[1] Bertschinger, N.; Natschläger, T. (2004): Real-Time Computation at the Edge of Chaos in Recurrent Neural Networks. *Neural Computation, 16(7):1413-1436.*

[2] Lau, P.-M.; Bi, G.-Q. (2005): Synaptic mechanisms of persistent reverberatory activity in neuronal networks. *PNAS, 102(29):10333-10338.*

[3] Li, XY; Liu, HJ; Sun, XX; Bi, GQ; Zhang, GQ (2013): Highly Fluorescent Dye-Aggregate-Enhanced Energy-Transfer Nanoparticles for Neuronal Cell Imaging. *Advanced Optical Materials, 1(8):549-553.*

[4] Morita, S. (2006): Crossovers in scale-free networks on geographical space. *Physical Review E, 73(3):035104-4.*

[5] Potter, S. M. (2008): How should we think about bursts?. *Conference Proceedings of the 6th International Meeting on Substrate-Integrated Micro Electrode Arrays, 5:22-25.*

[6] Sun, J.-J.; Kilb, W.; Luhmann, H. J. (2010): Self-organization of repetitive spike patterns in developing neuronal networks in vitro. *European Journal of Neuroscience, 32(8):1289-1299.*

[7] Volman, V.; Gerkin, R. C.; Lau, P.-M.; Ben-Jacob, E.; Bi, G.-Q. (2007): Calcium and synaptic dynamics underlying reverberatory activity in neuronal networks. *Physical Biology, 4(2):91-103.*

A Multivariate Spike-Detection Algorithm to Assess Activity Patterns of Three-Dimensional In Vitro Models

Andreas W. Daus[1*], Robert Bestel[1], Christiane Thielemann[1]

1 biomems lab, University of Applied Sciences Aschaffenburg, Germany
* Corresponding author. E-mail address: andreas.daus@h-ab.de

Abstract
Multichannel recording of cell cultures coupled to microelectrode arrays (MEAs) are a widespread approach to study electrophysiological properties of developing and mature neuronal networks. Spike detection however is still a crucial point, especially if three-dimensional (3D) in vitro systems are employed. 3D cultures are considered to increase the physiological relevance of in vitro studies, but their 3D architecture results in complex cell-electrode-configurations and enhanced cell densities around the electrodes. Hence a higher number of cellular signals with partly weak amplitudes participate in the recordings and common threshold-based detection-algorithm would deliver biased results. We developed a robust spike-detection algorithm, based on a multivariate approach with dynamic thresholds, ready for multichannel recordings of 3D in vitro systems.

1 Background/Aims

Adherent monolayer cell cultures on microelectrode arrays (MEAs) can give physiological and functional information on the effect of extrinsic stimuli, and are considered as an appropriate paradigm to mimic in vivo-like conditions e.g. in pharmacology, toxicology or developmental biology. However, cells within a tissue are organized in a complex three-dimensional (3D) arrangement and cellular interactions are not limited to a biased two-dimensional (2D) environment. In vitro models of primary cells or appropriate stem cells that reestablish a 3D architecture circumvent this disadvantage, while they still profit from defined cell culture conditions.

We combined the MEA technique with a 3D cell culture model [1,2]. Single dissociated neurons from avian embryonic brain were reaggregated to so-called spheroids in rotation-culture (Fig. 1). These spheroids were approximately 200–400µm in diameter and developed spontaneous electrical activity starting at 5 days in vitro. Signal analysis however was challenging, as (*i*) compared to monolayer experiments, an increased number of cellular signals with partly week amplitudes participated in the recordings and (*ii*) bursts were accompanied by extensive low-frequency signal components (see Fig. 2).

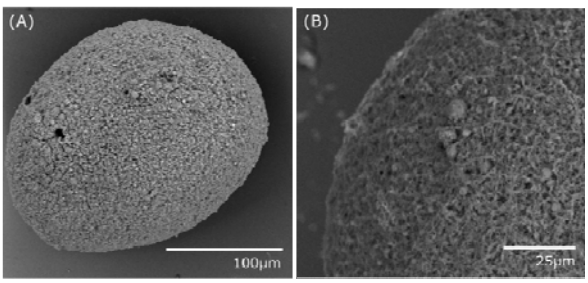

Fig. 1. SEM micrographs of neuronal spheroids. (A) Single dissociated cells reaggregated to 3D spherical networks in rotation-culture. (B) Close-up of a spheroid [4].

2 Methods

To ensure robust signal assessment, we developed a multivariate spike-detection algorithm based on a multi-level analysis: In the first step, amplitudes of the signals were evaluated using a dynamic threshold. In contrast to common static threshold models, which usually claim high-pass filtering to reduce detection artefacts in bursts, the dynamic threshold was calculated by smoothing the whole signal according to Savitzky-Golay with a negative shift based on the median absolute deviation (Fig. 2).

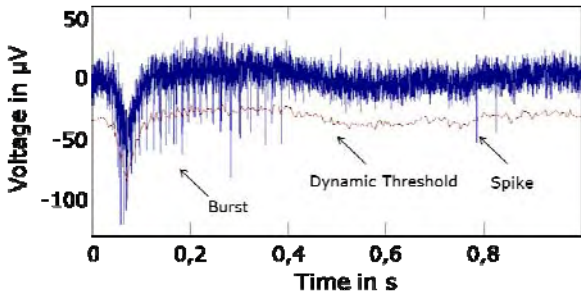

Fig. 2. Electrical activity of 3D neuronal spheroids. Burst were accompanied by extensive low frequency signal components. The dynamic threshold was attuned to these oscillations.

Solely amplitude evaluation however delivered biased results. In a second step, we therefore defined a variety of further geometric, Wavelet- and Principal component-based attributes and spike-noise-separation was performed using in total 17 features:

- positive and negative amplitude
- angle of falling and rising edge
- signal duration
- positive and negative signal energy

- NEO coefficient
- 1. – 3. Principal component
- 1. – 3. Wavelet distribution
- 1. – 3. Wavelet Shannon entropy coefficient

Subsets of these features, most suitable for robust spike determination were estimated from their particular distributions and clusters of spikes and noise were figured as multidimensional scatterplots [3]. Spike determination was subsequently carried out using an expectation maximization algorithm.

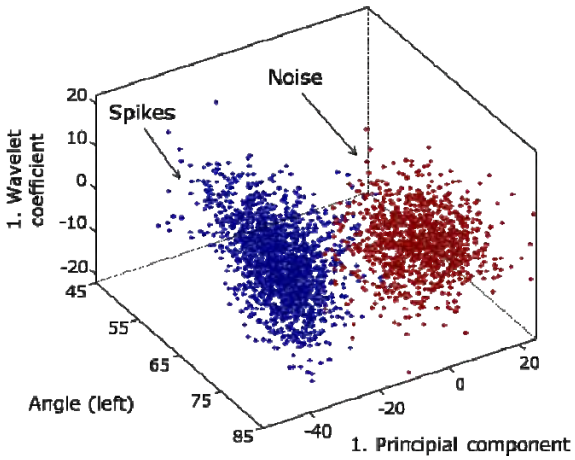

Fig. 3. Subsets of features figured as multidimensional scatterplot. An expectation maximization algorithm was employed for clustering.

3 Results

The novel spike detection algorithm was tested with data obtained from 3D neuronal spheroids coupled to MEAs [4]. We found, that the algorithm delivers robust results and is highly suitable to analyse in particular multi-layered in vitro models. Even spikes with low amplitudes were detected reliably by evaluation of suitable subsets of features in the time- or frequency domain.

In pharmacological experiments, the algorithm was employed to investigate activity patterns of neuronal networks after treatment with GABA and Bicuculline. GABA administration resulted in a dose-depend decrease in spike- and burstrate according to Figure 4, while Bicuculline led to a disinhibition of neuronal network activity.

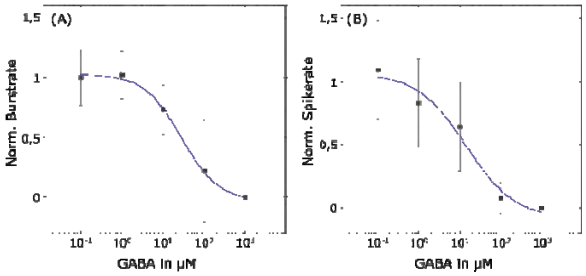

Fig. 3. GABAergic modulation of the network activity. Administration of GABA inhibited burstrate (A) and spikerate (B).

4 Conclusion

Spike detection is still a crucial point in multichannel recordings of neuronal in vitro systems. Particularly with regard to 3D cultures, solely amplitude evaluation with common static thresholds deliver biased findings. We have presented a novel spike-detection algorithm based on a multivariate approach with dynamic thresholds. The algorithm delivered robust results even when applied to complex data obtained from multi-layered networks.

Consequently we propose multivariate analysis instead of solely threshold-based algorithm as robust spike detection technique.

References

[1] Daus, A. W., Goldhammer, M., Layer, P. G., Thielemann, C. 2011, Electromagnetic exposure of scaffold-free three-dimensional cell culture systems. Bioelectromagnetics, 32: 351–359.

[2] Daus, A. W., Layer, P. G., Thielemann, C. 2012. A spheroid-based biosensor for the label-free detection of drug-induced field potential alterations. Sensors and Actuators B, 165: 53–58.

[3] Bestel, R., Daus, A. W., Thielemann, C. 2012. A novel automated spike sorting algorithm with adaptable feature extraction. Journal of Neuroscience Methods 211: 168–178.

[4] Daus, A. W. 2013, Zellbasierte Biosensoren – Hybride Systeme aus dreidimensionalen in vitro Netzwerken und Mikroelektroden Arrays, Dissertation TU Darmstadt, http://tuprints.ulb.tu-darmstadt.de/3419/

Partial Correlation Analysis for Functional Connectivity Studies in Cortical Networks

Daniele Poli[1]*, Vito Paolo Pastore[1], Simonluca Piazza[1], Paolo Massobrio[1] and Sergio Martinoia[1]

1 Department of Informatics, Bioengineering, Robotics and Systems Engineering (DIBRIS), University of Genova, Genova, 16145, Italy
* Corresponding author. E-mail address: Daniele.Poli@edu.unige.it

Abstract
The main goal of this work is to present a methodological approach to estimate the functional connectivity from the spontaneous activity of *in vitro* cortical assemblies coupled to Micro-Electrode Arrays (MEAs). We focused on the Partial Correlation (PC) method compared to Transfer Entropy and Cross Correlation (CC) algorithms. After the implementation and validation of the aforementioned methods on synthetic data generated by a realistic computational model, we assessed the statistical significance of the different performances, showing the best approach to infer functional mapping of biological *in vitro* cortical networks.

1 Introduction

The use of *in vitro* model systems and computational models has strongly contributed to the understanding of relevant neurophysiological principles, thanks to the advantages offered by a much better observability and controllability than intact brains.

The main goal of this work is to present a methodological approach to infer the functional connectivity from the spontaneous activity of dissociated cortical neurons developing *in vitro* and coupled to Micro-Electrode Arrays (MEAs) by means of correlation and information theory-based methods. In particular Partial Correlation (PC) analysis [1] compared to Transfer Entropy [2] and Cross Correlation (CC) [3] algorithms have been taken into account. We applied the algorithms to a neural network model made up of 60 spatially distributed and synaptically connected Izhikevich neurons [4] by sweeping the connectivity degree of each neuron in order to mimic different experimental conditions (i.e., low- and high density assemblies). Then we evaluated the methods' performances through receiver operating characteristic (ROC) curves and the values of the areas under these curves (AUC). By sweeping the connectivity degree over the all range, the algorithms show (Figure 1) different performances: Partial Correlation would seem to be the best method to infer functional connectivity. These results and the likelihood of the *in silico* model with experimental data allow us to indicate Partial Correlation as the best candidate to infer functional connectivity of *in vitro* cortical networks.

2 Materials and Methods

2.1 Materials

***In silico* model:** We developed a neural network model made up of 60 spatially distributed and synaptically connected neurons described following the Izhikevich equations [4]. The model simulates the spontaneous electrophysiological activity of cultured cortical neurons. Network model includes excitatory and inhibitory connections. In this configuration, two different types of neuron model excitatory and inhibitory populations: the former type belongs to the family of regular spiking neurons, and the latter to the family of fast spiking neurons [4-5]. Regular spiking neurons fire with a few spikes characterized by short Inter Spike Interval (ISI) at the onset of an input. Differently, fast spiking neurons exhibit periodic trains of action potentials at higher frequencies without adaptation. To preserve the main characteristics of the structure of the *in vitro* cortical neurons, the ratio between excitatory and inhibitory neurons was set to 4:1. These two neuron families were randomly connected by sweeping the average degree from 10 to 60. Synaptic weights are normally distributed. Spontaneous activity was obtained by introducing a randomly distributed stimulation reproducing the effect of fluctuation in the membrane potential due to the distributed background activity. All the simulations (20 realizations for each connectivity degree) were performed in Matlab environment (The Mathworks, Natick MA, USA).

***In vitro* model:** Dissociated cortical neurons have been extracted from rat embryos and plated on 60-channel MEAs precoated with adhesion promoting molecules (poly-D-lysine and laminin), at the final density of 1200–1400 cells/mm2. They were maintained in culture dishes, each containing 1 ml of nutrient medium (e.g. serumfree Neurobasal medium supplemented with B27 and Glutamax-I) and placed in a humidified incubator having an atmosphere of 5% CO2 and 95% O2 at 37C. The network electrophysiological activity was recorded after the third-fourth week in vitro to allow the maturation of synaptic connections among the cells of the network. The experi-

mental set-up was based on the MEA60 System (Multi Channel Systems, MCS, Reutlingen, Germany). The electrophysiological activity has been recorded without any chemical or electrical stimulation (i.e., it was referred only to the spontaneous activity).

2.2 Methods

CC: It measures the frequency at which one particular neuron or electrode fires ("target") as a function of time, relative to the firing of an event in another network ("reference"). Mathematically, CC reduces to a simple probability $Cxy(\tau)$ of observing an event in a train Y at time $(t+\tau)$, because of an event in another train X at time t; τ is called time shift or time lag. CC function was evaluated considering all the pairs of peak trains. Connection strength among neurons was evaluated on the basis of the peak value of the CC function. The highest CC values should correspond to the strongest connections.

PC: It is a measure to identify the functional neural connectivity from simultaneously recorded neural spike trains. Partial correlation analysis allows to distinguish between direct and indirect connections by removing the portion of the relationship between two neural spike trains that can be attributed to linear relationships with recorded spike trains from other neurons [1].

TE: It is an information theoretic measure which allows to extract causal relationships from time series [2]. It estimates the part of the activity of one single neuron which does not depend only on own past, but which depends also by neural past activity of another cell; moreover, it allows to analyzes the information flow between two different cortical regions.

TE can represent a general way to define the causality strength between peak trains generated by several populations. It is not symmetric with respect to the exchange of the variables X and Y and it is sensitive to linear as well as non nonlinear causal interactions. For this reason TE is seen as a promising technique to infer connectivity maps, gaining more and more popularity in the field of neuroscience for the analysis of complex stochastic dynamics.

ROC: These curves can be reduced to a single scalar value (AUC) representing the obtained performance. Since AUC represents the area of a portion of the unit square, its value will be always between 0 and 1 (see Figure 1). However, since random guessing produces the diagonal line between (0, 0) and (1, 1), which has an area of 0.5, a classifier should have an AUC higher than 0.5 (good classifiers should have AUC values close to 1). A ROC curve was obtained by comparing the Synaptic Weight Matrix (SWM; the matrix which takes into account the morphological connections of the model) and the Thresholded Connectivity Matrix (TCM), calculated by the previously described methods. For a given threshold, all TCM elements were considered as possible functional connections.

3 Results

By varying the connectivity degree of each neuron from 10 to 60 it is possible to observe that the Partial Correlation presents the best performances (Figure 1). In particular, we can summarize that:

- With connectivity degree equal to **10**, CC turns out to be statistically significant ($p < 0.01$, Kruskal-Wallis, non-parametric test) and different from the PC, TE and random case (identified with the limit value 0.5).
- For the others cases (connectivity degree **20**, **30**, **40**, **50**, **60**), PC shows the best performances and, also, a statistical difference ($p < 0.01$) from CC, TE and random case.

Therefore the results achieved, and the likelihood of the *in silico* model with experimental data, support the idea that Partial Correlation is the best functional connectivity approach for *in vitro* cortical networks. For this reason, the next step will be to apply PC to assemblies of dissociated cortical neurons, obtaining functional maps and extracting, through graph theory, relevant topological features.

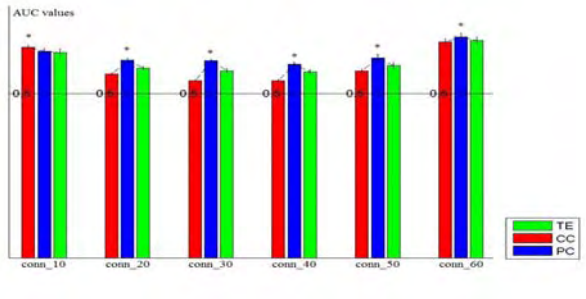

Fig. 1. AUC values. Comparison among the three algorithms.

4 Conclusion/Summary

The current work contributes, in general, to the study of functional connectivity in *in vitro* and *in silico* models suggesting as the best methodological approach the Partial Correlation.

References

[1] M. Eichler, R. Dahlhaus, J. Sandkuhler, "Partial Corrleation analysis for identification of synaptic connections", Biol. Cybern. 2003, 89:289-302.

[2] M. Lungarella, A. Pitti, Y. Kuniyoshi, "Information Transfer at multiple scales" Physical Review E 2007, 76:0561171-05611710.

[3] E. Salinas, T.J. Sejnowski, "Correlated neuronal activity and the flow of neural information" Nature Reviews Neuroscience 2001, 2:539-550.

[4] E.M. Izhikevich, "Simple model of spiking neurons" IEEE Transactions on Neural Networks 2003, 6:1569-1572.

[5] E.M. Izhikevich "Which model to use for cortical spiking neurons?" IEEE Transactions on Neural Networks, 2004 15: 1063-1070.

Modulating Functional Connectivity in Hippocampal Cultures Using Hebbian Electrical Stimulation

Víctor Lorente[1*], José Manuel Ferrández[1], Eduardo Fernández[2], Félix de la Paz[3]

1 Departamento de Electrónica, Tecnología de Computadores y Proyectos, Universidad Politécnica de Cartagena, Spain
2 Instituto de Bioingeniería, Universidad Miguel Hernández, Alicante, Spain
3 Departamento de Inteligencia Artificial, UNED, Madrid, Spain
* Corresponding author. E-mail address: victor.lorente@upct.es

Abstract
Electric stimulation has been widely used to induce changes in neuronal cultures coupled to multielectrode arrays (MEAs). In this paper we used different electrical stimulation protocols, such as low-frequency current stimulation and voltage tetanic stimulation, on hippocampal cultures for modifying its functional connectivity represented by functional connectivity graphs. We show that persistent and synchronous stimulation of adyacent electrodes induces a neural spike activation that leads to an increase of cross-correlation, creating a functional connection between them.

1 Introduction

The use of dissociated cortical neurons cultured onto MEAs represents a useful experimental model to characterize both the spontaneous behavior of neuronal populations and their activity in response to electrical and pharmacological changes, and permit the construction of real biological platforms.

Learning is a natural process that needs the creation and modulation of sets of associations between stimuli and responses. Many different stimulation protocols have been used to induced changes in the electrophysiological activity of neural cultures looking for achieve learning [1,2]

Hebbian learning describes a basic mechanism for synaptic plasticity wherein an increase in synaptic efficacy arises from the presynaptic cell's repeated and persistent stimulation of the postsynaptic cell. In previous papers, we used a specific low-frequency current stimulation on dissociated cultures of hippocampal cells to study how neuronal cultures could be trained with this kind of stimulation [3,4]. We showed that persistent and synchronous stimulation of adjacent electrodes may be used for creating adjacent

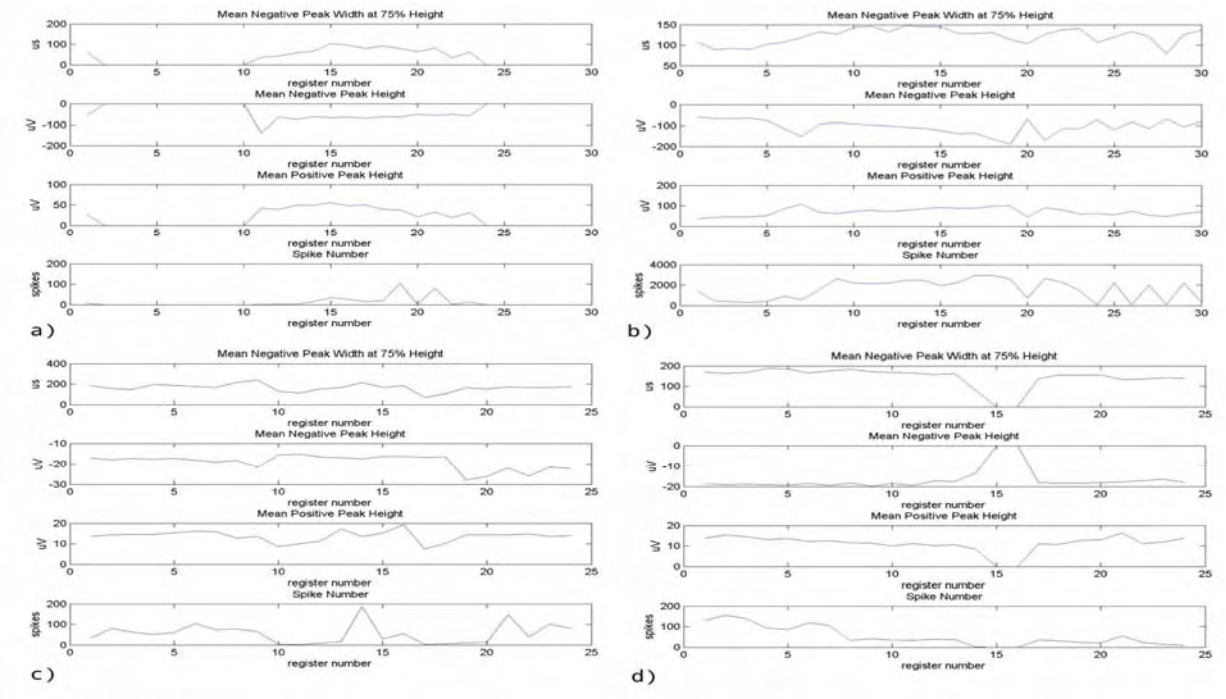

Fig. 1. For each electrode, Mean Negative Peak Height, Mean Positive Peak Height and Spike Number are represented. a) and b) graphs are for Electrode 31 and 42 from culture ID48. c) and d) graphs are from Electrode 62 and 72 from culture ID86.

physical or logical connections in the connectivity graph following Hebb's Law.

In this paper we used different electrical stimulation protocols, such as low-frequency current stimulation and voltage tetanic stimulation, on hippocampal cultures for modifying its functional connectivity represented by functional connectivity graphs. We show that persistent and synchronous stimulation of adyacent electrodes induces a neural spike activation that leads to an increase of cross-correlation, creating a functional connection between them.

2 Methods

A total of 24 dissociated cultures of hippocampal CA1-CA3 neurons were prepared from E17.5 sibling embryos. Cell density for each culture was roughly 200000 cells. Cells were kept in an incubator at 37˚ C in 6% CO2.

The cultures were used in five experiments of 2-3 weeks duration. In every experiment 4-5 cultures were stimulated with a specific electrical stimulation protocol. In experiments E1 to E3 a low frequency current stimulation with different parameters for each experiment was used. Experiments E4 to E5 used a more aggressive stimulation called Tetanization. Experiments were started when neural cultures had 14 Days in Vitro (DIV) and were carried out during 2-3 weeks.

The spontaneous activity of the cultures before and after the stimulation experiments was observed, as well as their evoked response to the applied stimulus. Extensive spike analysis, instantaneous firing frequencies analysis, inter-spike intervals analysis, functional connectivity graphs and spike characteristics analysis were the procedures used in this study.

Functional connectivity captures patterns of deviations from statistical independence between distributed neurons units, measuring their correlation/covariance, spectral coherence or phase locking.

The physiological function of neural cells is modulated by the underlying mechanisms of adaptation and reconfiguration in response to neural activity. Hebbian learning describes a basic mechanism for synaptic plasticity wherein an increase in synaptic efficacy arises from the presynaptic cell's repeated and persistent stimulation of the postsynaptic cell.

3 Results

Low-frequency current stimulation and tetanic stimulation had both an impact on the electrophysiological responses of the cultures, which can be analytically observed with raster plots, instantaneous firing frequencies and the interspike intervals of the neural cultures. Connectivity maps represent the functional connectivity of the neural cultures showing only the best three output logical connections per electrode in terms of strongest correlation. These diagrams showed some kind of connections reorganization after stimulations, concentrating them in a few electrodes. Furthermore, adjacent physical or logical connections in the connectivity graph following Hebb's law appeared in some pairs of stimulated electrodes. The creation of a new logical connection implies that this new value is between the three best values compared with the rest of the electrodes. There exists a positive evolution on the correlation that induces the origin of logical connections.

Analysing spike parameters such as peaks heights and widths and number of spikes showed that both stimulations produced a reactivation of neurons over time, which lead to the creation of adjacent physical or logical connections in the connectivity graph following Hebb's Law. We can observe in Fig. 1. that each electrode presented a good evolution of its parameters until register number 20. Negative peak height decreased, positive peak height increased, width of negative peak slightly increased and number of spikes increased. This positive evolution of the parameters was due to the activation of more new neurons near the electrodes, which produced a higher value of the spikes parameters.

4 Conclusion

When using low-frequency stimulation and tetanization it is possible to create adjacent physical or logical connections in the connectivity graph following Hebb's Law and such connections induce changes in the electrophysiogical response of the cells in the culture, which can be observed in the different analysis performed. These processes may be used for imposing a desired behaviour over the network dynamics. In this work a stimulation procedure is described in order to achieved the desired plasticity over the neural cultures.

References

[1] Bologna, L.L., Nieus, T., Tedesco, M., Chiappalone, M., Benfenati, F.: Low- frequency stimulation enhances burst activity in cortical cultures during development. Neuroscience 165, 692–704.

[2] Ide, A.N., Andruska, A., Boehler, M., Wheeler, B.C., Brewer, G.J.: Chronic network stimulation enhances evoked action potentials. J. Neural. Eng. 7(1) (February 2010).

[3] V. Lorente, J.M. Ferrández, E. Fernández y F. de la Paz. Enhancing Hebbian Learning in Biological Neural Cultures Through Electrical Stimulation. *Future Computing 2013*, pp. 20-25, 2013.

[4] V. Lorente, J.M. Ferrández, F.J. Garrigós, F. de la Paz, J.M. Cuadra, J. R. Álvarez y E. Fernández. Neural Spike Activation in Hippocampal Cultures Using Hebbian Electrical Stimulation. *Natural and Artificial Models in Computation and Biology Lecture Notes in Computer Science*, Volume 7930, 2013, pp 37-47. DOI: 10.1007/978-3-642-38637-4_5.

Learning and Plasticity in Hippocampal Cultures Using Antiepilectic Drugs

José Manuel Ferrández[1*], Victor Lorente[1], Arancha Alfaro[3], Eduardo Fernández[2]

1 Departamento de Electrónica, Tecnología de Computadores y Proyectos, Universidad Politécnica de Cartagena, Spain
2 Instituto de Bioingeniería, Universidad Miguel Hernández, Alicante, Spain
3 Departamento de Neurología, Hospital Vega Baja de Orihuela, Alicante, Spain
* Corresponding author. E-mail address: jm.ferrandez@upct.es

Abstract
Electric stimulation has been widely used to induce changes in neuronal cultures coupled to multielectrode arrays (MEAs). In this paper we used different electrical stimulation protocols, such as low-frequency current stimulation and voltage tetanic stimulation, on hippocampal cultures for modifying its functional connectivity represented by functional connectivity graphs. We show that persistent and synchronous stimulation of adjacent electrodes induces a neural spike activation that leads to an increase of cross-correlation, creating a functional connection between them.

1 Introduction

The mechanisms underlying the development of plasticity in epilepsy are complex and not fully understood. In order to establish neural learning paradigms to work in tandem with the chemical stimulation, patterns of neural stimulation and response to antiepilectic drugs need to be characterised. In-vitro recording experiments in hippocampal neural cultures via extracellular high-density recordings from embryonic rats have been successfully used to study simple hebbian associative learning. Therefore the main aim of this work was to test the usefulness of these paradigms for better understanding of the mechanisms specifically associated with antiepilectic drug responsiveness.

2 Methods

Different cultures of hippocampal CA1-CA3 neurons were prepared from E17.5 sibling embryos. Cell density for each culture was roughly 200000 cells. Fugure1. Cells were kept in an incubator at 37˚ C in 6% CO2.

The cultures were used in five experiments of 2-3 weeks duration. In every experiment 4-5 cultures were stimulated with a specific electrical stimulation protocol. In experiments E1 to E3 a low frequency current stimulation with different parameters for each experiment was used. Experiments E4 to E5 used a more aggressive stimulation called Tetanization. Experiments were started when neural cultures had 14 Days in Vitro (DIV) and were carried out during 2-3 weeks.

The spontaneous activity of the cultures before and after the stimulation experiments was observed, as well as their evoked response to the applied stimulus. Extensive spike analysis, instantaneous firing frequencies analysis, inter-spike intervals analysis, functional connectivity graphs and spike characteristics analysis were the procedures used in this study.

Functional connectivity captures patterns of deviations from statistical independence between distributed neurons units, measuring their correlation/covariance, spectral coherence or phase locking.

The physiological function of neural cells is modulated by the underlying mechanisms of adaptation and reconfiguration in response to neural activity. Hebbian learning describes a basic mechanism for synaptic plasticity wherein an increase in synaptic efficacy arises from the presynaptic cell's repeated and persistent stimulation of the postsynaptic cell.

Fig. 1. Hippocampal CA1-CA3 culture (21 DIV) on a microelectrode array

Free growing cultures were stimulated through pairs of electrodes from where there no existed previous functional connectivity. A train of balanced pulses were delivered with different temporal schemes over multielectrode arrays using Hebbian electrical learning. Several antiepilectic drugs were added to the culture with different temporal schemes. The spontaneous activity connectivity maps were computed before

and after the stimulation to analyse potential connectivity changes, as well as their evoked response to the applied stimulus.

Instantaneous firing frequencies analysis, interspike intervals analysis, functional connectivity graphs and spike characteristics analysis were used to study population activity.

Sodium valproate is an anticonvulsant used in the treatment of epilepsy as well as other psychiatric conditions requiring the administration of a mood stabilizer. Research has shown that histone-deacetylase inhibitors enable adult mice to establish perceptual preferences that are otherwise impossible to acquire after youth. In humans, it was found that adult men who took valproate (VPA) (a HDAC inhibitor) learned to identify pitch significantly better than those taking placebo—evidence that VPA facilitated critical-period learning. (1)

Lacosamide is a medication for the adjunctive treatment of partial-onset seizures and a functionalized amino acid that has activity in the maximal electroshock seizure test, that act through Voltage gated sodium channels undergo slow inactivation. This inactivation prevents the channel from opening, and helps end the action potential. Secondly, it will join the protein related to colapsine type2 (CRMP-2). This protein is related to neural growth and neural differentiation, used for neural circuitries shaping.

3 Results

The cultures show dynamical reconfiguration and are able to adapt to external electrical stimulation using different stimulation patters. Hippocampal neurons are able to establish neural induced connections, learn the paired stimulation patterns and create new neural circuitries. Therefore this approach can be used for testing the pharmacological effects of new anticonvulsant drugs in learning processes, for analyzing its facilitating profile for neural circuitries creation, and for determining the role of antiepilectic drugs in neural plasticity and learning modulation. Our preliminary results suggest that multielectrode recordings from hippocampal cultures is a suitable model for a better understanding of the interactions between antiepilectic drugs and neuronal populations.

4 Conclusion

A neural culture from hippocampal embryonic neural cells connected to a multielectrode array is an adequate platform for testing antiepilect drugs and its effects on different learning schemes. It is know that antiepilect drugs affects bursting patterns neural cultures, decreasing the neural activity [2], and it is also know that antiepilectic drugs affects learning capabilities in human adults. In future works we will test the learning performance and the forgetting parameters of the neural cultures using connectivity maps creation [3] and antiepilectic drugs release.

References

[1] Valproate reopens critical-period learning of absolute pitch. Judit Gervain, Bradley W. Vines, Lawrence M. Chen, Rubo J. Seo, Takao K. Hensch, Janet F. Werker, and Allan H. Young. Front. Syst. Neurosci., 03 December 2013 | doi: 10.3389/fnsys.2013.00102. [2]

[2] Ilaria Colmobi, Sameehan Mahajani, Monica Frega, Laura Gasparini and Michela Chiappalone. Enhancing Effects of antiepileptic drugs on hippocampal neurons coupled to microelectrode arrays. *Front Neuroeng. 2013; 6: 10. doi: 10.3389/fneng.2013.00010*, 2013.

[3] V. Lorente, J.M. Ferrández, F.J. Garrigós, F. de la Paz, J.M. Cuadra, J. R. Álvarez y E. Fernández. Neural Spike Activation in Hippocampal Cultures Using Hebbian Electrical Stimulation. *Natural and Artificial Models in Computation and Biology Lecture Notes in Computer Science*, Volume 7930, 2013, pp 37-47. DOI: 10.1007/978-3-642-38637-4_5.

A Web-Based Framework for Semi-Online Parallel Processing of Extracellular Neuronal Signals Recorded by Microelectrode Arrays

Mufti Mahmud[1,2], Rocco Pulizzi[1], Eleni Vasilaki[3], Michele Giugliano[1,3,4,*]

1 Theoretical Neurobiology & Neuroengineering Lab, Dept. of Biomedical Sciences, University of Antwerp, Wilrijk, Belgium
2 Institute of Information Technology, Jahangirnagar University, Savar, Dhaka, Bangladesh
3 Department of Computer Science, University of Sheffield, Sheffield, UK
4 Brain Mind Institute, Swiss Federal Institute of Technology Lausanne, Lausanne, Switzerland
* Corresponding author. E-mail address: Michele.Giugliano@uantwerpen.be

Abstract

To study brain (dys)functions *in vitro*, substrate integrated Micro-Electrode Arrays (MEAs) has been proven as an effective experimental tool. Statistically significant conclusions can only be drawn from a set of typical MEA experiments when there is enough raw data which, in usual cases, are in Gigabytes and require extensive, automated and time-demanding preprocessing. In this paper, we present an effective, web-based, semi-online, client-server based open-source software workflow for processing and analysis of extracellular multi-unit activity acquired by a standard MEA platform. The workflow continuously streams data from an acquisition computer to an analysis computer where each recorded channel is preprocessed in parallel. Our results suggest that by delegating the preprocessing of different channels to available cores of a multicore computer and executing them in parallel, as in case of distributed computing, a significant reduction in the processing time can be achieved.

1 Introduction

Substrate integrated Micro-Electrode Arrays (MEAs) has recently emerged as an effective tool to investigate brain (dys)functions in *in vitro* experimental models, such as primary neuronal cultures and organotypic brain slices [1, 2]. Both in academia and pharma industry, MEAs are employed to monitor non-invasively the electrical activity of large neuronal networks developing *ex vivo*. To have statistical significance, each experiment typically lasts long enough to generate several Gigabytes of raw data per MEA (i.e., 60 channels, 16 bits A/D conversion, 20 kHz sampling rate). Rigorous and automated preprocessing of the data thus becomes imperative, as soon as a large number of routine experiments are performed [3, 4].

To this aim, we developed an effective, web-based, semi-online, client-server software workflow for processing and analysis of extracellular multi-unit activity acquired by a standard MEA platform. The concept behind it is, to delegate stereotyped CPU-intensive signal processing steps to a powerful, multi-core computer where independent operations for each channel (e.g., de-multiplexing individual channel data from the multiplexed file (*.mcd), filtering, peak-detection, and spike sorting) are performed in parallel while data acquisition is performed by a general purpose computer. Thus, exploiting open source tools for web-server configuration and distributed parallel computing [5] under Linux, the semi-online workflow continuously streams data from the acquisition computer during an experiment, performs in parallel the jobs of processing each recorded analog channel, and returns the results back to the user. This turns a long and tedious manual offline process in an automated and semi-online data analysis where the scientists will have the results ready at the end of the experiment [6].

2 Methods

The workflow is based on client-server architecture (Fig. 1A) with a stand-alone workstation, or a master-node of a computer cluster as server, and the signal acquisition setup computer as client (Fig. 1B). The processor cores of the server are configured as distributed computing nodes, as in a high-performance computing intranet. The master node also runs a web server software, capable of launching a series of server-side operations (e.g., via the common gateway interface, CGI, as in web applications) when instructed by a client computer connected to the same network.

The data streaming and preprocessing performed by the workflow includes several steps executed in a sequence (Fig. 1A). Before starting the data acquisition, the user is required to initiate a streaming and processing session in the server. The server then securely connects to the acquisition setup computer and scans for any *.mcd files available for streaming in a pre-specified directory. The server repeatedly executes the following steps of the workflow for each streamed *.mcd file. The streaming stops when for a certain amount of time no new files are made available.

(1) a fast, secure, and automated SFTP based raw data transfer (i.e., data streaming), from the data acquisition setup storage hard drive to the computer(s) dedicated for data preprocessing;

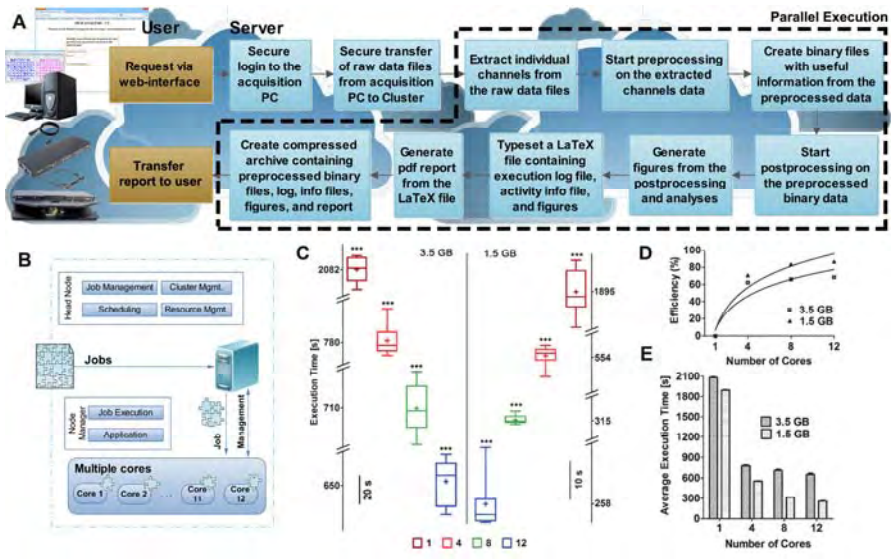

Fig. 1. Steps and performance of the workflow. A. Once an experiment is started by a scientist, the streaming and data processing is initiated through the web-interface of the workflow. B. The jobs are scheduled and distributed among different cores. C. Box plots showing significant decrease of processing times with increasing number of employed cores during the processing of two different file sizes (3.5 GB and 1.5 GB). D, E: The workflow execution efficiency increases, and the average execution times of the processing decreases significantly for both representative file sizes.

(2) the conversion of each multiplexed raw data file into several binary files, each containing data points from a distinct recording channel;

(3) the preprocessing of each file using fully extensible MATLAB (The Mathworks, Natick, USA) scripts which include: band-pass filtering, artifact removal, spike detection and elementary spike-sorting;

(4) MATLAB script based analysis of (multi)unit activity extracted in the previous step to view experimental outcomes (e.g., MEA-wide synchronous bursting rate, single-channel and MEA-wide firing rate, intra-burst instantaneous discharge probability, etc.);

(5) the automated typesetting of a PDF report from a dynamically generated and compiled LaTeX source file, including both textual and graphical information, extracted by the previous step. It then securely delivers the PDF report and of all intermediate and final preprocessed files (e.g., spike time-stamps, spike waveforms, spike count) to the client computer, as a compressed file archive.

3 Results

We configured and run our workflow on sample binary (*.mcd) data files of two different sizes (i.e., ~1.5 GB for 8 min and ~3.5 GB for 20 min recording). We employed four distinct predefined queues (i.e., with 1, 4, 8, and 12 reserved cores) to compare the User Execution Times (Fig. 1C). Confirming the embarrassingly parallelization of the task, we found that execution time reduced significantly ($p<0.05$, ANOVA; sublinearly) with an increasing number of cores available (see Fig. 1C), with maximum and minimum execution times ranging from 34.7 mins ± 10 s to 10.8 mins ± 17 s or from 31.5 min ± 5 s to 4.3 min ± 6 s for large and small files, respectively. As expected, the execution efficiency increases (Fig. 1D) and the mean execution time maintains a decaying trend (Fig. 1E) with increasing number of cores used.

4 Conclusion

As the availability of new, high-density MEAs for both in vitro and in vivo applications is becoming increasingly widespread, it is our strong opinion that disseminating our strategy and workflow will facilitate the adoption of neuroinformatic tools in the MEA electrophysiological community.

Acknowledgement

Financial support from the EC FP7 (Marie Curie Actions ‘NAMASEN’ & ‘NEUROACT’, contract nos. 264872 & 286403; and FET project “ENLIGHTENMENT”, contract no. 284801), the FWO (grant no. G.0888.12N), and the IUAP are kindly acknowledged.

References

[1] Berdondini L. et al. (2009). Extracellular recordings from locally dense microelectrode arrays coupled to dissociated cortical cultures. *J Neurosci Methods 177,* 386-396.

[2] Liu M.G., et al. (2013). Long-term potentiation of synaptic transmission in the adult mouse insular cortex: multi-electrode array recordings. *J Neurophysiol, 110*, 505–521.

[3] Buzsaki G. (2004). Large-scale recording of neuronal ensembles. *Nat Neurosci, 7,*446-451.

[4] Stevenson I.H., Kording K.P. (2011). How advances in neural recording affect data analysis. *Nat Neurosci, 14,* 139-42.

[5] Denker M., et al. (2010). Practically trivial parallel data processing in a neuroscience laboratory. In: Grün S. & Rotter S., ed., *Analysis of Parallel Spike Trains, 7,* 413-36, Springer US.

[6] Mahmud M., Pulizzi R., Vasikali E., Giugliano M. (2014). QSpike tools: a generic framework for parallel batch preprocessing of extracellular neuronal signals recorded by substrate microelectrode arrays. *Front. Neuroinform. 8*, 26.

Comparison of Neuronal Dynamics in 2D and 3D In Silico Networks

Inkeri Vornanen, Jarno M. A. Tanskanen, Jari Hyttinen, Kerstin Lenk*

Tampere University of Technology, Department of Electronics and Communications Engineering, and BioMediTech, Tampere
* Corresponding author. E-mail address: kerstin.lenk@tut.fi

Abstract
Neurons form in their natural environment three-dimensional structures, but most of the *in vitro* cultures of neurons have been planar 2D systems. As 3D space offers more possible structures for the neuronal network, it can be expected that also the behavior of the networks differ in 2D and 3D. Here we constructed computational models of 2D and 3D neuronal networks to predict how the network dynamics differ, when the network is 3D instead of 2D. The network model was based on a previously presented model called INEX, to which the spatial 2D and 3D topology models were added: randomly distributed neurons were connected to their neighbors inside a certain radius resulting in approximately 10%-connectivity. The spiking behavior of the simulated 2D networks was tuned to match the *in vitro* cultured human embryonic stem cell (hESC) derived neurons on 2D microelectrode arrays (MEAs). The same parameters were used for the 3D network simulation. Our simulations showed a clear difference between 2D and 3D networks: E.g. the 3D networks were more active than 2D networks. Our results suggest that the dimensionality plays an important role in the neuron network dynamics. The developed model enables us to test also other neuronal topologies and connectivity hypotheses.

1 Introduction

Neurons form three-dimensional structures in their natural environment. However, most of the *in vitro* cultures of neurons are two-dimensional to enable the use of planar microelectrode array (MEA) systems. As 3D space allows much more complex structures for the neuronal networks, it could be expected that the network behavior also differs in 2D and 3D.

Computational modelling of neuronal networks enables the study of fully known and controlled networks, where different hypothesis, such as topologies, can be tested easily. There are many models for describing *in vitro* neuronal cultures [1-3], but not so many with spatial topology [4].

In this study, we constructed 2D and 3D topology models on top of a previously presented neuronal network model called INEX [1]. The aim was to see, if and how the change of the dimensionality affects the behavior of the network. To ensure biologically plausible behavior of the network model the spiking and bursting behavior of the simulated 2D networks was tuned to match *in vitro* neuronal networks consisting of human embryonic stem cell (hESC) derived neurons measured with MEAs [5,6].

2 Methods

2.1 Network model

Our network model was based on a network model called INEX [1,6] which is a probabilistic neuronal network model with both excitatory and inhibitory Poisson neurons. As the original INEX model has no spatial topology, both the 2D and 3D topologies were added to the model: First 1000 neurons were placed randomly in 2D or 3D space. Thereafter each neuron was connected to all of its neighbors inside a certain range. The range was chosen so that the resulting network was approximately 10%-connected. The topology models are demonstrated in Fig. 1. The spike trains were recorded from 64 *in silico* neurons, which were picked from grid positions, see Fig. 1.The parameters of the 2D networks were tuned so that their spiking behavior matched the hESC-derived neuronal cultures [6]. Thereafter, the 3D networks were simulated using the same parameters to see the difference between the 2D and 3D networks. All the simulations were performed using the Neural Simulation Tool NEST [7].

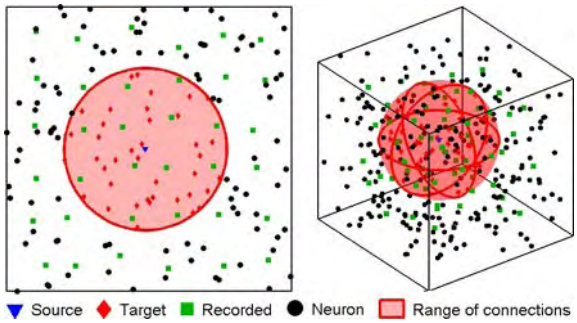

Fig. 1. Demonstration of the topology model in 2D and 3D. Figures present the connections of one example neuron (blue triangle). The red diamonds are the neurons with which the source is connected. Also the range of the connections is shown. The green rectangles mark the neurons whose spike trains are recorded. The black dots mark other neurons in the network. Not all 1000 neurons are shown.

2.2 Statistics

To compare the spiking activity of the simulated 2D and 3D, and the 2D cultured neuronal networks on

MEAs, statistics of the spiking and bursting were calculated. The bursts were detected using the Cumulative Moving Average algorithm [8], which is designed for use with variably spiking neuronal networks, such as hESC-derived. The calculated statistics were: the mean spike rate, burst rate, burst duration and the number of spikes in burst over the measurement/simulation period for each electrode/neuron. Of these means we calculated the medians and upper and lower quartiles in each cultured/simulated network. The statistical analysis was performed in Matlab.

3 Results

The statistics of the spiking behavior of the simulated networks are presented in Fig. 2. The activity of the simulated 2D networks corresponded to the activity of the cultured planar networks: All the calculated statistics of the 2D network lay between the quartiles of the MEA data.

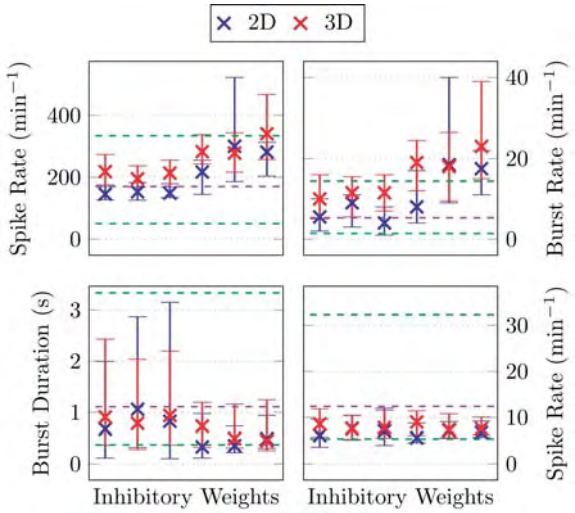

Fig. 2. The spiking statistics of the 2D and 3D networks. For comparison the purple and green horizontal lines mark the median and quartiles, respectively, of the hESC-derived neuronal networks.

As the 2D networks were transformed to 3D using the same parameters, a clear difference in the behavior of the networks was seen: The 3D networks were more active than the 2D networks with the same parameters. The mean spike rate in the 3D networks is about 30% higher than in 2D. The mean burst rate increases also even more. Additionally, the bursts in 3D networks were shorter: Both the burst duration and number of spikes per burst were 20-30% lower in 3D than 2D.

4 Conclusions/Summary

The 2D network model was tuned so that its spiking behavior matched the hESC-derived neuronal cultures. When the network was transformed to 3D , a clear change in the behavior was seen. In general, the 3D networks were more active than the 2D networks. A recent study [9] has shown how the activity in 3D cultures is less synchronized than in 2D cultures.

The relatively simple topology model used in this study was able to induce a clear difference in the behavior of the 2D and 3D networks, even though the general connectivity or the number of neurons was not changed. Additionally, the simulations do not include delays in communication. Therefore, all changes were based on purely the dimensional change. This suggests that the dimensionality of the neuronal network greatly affects the dynamics of the network.

The bursts in the model networks were typically shorter than in the biological networks, which suggests that the model should be further improved towards a more biologically plausible one. Moreover, the behavior of the biological 3D networks was not verified here, as 3D culture systems and MEAs are still under development e.g., in the EU project “3DNeuroN”.

Acknowledgement

This research has been supported by the 3DNeuroN project in the European Union's Seventh Framework Programme, Future and Emerging Technologies, grant agreement n°296590. We also want to thank Adj. Prof Narkilahti, NeuroGroup, BioMediTech, University of Tampere for providing the biological data used in this study.

References

[1] Lenk, K. (2011): A simple phenomenological neuronal model with inhibitory and excitatory synapses. *Advances in Nonlinear Speech Processing, 7015, 232-238*

[2] Gritsun, T.A., le Feber, J., Stegenga, J. & Rutten, W.L.C. (2010): Network bursts in cortical cultures are best simulated using pacemaker neurons and adaptive synapses. *Biological Cybernetics, 102, 293-310.*

[3] Brunel, N. (2000): Dynamics of sparsely connected networks of excitatory and inhibitory spiking neurons. *Journal of Computational Neuroscience, 8, 183-208.*

[4] Abbott, L.F. & Rohrkemper, R. (2007): A simple growth model constructs critical avalanche networks. *Computational Neuroscience: Theoretical Insights into Brain Function, 165, 13-19.*

[5] Heikkilä, T.J., Ylä-Outinen, L., Tanskanen, J.M.A., Lappalainen, R.S., Skottman, H., Suuronen, R., Mikkonen, J.E., Hyttinen, J.A.K. & Narkilahti, S. (2009): Human embryonic stem cell-derived neuronal cells form spontaneously active neuronal networks in vitro. *Experimental Neurology, 218, 109-116.*

[6] Lenk, K.., Priwitzer, B., Ylä-Outinen, L., Tietz, L., Narkilahti, S. & Hyttinen, J.A.K. (2014): Simulation of developing human neuronal cell networks. *Frontiers in Neuronal Circuits* (submitted).

[7] Gewaltig M.-O. & Diesmann M. (2007): NEST (NEural Simulation Tool). *Scholarpedia 2(4).*

[8] Kapucu, F.E., Tanskanen, J.M.A., Mikkonen, J.E., Ylä-Outinen, L., Narkilahti, S. & Hyttinen, J.A.K. (2012): Burst analysis tool for developing neuronal networks exhibiting highly varying action potential dynamics. *Frontiers in Computational Neuroscience, 6(38).*

[9] Frega, M., Tedesco, M., Massobrio, P., Pesce, M. & Martinoia (2012): 3D neuronal networks coupled to microelectrode arrays: an innovative in vitro experimental model to study network dynamics. *8th International Meeting on Substrate-Integrated Microelectrode Arrays, 40-42*

Estimating Stationary Functional Connection Underlying Switching-State Network Activity

Yuichiro Yada[1,2,3*], Osamu Fukayama[1], Takayuki Hoshino[1], Kunihiko Mabuchi[1]

1 Graduate School of Information Science and Technology, The University of Tokyo, Tokyo, Japan
2 Research Center for Advanced Science and Technology, The University of Tokyo, Tokyo, Japan
3 Research Fellow of the Japan Society for the Promotion of Science, Tokyo, Japan
* Corresponding author. E-mail address: yuichiro_yada@ipc.i.u-tokyo.ac.jp

Abstract
Activity levels of cultured neuronal networks show repeating transition between up states and down states. Therefore, when estimating the underlying stationary structures of the networks from their activities, it is harmful to handle data from both states as continuous time series. A preceding research reported improvement of estimation when analysing only down states. However, we assumed that up "bursting" states also reflect useful information for estimating a structure. In this paper, we proposed a novel transfer-entropy-based estimation method that process data from each state separately, but uses both data for estimation. The method showed better and robust performance for detecting neuronal connections in simulation and estimated more realistic structure in actual cortical networks.

1 Background

Multielectrode arrays (MEAs) are effective experimental systems for recording spikes from wide fields of cultured neuronal networks because of its stability and high temporal resolution in recording and thus widely used for investigating functional structures of neuronal networks. Cultured neuronal networks show bursting activities, which are characteristic dynamical activity-level transition between active bursting states and inactive resting states. The network bursts are considered to play fundamental roles in neuronal development.

Transfer entropy [1] is one of the promising methods for estimating causality between multiple time series, but it is not designed for evaluating information transfer in switching-state activities. Stetter *et al*. proposed a connection estimation method that combined calcium imaging and transfer entropy, where they used data from only non-bursting states for estimation [2]. They reported remarkable improvement against original transfer entropy in simulated calcium imaging data.

However, as a bursting activity isn't structural change but transient of activity modes, it is assumed that information of the structure is reflected in both states. Here, we proposed a transfer-entropy-based connection estimation method for bursting networks that used both bursting "up" state and resting "down" state for estimation.

2 Methods

Transfer entropy (TE) from a spike train $\{t_i\}$ to another spike train $\{t_*\}$ is described as

$$TE = \sum p\left(t_{t+1}, t_t^{(k)}, f_{t+1-d}\right) \log \frac{p\left(t_{t+1} \middle| t_t^{(k)}, f_{t+1-d}\right)}{p\left(t_{t+1} \middle| t_t^{(k)}\right)}$$

where d is transfer delay and $t_t^{(k)}$ means $t_t, t_{t-1}, \cdots t_{t-k+1}$. Here, we expressed *TE* as an original index that uses all data for continuous time series, *TErest* as the index that analyzes data from resting states only and *TEburst* as that uses data from bursting states only. Our proposed index was described as

$$NTErest + NTEburstCI,$$

where *NTErest* is normalized *TErest* and *NTEburstCI* is normalized Coincidence Index [3] of *TEburst.* The resting states and the bursting states were identified by Gaussian smoothed total output spikes from all neurons belong to a neuronal network. Pairs of neurons were identified as connected when these indices were over thresholds.

We evaluated the method with data from simulated spiking neuronal networks consist of 500 Izhikevich-model neurons and dynamical synapses. The 400 excitatory and 100 inhibitory neurons were randomly connected, where inhibitory-inhibitory connections were not made. The structures were stable thorough simulation. Synaptic efficacies fluctuated according to short-term plasticity model, but no long-term plasticity models, such as spike-timing dependent plasticity (STDP), were included. Performance of each method was evaluated with accuracy of connection detection with the receiver operating characteristics (ROC) curve. Thresholds were set for detecting specific rates of false connections. The ROC curve was depicted as mean values of 100 samples.

The proposed method was also applied to recorded data from living neuronal networks. Cortical neurons derived from E18 Wister rats were cultured on 64 Ch. MEAs (MED-P210A; Alpha MED Scientific Inc.)

for 27 days *in vitro*. Spontaneous activities were recorded for 10 minutes with sampling rate at 20 kHz. Then, recorded signals were band-pass filtered at 300-3000 Hz and spike trains were acquired after spike-detection and spike-sorting processes.

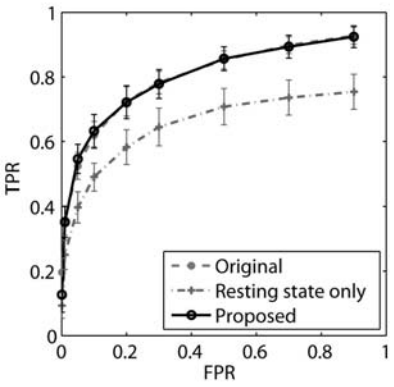

Fig. 1. ROC curve that acquired from simulated sparse random-connected neuronal networks. (Connection prob.=0.02, N=20, error bar: s.d.)

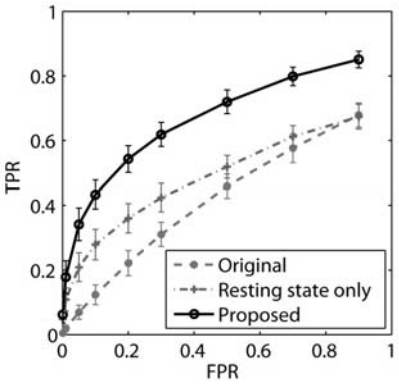

Fig. 2. ROC curve that acquired from simulated dense random-connected neuronal networks. (Connection prob.=0.05, N=20, error bar: s.d.)

3 Results

The Proposed method showed good and robust results in detecting connections in simulated bursting neuronal networks. Fig. 1 shows ROC curves acquired from sparse connected random networks. Performance of the proposed method was as good as that of an identification method using original *TE*. *TErest* showed inferior performance against original *TE* in sparse networks, but performed better than original *TE* in more densely connected networks, as shown in Fig. 2. However, The proposed method showed superior performance against both *TE* and *TErest* in this data. This indicates bursting states had considerable useful information for estimating connection.

Using both-states data for detecting connections in actual living neuronal networks, more non-localized networks were detected. Fig. 3 shows detected networks from cultured networks. When using data from only resting states, few neurons had most part of connections and sometimes unnaturally localized networks were estimated (Fig. 3(a)), whereas proposed method detected non-localized structures (Fig. 3(b)). As not all neurons fired in both resting states and bursting states, it was possible to detect realistic stationary structure when considering activities from both states.

4 Conclusions

The proposed estimation method that deals information from both up and down state showed improvement in detecting connections in simulated bursting neuronal networks and was available to estimate non-localized realistic networks in actual living cultured networks. This suggests both resting states and bursting states contains useful information and should be considered for network estimation.

Acknowledgement

This work was partly supported by Sasakawa Scientific Research Grant (25-219) from Japan Science Society.

References

[1] Schreiber, T. (2000): Measuring information transfer. *Physical Review Letters*, 85(2), 461-464.

[2] Stetter, O. (2012): Model-free reconstruction of excitatory neuronal connectivity from calcium imaging signals. *PLOS Computational Biology*, 8(8), e1002653.

[3] Ito, S. (2011): Extending transfer entropy improves identification of effective connectivity in a spiking cortical network model. *PLOS One*, 6(11), e27431.

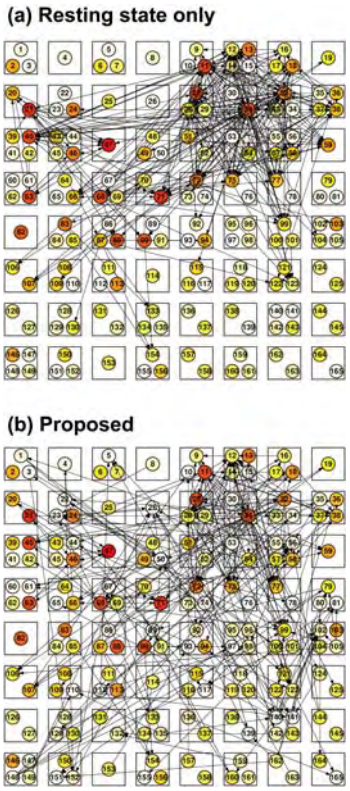

Fig. 3. Detected network structure from an actual cortical culture using (a) *TErest* and (b) the proposed index. Squares and circles mean electrodes of MEA and neurons respectively. Colors of neurons indicate their firing rates.

Network Dynamics in Connected Neuronal Sub-Populations During In Vitro Development

Marta Bisio[1#], Alessandro Bosca[1#], Valentina Pasquale[1], Luca Berdondini[1] and Michela Chiappalone[1*]

1 Istituto Italiano di Tecnologia (IIT), Genova, Italy
# Equal Contribution
* Corresponding author. E-mail address: michela.chiappalone@iit.it

Abstract
Uniform and modular primary hippocampal cultures from embryonic rats were grown on commercially available Micro-Electrode Arrays to investigate network activity with respect to development. Modular networks, consisting of active and inter-connected sub-populations of neurons, were realized by means of bi-compartmental polydimethylsiloxane structures. Spontaneous activity in both uniform and modular cultures was periodically monitored during their development.

1 Backround

Although very informative, in vivo experiments do not allow controlled manipulation of the spatio-temporal dynamics of neuronal networks, while in vitro systems can be more easily accessed, monitored and modeled [1]. Indeed, in order to provide a simplified but plausible representation of interacting neuronal assemblies, in vitro systems should be organized in connected ('modular') neural sub-populations [2].

The integration of Micro Electrode Arrays (MEAs) with microfluidic structures designed for growing *in vitro* modular cultures allowed us to characterize the neurodynamics of reduced biological models of the brain over extended timescales.

2 Methods and Statistics

To achieve a long-term segregation of the network into two distinct yet interconnected neuronal populations, a cell-confinement system was assembled on standard MEAs. The polymeric structure for the physical confinement of neuronal cultures has been realized in polydimtheylsiloxane (PDMS) by soft lithography and by using a photolithographically defined EPON SU-8 master on a silicon substrate. As experimental model, we used dissociated neurons from the hippocampus of embryonic rats at gestational day 18 [3].

We performed experiments on 16 cultures (8 modular, i.e. with physical confinement, and 8 uniform) monitored from 16 up to 55 Days In Vitro (DIVs), divided into four DIV ranges: *i)* 16- 25 DIVs; *ii)* 26 - 35 DIVs; *iii)* 36 - 45 DIVs; *iv)* 46 - 55 DIVs. The normal distribution of experimental data was assessed using the Kolmogorov-Smirnov normality test. According to the distribution of the data, we performed either parametric or non-parametric tests and p-values < 0.05 were considered significant. We applied the Mann-Whitney U-test when comparing two experimental groups (e.g. modular vs uniform cultures) at each developmental stage. For multiple comparisons (e.g. same experimental group at different DIVs), we performed either the one-way ANOVA statistical test or the Kruskal-Wallis ANOVA on Ranks.

3 Results

Spontaneous activity in both uniform and modular cultures was periodically monitored, from a few days up to eight weeks after plating. In particular, we found that: *i)* in uniform cultures channels fire in a synchronous way (Fig. 1A, left), while modular cultures shows a desynchronization among the two compartments activity (Fig. 1A, right), more pronounced at the beginning of the development (DIV 16-25); *ii*) the Coefficient Variation (CV) of the Mean Firing Rate is lower in case of modular cultures (Fig. 1B, left, red bars) during the entire development and presents a lower variation compared to uniform cultures (Fig. 1B, right, black bars), while the CV of the Mean Bursting Rate indicates a comparable level of variability between the two cultures (Fig. 1B, right); *iii)* uniform cultures are globally characterized by a higher level of correlation (Fig. 1C, left), but this difference disappears for older cultures (data not shown); *iv)* for modular cultures, a lower inter-compartmental correlation is observed (Fig. 1C, right) compared to the intra one during the entire development, thus suggesting a delay in the signal propagation and a coexistence of segregation and integration of activity; *v)* the synchronized bursting activity shown by modular networks was preferentially originated and propagated in one of the two compartments ('dominant'), even in cases of balance of firing rate between the two compartments, and this dominance was generally maintained during the entire monitored developmental frame (data not shown).

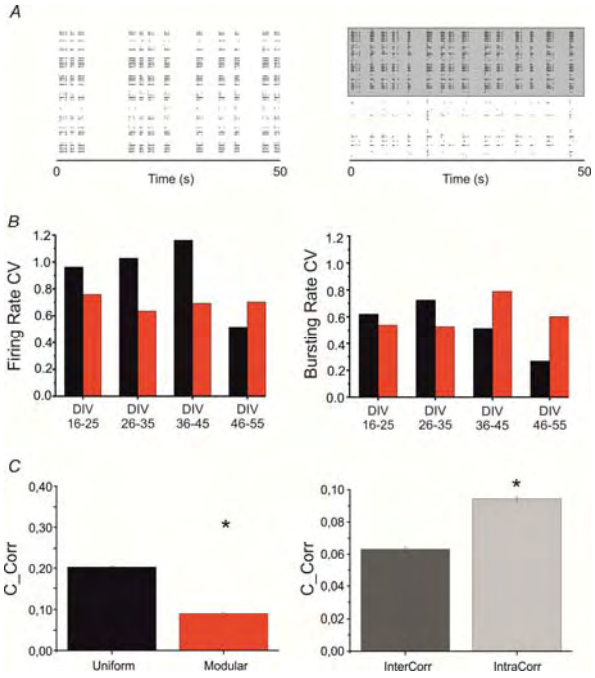

Fig 1. A. 50-seconds raster plots of spontaneous activity of a representative uniform (*left*) and modular culture (*right*) at the beginning of the development (DIV 16-25). The grey area indicates the upper compartment. **B.** *Left.* Comparison between the Coefficient of Variation (CV) of the Mean Firing Rate of uniform (black bars) and modular cultures (red bars). *Right.* Comparison between the CV of the Mean Bursting Rate of uniform (black bars) and modular cultures (red bars). **C.** *Left.* Comparison between the Cross Correlation value (C_Corr, i.e. peak of the cross-correlogram), computed for each couple of active channels, for uniform and modular cultures at the beginning of the development (DIV 16-25). *Right.* Comparison between the Cross Correlation computed inside each compartment (IntraCorr) and between the two compartments (InterCorr) at the beginning of the development. Statistical analysis has been performed by using the Mann-Whitney U test [*p<0.05]

4 Conclusion/Summary

The described approach allowed us to implement a low-complexity biological model used to investigate, in a controlled and reproducible way, the interplay between two connected neuronal populations during development, and to perform an unbiased comparison with the activity of uniform networks. Our results constitute important evidence that engineered neuronal networks are a powerful platform to systematically approach questions related to the dynamics of neuronal assemblies. Unlike networks *in vivo*, in which multiple activation pathways are impinging on any recorded region, these partially confined networks can be studied in a controlled environment. Moreover, such a system can be easily interfaced to robotic artifacts in order to better investigate coding properties towards the final goal of integrating brains and machines [4].

Acknowledgement

The research leading to these results has received funding from the European Union's Seventh Framework Programme (ICT-FET FP7/2007-2013, FET Young Explorers scheme) under grant agreement n° 284772 BRAINBOW (www.brainbowproject.eu).

References

[1] Bonifazi, P., DIfato, F., Massobrio, P., Breschi, G. L., Pasquale, V., Levi, T., Goldin, M., Bornat, Y., Tedesco, M., Bisio, M., Kanner, S., Galron, R., Tessadori, J., Taverna, S., and Chiappalone, M. (2013): In vitro large-scale experimental and theoretical studies for the realization of bi-directional brain-prostheses. *Frontiers in Neural Circuits, 7, 40.*

[2] Levy, O., Ziv, N. E., and Marom, S. (2012): Enhancement of neural representation capacity by modular architecture in networks of cortical neurons. *European Journal of Neuroscience, 35, 1753-1760.*

[3] Colombi, I., Mahajani, S., Frega, M., Gasparini, L., and Chiappalone, M. (2013): Effects of antiepileptic drugs on hippocampal neurons coupled to micro-electrode arrays. *Frontiers in Neuroengineering, 6, 10.*

[4] Tessadori, J., Bisio, M., Martinoia, S., and Chiappalone, M. (2012): Modular neuronal assemblies embodied in a closed-loop environment: toward future integration of brains and machines. *Front Neural Circuits, 6, 99.*

Evoked Activity of Major Burst Leaders in Cultured Cortical Networks

Valentina Pasquale[1*], Sergio Martinoia[2], Michela Chiappalone[1]

1 Department of Neuroscience and Brain Technologies, Istituto Italiano di Tecnologia, Genova, Italy
2 Department of Informatics, Bioengineering, Robotics and System Engineering, University of Genova, Genova, Italy
* Corresponding author. E-mail address: valentina.pasquale@iit.it

Abstract
We electrically stimulated rat cortical networks cultured on micro-electrode arrays (MEAs) from different locations, being either leaders of the spontaneous bursting activity or not, and we compared the evoked activity of major burst leader (MBL) sites to the one shown by non-MBLs (nMBLs). We also compared network responses obtained by MBL stimulation with respect to nMBL stimulation. Stimulation usually evoked stronger and faster responses on MBLs than on nMBLs. Moreover, stimulation of MBLs evoked faster (but not stronger) network responses than stimulation of nMBLs.

1 Background

Recent studies about the spontaneous generation and propagation of coordinated activity in cultured neuronal networks reported the existence of privileged sites that consistently fire earlier than others at the onset of network bursts (NBs), which have been termed major burst leaders (MBLs) [1, 2]. In this study, we investigated the existing relationship between spontaneous and evoked activity of MBLs with respect to non-MBLs (nMBLs). Moreover, we also compared network responses evoked by either MBLs or nMBLs.

2 Methods and statistics

2.1 Experimental protocol

Primary cultures of rat cortical neurons were plated on planar micro-electrode arrays (8×8 grid, Multi Channel Systems, Reutlingen, DE). Our dataset comprises 20 recordings from mature cultures (> 3 weeks *in vitro*). After recording spontaneous activity, we delivered to each culture a test stimulus from eight selected channels of the array, four of which were classified as MBLs and the rest as nMBLs. MBLs were selected according to their leadership score (LS) (i.e. electrodes leading at least 4% of all NBs). The test stimulus consisted of a train of 100 voltage pulses at 0.2 Hz, each of which being a positive-then-negative square wave (amplitude ±750 mV, duration 500 µs, duty cycle 50%).

2.2 Data analysis

First, we analysed spontaneous activity of our cultures by computing the main firing and bursting statistics of all MBL and nMBL channels and comparing the statistical distributions of these measures for these two groups (cf. Fig. 1).

Then, we characterized each response to electrical stimulation by measuring the area of the post-stimulus time histogram (PSTH), corresponding to the average number of evoked spikes, and the delay of the first evoked spike. These measures were normalized either to compare the effects of different stimulating sites on the same responding site (normalization 1) or to compare responses of different sites to the same stimulating site (normalization 2). Normalization 1 allowed to compare responses to MBL stimulations with responses to nMBL stimulations (cf. Fig. 2B-D), while normalization 2 allowed to compare MBL responses to nMBL responses (cf. Fig. 2A-C).

3 Results

We recorded neuronal electrophysiological activity from a total of 933 active channels (i.e. channels whose firing rate is > 0.1 spikes/s) in 20 cultures. Of these 933 channels, 108 (11.58%) were classified as MBLs (criterion: LS > 4% of all NBs). Firing rate, firing rate within bursts and burst duration of each electrode were normalized over the mean value obtained from each culture, considering all active electrodes. Statistical analysis has been performed by pooling normalized values of all cultures. MBLs present higher firing rates with respect to nMBL channels (Fig. 1A) and a high ratio of spikes within bursts (Fig. 1B). They also feature longer burst durations (Fig. 1D), but comparable values of firing rate within bursts (Fig. 1C). Altogether these results led us to conclude that MBL sites are highly active bursting channels. These results confirm previous similar findings [1, 3].

We also found that MBLs generally respond to stimulation with higher number of spikes (Fig. 2A) and more rapidly to electrical stimulation (Fig. 2C). Moreover, electrical stimulation from MBLs evokes, on average, earlier responses than the stimulation delivered from other locations (Fig. 2D), but does not evoke stronger responses (Fig. 2B). Apart from PSTH areas of MBL stimulations vs. nMBL stimulations

(Fig. 2B), all other statistical distributions reported in Fig. 2 are significantly different, as assessed by using two-sample Kolmogorov-Smirnov test (p-level = 0.01).

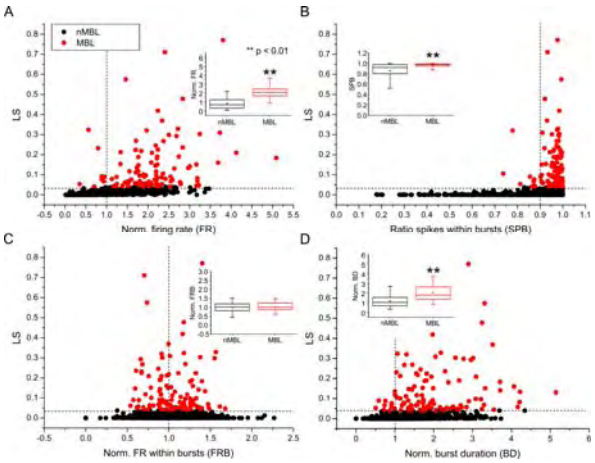

Fig. 1. MBL present higher firing rates and longer burst durations, together with poor random spiking activity. A, Burst leadership score (LS) VS normalized firing rate for all recorded electrodes (825 nMBLs, in black, 108 MBLs, in red). B, LS VS ratio of spikes within bursts. Same notation as in A. C, LS VS normalized firing rate within bursts. Same notation as in A. D, LS VS normalized burst duration. Same notation as in A. Insets report box plots of statistical distributions of the variables reported in the same panels, for nMBL (black) and MBL (red) respectively. Stars indicate statistical significance (p-level = 0.01), as assessed by non-parametric Mann-Whitney U-test.

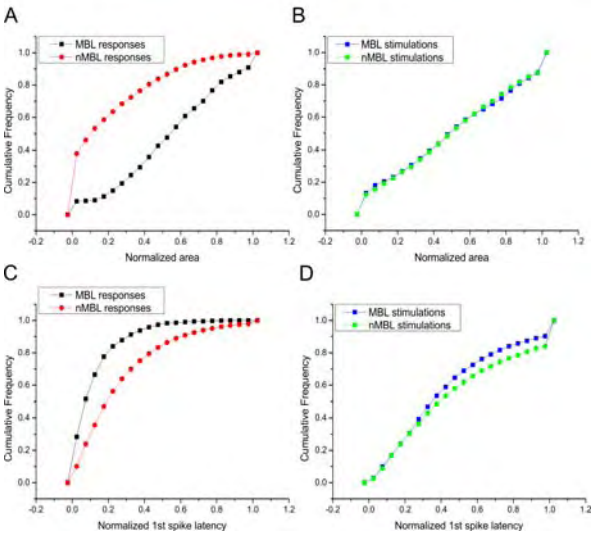

Fig. 2. Cumulative frequency of normalized PSTH area (A-B) and normalized first-spike latency (C-D). A-C, comparison of either MBL (black) or nMBL (red) responses; B-D, comparison of responses to either MBL (blue) or nMBL (green) stimulations.

4 Summary

To summarize, we showed that in the absence of any stimulation MBLs are highly active bursting channels, displaying poor random spiking activity.

Moreover, they also play a role in coordinating and driving the evoked bursts of activity, featuring more intense and faster responses to electrical stimulation. Finally, the network generally responds with shorter latencies when stimulated from MBLs.

Acknowledgement

The research leading to these results has received funding from the European Union's Seventh Framework Programme (ICT-FET FP7/2007-2013, FET Young Explorers scheme) under grant agreement n° 284772 BRAINBOW (www.brainbowproject.eu).

References

[1] Ham, M. I., Bettencourt, L. M., McDaniel, F. D., and Gross, G. W. (2008): Spontaneous coordinated activity in cultured networks: analysis of multiple ignition sites, primary circuits, and burst phase delay distributions. J Comput Neurosci, 24, 346-57.

[2] Eckmann, J. P., Jacobi, S., Marom, S., Moses, E., and Zbinden, C. (2008): Leader neurons in population bursts of 2D living neural networks. New Journal of Physics, 10,

[3] Eytan, D. and Marom, S. (2006): Dynamics and effective topology underlying synchronization in networks of cortical neurons. J Neurosci, 26, 8465-76.

Use of Entropy to Discriminate Between Different Conditions in MEA Recordings

Capurro Alberto[1*], Perrone Sandro[1], Heuschkel Marc[2], Makohliso Solomzi[2], Baez Candise[1] and Luthi-Carter Ruth[1]

1 Department of Cell Physiology and Pharmacology, University of Leicester, UK
2 Qwane Biosciences SA, EPFL Innovation Park, Lausanne, Switzerland
* Corresponding author. E-mail address: ac331@le.ac.uk

Abstract
We have identified Shannon entropy as a sensitive single parameter to detect changes in electrophysiologic behaviour of neuronal cells cultured on MEAs. We demonstrate the use of this measure using an *in vitro* model of Huntington's disease (HD). The spike time histograms of the population activity recorded in the MEAs had larger values of Shannon entropy when they were treated with brain-derived neurotrophic factor (BDNF), a known neuroprotectant and neuromodulatory factor.

1 Backround / Aims

We are interested in the identification of quantities suitable to discriminate between different conditions in MEA recordings that may represent human disease-related abnormalities in neuronal connectivity.

2 Methods / Statistics

Spontaneous recordings were conducted to compare the spiking activities of rat P1 dissociated primary neuronal cultures under different disease-related conditions [e.g., 1]. The spike detection and data analyses were performed with customized R codes run using a cluster computer ("Alice") at the University of Leicester. We constructed time histograms of the population spiking activity (Fig. 1).

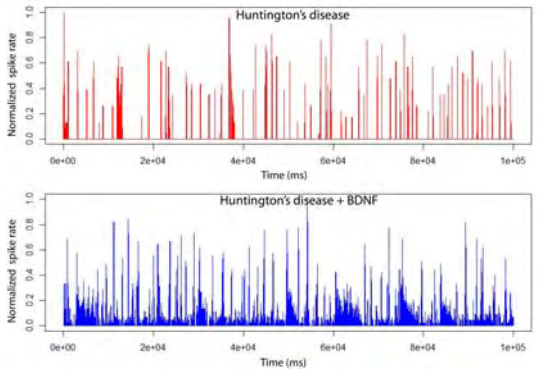

Fig. 1. Spike time histograms in HD (red) and HD+BDNF (blue).

The Shannon entropy [2] of the number of spikes per bin was used to evaluate the effect of BDNF treatment on the spiking activity of the cultures in comparison with the mean values of the same time series.

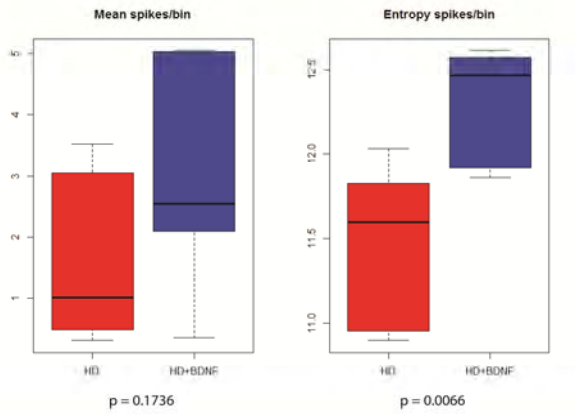

Fig. 2. Effects of BDNF on the HD culture measured using the mean number of spikes per bin (left panel) and using the entropy of the number of spikes per bin (right panel). N= 6 cultures in each condition.

3 Results

The mean number of spikes per bin tended to increase with the BDNF treatment but did not reach significance due to the variability found between different cultures (Fig. 2, left panel). Conversely, the entropy was significantly larger after BDNF (Fig. 2, right panel) because it showed less variability in different cultures. The entropy-based measure therefore proved more sensitive to discriminate the effect of BDNF than the mean value of the same time series (DIV20, Fig. 2).

4 Conclusion/Summary

Shannon entropy provided an effective way to discriminate between two conditions using a single parameter. To understand why the entropy increased with the BDNF treatment we constructed amplitude histograms of the time series shown in Fig 1. In these histograms (Fig. 3) we can see that most cases are

classified in the first bar of the left, both with and without BDNF (Panels A and B). However, in the cultures treated with BDNF there are more cases that fall in the classes corresponding to the bars 2 to 10 of the histogram. This can be better appreciated by focusing onto the lower portion of the ordinate scale, as illustrated in panels C and D. Thus, the uncertainty of the classification is larger with BDNF and this is reflected in a larger entropy value.

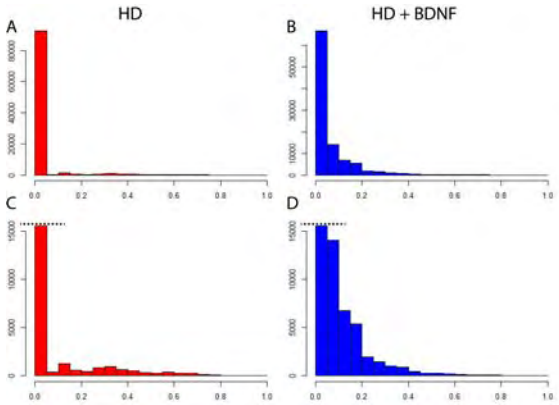

Fig. 3. Amplitude histograms of the time series shown in Fig. 1. Upper panels depict full scale and lower panels show lower ordinates in detail by cutting the first bar as indicated with dotted lines.

In this poster we highlight the use of the entropy measurement as a sensitive analysis parameter and discuss its application to different time series derived from the MEA recordings. Regarding BDNF our results support the conclusions of a previous report [1], demonstrating that the impairment of the synaptic coupling caused by the mutant Huntingtin gene could be reversed with this treatment. In the future, our data processing approach will be used to study the positive effects of other prospective treatments for HD and the deleterious effects at synapses in other neurodegenerative diseases.

Acknowledgement

This research was supported via a grant from the European Community's Seventh Framework Program FP7-PEOPLE-2011-IAPP under Grant Agreement n°286403 – NEUROACT.

References

[1] Gambazzi L et al. (2010) J. Pharmacol Exp Ther 335 (1), 13-22.
[2] Shannon, C E (1948) Bell Syst. Tech. J. 27, 379-423, 623-656.

Initiation of Spontaneous Bursts in Dissociated Neuronal Cultures Is Poisson Process

Arthur Bikbaev[1*], Abdelrahman Rayan[2], Martin Heine[1]

1 AG Molecular Physiology, Leibniz Institute for Neurobiology, Magdeburg, Germany
2 AG Molecular Neuroplasticity, Deutsches Zentrum für Neurodegenerative Erkrankungen, Magdeburg, Germany
* Corresponding author. E-mail address: abikbaev@lin-magdeburg.de

Abstract
The Poisson process is one of the most commonly used models of spike trains in neural networks. To address the question whether the neuronal firing in cultured neuronal networks can indeed be considered as Poisson process, we analyzed the features of spontaneous spike trains recorded during development in dissociated hippocampal cultures grown on microelectrode arrays (MEAs).

1 Methods

All experimental procedures were carried out in accordance with the EU Council Directive 86/609/EEC and were approved and authorised by the local Committee for Ethics and Animal Research (Landesverwaltungsamt Halle, Germany).

Neuronal cultures were prepared from Wistar rat embryos at gestation day 18 (E18) as described previously [2]. The suspension of dissociated hippocampal cells was plated on 60 channel (inter-electrode distance 200 µm) MEAs (MultiChannel Systems, Reutlingen, Germany). Cultures were incubated in serum-free Neurobasal medium at 37°C in a humidified atmosphere (95% air and 5% CO_2), with culture medium being partially exchanged once a week.

The neuronal activity in rat hippocampal cultures (n = 10 MEAs) was sampled at 10 kHz using MEA1060INV-BC system and MC_Rack software (MultiChannel Systems, Reutlingen, Germany) on a weekly basis from day *in vitro* (DIV) 14 to 35. No external stimulation was applied to cultures during this period. The analysis was performed on 600-s long epochs of activity recorded at each time point in each individual culture. The threshold-based spike detection (± 6SD of noise) in high-pass filtered (300 Hz) records was followed by burst identification (≥ 5 spikes with inter-spike interval (ISI) < 100 ms). Obtained spike and burst time-stamps were used further for calculation of the mean firing rate (MFR) and the mean bursting rate (MBR) per minute. Due to relatively low amount of activity in immature cultures at DIV14, absolute MFR and MBR values for each individual channel were normalized to respective values obtained at DIV28 (taken as 100%). Processing and analysis of recorded signals were carried out using Spike2 software (Cambridge Electronic Design, Cambridge, UK).

Statistical analysis included the protected one-way ANOVA for *development* factor followed by Duncan's *post hoc* test, which were performed using STATISTICA data analysis system (Statsoft, Inc., Tulsa, USA). Factorial effects and differences were considered as significant at $p < 0.05$. Results are presented as mean±S.E.M.

2 Results

The analysis of developmental profile of spontaneous neuronal activity revealed that both the MFR and the MBR were significantly influenced by developmental factor ($F_{3,1132}$=21.6 and $F_{3,701}$=30.0, respectively; both $P < 0.00001$). The third week *in vitro* was characterized by dramatic enhancement of neuronal activity, with DIV21 being associated with peak levels of the MFR and MBR (Fig. 1A). In contrast, the fourth week of culturing was accompanied by significant reduction of spiking and bursting activity, while only marginal changes were observed after DIV28. Bursting is known to become a predominant pattern of activity in cultured neuronal networks during development [1,3]. Such burstinness of spontaneous spike trains results in heavy-tailed distribution and high variation of ISIs due to coexistence of numerous short intra-burst ISIs and rarer but long ISIs between bursts (i.e., IBIs). Indeed, the mean coefficient of variation of ISI (CV_{ISI}) throughout analyzed period (DIV14-35) was in the range between 2.6 and 3.0 (Fig. 1B). However, for IBIs we found remarkably lower variation with $CV_{IBI} \approx 1$, suggesting that *initiation* of bursting remains a Poisson process despite large-scale fluctuations of spiking and bursting rates in neuronal cultures during development. To clarify this, we calculated the Fano factor for bursting rate (F_{BR}) in various time bins ranging from 0.1 to 1.0 s. We found that $F_{BR} \approx 1$ for most conditions, except F_{BR} values obtained for lengthy time bins (> 500 ms) in immature two-week old cultures (Fig. 1B).

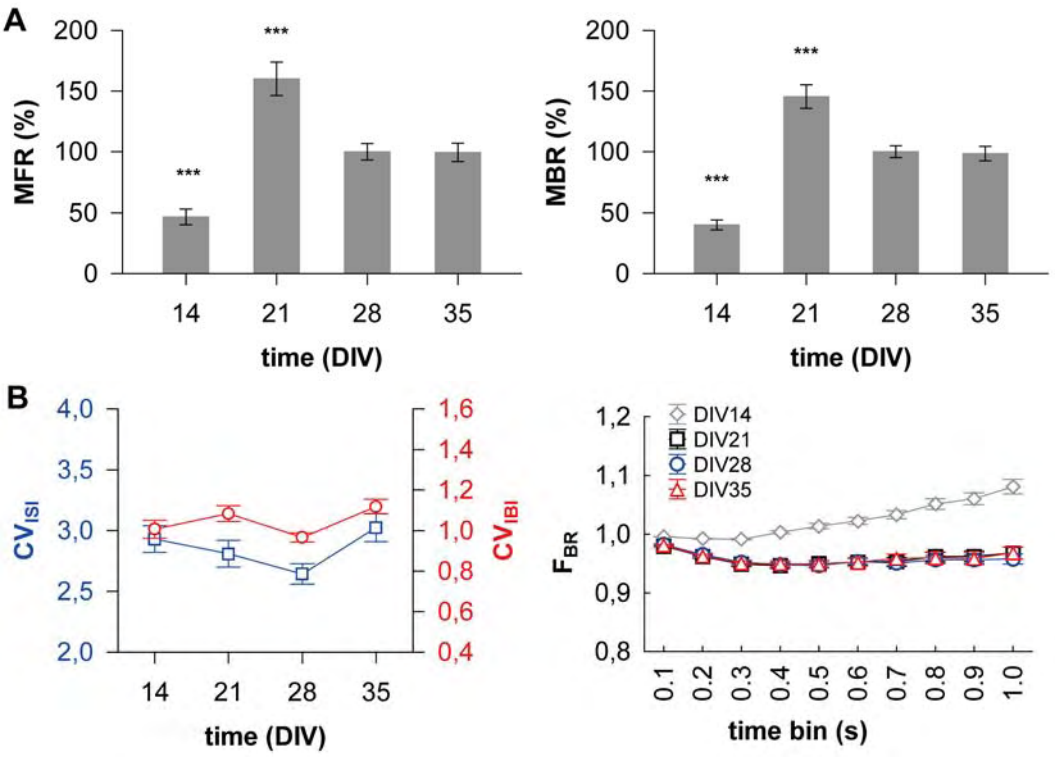

Fig. 1. The spontaneous initiation of bursts in dissociated hippocampal cultures remains stochastic during development and can be considered as Poisson process. **A**. Dramatic changes of spiking and bursting rates during third and fourth weeks *in vitro* are followed by steady-state stabilization after DIV28. **B.** Despite large-scale fluctuations of the MBR during development, both the coefficient of variation of IBIs and the Fano factor for bursting rate are ≈1 and remain relatively stable in developing and mature hippocampal cultures grown on MEAs.

3 Conclusion

Several properties of bursting activity are subject of strong developmental regulation reflecting the maturation of synaptic connectivity and circuitry formation. However, the initiation of bursts in developing neuronal cultures is stochastic Poisson process, and remains as such upon maturation. Our data suggest that bursts represent a rather complex phenomenon with distinct probabilities of the first spike and the following ones in each individual bursting episode.

Acknowledgement

This work was supported by the Federal State Sachsen-Anhalt (grant LSA RG Molecular Physiology) and the DFG (grant HE-3604/2-1).

References

[1] Corner, M.A. (2008). Spontaneous neuronal burst discharges as dependent and independent variables in the maturation of cerebral cortex tissue cultured *in vitro*: A review of activity-dependent studies in live 'model' systems for the development of intrinsically generated bioelectric slow-wave sleep patterns. *Brain Research Reviews*, 59, 221-244.

[2] Kaech, S., Banker, G. (2006). Culturing hippocampal neurons. *Nature Protocols*, 1, 2406-2415.

[3] Marom, S., Shahaf, G. (2002). Development, learning and memory in large random networks of cortical neurons: lessons beyond anatomy. *Quarterly Reviews of Biophysics*, 35, 63-87.

Selective Laser Ablation of Interconnections Between Neuronal Sub-Populations: A Test-Bed for Novel Neuroprosthetic Applications

Alberto Averna[1#], Marta Bisio[1#], Valentina Pasquale[1], Paolo Bonifazi[2], Francesco Difato[1] and Michela Chiappalone[1*]

1 Department of Neuroscience and Brain Technologies, Istituto Italiano di Tecnologia, Genova, Italy
2 School of Physics and Astronomy, Tel Aviv University (TAU), Israel
[#] Equal Contribution
* Corresponding author. E-mail address: michela.chiappalone@iit.it

Abstract
Cortical and hippocampal patterned networks, composed of inter-connected modules of different size, were grown on commercially available Micro-Electrode Arrays to investigate neurodynamics. Such patterned networks, realized by means of multi-compartmental polydimethylsiloxane structures, represent an in vitro model to study electrophysiological activity of damaged neuronal networks in the central nervous system. A laser microdissector has been used to selectively cut the neural connections between different modules, thus mimicking a pathological condition. Spontaneous and evoked activity of modular neural networks has been characterized in both healthy and damaged cultures.

1 Background

In the last decades, great efforts have been made to focus on studying neuro-prostheses targeting lesions at the level of the CNS and aimed at restoring lost cognitive functions [1, 2]. Simplified *in vitro* models of cell assemblies can provide useful insights for the design of future cognitive brain prostheses. In particular, studies of healthy and lesioned *in vitro* neuronal networks can be exploited as a test-bed for the development of innovative neuro-prostheses [3]. To investigate the inherent properties of neuronal cell assemblies as a complement to artificial computational models, engineered networks of increasing structural complexity, from isolated finite-size networks up to inter-connected modules, were grown on Multi Electrode Arrays (MEAs). Here, we characterized the spontaneous and evoked activity of 2D neuronal cultures, before and after selective laser dissection of physical connections between neuronal sub-populations [4]. The quantitative characterization of the lesion-induced changes in activity represents a reproducible injury model to possibly test innovative ‘brain-prostheses‘.

2 Methods

All experimental procedures and animal care were conducted in conformity with institutional guidelines, in accordance with the European legislation (European Communities Directive of 24 November 1986, 86/609/EEC).

Primary neuronal cultures were obtained from cerebral cortices and hippocampi of rat embryos at gestational day E18. In order to provide the physical confinement of neuronal cultures, a polymeric structure in polydimethylsiloxane (PDMS), composed of different modules, has been realized through soft lithography [5]. The PDMS mask is positioned on the MEA substrate before the coating procedure, performed by putting a 100-µl drop of laminin and poly-D-lysine solution on the mask and leaving it in the vacuum chamber for 20 minutes. Then, the mask is removed and cells plated afterwards. The used MEAs (Multi Channel Systems, Reutlingen, Germany) can present three different geometrical layouts: “4Q”, where 60 electrodes are organized in 4 separate quadrants; “8x8”, where electrodes are placed according to a square grid; 6x10, rectangular grid. The nominal cell density is around 500 cells/µl (~100 cells per network module).

Experiments on both cortical and hippocampal modular networks, recorded between 20 and 25 Days In Vitro (DIVs), have been carried out. Results have been obtained from a dataset of 17 modular networks (7 hippocampal and 10 cortical). The used experimental protocol consisted of 5 consecutive phases: *i)* One-hour recording of spontaneous activity; *ii)* Stimulation session I, which consists of stimulating at least two electrodes per cluster using a train of 50 positive-then-negative pulses (1.5 V peak-to-peak, duration 500 µs, duty cycle 50%) at 0.2 Hz; *iii)* Laser ablation of inter-cluster neural connections, whose aim is to isolate a cluster which is physically and functionally connected to at least another one; *iv)* One-hour recording of spontaneous activity after performing the lesion; *v)* Stimulation session II, from the same electrodes of phase *ii*.